An Evaluation of Miniaturised Field Asymmetric Waveform Ion Mobility Spectrometry Hyphenated With Time-Of-Flight Mass Spectrometry

Robert W. Smith

A thesis submitted in partial fulfilment of the requirements for the award of Doctor of Philosophy (PhD) of Loughborough University

September 2014

Acknowledgements

I would not have been able to write this thesis on my own.

I am most grateful to my supervisor, Colin Creaser, whose guidance, attention to detail and no-nonsense feedback has prepared me for the real world, this work would not have been possible without your support.

I give thanks to Jim Reynolds, who has been very supportive throughout and someone to talk to. I greatly appreciate the financial and technical support from Owlstone, in particular Danielle Toutoungi and Billy Boyle and the rest of FAIMS academy (ALOA). The provision of instrumentation supplied by Agilent made this work possible. I would like to thank Jon Roach for fixing everything, a rare privilege for a PhD student.

I would like to thank the research group: Lauren, Neil and Caitlyn, Aadi, Vicky, Helen, Matt, Shuo, Dorota, Cristina, Corrinne, Little Vic, Liam, Alex, Emily, everyone else at the third floor lab. There was never a dull moment, it's the end of an era!

All my family and friends, I thank you for your support and encouragement. Nick and Charles for giving me perspective and helping me have fun.

Kung fu for keeping me sane.

Last, but by no means least, I thank my wife, Kaira, for your infinite patience (I wasn't snapping), wisdom and understanding.

Abstract

In this thesis, the performance of a miniaturised field asymmetric waveform ion mobility spectrometry (FAIMS) device hyphenated with time-of-flight mass spectrometry is studied and evaluated for analysis of a variety of compounds in different sample matrices. FAIMS is a selective spectrometer which is highly orthogonal to mass spectrometry and has the potential for enhancing sensitivity and improve selectivity of rapid analyses.

In Chapter 2, the performance of the miniaturised FAIMS device is tested for stability and transmission under a wide range of ion source conditions. An investigation of three different systems, including pairs of isobaric, isomeric and near-mass ions shows that miniaturised FAIMS has the ability to distinguish between analytes that are challenging to separate by mass spectrometry. Chapter 3 explores the effect of changing the composition of the carrier gas by observing the effect of adding gas modifiers on the FAIMS spectra of small molecules, peptides and proteins. Chapter 4 investigates the advantages of combining a fast FAIMS separation with mass spectrometry in the analysis of nitrogen-containing pharmaceutical impurities, where FAIMS is found to offer additional selectivity. In Chapter 5, the development of a UHPLC-FAIMS-MS method for the quantitative determination of a drug metabolite in urine is reported. UHPLC-FAIMS-MS shows improvements in signal-to-noise and linear dynamic range as well as a reduction in chemical noise, demonstrating the potential of combining FAIMS with mass spectrometry.

Contents

Appendices

Chapter One

Introduction

1. An Introduction to Ion Mobility and Differential Mobility Spectrometry

High-field asymmetric wave ion mobility spectrometry (FAIMS), also known as differential mobility spectrometry (DMS), originated from Russia in the early 1980s and details of the technique were first published in English by I. A. Buryakov in 1993.[1] Since then, FAIMS devices are used for a wide variety of applications across different industries worldwide; the development of different designs and interfaces with a number of ionisation and detection methods have made it a versatile technique for chemical detection.[2]

Ion mobility defines the velocity of an ion in the presence of an electric field and a buffer gas, a phenomenon that can be used for chemical analysis on a time-scale many times faster than many other analytical techniques. FAIMS distinguishes ions in the gas phase based on differences in ion mobility in the presence of low and high electric fields. The low and high electric fields are alternated in an asymmetric waveform, known as dispersion field (DF), which separates ions as they travel between two electrodes at atmospheric pressure. FAIMS technology differs from conventional drift tube ion mobility spectrometry (IMS) by controlling the stream of ions that traverse the device depending on differential mobility, rather than separation based on ion drift time, determined by size, shape and charge at low electric fields. In FAIMS, interfering ions are neutralised and removed while the analyte ion is selectively transmitted based on its differential mobility.

The separation parameter of FAIMS is compensation field (CF); which can be scanned to produce a CF spectrum of all ions entering the device or fixed at a single CF for the selective transmission of ions of a particular differential mobility.[3] The mechanism for FAIMS separation is distinct from mass spectrometry (MS) and high performance liquid chromatography (HPLC), making it ideal for hyphenation with these techniques,[4] offering a rapid separation step which can potentially remove the need for time consuming sample preparation and chromatography steps of analyses.[5,6] Improvements in signal to noise ratio by removing chemical interferences can enhance quantitative performance and increase linear dynamic ranges.[7] FAIMS has been used to separate isobaric ions[8], isomers[9] and conformers.[10]

In this chapter, the theories that describe the behaviour of ions in FAIMS devices and how these can be utilised for improving separations will be described. The focus of the introduction will be to highlight each technique that is used in this thesis, from sample introduction to detection. The advantages offered by combining FAIMS with other analytical systems will be discussed.

1.1 Principles of Ion Mobility Spectrometry

An ion subjected to an electric field in a drift gas will travel along the electric field with a velocity (V) defined by:

$$V = KE \qquad \text{(Equation 1.1)}$$

Where E is the electric field strength and ion mobility constant (K) is a constant unique to an ion.[11] The time taken for an ion to traverse an ion mobility drift cell in the presence of an electric field and a drift gas is therefore dependent on K. Separation in a drift cell is related to mass, charge and collisional cross section of the ion as shown in Equation 1.2.[12] Ion mobility spectrometry (IMS) is able to resolve ions by drift time in the gas phase with a low electric field applied. The mobility of an ion is defined:

$$K = \left(\frac{3q}{16N}\right)\left(\frac{2\pi}{kT_{eff}}\right)^{\frac{1}{2}}\left(\frac{m+M}{mM}\right)^{\frac{1}{2}}\left(\frac{1}{\Omega}\right) \qquad \text{(Equation 1.2)}$$

And depends on charge (q), number density of the gas (N), effective temperature of the ion (T_{eff}), the mass of the buffer gas (m), the mass of the ion (M), and the collisional cross section of the ion (Ω, also CCS).[13,14] However, the mobility of an ion is independent of electric field strength only at low electric field conditions.

1.2 Field Asymmetric Waveform Ion Mobility Spectrometry

The first mention of FAIMS in English literature was in 1993 by Buryakov[1] and given the name Field Ion Spectrometry (FIS). The technology was investigated for its applicability to explosive detection in North America by Mine Safety Appliances (MSA).[15] At this stage, the design featured two planar electrodes. MSA collaborated with MDS Sciex and the National Research Council of Canada to investigate the use of cylindrical electrodes.[2] Ionalytics Corporation was the first company to produce a commercialised FAIMS system which was subsequently taken over by Thermo Fisher Scientific. While development of cylindrical FAIMS continued, Nazarov with the research group at the Charles Stark Draper Laboratory Inc. and researchers of the New Mexico State University collaborated to develop a micro-machined planar FAIMS device, commonly referred to as Differential Mobility Spectrometry (DMS) in literature.[15] The planar FAIMS device was commercialised by the Sionex Corporation and consequently incorporated into the ABSciex SelexIon Spectrometer. More recently, a number of electrode designs with cylindrical and planar configurations have been

explored. The most recent being the ultraFAIMS device, or chip-based FAIMS, (Owlstone Ltd.) utilising multiple planar channels with small electrode gaps, achieving higher electric field strength.[3,16]

1.2.1 Ion Mobility Behaviour at Low and High Electric Field Strengths

If E exceeds around 1-10 Td (1 Td = 10^{-17} V cm^2), ion mobility (K) becomes dependent on electric field strength (E) and equation 1.1 no longer holds true.11 The threshold of non-linearity (E_0) can be calculated by dividing the dispersion field (DF) applied to the plate (U_0) by the distance between the plates (d); that is $E_0 = U_0/d$. So where, $E > E_0$ then $k(E) \neq k_0$. FAIMS uses an asymmetric waveform such that:[17]

$$E_h t_h + E_l t_l = 0 \qquad \text{(Equation 1.3)}$$

where t is the time that the electric field (E) is applied and the subscripts h and l relate to high and low electric field conditions respectively. The geometry of FAIMS electrodes varies between devices (Section 1.2.3), despite this they all utilise a gas flow that carries ions through the device and an asymmetric waveform of high and low electric field strengths is applied across the gap.[18] Typically, E_h will be double in magnitude with an opposite polarity and applied for half the time compared to E_l (2:1 ratio), but other asymmetric waveforms have been studied.[19,20,21] After each asymmetric waveform, a difference between low and high field components in mobility will cause an ion to have a displaced trajectory through the electrodes resulting in a neutralising collision with an electrode before the ion can traverse the device; this displacement is corrected by a compensation field (CF) applied to one of the electrodes. The CF can be scanned as an extra dimension of separation or to determine the optimum transmission conditions for the ion of a particular differential mobility which can then be fixed to selectively transmit the ion.[15] Figure 1.1 demonstrates the three different ways ion mobility can behave with increasing electric field strength: increasing (type A ions); increasing to a maximum before decreasing (type B ions); or decreasing (type C ions).

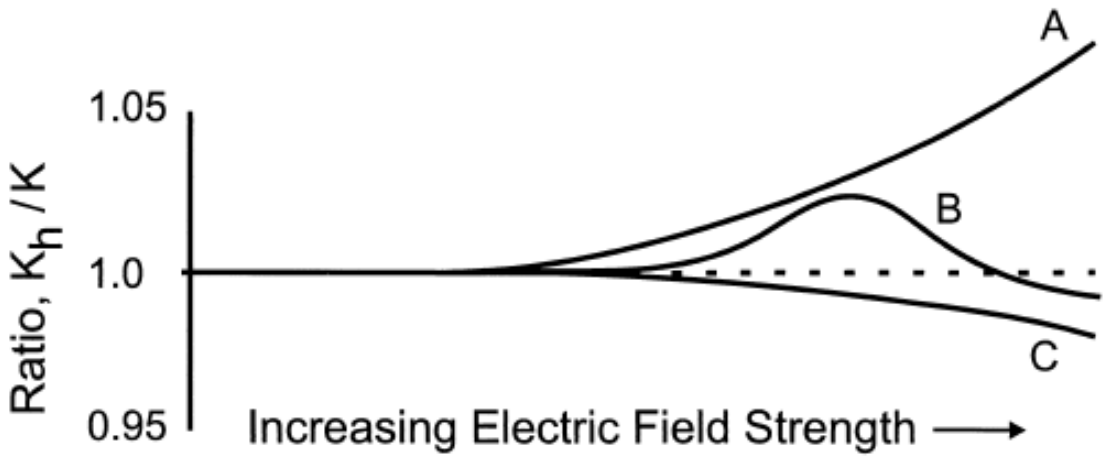

Figure 1.1 The dependence of ion mobility on electric field strength is shown by A, B and C[22] [Reprinted (adapted) with permission from Guevremont, R.; Purves, R. W. J. Am. Soc. Mass Spectrom. 1999, 10, 492–501. Copyright 1999 American Society for Mass Spectrometry]

The change in behaviour of tryptic peptides ions in a drift tube ion mobility spectrometer using high electric fields shows the upper limit of low electric field limit plotted against mass (Figure 1.2). The upper limit increases with mass and starts to plateau above 1000 amu showing that the low-field limit is mass dependent.[23]

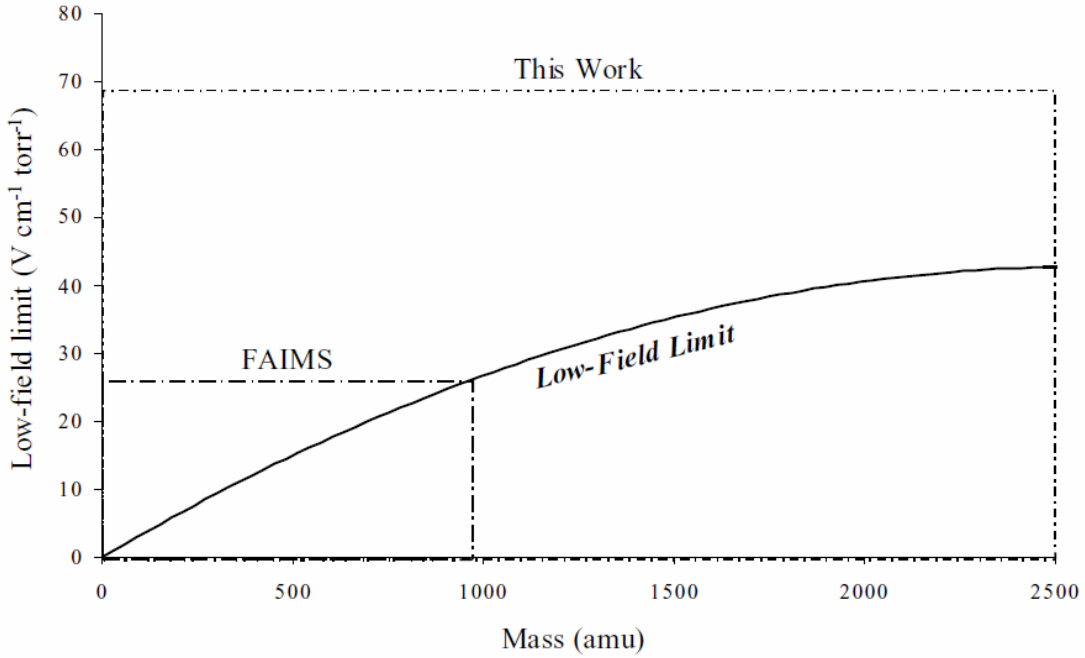

Figure 1.2 Low-field limit against mass for tryptic peptide ions showing the working range of FAIMS and high-field drift tube IMS[23] [J. Am.Soc. Mass Spectrom., 15, 2005, 158, The influence and utility of varying field strength for the separation of tryptic peptides by ion

mobility-mass spectrometry, B.T. Ruotolo, Figure 6, Copyright 2004 American Society for Mass Spectrometry reproduced with kind permission from Springer Science and Business Media]

The dependence of K on electric field strength at higher field strengths is defined by:

$$K(E) = K_0 \left[1 + \alpha\left(\frac{E}{N}\right)\right] \qquad \text{(Equation 1.4)}$$

where K_0 is the mobility at zero electric field; and α(E/N) is defined by an even power series $\alpha_2(E/N)^2 + \alpha_4(E/N)^4 + \ldots\alpha_n(E/N)^n$ where expressions beyond n = 4 are normally negligible.[24,25] Electric field strength is defined by (E/N) where E is the voltage applied and N is the neutral gas density (atoms/cm^3). The α function is used as a method for determining K(E/N) (mobility as a function of electric field strength and gas number density) giving information about an ion's behaviour in FAIMS and enabling comparisons between different systems.[2]

The α functions for a homologous series of ketones plotted against electric field strength are shown in Figure 1.3.[26] Plotting the α function for a group of ions can be used to probe their behaviour under high field conditions. The difference in the differential mobility behaviour between singly protonated monomers and dimers is distinct. Where the monomers have a positive α value which increases with electric field strength, most of the dimers have a negative α value that decreases with electric field strength. The larger monomers and smaller dimers are similar, suggesting that when functionality is the same, size can influence α values and the peak position. Theoretically and experimentally derived CF values were found to be in agreement.[26] The correlation between α function and ion mass demonstrates the potential for predicting the mobility behaviour of ions with similar functionality. Further elucidation of the relationship between CF and *m/z* showed trends but also states that the deviations of CF values from a single trend that were observed make FAIMS a more valuable analytical technique.[27] A method for determining the alpha parameter was determined by using a spectrometer of ion mobility increments (SIMI)[17] and a more comprehensive attempt to explain the theory of FAIMS without the alpha coefficient was made by Spangler *et al*.[28] The purpose of the latter work was to estimate where an ion would appear in the compensation field spectrum. The resulting equation (not shown) worked best for small ions in a light gas and gave an accuracy of 50%. Currently, the best approach for testing the potential for a FAIMS separation of a new analyte is still by running a scanning CV experiment at multiple

dispersion fields. Research continues in this area, with the aim to use computer modelling to calculate optimum conditions for separations. Another method for modelling the behaviour of ions in FAIMS analysers is called the Monte Carlo simulation.[29,30]

Dispersion field (DF) and compensation field (CF) are measured in Townsend (1 Td = 10^{-17} V cm^2) which is calculated from E/N; this is more accurate for measuring electric field strengths than the voltage over the gap (V/cm) because changes in pressure/flow and temperature are taken into account which aids in instrumental stability and repeatability. The use of Townsend is simpler for comparing between different systems and changes in carrier gas properties where different gap sizes, temperatures, gas flows and pressures influence the electric field strength.[31]

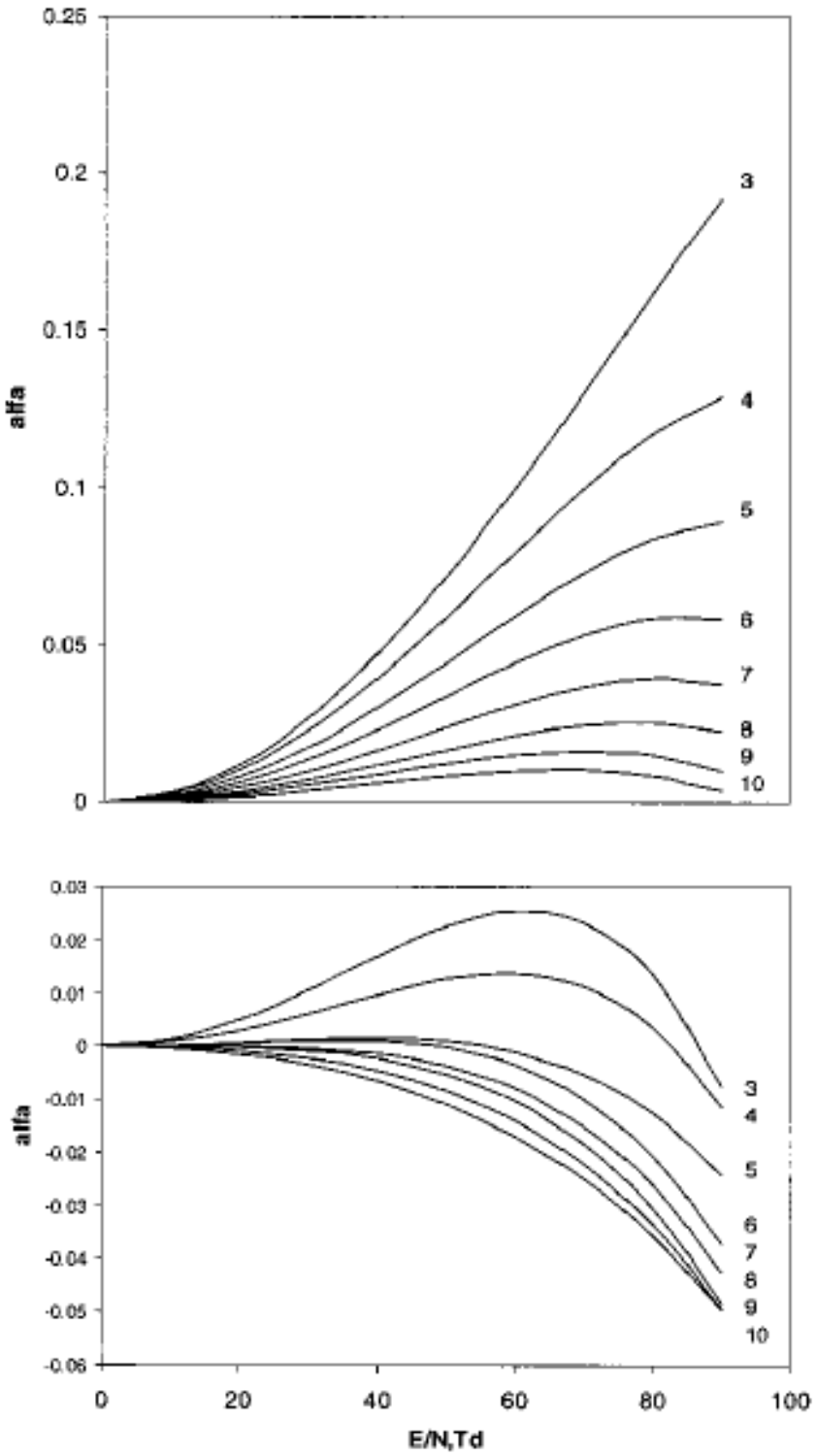

Figure 1.3 α(E/N) plot for protonated monomer (top) and proton bound dimer (bottom) ketones. Each data series is labelled with a number which indicates the number of carbons in the ketones.[26] [Reprinted with permission from Krylov, E.; Nazarov, E. G.; Miller, R. A.; Tadjikov, B.; Eiceman, G. A. *J. Phys. Chem. A*. **2002**, *106*, 5437–44. Copyright 2002 American Chemical Society]

1.2.2 Mechanisms of Differential Mobility Separation

The mechanisms that best describe the behaviour of ions in alternating low and high electric field strengths will be discussed in this section.

Clustering/Declustering

Under low electric field conditions, an ion is clustered with small neutral molecules, such as water, *via* non-covalent interactions. The increase in velocity resulting from a higher electric field increases the number of collisions with the carrier gas resulting in the ion experiencing a higher temperature than the carrier gas molecules, a phenomenon called 'field heating' which causes the clustered ion to decluster (Figure 1.4.a). The removal of neutral molecules results in a smaller CCS and increases the ion velocity, hence mobility in high field conditions is higher than in low electric field conditions (type A ions).[32] The magnitude of the difference between low and high field mobility is inversely related to the size of ions with the same charge because a smaller ion will experience a larger relative change in CCS.[33] It is possible to add different neutral molecules to the carrier gas to change the composition of clustering. Clustering with larger molecules, such as 2-butanol, can potentially increase the size of the clustered ion and subsequently increase the difference between the size of clustered and declustered ions (Figure 1.4.b). The advantage of utilising the clustering/declustering mechanism by modifying the carrier gas with different solvent molecules will be discussed in section 1.2.5.

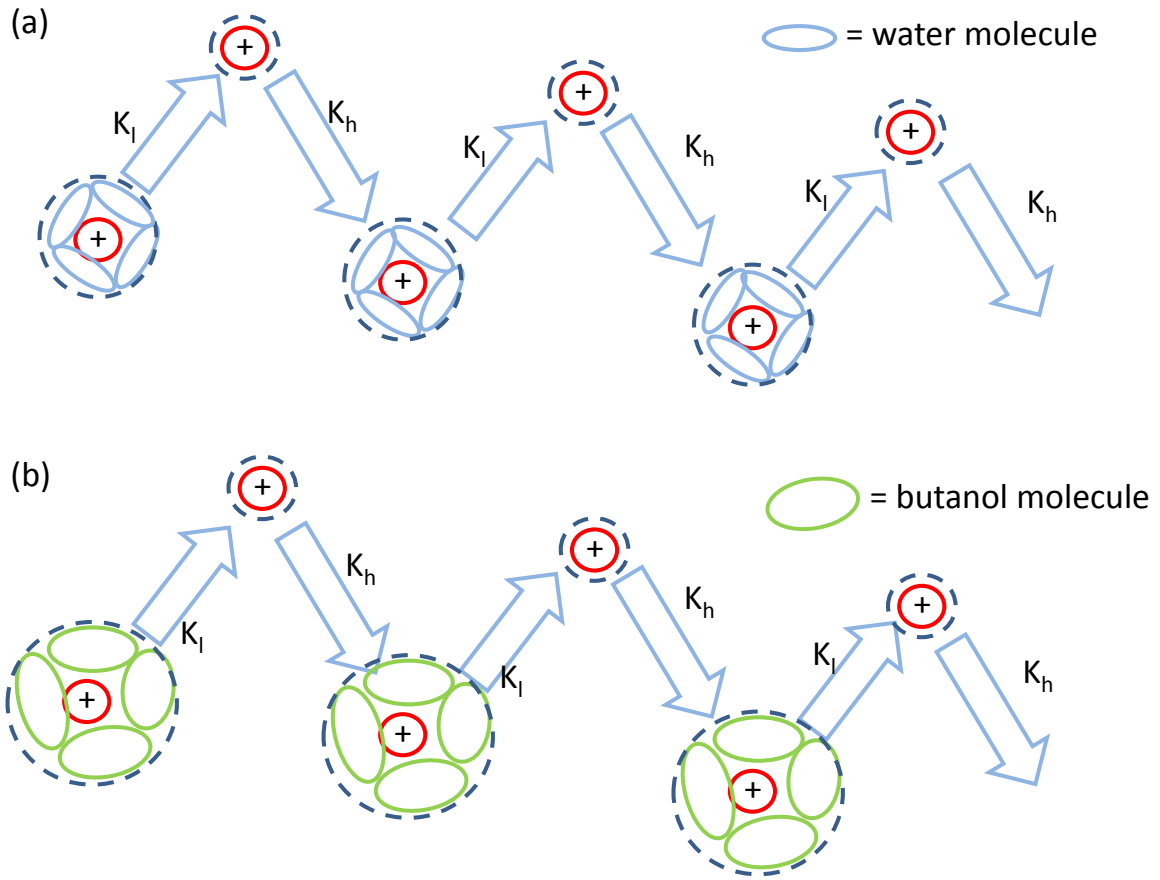

Figure1.4. Schematic of clustering/declustering mechanism of a positive ion with (a) water molecules, and (b) butanol molecules

The effect of moisture on the differential mobility of organophosphorus compounds has been studied in detail, supporting the clustering/declustering mechanism.[34] Moisture levels between 0.1 and 15000 ppm were explored and a threshold of at least 50 ppm was required before a trend of increasing α for ions occurred with increasing water concentration was observed. The authors suggested that at low hydration levels, the kinetics for an ion to form a cluster with water molecules are too slow to occur in the low-field portion of the asymmetric waveform. In another study, four different gas modifiers at increasing concentrations influenced the differential mobility of 2,6-dinitrotoluene. The gas modifiers compete with molecules that would ordinarily cluster with the ion, potentially producing a much larger CCS and requiring a higher compensation voltage for it to be successfully transmitted. Different modifiers in the carrier gas changed the order of the ions in the FAIMS spectrum showing that a degree of selectivity results from the non-covalent interactions between analyte ions and gas modifier molecules and that neutral molecules in the carrier gas have an active role in the clustering/declustering mechanism.[25] It has been proposed that polar gas

modifier molecules compete with the gas molecules in the buffer gas via intermolecular forces (like H-bonding and Van der Waals forces) to increase an ion's CCS in low field conditions. Gas modifiers can be used to exploit this mechanism and potentially improve separation.[35] The effect of gas modifiers on separation will be discussed in greater detail in Section 1.2.5.

Conformation Switching

Field heating can cause conformational changes to ions in a FAIMS device. For example, peptide and protein ions can adopt a less folded conformation during the high-field portion of the asymmetric waveform, resulting in the peptide/protein switching between open and closed conformations with the cycles of low and high electric fields. Open conformations have greater CCSs than closed conformations resulting in a reduction in ion mobility at high fields (type C ions). FAIMS was combined with IMS-MS to investigate conformation switching of ubiquitin ions and corresponding CCS for each resolved conformer and charge state were determined using IMS-MS. FAIMS caused ubiquitin to unfold to the extent that is equivalent to 50°C heating above room temperature, although calculations predicted field heating would contribute 10°C. Shvartsburg recommended cooling by 75°C to remove these effects for more accurate structural characterisation.[10,36]

Dipole Alignment

Dipole alignment occurs when a high electric field imposes orientation on ions with a permanent electric dipole of at least 400 Debye. An average CCS will typically define ion mobility because free rotation permits a number of different orientations, each with their own CCS to give an average CCS. An imposed orientation means that the directional CCS will define mobility instead of the average CCS. An ion will have an average CCS and directional CCS in low and high electric field conditions respectively as it travels between the electrodes, creating a difference between low and high field conditions. Type B behaviour (Figure 1.1) can result, where cluster/declustering is the primary mechanism resulting in the initial increase in mobility in the high field but when the high field becomes sufficiently strong enough to impose orientation giving a directional CCS and a decrease in high field mobility.[37] Recently developed FAIMS microchips feature smaller gaps than other devices, making higher field strengths achievable (up to 60 kV/cm); it was used to explore the influence of higher field conditions on bovine ubiquitin and bovine serum albumin (BSA), small and large proteins.[38] For a protein to exhibit a dipole moment large enough for dipole

alignment to occur the mass needs to be ~ 20-25 kDa, dipole moment increases with protein mass. BSA is large enough, ~66 kDa, for dipole alignment to occur. The results shown in Figure 1.5 support this theory, where BSA can be distinguished from the smaller protein ubiquitin because BSA exhibits type A behaviour opposed to type C as seen with smaller proteins and peptides. Dipole alignment makes it possible to resolve peptides and proteins from larger proteins (like BSA) potentially allowing larger proteins to be filtered from complex biological environments.

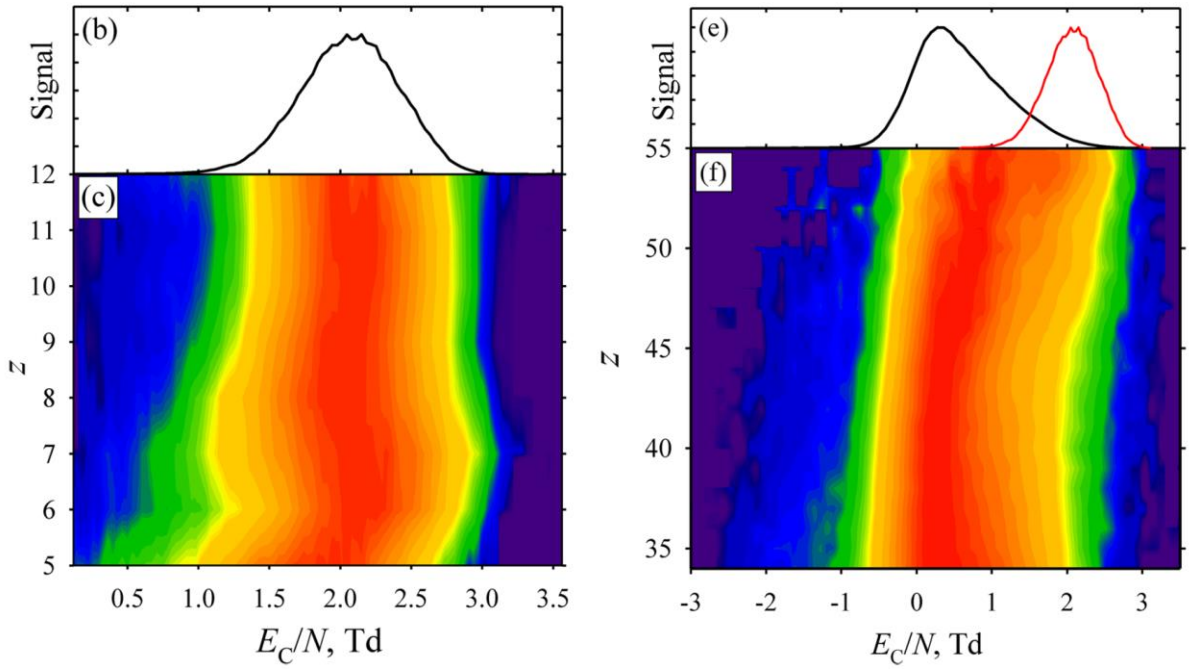

Figure 1.5 CF spectra at 60 kV/cm of ubiquitin (left) and BSA (right, black line), showing the sum of all the charge states (top), and the individual charge states using a heat map (bottom); ubiquitin (red trace) is included on the BSA spectrum for comparison between the two proteins[38] [Reprinted (adapted) with permission from Shvartsburg, A. A.; Smith, R. D. Anal. Chem. 2012, 84, 7297–300. Copyright 2012 American Chemical Society]

1.2.3 Instrumentation for Field Asymmetric Waveform Ion Mobility Spectrometry

Two fundamental electrode designs exist for FAIMS: planar (Figure 1.6) and cylindrical (Figure 1.7). In the literature, cylindrical is commonly (but not always) referred to as FAIMS and planar as DMS.[15] There are a number of devices that fall under the category of cylindrical and planar electrode designs but their performance characteristics generally correlate to either cylindrical or planar geometries.

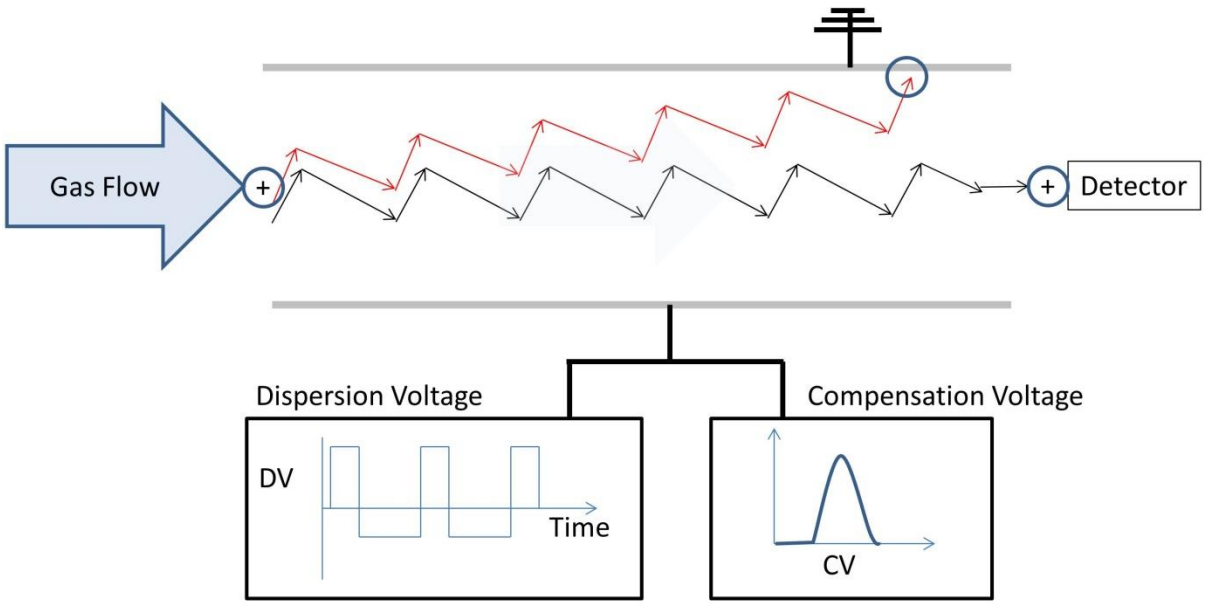

Figure 1.6 A diagram of a planar geometry FAIMS, showing the dispersion and compensation voltages applied to one electrode (although they can also be applied to different electrode plates)[18]

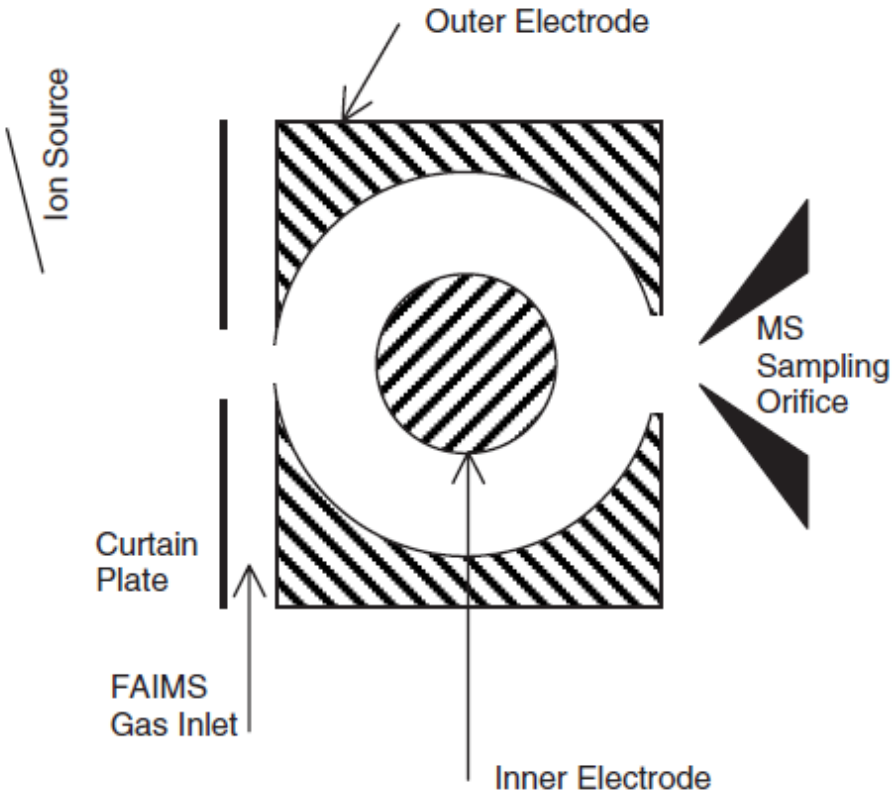

Figure 1.7 Cylindrical FAIMS electrode design (cube/dome) with ESI-MS interface[39] [Reprinted with permission from Kapron, J. T.; Jemal, M.; Duncan, G.; Kolakowski, B.;

Purves, R. Rapid Commun. Mass Spectrom. 2005, 19, 1979–1983. Copyright 2005, John Wiley & Sons, Ltd.]

The planar devices can simultaneously analyse positive and negative ions due to the uniform distance between the electrodes.[18] The cylindrical electrode FAIMS design can result in an ion focussing effect giving an improvement in transmission, however analysing in an opposite polarity can cause either ion focussing or ion defocussing effect.[15,40] Running experiments in FAIMS off mode can be challenging with cylindrical devices due to a 93% loss in signal compared to 20-30% loss observed with a planar device with the same gap diameter. The ability to run in FAIMS off mode with a FAIMS device in place with acceptable signal loss saves the need to remove the FAIMS device from a mass spectrometer whenever a FAIMS separation is not required, making it simpler to use. When ion focussing conditions are met with cylindrical FAIMS devices, transmission is increased which exceeds transmission of a planar device.[41] Ion focussing in cylindrical devices reduces the coulombic ion-ion repulsion, enabling longer residences times for improved resolution. In a planar device, longer residence times would increase ion loss due to diffusion effects.[18] Reversing polarities dramatically changes the CV spectrum of an ion because the ion focussing effect reverses, defocussing ions with increasing electric field strength (Figure 1.8). Ion focussing conditions cannot be met for all ions. No focussing occurs with planar devices where the velocity increases with dispersion field resulting in more neutralising collisions with the electrodes and reducing transmission.[2] In the past, ion focussing made cylindrical FAIMS designs the favourable for interfacing with MS due to a focussed ion beam exiting the FAIMS device.

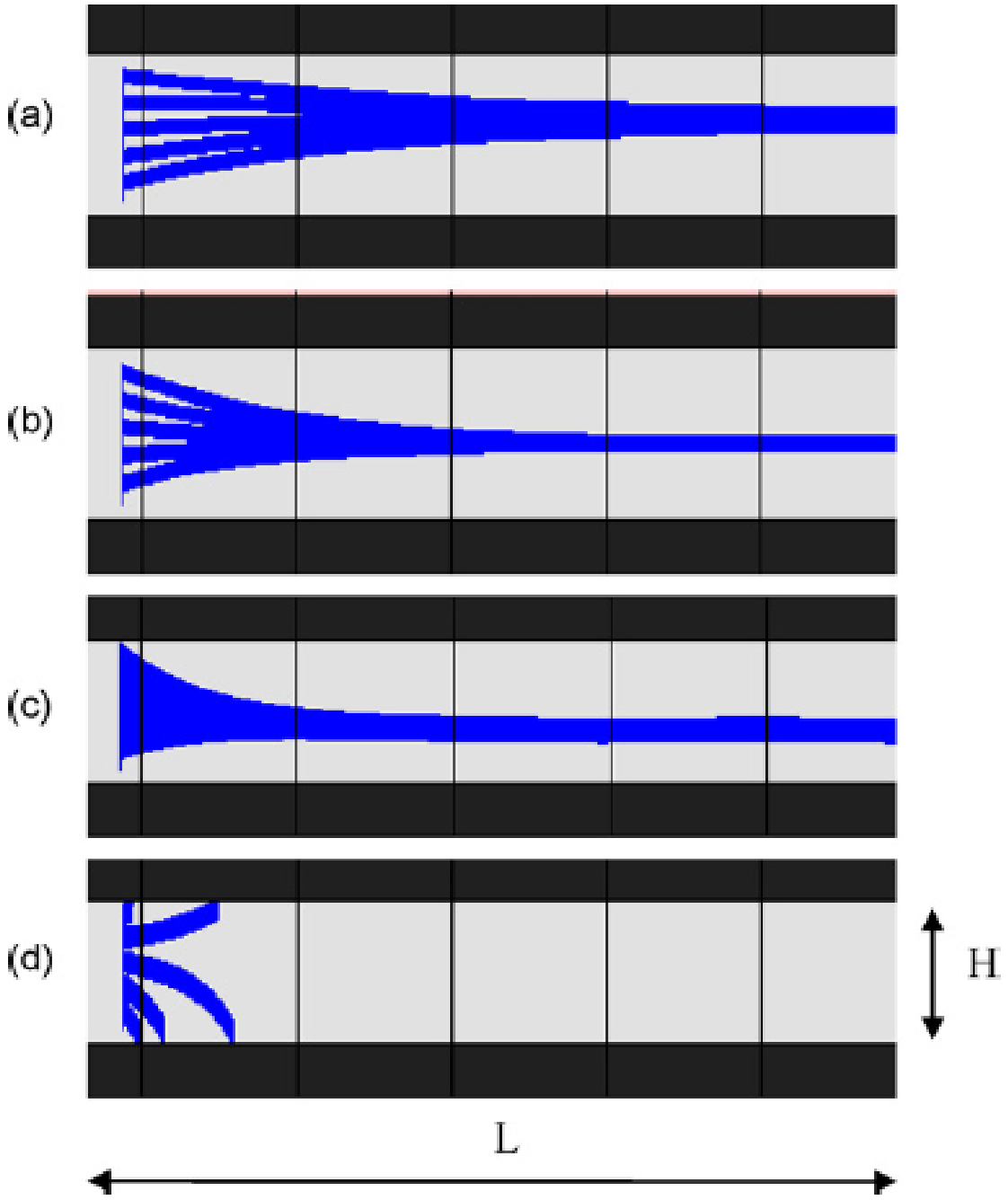

Figure 1.8. Simulated ion focussing/defocussing in a cylindrical FAIMS device showing: (a) weak, (b) moderate, (c) strong focussing conditions; and (d) defocussing conditions[18] [Reprinted (adapted) with permission from Schneider, B. B.; Covey, T. R.; Coy, S. L.; Krylov, E. V; Nazarov, E. G. Int. J. Mass Spectrom. 2010, 291, 108–117. Copyright 2010 Elsevier B.V.]

The cylindrical devices described in the literature include cylinder, dome and cube designs; cylinder design being the earliest cylindrical device which features two cylinders, an inner and outer cylinder electrode with ~2 mm gap for ion separation.[39,43] Development of the dome device, featuring two concentric cylinders and a semi-spherical end, has been hindered by only tolerating < 5 µl/min liquid flow rates. The cube electrode design (sometimes referred to as dome) was able to cope with higher flow rates when combined with a heated electrospray ionisation source which was marketed by Thermo Fisher FAIMS interface (Figure 1.7). A drawback of this device was that the source heated the FAIMS electrodes resulting in unstable CV values and requiring warm up periods of up to 2 hours.[15,42] The dome design was used for an increase in sensitivity for the analysis of an unnamed amine drug in the presence of its metabolites.[39] Good precision was observed for replicates and the FAIMS device found to be compatible with current sample preparation and sampling procedures.

Ion residence time in a planar device is ~1 ms, compared to ~300 ms in a typical cylindrical device. Miniaturised FAIMS features 35-100µm gaps and 300-700µm path lengths, enabling residence times between 50 and 250µs. The time an ion resides in a FAIMS device will affect the resolution, sensitivity and potential CF scanning speed. A longer residence time can improve resolution but compromises CF scanning speed and may increase signal loss.[15] Cycling between two CF values cannot be carried out faster than 1 cycle of ions per second, limiting the speed at which CV can be ramped or hopped. A short residence time is required for fast scanning times enabling full CF scan data within the elution time of a chromatographic peak and for rapid method optimisation. Longer residence time has the potential for improving separation for FAIMS-MS experiments, but the timescale is not compatible with chromatography.[2] Switching between static CF/DF settings (hopping) is required to make cylindrical FAIMS compatible with LC-MS instruments.[44] The ion selectivity of cylindrical and planar devices with similar ion residence times were compared, the planar devices were found to have 3-5 times better separation.[45]

A planar FAIMS device interfaced to MS and subjected to conditions of high sample contamination was found to be suitable for high throughput and high quantitative accuracy environments.[18] Planar FAIMS devices are easier to manufacture, making them cheaper and more reproducible.[15] Such devices have been used with nanoESI-FAIMS-MS for the quantitative analysis of a semi-complex peptide mixture, spiked with 2 µg/ml angiotensin.[35] In the past, interfacing planar FAIMS devices with MS was found to be challenging due to

the ion beam being unrestrained from expanding in the gap leading to large losses. Introduction of a slit-shaped entrance and exit aided transmission giving an order of magnitude increase in signal intensity.[46] Planar FAIMS devices were found to tolerate higher liquid flow rates (< 50 µL/minute) making them better suited to HPLC and MS systems, although introduction of the heated electrospray source (HESI) made the Thermo 'cube' FAIMS more compatible with higher flows.[15]

Miniaturised, chip-based FAIMS

The research described in this thesis was carried out using a new miniaturised, chip-based planar FAIMS design (Figure 1.9). The FAIMS chip consists of 47 parallel electrodes with 35 µm gaps, or ~20 electrodes with 100 µm gaps. The small gap generates far higher dispersion fields than any other FAIMS devices without causing electric breakdown of the carrier gas, up to 60 kV/cm (320 Td). Ion residence time is 50-250 µs, 1% of the shortest residence times in other FAIMS devices, enabling faster CF scans and decreasing the time for ion loss from diffusion to occur. The waveform frequency is 22 – 27 MHz compared to ~3 MHz in other devices, making the number of asymmetric waveforms experienced by ions comparable to other FAIMS devices despite the shorter ion residence times. The parallel arrangement of the gaps (Figure 1.9) relaxes the coulombic repulsion by spreading the charge between the channels for improved transmission, where transmitting the same number of ions through a single gap would result in much higher loss of ions. Low residence times cause broader peaks when compared with other planar devices but enables fast CF scanning times for full CF scans within LC peak timescales.[16] Other planar and cylindrical FAIMS devices have ion residence times of 100 ms (Thermo Fisher) and 20 ms (ABSciex SelexIon),[47] although modified devices may have different residence times. The Owlstone ultraFAIMS stand-alone system was first used for homeland security[48] and has now been interfaced to LTQ ion trap MS (Thermo Fisher) and 6230 ToF MS (Agilent Technologies) spectrometers.[3,49] Miniaturised FAIMS is discussed in detail in other publications.[16,50]

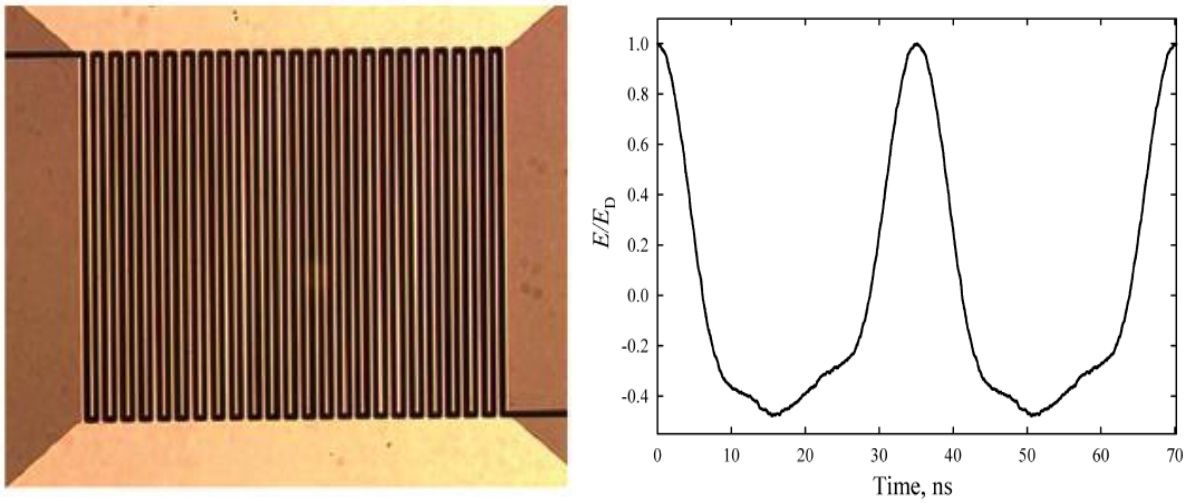

Figure1.9: Ultra-FAIMS microchip: (a) diagram showing arrangement of microchannels and (b) showing asymmetric waveform[16] [Reprinted (adapted) with permission from Shvartsburg, A. A.; Smith, R. D.; Wilks, A.; Koehl, A.; Ruiz-Alonso, D.; Boyle, B. *Anal. Chem.* **2009**, *81*, 6489–95. Copyright 2009 American Chemical Society]

Each design of FAIMS has its own advantages and disadvantages which need to be considered when deciding the most suitable device for a particular application. The research discussed in this thesis investigates the performance of the prototype Owlstone ultraFAIMS interfaces with TOF MS and explores the enhancements it can offer to liquid chromatography and mass spectrometry for small molecule analysis.

1.2.4 Effect of Instrumental Parameters on FAIMS Performance

The development of a FAIMS analysis includes a CF/DF stepping experiment to determine optimum DF for separation. Once determined, the CF will be either scanned, fixed or cycled between several fixed CF values depending on the sensitivity and selectivity the analysis requires. There are also a number of other parameters that can be changed to improve analytical performance. These include: carrier gas composition/flow, electrode gap size, ion residence time, type of asymmetric waveform and temperature. The importance of each of these factors on changing separation, sensitivity and selectivity will be discussed in this section.

Electrode Gap Size, Carrier Gas Flow and Ion Residence Time

A smaller electrode gap size increases the maximum dispersion field achievable without causing electrical breakdown of the carrier gas.[16] A larger gap size can increase ion residence time if the carrier gas flow is not adjusted accordingly, which will improve resolution at the cost of transmission. Gas flow and gap size are independent, but when one is changed both should be considered.[51] Changing ion residence time by altering gas flow/gap size affects selectivity and sensitivity because decreasing ion residence time increases transmission, but compromises peak resolution, and increasing ion residence time will improve resolution at the expense of transmission. Ion residence time is more critical for smaller electrode gap sizes, where signal loss is greater when compared to a larger gap size (Figure 1.10).

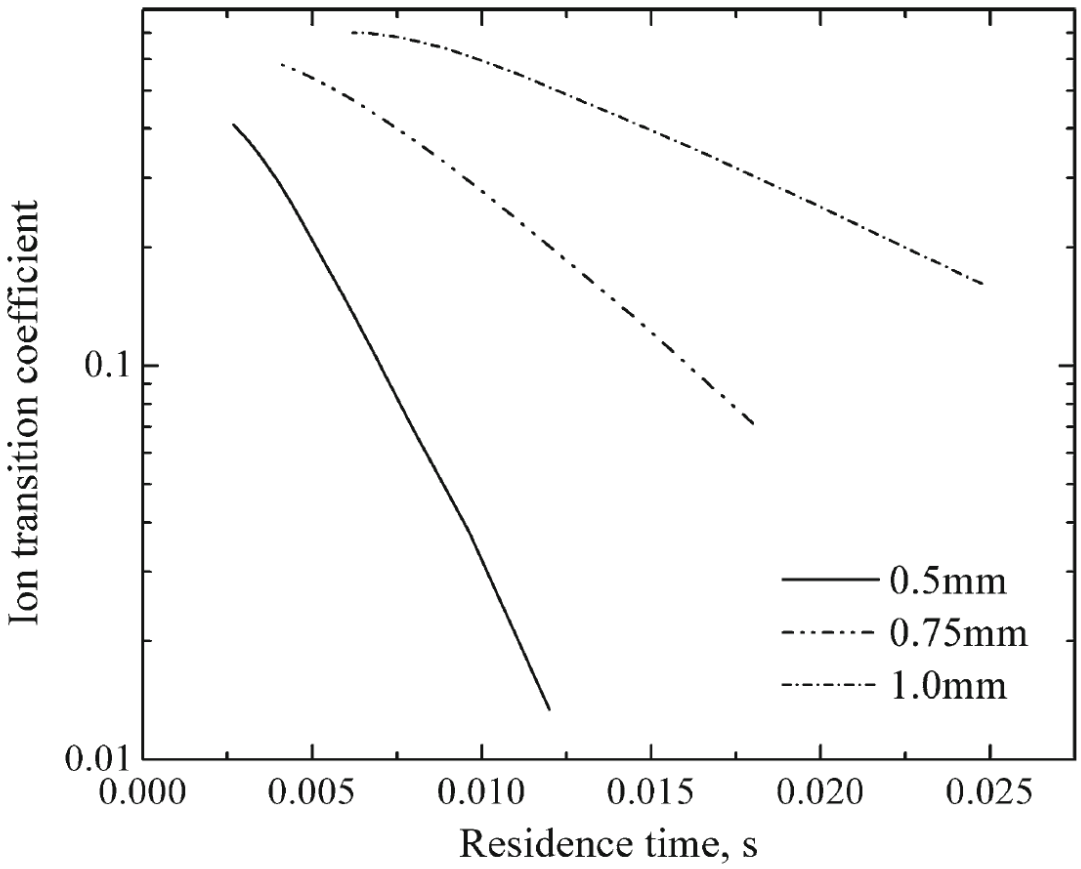

Figure 1.10 Ion transmission coefficient for positive reactant ions $(H_2O)_nH^+$ against residence time for different gap sizes (DF 45 Td)[51] [Reprinted (adapter) with permission from Krylov, E. *Int. J. Ion Mobil. Spectrom.* **2012**, *15*, 85–90. Copyright 2012 Springer-Verlag]

Optimising sensitivity and selectivity often require a compromise of one against the other. Kyrlov's work in 2012 on optimising analytical characteristics of planar FAIMS discussed analytical quality, where a balance between sensitivity and selectivity for a particular application can be determined by relating ion transmission and peak width. Ion transmission coefficient (G) is defined by:

$$G = \exp(-\frac{t_{res}D\pi^2}{g^2}) \qquad \text{Equation 1.5}$$

where residence time (t_{res}) and diffusion (D) reduce transmission and effective gap size (g) improves transmission; peak width (W) is related by:

$$W = \frac{g}{Kt_{res}} \qquad \text{Equation 1.6}$$

where the effective gap width (g) and residence time (t_{res}) are inversely related. G and W define analytical quality (A):

$$A = \frac{G}{W}$$ Equation 1.7

Analytical quality can be plotted against residence time (Figure 1.11.a) which clearly shows that optimum residence time will change depending on the electrode gap size. Figure 1.11.b shows the results at the same gap size (0.75 mm) but with different mobilities, showing that diffusion (related to mobility) can also influence analytical quality which suggests that even if ion residence time is optimised for a set of compounds, it may not necessarily be the optimum condition for a different set of compounds.

A recent publication by Barnett and Ouellette addresses the issue of cost for high flow rates of helium in gas mixtures for peptide analysis and an approach for removing the need for gas mixtures by decreasing the gap (2.5 mm to 1.25 mm) between the electrodes of a cylindrical design. The modified design was found to have a significantly improved performance (in pure N_2) than commercial FAIMS designs using an equal gas mixture of N_2/He with 2.5 mm gap.[52] This example demonstrates the importance of gap size on FAIMS devices.

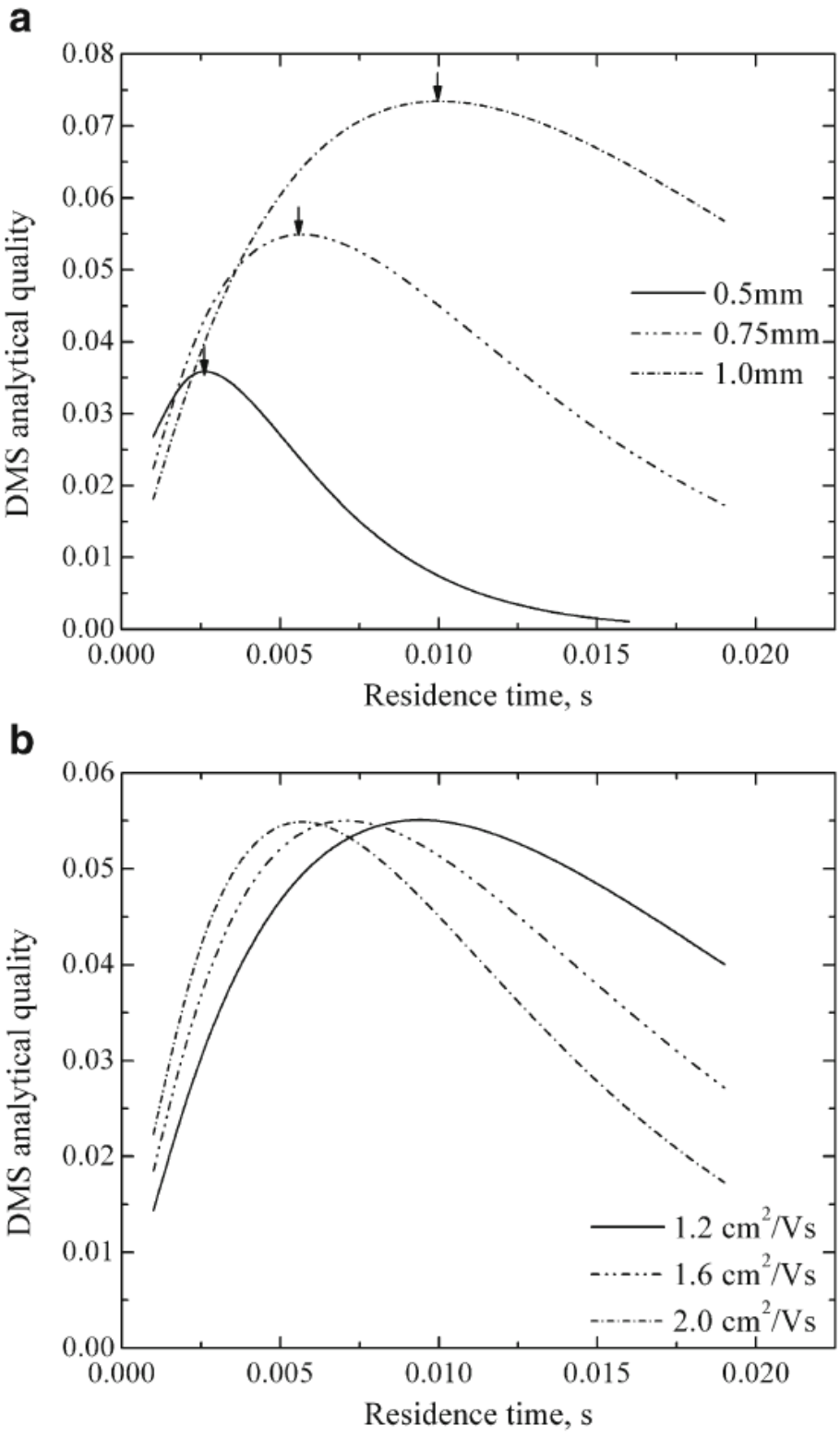

Figure 1.11 Analytical quality has been plotted against residence time with: (a) different gap sizes (K = 2 cm^2/Vs), and (b) different ion mobilities (gap = 0.75 mm)[51] [Reprinted (adapter) with permission from Krylov, E. *Int. J. Ion Mobil. Spectrom.* **2012**, *15*, 85–90. Copyright 2012 Springer-Verlag]

Temperature and Pressure effects

Changes in temperature and pressure can influence where peaks appear in the compensation field spectrum.[31] Figure 1.12 shows FAIMS spectra of methyl salicylate under different pressures and temperatures. The dispersion field and a compensation field axis (in Td) are adjusted to temperature and pressure. The influence of different pressures results in small changes in the position of the positive methyl salicylate ions on the CF axis (Figure 1.12.a), although there are large changes in peak height. Temperature has a much larger effect, causing a positive shift of peak location in the CF axis (Figure 1.12.b). The influence of temperature on the differential mobility of amine ions was the subject of an in-depth study published in 1989.[53] The mobilities of a series of aliphatic and aromatic amines were explored in helium, air, CO_2 and SF_6 over a temperature range 87 to 250 ˚C. Temperature has the potential to change differential mobility of ions and may be useful for improving selectivity, but caution should be taken when changing temperatures of the ionisation source which may result in a different FAIMS spectra and a loss of separation.

The Asymmetric Waveform

The asymmetric waveform was not changed in the results described in this thesis, but it is important to briefly discuss its effect. Evaluations of the effects of different asymmetric waveforms to improve analytical performance have been reported.[19,20,21,54] Despite the advantages of selecting the best asymmetric waveform for better performance, changing the waveform can be complex and challenging and is rarely included in routine FAIMS optimisation. Optimising waveforms is generally left to manufacturers rather than the individual analyst, but certainly should not be neglected entirely in method development.

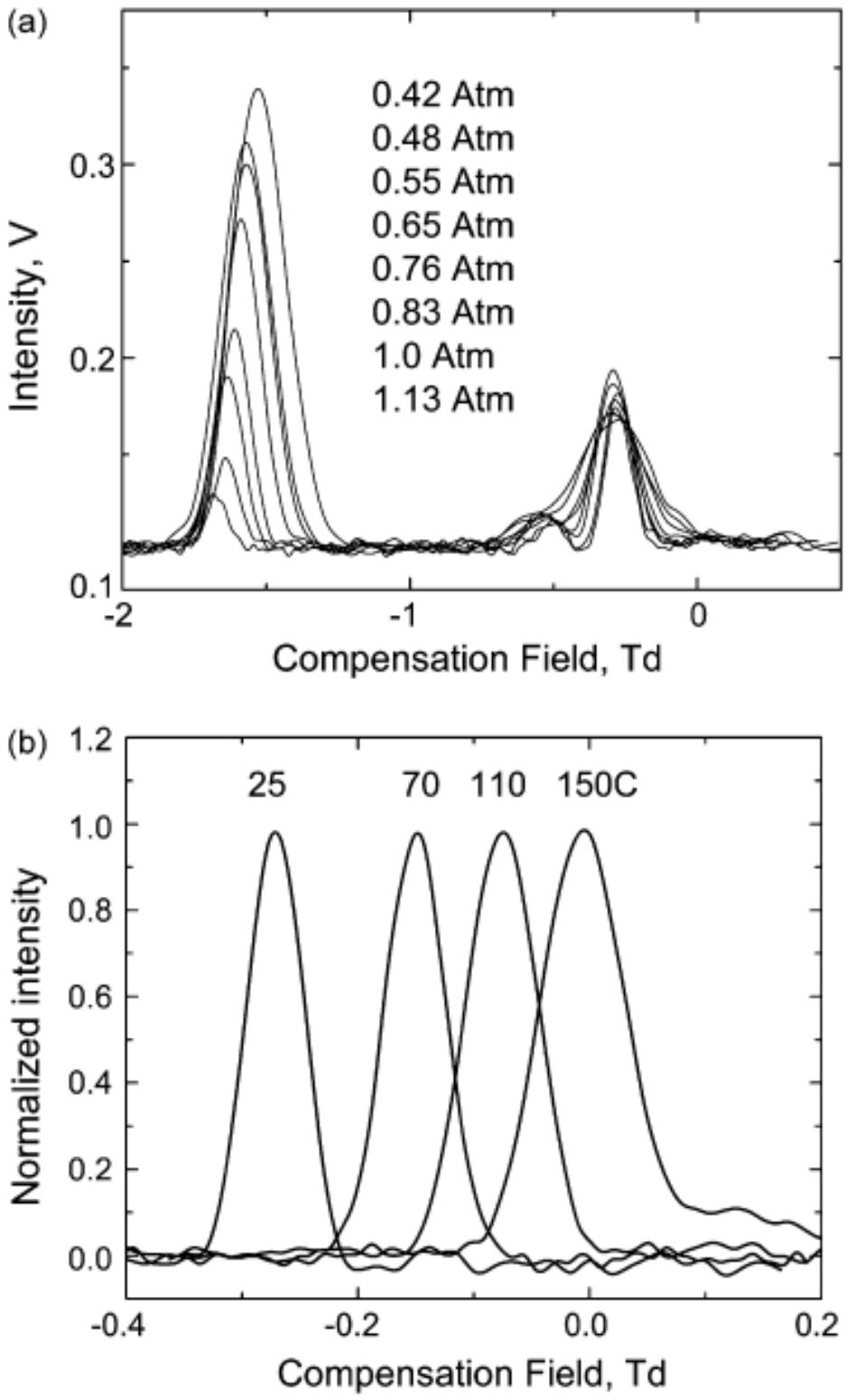

Figure 1:12 Positive FAIMS spectra of methyl salicylate ions with a dispersion field of 100 Td with (a) different gas pressure, and (b) different temperatures[31] [Reprinted (adapted) with permission from Krylov, E.; Coy, S.; Nazarov, E. Int. J. Mass Spectrom. 2009, 279, 119–125. Copyright 2008 Elsevier B.V.]

1.2.5 The Importance of Carrier Gas

Gas Mixtures

Typically, nitrogen or air are used as the carrier gas for FAIMS analysers. This section will discuss the effect that changing the carrier gas composition of the carrier gas has on separation, selectivity, sensitivity and transmission.

Different gases will interact with ions in different ways depending on the size and polarisability of gas molecules with the potential to change FAIMS separation and sensitivity. Nitrogen has been commonly mixed with helium and/or carbon dioxide, although other gases, such as hydrogen, have also been studied.[55] An increase in the size and polarisability of the neutral carrier gas decreases mobility of an ion due to increased collisions which can improve separations and, in some cases, peak resolution and transmission. Another way to influence differential mobility is to impose a change in the clustering mechanism. Gas modifiers are solvent molecules in the vapour phase that change the non-covalent interaction of analyte ions with neutral molecules in the carrier gas, changing the collisional cross section of the clustered ion and making a bigger difference between mobility in the low field and high field.[32]

Polarisability and reduced mass are important factors affecting ion mobility. Polarisability is the interaction potential between a gas molecule and an ion, reduced mass depends on the ion mass and gas molecule mass given in Equation 1.2. The mobilities and CCS of aliphatic and aromatic amines were determined with six different gases,[56] with increasing polarisability ($Å^3$) as follows: helium (0.205), argon (1.64), air (1.73), nitrogen (1.76), carbon dioxide (2.59) and sulfur hexafluoride (4.48). The addition of helium to a nitrogen carrier gas is common place for users of cylindrical FAIMS devices and often benefits separation.[57] Helium has a lower polarisability than nitrogen which increases the mobility of ions whereas carbon dioxide has a higher polarisability than nitrogen which decreases mobility.[56] Helium can result in broader peaks, but improve sensitivity, carbon dioxide may cause a loss in signal, but can reduce peaks widths. Anabolic androgenic steroid metabolite detection in urine using LC-FAIMS-MS/MS,[58] the separation of prostanoids,[59] peptide sequence isomers,[60] glycopeptides with differing sites of glycosylation61 are just a few of many examples where gas mixtures have been used to improve FAIMS performance. High helium fractions, often up to 50% of the carrier gas, can make analyses considerably more expensive

for routine analysis. The addition of CO_2 can worsen separation but combined with He and N_2 can give optimum performance by compromising between separation and sensitivity.[62]

The balance between different gases may be optimised for specific applications. Shvartsburg *et al*. recently experimented with hydrogen and helium mixed with nitrogen to improve resolving power of a planar FAIMS device, using a 50:50 He/N_2 mixture revealed four partially resolved conformers of Ubiquitin +12H,[63] and up to 90% H_2 was used to separate amino acid sequence isomers.[55] The addition of H_2 to the carrier gas is advantageous compared to He because higher fractions of H_2 (up to 90%) are possible than with He (up to 50%) due to the higher electrical breakdown threshold of H_2, benefiting separation. Greater signal losses were observed for the more mobile ions in the presence of H_2, and the authors suggested that a larger gap with a higher voltage to maintain the same electric field over the gap would recover some of the signal.

The benefits of gas mixtures and modifiers are still being explored; however, work discussed previously in this section shows that despite the improvement gained when using gas mixtures, the cost of running methods with high helium consumption make it less suitable for routine analyses;[52] alternative methodologies such as the introduction of gas modifiers to the carrier gas that are more financially viable are being explored.

Gas Modifiers

The effect of gas modifiers was first reported in 1993 when Buryakov et al. observed a change in the α coefficient of triethylamine with different humidity levels.[1] The moisture effect was later studied by Eiceman et al.[34] where the α coefficient of organophosphorus compounds changed with different levels of moisture. In 2004, an extension of this work focused on improving separation by the addition of other solvent gas modifiers to the carrier gas. Water, acetone, propanol and methylene chloride were studied and methylene chloride was found to cause 2,6-dinitrotoluene to have the biggest shift in CV, so it was used for increasing 'analytical space' for analysing a mixture of explosives (Figure 1.13). A comparison of the effect on the α function of explosive ions in pure air and in the presence of a methylene chloride demonstrates the potential for greater separation by using gas modifiers (Figure 1.14).[25]

Gas modifiers need to be introduced in to the carrier gas of a FAIMS analyser and there are two published methods for carrying out this process: a gas bubbler[35] (Figure 1.15) or liquid infusion.[64] The studies discussed in this section have utilised both of these modifier introduction techniques. The first commercial instrument with a built-in gas modifier system, the ABSciex SelexION^{TM} Technology[65], has recently been released. The investment in user-friendly gas modifier technology on a commercial system shows that gas modifiers are becoming established as routine for improving FAIMS separations.

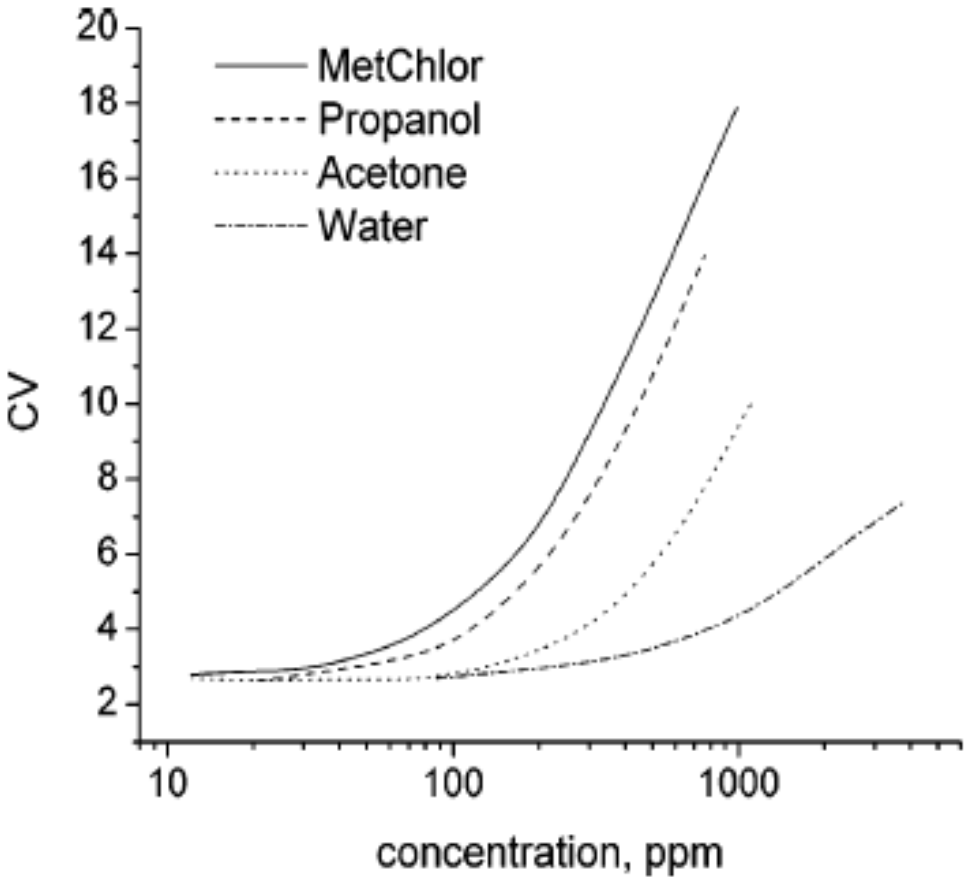

Figure 1.13 The change in CV against concentration of gas modifier for the detection of 2,6-dinitrotoluene (50 ppb) at DV (20 kV/cm) [25] [Reprinted (adapted) with permission from Eiceman, G. A.; Krylov, E. V; Krylova, N. S.; Nazarov, E. G.; Miller, R. A. Anal. Chem. 2004, 76, 4937–44. Copyright 2004 American Chemical Society]

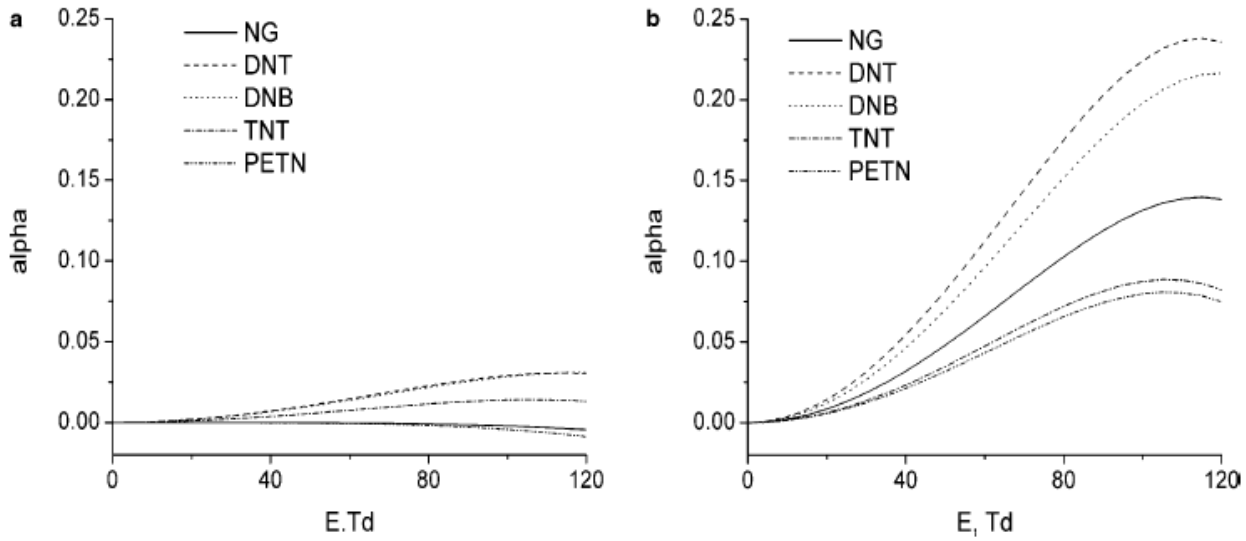

Figure 1:14 α functions of explosive ions in (a) pure air and (b) methylene chloride (1000 ppm) in air[25][Reprinted (adapted) with permission from Eiceman, G. A.; Krylov, E. V; Krylova, N. S.; Nazarov, E. G.; Miller, R. A. Anal. Chem. 2004, 76, 4937–44. Copyright 2004 American Chemical Society]

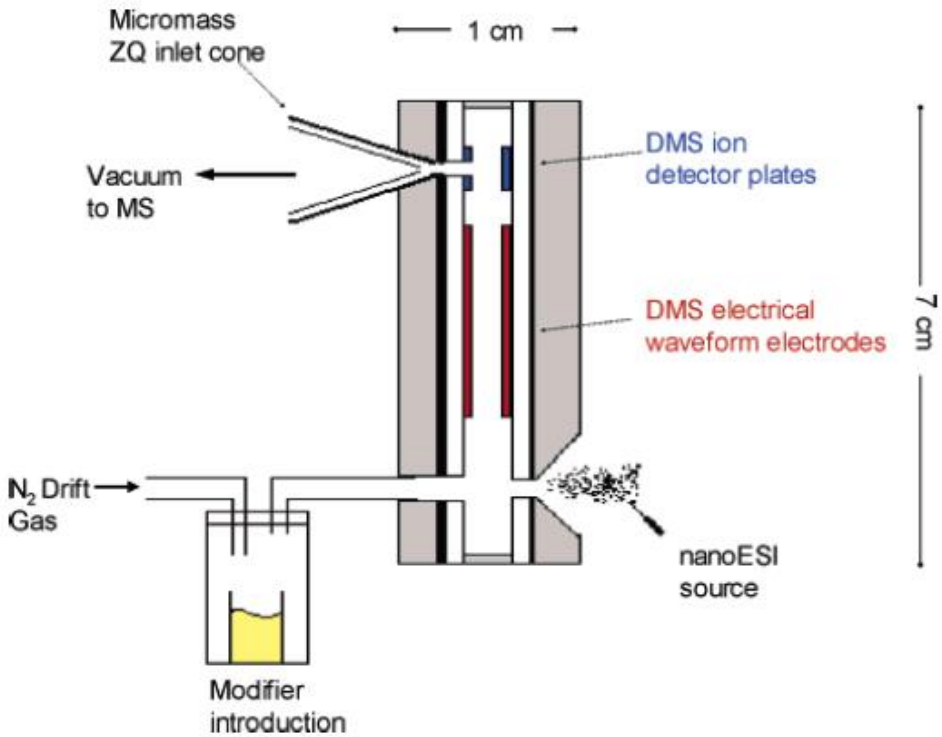

Figure 1.15 A diagram showing a gas bubbler used to introduce a gas modifier into a FAIMS-MS system[35] [Reprinted (adapted) with permission from Levin, D. S.; Miller, R. A; Nazarov, E. G.; Vouros, P. Anal. Chem. 2006, 78, 5443–52. Copyright 2006 American Chemical Society]

Gas modifiers have been shown to compete with water and other small molecules present in the nitrogen or air carrier gas, with hydrogen bonding and Van der Waals forces leading to cluster formation. This increases the CCS of the clustered ions under low field conditions and making a bigger difference between clustered and declustered/partially declustered ions. However, the behaviour of differential mobility in the presence of gas modifiers cannot be explained by ion-neutral molecule interactions alone: dimer/trimer formation; competitive clustering resulting from hydrogen bonding and electrostatic attraction; steric repulsion and conformation changes all make significant contributions.[66]

Nazarov *et al.* compared the use of nitrogen, nitrogen with 1.5 % 2-propanol and nitrogen with 44% helium for large mixture of compounds: 70 in positive ion mode and 24 in negative ion mode.[32] The effect of the different carrier gas conditions were discussed in terms of separation (selectivity) and signal intensity (sensitivity). Figure 1.16 shows the results of these experiments. When 2-propanol or helium was added to the carrier gas, only ions that maintained greater than 5% of the original signal in nitrogen were included. The addition of helium reduced the signal for all ions below a threshold of *m/z* 195 below this threshold, likely due to the increase in velocity and a less polarisable carrier gas having a larger influence on smaller ions. Modifiers can also cause loss in signal, however this is not related to the size of ions but rather the gas phase chemistry. Gas modifiers with a greater gas phase proton affinity than that of an analyte ion will be likely to suppress ions in positive ion mode. Signal loss with the addition of modifiers has been reported elsewhere.[64] The authors also observed a stabilising effect, where gas modifiers aided the transmission of ions compared to ions that were easily lost due to fragmentation or scattering at DF above 104 Td in insert gases. It was suggested that excess energy that would usually result in fragmentation is absorbed by the ion-neutral cluster bonds. Overall, the addition of 2-propanol benefited separation but in some cases a nitrogen/helium mixture separated compounds which were not resolved by 2-propanol. There is certainly a complex relationship between modifier and analyte that has to be taken in consideration when developing a FAIMS separation.

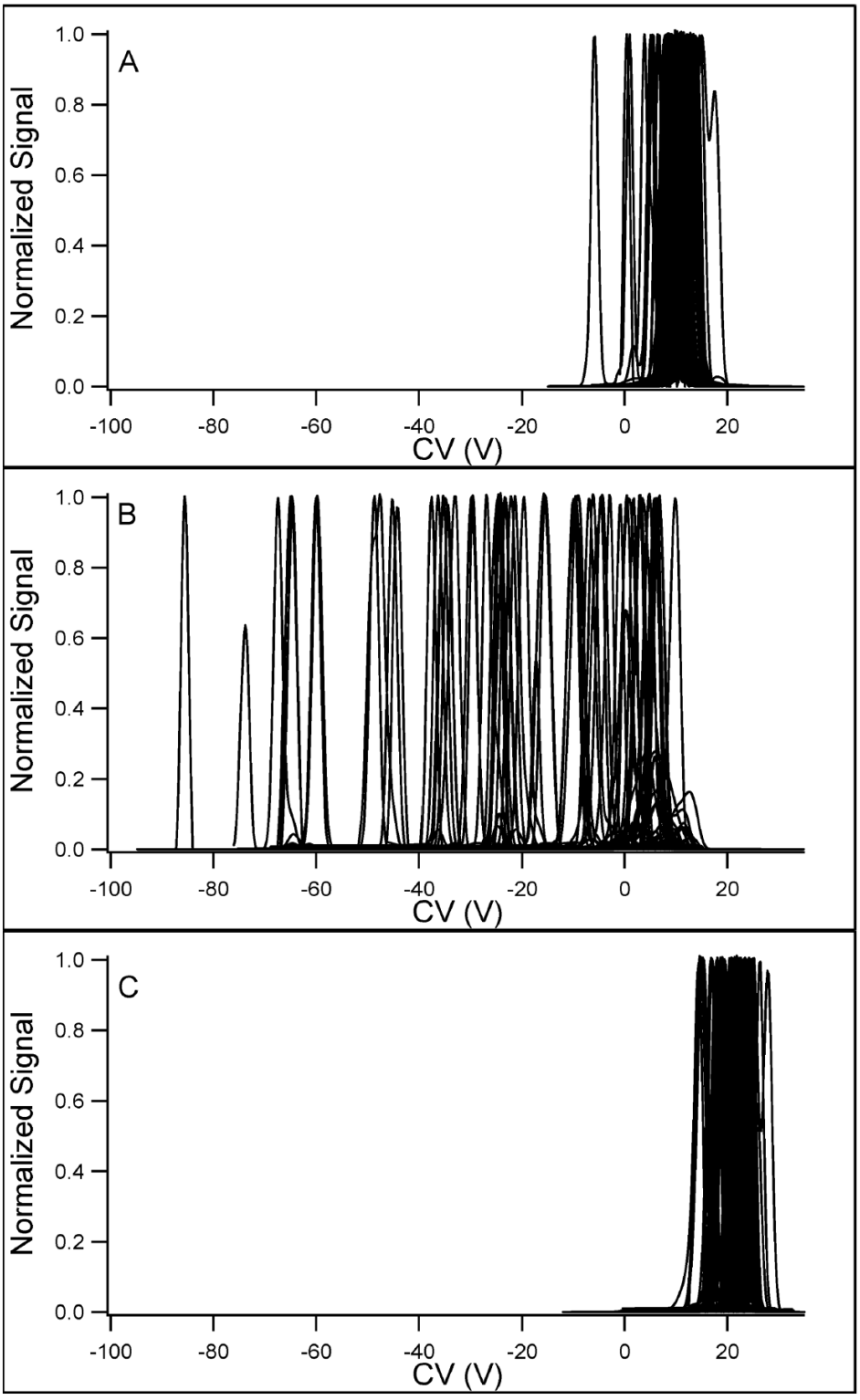

Figure 1.16 FAIMS spectra (DF 132 Td) of a 70-compounds mixture with different carrier gas conditions: (a) nitrogen; (b) nitrogen with 1.5% 2-propanol; and (c) nitrogen with 44% helium.[32] [Reprinted (adapted) with permission from Schneider, B. B.; Covey, T. R.; Coy, S. L.; Krylov, E. V; Nazarov, E. G. Anal. Chem. 2010, 82, 1867–80. Copyright 2010 American Chemical Society.]

The separation of a mixture three phthalic acid isomers has been achieved by adding water and methanol (separately) as gas modifiers (Figure 1.17) where little or no resolution was observed without modifiers.[67] Interestingly, going from dried nitrogen to nitrogen with water or methanol, the para- and ortho-phthalic acids switch in order, which suggests there is a non-covalent interaction between phthalic acid and modifier that is specific to the position of the acid groups. The addition of methanol (8000 ppm) to a FAIMS device has been used to separate oligosaccharides, maltopentaose and maltoheptaose. Lacto-N-fucopentaose I (LNFP I) and lacto-N-fucopentaose II (LNFP II) remained unresolved, successful separation by gas modifiers may be application dependent or perhaps that the correct modifier for a selective interaction is yet to be determined.[68]

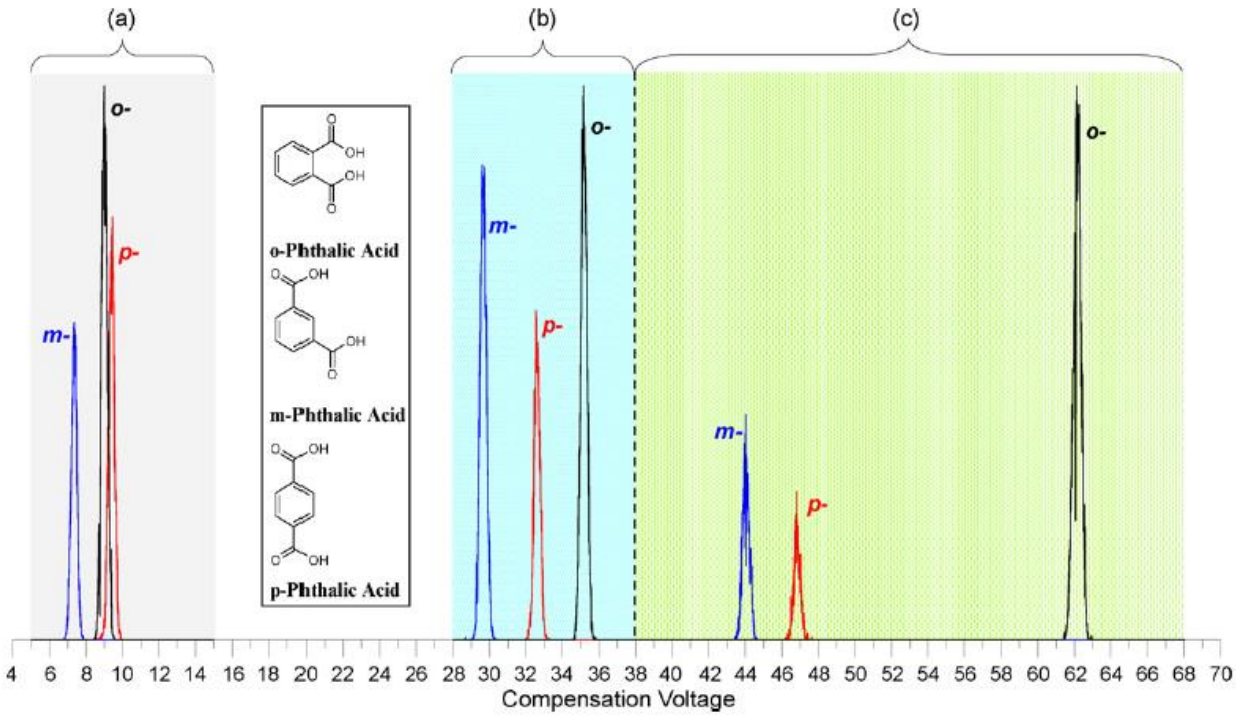

Figure 1.17 CV scans of a mixture of three phthalic acid isomers acquired with (a) dry nitrogen, (b) water vapour added to dry nitrogen(~7000 ppm), and (c) methanol vapour added to dry nitrogen (15,000 ppm)[67] [Reprinted (adapted) with permission from Rorrer III, L. C.; Yost, R. A. Int. J. Mass Spectrom. 2010, 300, 173–181. Copyright 2010 Elsevier B.V.]

An extension of this work focussed on the effect of different gas modifiers on groups of structurally similar componds.[69] 2-propanol is commonly used as a modifier of choice,[70] Figure 1.18 shows FAIMS spectra of ketamine and sulfadiazine under a number of different modifiers. Interestingly, separation is not achieved using 2-propanol (1.5 %) but the best is

observed with ethylacetate. Acetonitrile and acetone also resolve the two compounds well. In contract to 2-propanol, methanol resolves the two ions, suggesting that the presence of the alcohol group is not the only factor which determines whether a separation is achievable or not, steric hindrance around a functional group can influence clustering.

It has been suggested that by subtracting the CF value observed with one set of conditions from a CF value observed with a different set of conditions can be used to determine 'orthogonality' between the two experimental conditions.[70] Comparisons were made with three different carrier gas conditions and nitrogen; 2-propanol (1.5 %) was found to be considerably more orthogonal than hexane (1.5 %) or helium (44 %) when compared with nitrogen (data not shown). Selectivity (estimated by orthogonality) is important when developing a method because when one modifier does not give the required performance, the best chance of achieving separation will be with a modifier that behaves chemically very differently rather than one that behaves similarly. Modifiers that are highly orthogonal will interact differently and improve the chances of finding the suitable modifier for a separation. The differences in selectivity between 2-propanol, ethylacetate, acetonitrile and acetone are shown in Figure 1.19. 2-propanol was found to be highly orthogonal to ethylacetate and acetonitrile, suggesting that it would be worth investigating each of these modifiers. Figure 1.19.c shows that there is little orthogonality between acetonitrile and acetone; if one of these did not produce a separation, it might be preferable to try an alternative modifier to either of these as there will be little difference in gas phase chemistry.

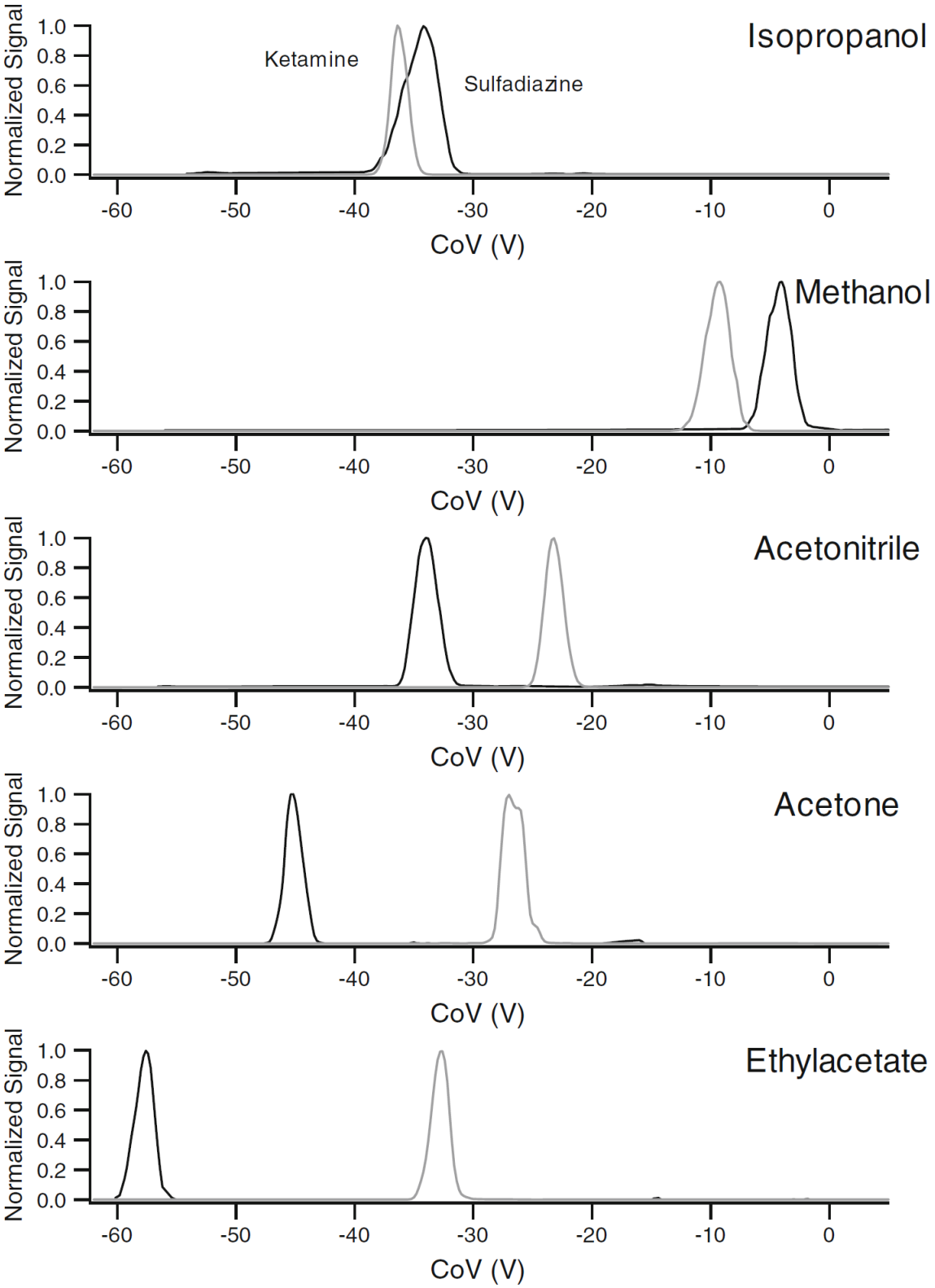

Figure 1.18 FAIMS spectra of sulfadiazine (black) and ketamine (grey) at DF 132 Td with a number of modifiers, each at 1.5 % in a nitrogen carrier gas[69] [Reprinted (adapted) with permission from Schneider, B. B.; Nazarov, E. G.; Covey, T. R. Int. J. Ion Mobil. Spectrom. 2012, 15, 141–150. Copyright 2012 Springer-Verlag]

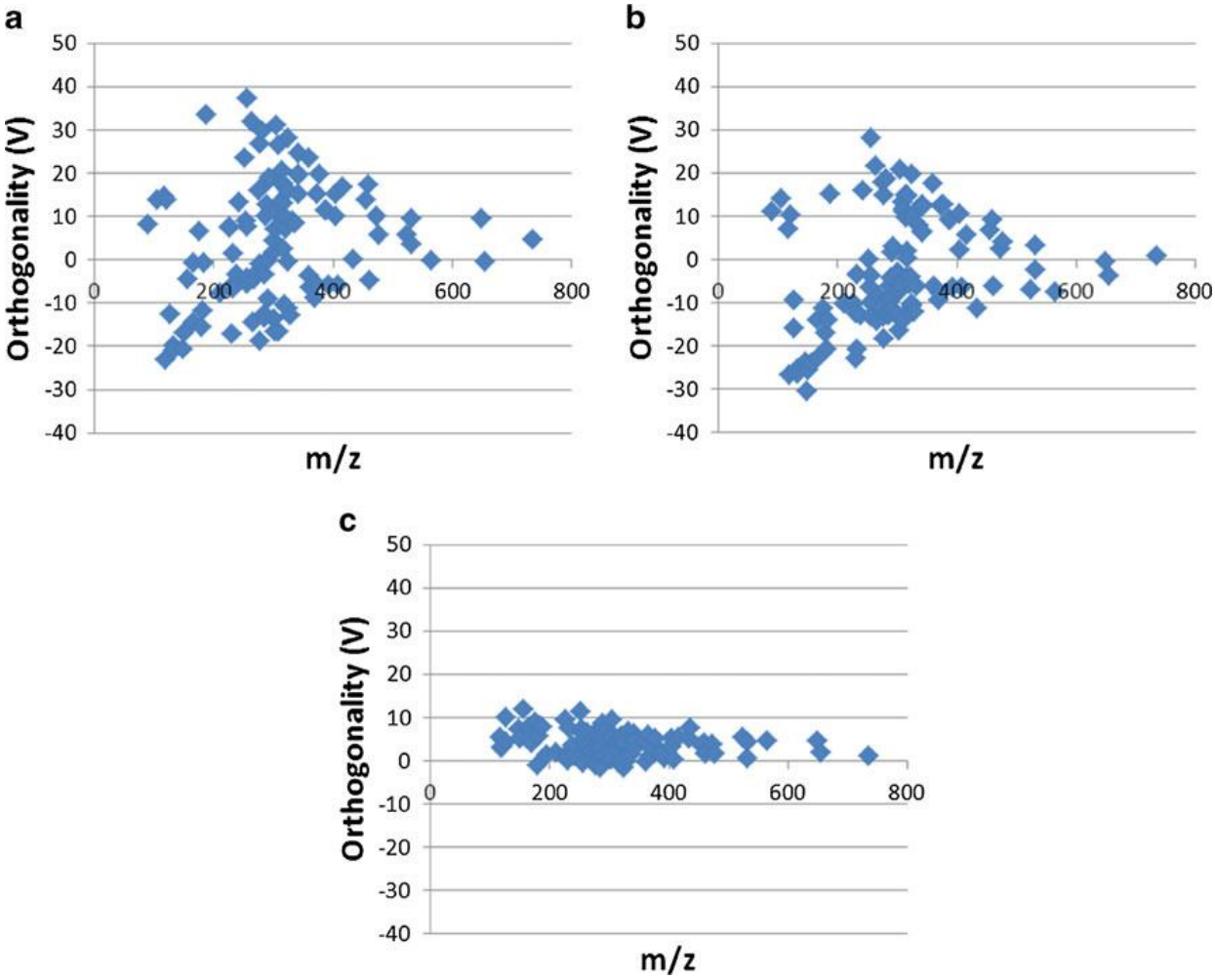

Figure 1.19 Orthogonality plotted against *m/z* for a mixture of 140 compounds at DF 132 Td between 1.5 % of the following modifiers: (a) 2-propanol and ethylacetate; (b) 2-propanol and acetonitrile; (c) acetonitrile and acetone[70] [Reprinted (adapted) with permission from Schneider, B. B.; Covey, T. R.; Nazarov, E. G. Int. J. Ion Mobil. Spectrom. 2013, 16, 207–216. Copyright 2013 Springer-Verlag Berlin Heidelberg]

Nazarov *et al.* have advanced our understanding of the use of modifiers in FAIMS systems by comparing modifiers with other carrier gas conditions and drawing comparisons between different modifiers. However, the complex nature of gas phase chemistry between different analytes and different modifiers make it hard to predict which modifier would be best for a given set of compounds (if modifiers are even needed at all).

Gas mixtures and modifiers may not always provide sufficient separation. A recent publication achieved further improvement with an ultrahigh-resolution FAIMS device. A standard cylindrical Thermo FAIMS device decreased flow rates of gas mixture from 50 – 75% He (from 2 L/min to 0.5 L/min) to increase the ion residence time (from 0.2 seconds to

0.8 seconds). Resolving power was increased up to 300 for multiply charged peptides. Phosphorylated peptides with variations in sites of phosphorylation have been resolved, previously unresolved by this system at standard flow rates. Further progression for improving resolving power of FAIMS is still of great interest.[71]

Adduct Formation

Separation of isobaric ions in the gas phase using ion mobility is desirable because of much faster analysis times, although separation cannot always be achieved under conventional conditions. For example, it has been shown that it is possible to separate disaccharide anomers, linkage isomers and positional isomers by observing disaccharide isomers adducts.[72] In positive mode, metal adducts (Na, Li, K, Rb, Cs) and ammonium were investigated; in negative mode, CV positions of chloride and acetate adducts with disaccharides (acetate, monochloroacetate, monobromoacetate, bromochloroacetate etc.) were determined (Figure 1.20). The salts added for cation/anion adduct formation in positive/negative modes improved separation when compared with conventional protonated/deprotonated ions.[72] The authors propose that separation results from dipole alignment, where disaccharides align with the high field portion of the asymmetric waveform.

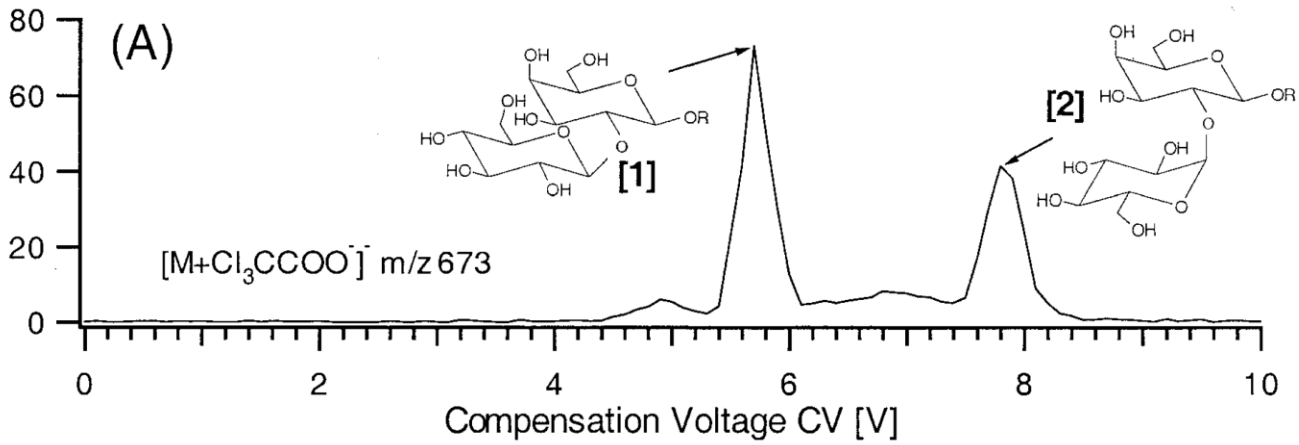

Figure 1.20 Separation of anomer disaccharides using trichloroacetate (TCA^-) to form an adduct with analytes in negative ion mode[72] [Reprinted (adapted) with permission from Gabryelski, W. J. Am. Soc. Mass Spectrom. 2003, 14, 265–277. Copyright 2003 American Society for Mass Spectrometry]

1.3 Introduction to Mass Spectrometry

Mass spectrometry is a tool that has become well established in many areas of chemical analysis, including: pharmaceutical, environmental, forensic, biological, food science and many more. The ability to measure the mass-to-charge ratio of ions makes mass spectrometry a powerful, informative method of detection. Steps in the work flow of a mass spectrometry analysis from sample introduction/separation to detection and data analysis are shown in Figure 1.21 and discussed.

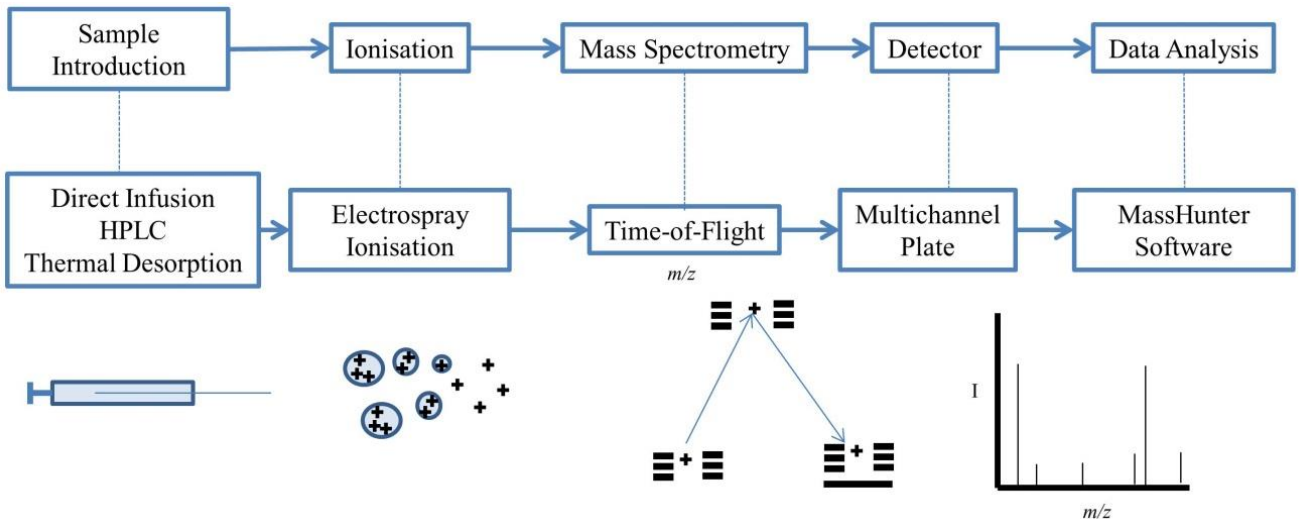

Figure 1.21 Schematic of workflow of typical mass spectrometry experiments

The first mass spectrometer (a parabola spectrograph) was reported in the literature by J.J. Thomson in 1912. Mass spectra of N_2, O_2, CO, CO_2 and $COCl_2$ were obtained and in 1913 isomers of Neon (20 and 22) were discovered.[73, 74] Mass spectrometers have continued to be developed, from early magnetic sector instruments with an electron ionisation source to a multitude of mass spectrometry systems for a broad range of applications used today. All mass spectrometers contain an inlet for sample introduction (e.g. from an HPLC), an ionisation source to produce ions, one or more mass analysers, a detector to count ions and a data processing system. The focus of this section is to describe each of the techniques used in the research presented in this thesis.

1.3.1 Sample Introduction

Samples can be introduced into a mass spectrometer using a variety of techniques. One method is to directly infuse a liquid sample into the ionisation source. The simultaneous ionisation of an entire sample is fast, but may result in suppression of analytes. In order to

avoid this, a separation method prior to ionisation is often used. High performance liquid chromatography (HPLC) is a common liquid phase separation technique where molecules are separated based on their interaction with the stationary phase of a column as they are carried through by a liquid mobile phase flow. Thermal desorption is an alternative method for the direct introduction of analytes. Using thermal extraction of an analyte by volatilisation from a less volatile matrix, interference and suppression from the matrix can be reduced. These techniques are discussed in more detail below.

1.3.2 High Performance Liquid Chromatography

The development of atmospheric pressure ionization techniques for mass spectrometry allowed the robust combination of high performance liquid chromatography with mass spectrometry (LC-MS) and is routinely used to separate complex mixtures.[75] The development of electrospray (ESI) dramatically improved the ionisation of high liquid flow rates from HPLC into a mass spectrometer.[76] Other ionisation sources that tolerate HPLC flow rates are thermospray, atmospheric pressure chemical ionisation and atmospheric pressure photoionisation.

Liquid chromatography originally utilised a hydrophilic stationary phase which has a strong affinity for hydrophilic molecules. Hydrophobic molecules will have a lower affinity for the stationary phase and elute from the column first. Elution of the hydrophilic molecules from the column is achieved by increasing the polarity of the mobile phase. This is referred to normal phase chromatography.

Reversed phase chromatography is the opposite of normal phase chromatography, in that a hydrophobic stationary phase (e.g. alkyl chains bonded to silica particles) is used to retain molecules based on hydrophobicity and the polar mobile phase elutes molecules with a higher polarity first. The elution of a compound can be controlled by the percentage of water and organic solvent (e.g. methanol, acetonitrile), where organic solvent will make hydrophobic molecules elute faster. High performance liquid chromatography (HPLC) is used to separate components of a liquid mixture. Samples are injected onto a column and carried through by a mobile phase with a flow up to 2 mL/min. A wide selection of stationary phases is available and can be selected based on their suitability depending on the analysis. Sample components are separated and commonly detected by either a UV diode-array detector or a mass spectrometer. The technique used in this thesis was reversed phase HPLC. HPLC hyphenated with mass spectrometry (LC-MS) is a powerful combination which

separates based on retention time and *m/z*. Reversed phase can be used for a wide range of analytes, it is robust and offers a range of controllable variables, including organic solvent concentration and type, pH and temperature.

1.3.3 Electrospray Ionisation and Extractive Electrospray Ionisation

All the work reported in this thesis is based on FAIMS interfaced with an electrospray ionisation (ESI) source of a mass spectrometer and the principles of ESI are discussed in this section. Before the introduction of ESI, ionisation methods like electron ionisation were fit for some analyses but not suitable for large, non-volatile and thermally labile molecules and unable to cope with high liquid flow rates. ESI was pioneered by Malcolm Dole in 1968, when his group reported the production of macroions by ESI.[77] The most significant developments of electrospray were made by John Fenn in the 1980s, for which he later received the Nobel Prize for Chemistry in 2002.[76, 78, 79] Since then, electrospray has become a well-established technique for mass spectrometers.[80]

In ESI, a flow of liquid (from LC or direct infusion) enters a capillary and flows into a needle. At the charged needle tip, a jet of droplets (electrospray) is produced. The charged needle tip removes ions carrying the opposite polarity to allow ions of the same polarity (as charged needle tip) to enrich at the tip of the Taylor cone (Figure 1.23).[81] Charged droplets produced from the Taylor cone decrease in size as solvent molecules evaporate from the droplet. The charge density on the surface increases until the droplet reaches its Rayleigh limit and becomes unstable, producing a cascade of smaller highly charged droplets.[79] The mechanism of ion formation after the small highly charged droplets have been produced is explained by two models (Figure 1.22) the charge residue model (CRM) and ion evaporation model (IEM).[80] In CRM an ion is formed after all solvent molecules have evaporated from the droplet containing a single ion. IEM involves the loss of an ion from a droplet, due to increasing coulombic repulsion at the surface of the droplet.[82] It is likely that a combination of both mechanisms occur for small molecules.

Desolvation is assisted by gas flows that are typically heated. A sheath gas/nebuliser gas creates and assists the initial spray; a counter flow desolvation gas (‘curtain’ or ‘drying’ gas) often situated at the orifice of the MS will hinder neutral solvent molecules from entering the MS and aid desolvation. Heating of the entrance to the MS either at the orifice or capillary, aids in the evaporation of neutral molecules from the ions. The capillary is positioned before

the skimmer lens, there is an electrical potential between the capillary and skimmer lens which can collisionally induce dissociation of any remaining clusters.[80]

An ESI source can produce multiply charged species and form ions of non-covalent complexes. ESI is concentration dependent making it suitable for quantitative analyses. The development of ESI was a big step for mass spectrometry because it has enabled combination of MS with the high liquid flow rate separation techniques, like HPLC; and the soft ionisation intact molecules. Competitive ionisation can occur where affinities of molecules for charged particles vary, meaning that one set of analytes may be preferably ionised over the other. It is possible for components within a sample matrix to have a higher proton affinity causing suppression of the analyte ions. In this case, extra steps may be required to remove the matrix by sample pre-treatment/chromatographic separation, although ion suppression still needs to be considered with LC-MS method development.[83] Regardless of this, the combination of HPLC and MS (LC-MS) is a well-established, routinely-used analytical technique with ESI as an important part for simple and robust ionisation.[75]

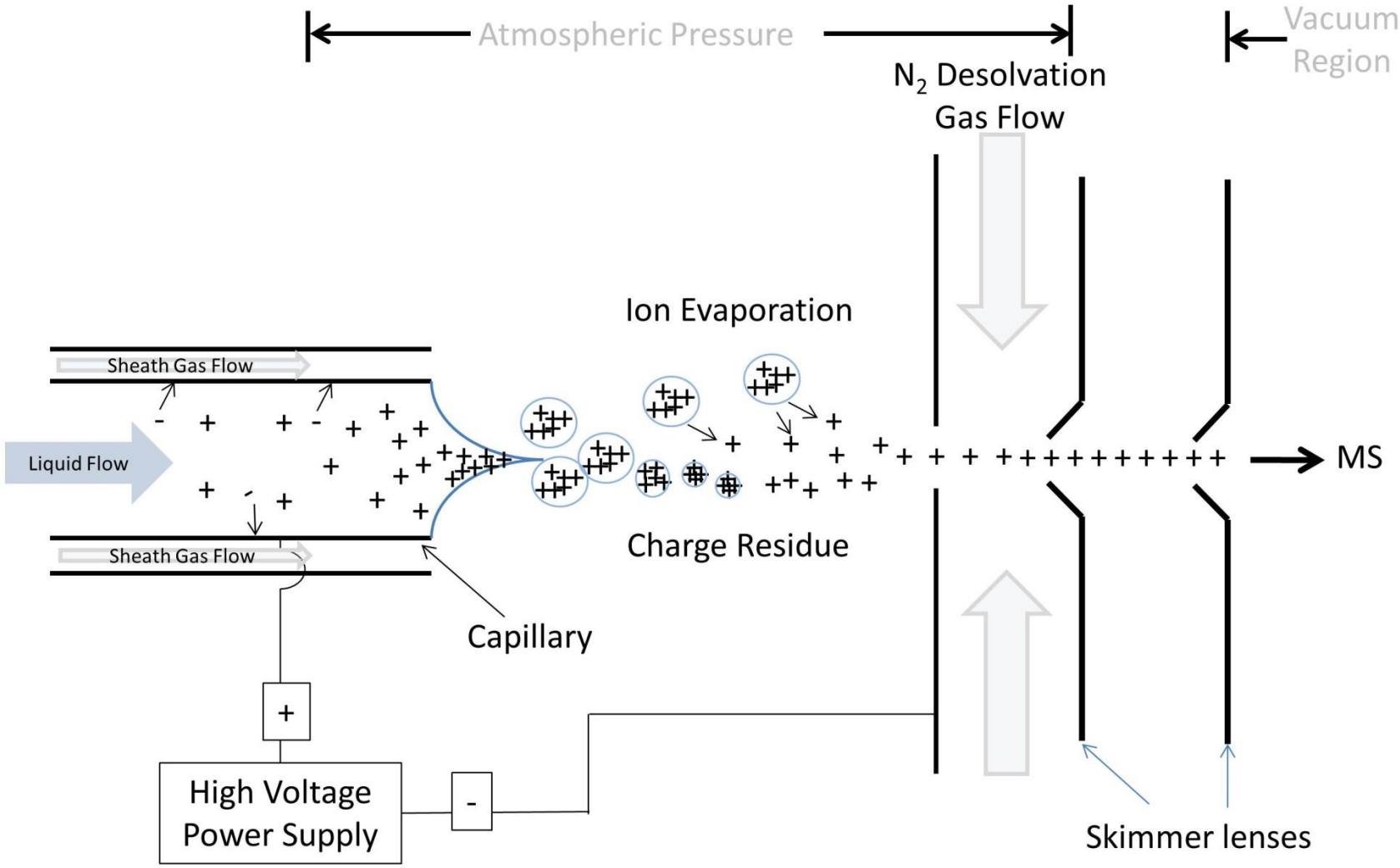

Figure 1.22 A non-specific schematic of an electrospray ionisation source, showing ion evaporation and charge residue models

Extractive electrospray ionisation (EESI) is a relatively new ambient ionisation technique developed in 2006 by Cooks et al.[84] Initially, a sample spray was directed into an electrospray plume where collisions between sample and charged microdroplets result in liquid-liquid extraction and ionization (Figure 1.23). Analytes in a sample matrix were extracted from urine, milk, and polluted water and ionised for analysis without sample preparation. The ESI spray consists of a standard ESI spraying solution (i.e. acidified water/organic solution).[85, 86] EESI is a promising ionisation method for ionising volatile organic compounds with potential to perform direct analysis of complex samples.[87]

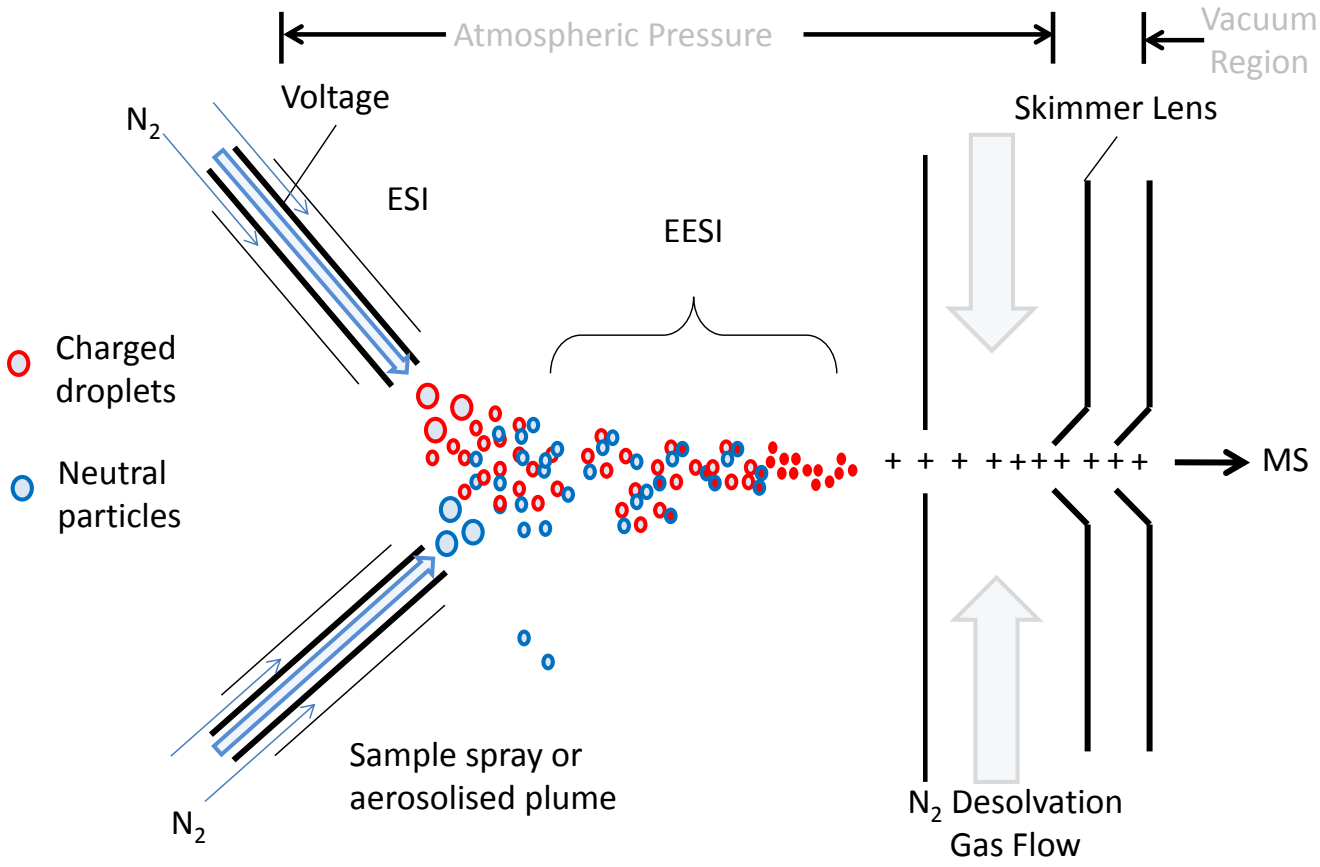

Figure 1.23 Schematic showing EESI mechanism

1.3.5 Collision induced Dissociation and In-source Collision Induced Dissociation

A number of ion fragmentation techniques are in use but only collision induced dissociation (CID) will be discussed in this section. CID is well established for ion fragment in tandem mass spectrometers. Ions colliding with neutral gas molecules become activated and the increase in internal energy, which induces fragmentation.[88] Precursor ions are selected before CID to give characteristic products for identification and structure elucidation. The precursor

ion can be mass-selected by monitoring a narrow mass window for selected ion monitoring (SIM); or precursor ion can be selected and fragmented to a product ion, this transition can be monitored for sensitive detection of a product ion by removal of background noise, selected reaction monitoring (SRM). CID is typically performed in a collision cell of a tandem mass spectrometer, usually a triple quadrupole, quadrupole time-of-flight (QTOF) or an ion trap mass spectrometer (ITMS). CID experiments are typically performed using mass-selection of a precursor ion prior to fragmentation for sensitive detection of an analyte.

Single mass analysers do not have a collision cell, but in-source CID (also known as cone voltage CID) can be used instead. In-source CID occurs in the interface of a mass spectrometer where reduced pressure causes ions to accelerate and collide with neutral molecules which induces fragmentation, allowing the acquisition of fragment data on a single mass analyser. This is less favoured than tandem MS because the inability to pre-select a precursor ion produces complex mass spectra containing a mixture of both multiple precursors and multiple product ions.

A separation stage prior to ionisation gives a degree of selectivity to in-source CID. For example, LC-MS systems have been used to separate oligopeptides before ionisation and in-source CID, giving a level of selection by fragmenting ions as they are eluted, aiding in identifying oligopeptide sequencing.[89] LC-in-source CID-MS has also been used to probe the fragmentation behaviour of peptide aldehydes and acetals[90] and organic bromine compounds.[91]

In-source CID is not only useful for single mass analysers but can be used to give tandem MS/MS an additional fragmentation step.[92] Analyses of tryptic peptides from bovine and human haemoglobin by tandem MS/MS with a Q-TOF were enhanced using in-source CID, helping to elucidate sequences.[93] Use of in-source CID can enhance but also complicate tandem MS/MS.[94] The reproducibility of in-source CID in six different instruments (four different manufacturers) was explored to improve identification when using spectral libraries.[95] A method for controlling the ions fragmented by in-source CID would reduce the complexity of fragment spectra. The following examples are all the FAIMS-in-source CID-MS techniques found in the literature.

The first reported combination of FAIMS and in-source CID showed a change in cluster distributions of leucine enkephalin ions in the CV spectrum between gentle and harsh conditions of an ESI source, where fragmentation was induced by the harsh ionisation

conditions. The authors described the in-source CID MS as comparable to using tandem MS/MS, although all further fragmentation in the paper was pursued using tandem MS/MS.[22] Eiceman *et al* described source conditions harsh enough to induce the fragmentation of chlorocarbons which complicated identification of ions separated by a Sionex planar FAIMS-MS system.[24] The FAIMS-MS analysis of 5 isobaric compounds (*m/z* 316.07559 – 316.23889), using a planar FAIMS device, used fragmentation induced by increasing the inlet cone voltage in the interface of a quadrupole MS to identify isobaric ions by matching CV peaks of fragments with CV peaks of standards.[8]

FAIMS selection prior to in-source CID MS has not yet been used to isolate ions prior to fragmentation for identification of a precursor ion by a product mass spectrum. A FAIMS-CID-MS system has the potential for gas phase pre-selection of ions prior to fragmentation giving single mass analysers the option of selective fragmentation. FAIMS interfaced with a tandem MS system (triple quadrupole, IT and QTOF) has the potential of two orthogonal methods of separation prior to fragmentation, making a highly selective system.

1.3.6 Time-of-Flight Mass Spectrometry

Mass spectrometry separates ions in a vacuum based on their mass to charge (*m/z*) ratio. There are several types of mass analysers, each with their own strengths and weaknesses, but for the purpose of describing the techniques used in this research the sole focus will be on time-of-flight mass spectrometry (TOF). The idea of TOF mass spectrometry was first proposed in 1946 by Stephens and the linear TOF design later published by Wiley and McLaren in 1955.[96] In the 1980s, significant progress was made possible with new developments in electronics to allow handling of high data flow and the use of the techniques increased because of the compatibility of TOF with laser desorption ionisation due to pulsing nature of both techniques.

In a TOF analyser, ions are accelerated by an electric field into a flight tube at vacuum. The ion velocity (v) is defined by:

$$v = \left(\frac{2zeV_s}{m}\right)^{1/2} \qquad \text{Equation 1.8}$$

Where an ion of mass (m) and total charge (ze) is accelerated by a potential (V_s). The velocity of the ion is constant after the initial acceleration, time (t) can be related to distance (L) and v:

$$t = \frac{L}{v} \qquad \text{Equation 1.9}$$

v in equation 1.8 can be substituted by equation 1.9, after rearrangement, t^2 relates to:

$$t^2 = \frac{m}{z}\left(\frac{L^2}{2eV_s}\right) \qquad \text{Equation 1.10}$$

where t^2 can be used to calculate *m/z* because the terms in brackets are constant. Ions with the same *m/z* will arrive at the detector at different times if there is an initial kinetic energy spread in the accelerated pulse of ions, which will result in peak broadening and a reduction in resolution (R):

$$\mathrm{R} = \frac{m}{\Delta m} = \frac{\mathrm{t}}{2\Delta \mathrm{t}} \qquad \text{Equation 1.11}$$

where Δm and Δt are the mass and flight time for the two adjacent peaks.

Removal of the variations in initial kinetic energy that result in peak broadening has been approached in a number of different ways. The first of these was developed by Wiley and McLaren in the 1950s,[96] a technique called Delayed Pulsed Extraction. Ions that vary in kinetic energy will reach the detector at different times; a delayed pulse increases the kinetic energy of lower kinetic energy ions correcting for the dispersion of energies of the ion population so that they arrive at the detector in a narrower time frame to improve resolution.

The first TOF mass spectrometer featured a linear flight tube, where the sample was introduced at one end and the detector situated at the opposite end (Figure 1.26.a). Samples with masses above 300 kDa can be analysed by linear TOF mass spectrometers and in principle there is no upper mass limit, although the mass resolution is low. A reflectron is another way to improve mass resolution, first proposed in 1973 by Mamyrin.[97] Ions travelling through the flight tube are reflected by a 'mirror' lens and reflected in the reverse direction towards the source. The reflectron features a series of equally-spaced ring electrodes with a resistive network of equal-value resistors. It is positioned at the end of the flight tube and the detector is placed at the opposite end, adjacent to the source (Figure 1.24.b). Ions with a high kinetic energy will travel further into the reflectron than ions with a lower kinetic energy, resulting in the high energy ions spending a longer time in the reflectron which reduces the difference between the flight times for ions to reach the detector. The reflectron focusses the energy of ions, consequently improving mass resolution. A reflectron TOF will have higher resolution than a linear TOF, but the upper mass limit and transmission are reduced due to the reflector.[97,98]

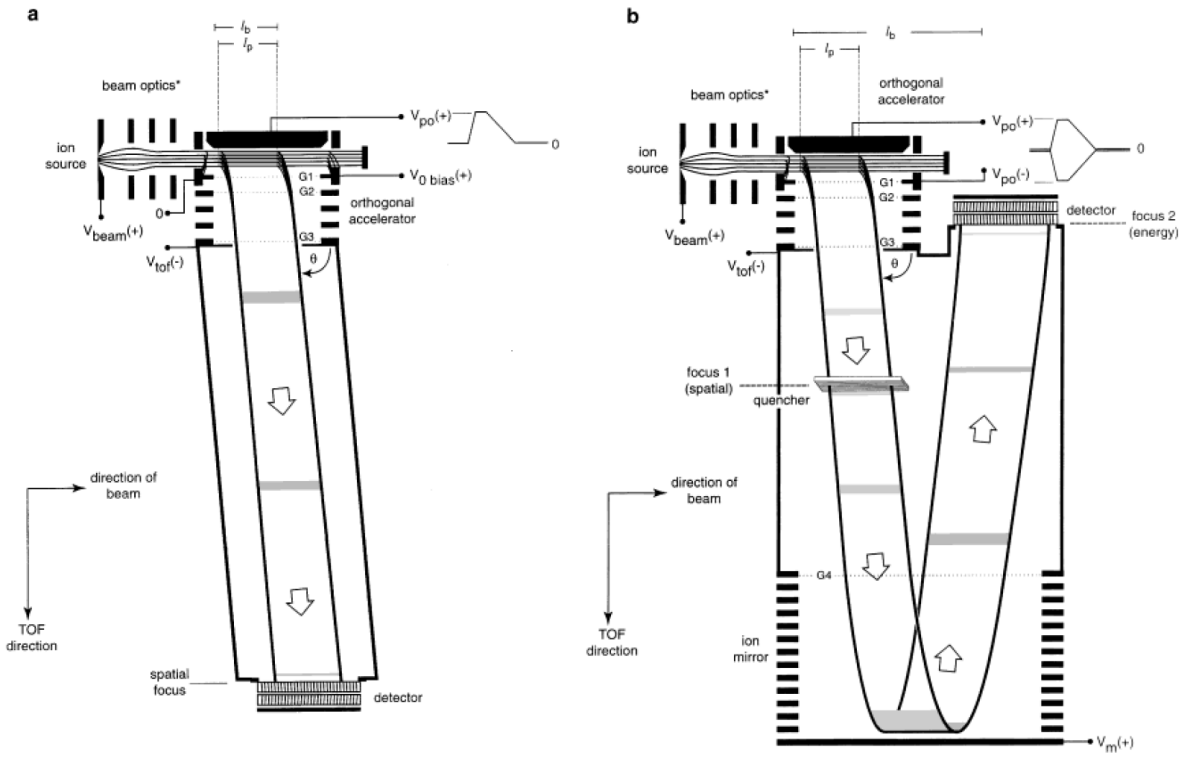

Figure 1.24 Schematic of (a) linear, and (b) reflectron time of flight mass spectrometers[99] [Reprinted (adapted) with permission from Guilhaus, M.; Selby, D.; Mlynski, V. Mass Spectrom. Rev. 2000, 19, 65–107. Copyright 2000 John Wiley & Sons, Inc.]

1.3.7 Quadrupole Mass Spectrometry

A quadrupole consists of four electrodes (two pairs) in symmetry around a *z*-axis in a vacuum with an oscillating field.[74] The opposing rod of each pair has the same polarity, but the two pairs of the four parallel rods have the opposite polarity by applying a dc voltage, U. An rf voltage, V, is superimposed over U creating a hyperbolic field. In this region, a positive ion will travel towards a negatively charged electrode, as the polarities switch between the pairs of electrodes the ion will be attracted to another electrode; this process continues as the pairs of electrodes switch in polarity and the ion takes a helical path through the quadrupole. The trajectory of an ion is related to its mass and charge (*m/z*), where an ion of a particular *m/z* will have a stable trajectory and ions with a different *m/z* will have unstable oscillations and collide with an electrode and neutralise.[100] This feature allows ions to be filtered based on mass and charge, where a low *m/z* can be selected using a low U and V and a high *m/z* using a high U and V. Ramping both U and V will produce a mass spectrum as ions with increasing *m/z* have a stable trajectory and can reach the detector. U and V can also be fixed to transmit only a selected *m/z*. Quadrupoles can be arranged in tandem, known as a triple quadrupole, where ions are analysed by mass and charge in several stages.

1.3.8 Detectors

A detector is required to record ions separated by *m/z*, changing ions into response in a mass spectrum. Electron multiplier detectors are the most widely used for mass spectrometry. They feature a system of dynodes that initially convert ions into electrons which are then amplified by the next dynode. The cascade of electrons travels down the set of dynodes; at the end, the flow of electrons supply an electrical current for detection. Another type of electron multiplier is a microchannel plate (MCP) which consists of a 3D array of detectors each of which features a single, continuous dynode. The amplifying region is a series of microchannels where the emissive surface initiates the burst of electrons from a ion. The cloud of electrons is directed onto an anode for the current to be detected. The short electron path length is only a few millimetres resulting in short electron pulse widths, making it the detector of choice for TOF MS.[74, 101]

1.4 Hyphenated Ion Mobility-Mass Spectrometry Techniques

A variety of analysis methods use mass spectrometers as the detector because of the information and selectivity offered by mass spectrometry. However, the complex nature of a chemical matrix means that not every compound can be resolved by mass spectrometry, hence the development of hyphenated ion mobility-mass spectrometry techniques (IM-MS) to add an extra stage of fast separation in the gas phase.

There are currently two widely used commercial systems based on the drift tube ion mobility spectrometers: the Waters Synapt, where a travelling wave is used to transport ions through the drift cell; and the Agilent 6560 which uses a static electric field gradient. These are important instrument for delivering added separation and the ability to measure the collisional cross sections of ions. The ion mobility drift tube is fully integrated into the mass spectrometer. However, FAIMS can be added to the inlet of a mass spectrometer with relatively minor modifications. This section will discuss the hyphenations of FAIMS with mass spectrometry and the benefits associated with differential mobility separation prior to MS detection.

1.4.1 FAIMS-MS Systems and Applications

Since the publication of Guevremont's FAIMS-MS system in 1999,[102] a number of new FAIMS-MS systems have been developed, including variations on both cylindrical and planar devices and a microscale chip-based FAIMS device. Publications or FAIMS-MS systems

have increased significantly since 1999, showing the growing interest in the combined technique.[103] Commercial FAIMS-MS interfaces include the Ionalytics/Thermo cylindrical FAIMS device, the ABSciex SelexIon planar FAIMS, the Owlstone chip-based 'multi-planar' FAIMS device.

The first interfacing of a FAIMS device with a mass spectrometer used a cylindrical FAIMS device set at a ~45˚ angle to the sampler cone/skimmer of a triple quadrupole mass spectrometer.[104, 105] Combining FAIMS with MS was shown to improve sensitivity when compared to mass spectrometry alone by reduction of chemical noise. Transmission of ions through FAIMS has a linear relationship with concentration which can help improve the linear range of a mass spectrometer at the lower end of a calibration plot by reducing noise and improving the signal-to-noise ratio.[102, 106, 107] The potential to separate isobaric ions gives information unattainable by MS alone that is significantly faster than other separation techniques used prior to MS analysis.[4]

The improvement FAIMS offers to mass spectrometry is dependent on the type of mass spectrometer it is being interfaced to. A comparison between MS, MS/MS, FAIMS-MS and FAIMS-MS/MS systems was made with trace analysis of amino acids introduced by ESI. Only when using FAIMS was it possible to separate isobaric amino acids, an advantage that enhances mass spectrometer performance where there is no unique selected reaction monitoring (MRM) transition that can distinguish fragments of the isobaric compounds. FAIMS has the ability to reduce background noise and increases the relative response of an analyte was demonstrated in a comparison of MS and MS/MS modes with and without FAIMS, made by observing the limits of detection obtained for 20 amino acids (Figure 1.25).[42] Sufficient FAIMS resolution and the best detection limits were seen with FAIMS-MS, making it the preferred method for amino acid analysis in a hydrolysed yeast matrix. An advantage of FAIMS-MS over MS/MS is that the former can enable separation and quantification of isobaric ions but little advantage was seen when considering limits of detection,[42] suggesting that FAIMS might have a greater benefit on standalone MS systems.

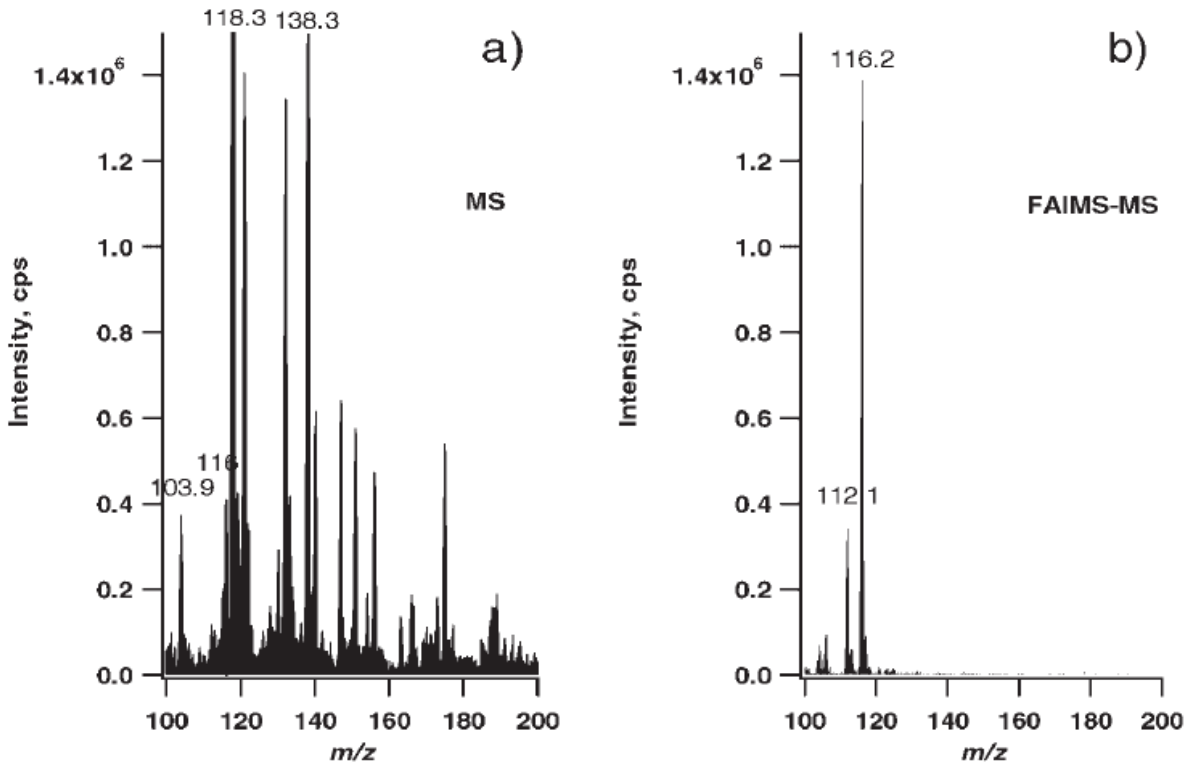

Figure 1.25 Protonated proline (*m/z* 116) in a hydrolysed yeast sample by (a) ESI-MS; and (B) ESI-FAIMS-MS (DV = 4000V, CV = -15V and N_2 flow at 2.5 $l.min^{-1}$) [42] [Reprinted (adapted) with permission from McCooeye, M.; Mester, Z. Rapid Commun. Mass Spectrom. 2006, 20, 1801–8. Copyright 2006 Crown in the right of Canada. Published by John Wiley & Sons, Ltd.]

An ESI-FAIMS-MS (triple quadrupole) method provided sufficient separation and sensitivity with far higher throughput to replace current LC methods in the analysis of ephedrine, pseudo ephedrine and their metabolites in a health tablet matrix.[5] Detection limits were in the range of 0.1 – 3 ng/ml with a linear range over 2 orders of magnitude. The diastereoisomers were resolved for the first time by FAIMS and quantitation required no clean-up step prior to analysis.5 Another technique achieved sufficient sensitivity and selectivity by combining SPME with ESI-FAIMS-MS to enable the removal of a chromatography step for the quantitative determination of amphetamine, methamphetamine and their methylenedioxy derivatives in urine. SPME was needed to remove the high salt content to improve the electrospray conditions.[6] The cylindrical FAIMS device gave significant improvements in S:N ratio and analysis times of the compounds in urine (Figure 1.26).

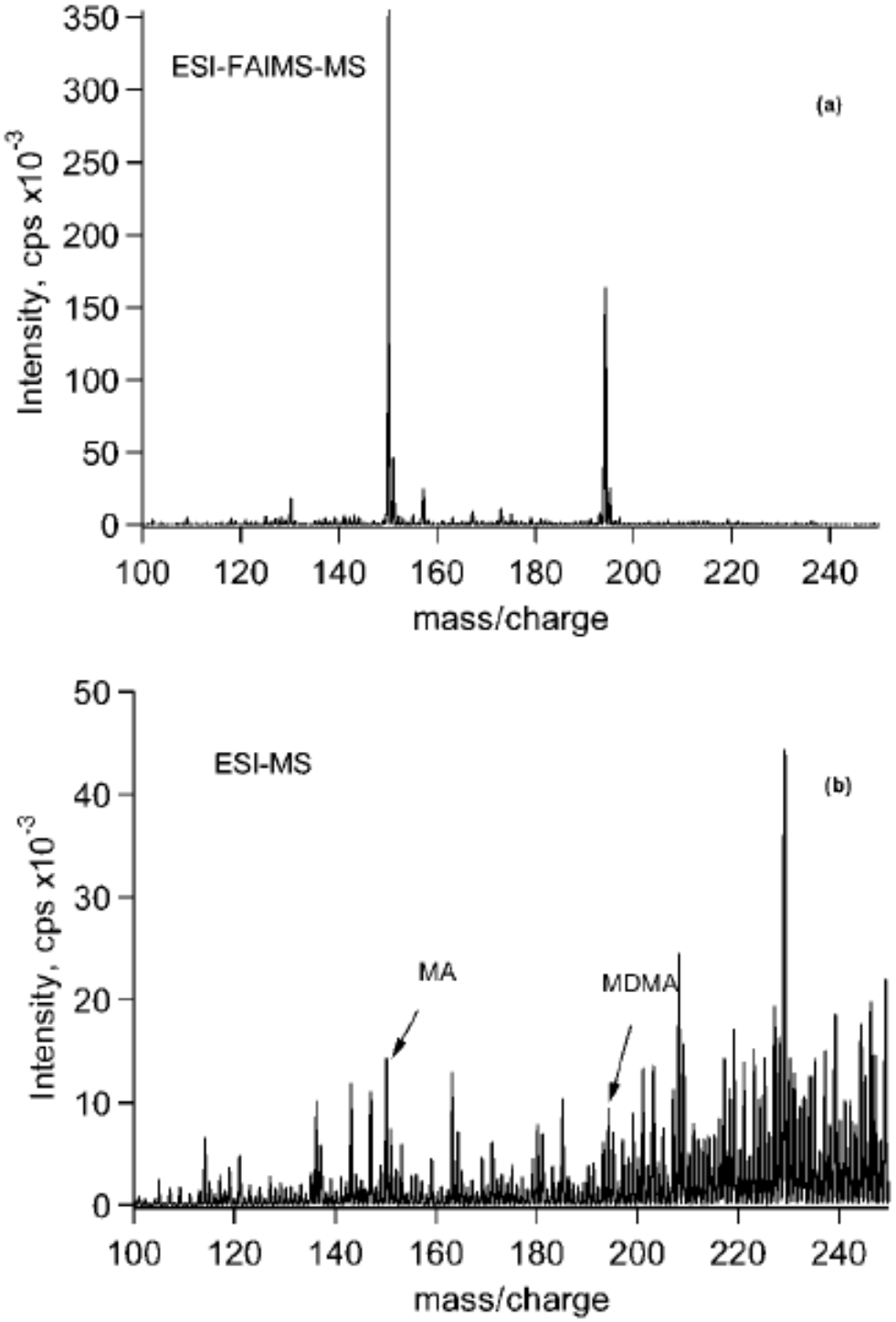

Figure 1.26 MS of a desorbed SPME sample with methamphetamine (MA) and 3,4-methylene-dioxymethamphetamine (MDMA) being transmitted (a) with FAIMS and (b) without FAIMS[6] [Reprinted (adapted) with permission from McCooeye, M. A.; Mester, Z.; Ells, B.; Barnett, D. A.; Purves, R. W.; Guevremont, R. Anal. Chem. 2002, 74, 3071–5. Copyright 2002 American Chemical Society]

A cylindrical FAIMS-MS system has made the removal of sample preparation and chromatographic separation possible and provided good agreement in terms of accuracy and precision with the routine GC-MS method for naphthenic acids analysis.[108] Also, a comparison between using ESI-FAIMS-quadrupole, ESI-FAIMS-QTOF and nanoESI-QTOF was carried out. Similar *m/z* and CV distributions were observed when using ESI-FAIMS-Q and ESI-FAIMS-QTOF, but the *m/z* distribution was significantly different without the FAIMS in system. The FAIMS-QTOF dissociated more of the fragile ions than with FAIMS-Q; however, the FAIMS-QTOF provided high mass resolution, quick detection speed, accurate mass and tandem mass spectrometry making it the preferred MS technique. Determining the elemental composition of NAs and fragments required less effort than the sample preparation steps required when using GC-MS. This was not possible with the single quadrupole where neither elemental composition nor structural detail could be obtained.[108] Gabryelski and Froese removed the sample preparation step in the analysis of tap water for haloacetic acids (HAA) by using ESI-FAIMS-MS (cylindrical); this was compared with current GC and GC-MS techniques.[109] The limits of detection were explored in a number of matrices, including tap water, urine and oil, and shown to be sufficient for routine analyses without pre-concentration.[110]

Guevremont *et al* have reported the separation of peptides into 'charge state families' and that simplifying interpretation of mass spectra was shown for a peptide mixture analysed using ESI sample introduction with cylindrical FAIMS and triple quadrupole MS.[111,112] The CV for a peptide mixture was plotted against *m/z* (Figure 1.27) showing no correlation between the two techniques. Good orthogonal separation shows the importance of FAIMS separation prior to mass analysis.[112]

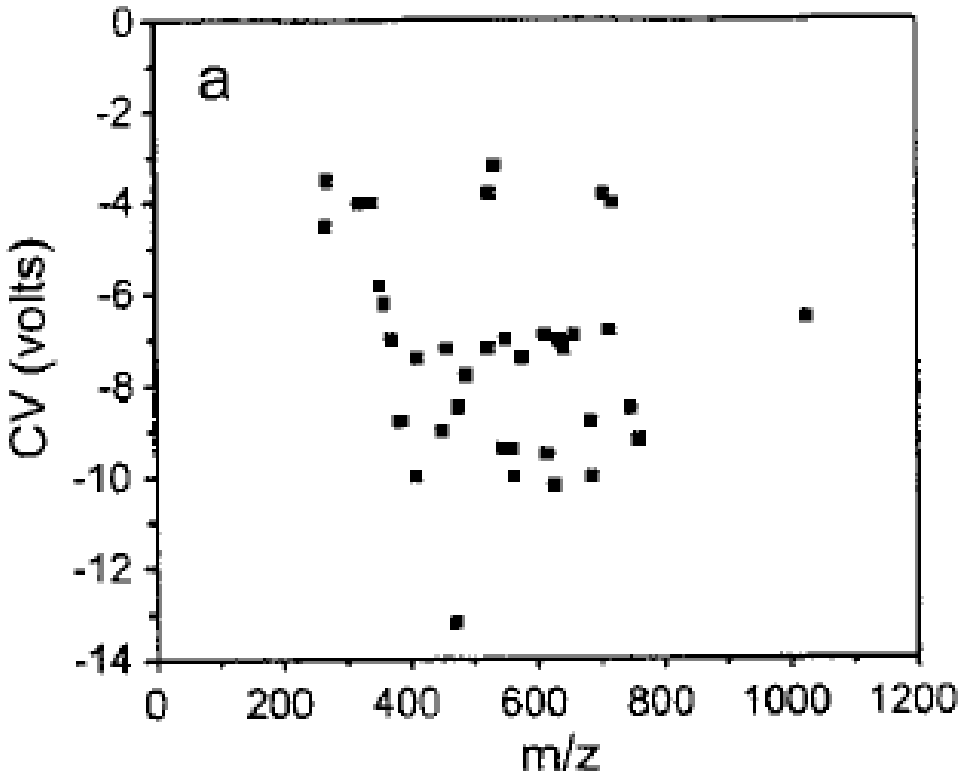

Figure 1.27 Separation of peptide mixture by FAIMS prior to MS[112] [Reprinted (adapted) with permission from Guevremont, R.; Barnett, D. A.; Purves, R. W.; Vandermey, J. Anal. Chem. 2000, 72, 4577–84. Copyright 2000 American Chemical Society]

A cylindrical FAIMS was combined with electron transfer dissociation (ETD) mass spectrometry for analysis of isobaric phosphopeptides with identical amino acid sequences but different sites of phosphorylation to aid in the identification of the location of the phosphorylation site. Partial separation was achieved which provided identification of the species in a mixture.[113]

NanoESI-FAIMS/IMS/MS (Q-TOF) giving a 2-dimensional ion mobility separation prior to MS was investigated for the analysis of a mixture of 11 common proteins and 19 typical peptides and the degree of orthogonal separation between FAIMS and drift tube IMS explored. Peptides with a +1 charge were found to have lower mobility and CV value than those with +2 or higher; despite this, the two techniques are different enough to justify interfacing them in tandem prior to MS. From a point in the CV spectrum, an IMS scan comprised of multiple MS scans gave 3 different gas-phase separation techniques.[114]

The addition of a nanoESI to FAIMS-MS was compared with a routine technique (LC-MS/MS) in drug discovery. The authors aimed to show the ability of nanoESI-FAIMS-MS to separate metabolite interferences and remove the chromatographic step to dramatically reduce run times. A liquid flow rate of 30 nL/min gave the optimum balance for shortening sample time and reducing ion suppression. LODs and LOQs were in the ng/mL range with a linear dynamic range of 50 – 10 000 ng/mL was observed, an order of magnitude greater than the standard LC-MS method. Concentrations determined by the two techniques were in agreement showing nanoESI-FAIMS-MS to be a faster alternative, although the exact improvements in run time were not detailed.[7]

An ultraFAIMS-MS system was used to isolate the singly protonated ions from a tryptic digest of α-1-acid-glycoprotein (AAG), giving MS similar to a MALDI-MS system (Figure 1.28). This greatly simplifies the data obtained from ESI which yields ions with single and multiple charge states, making protein identification simpler. A doubly charged peptide (*m/z* 877) was isolated with the FAIMS prior to fragmentation by the ion-trap MS. This reduced the complexity of the fragmentation spectrum and gave a 10-fold improvement in the signal to noise ratio. The fragmentation pattern was used to identify the protein from a Mascot database search.[3]

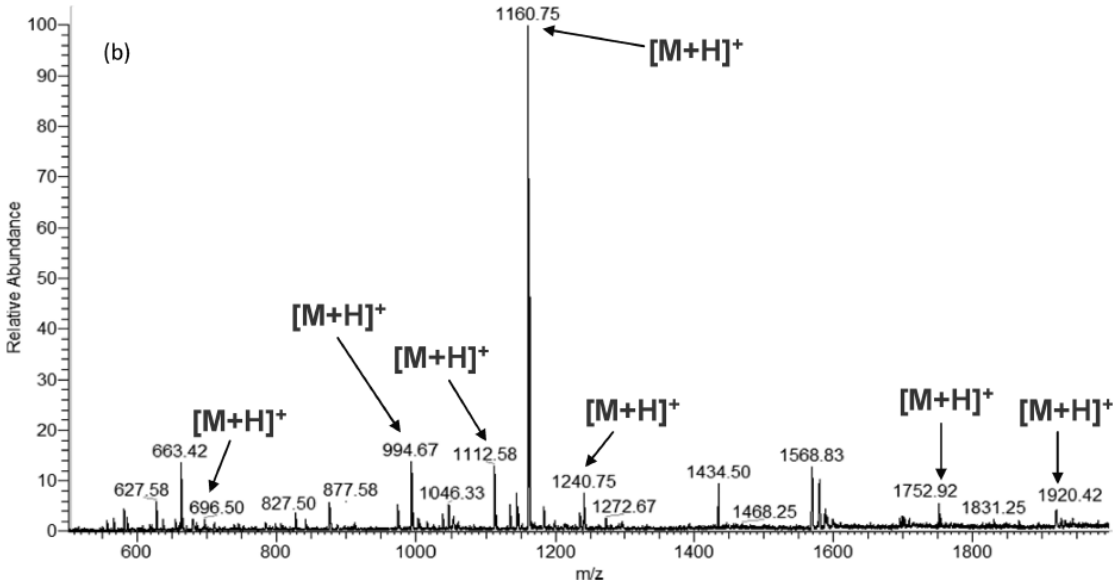

Figure 1.28 FAIMS-selected singly protonated tryptic digested peptides from AAG[3] [Reprinted (adapted) with permission from Brown, L. J.; Toutoungi, D. E.; Devenport, N. A.; Reynolds, J. C.; Kaur-Atwal, G.; Boyle, P.; Creaser, C. S. Anal. Chem. 2010, 82, 9827–34. Copyright 2010 American Chemical Society]

1.4.2 LC-FAIMS-MS

The previous section discusses removal of chromatography and sample preparation steps but FAIMS can be used to compliment chromatography-based separation like HPLC. FAIMS has been combined with other separation methods but the focus of this section will be on HPLC, the technique used in this thesis. A brief summary of FAIMS combined with LC is shown below.

Liquid-liquid extracted urine samples were analysed with LC-FAIMS-MS/MS to detect anabolic androgenic steroids in sports drug testing, enhanced by a 4 L/min gas mixture of N_2/He (50:50). The reduction of S/N ratio and interference reduced ambiguity in the data. Metandienone is a long-term metabolite that is only observable (when satisfying the criteria for positive finding) by LC-FAIMS-MS/MS where the LC-MS/MS method failed to provide a peak above LOD. Helium usage was reduced by only using it upon analyte elution. Positive tests can be produced with longer time periods after the drug abuse has occurred when enhancing LC-MS/MS with FAIMS.[58]

The addition of FAIMS separation to LC-MS/MS analysis of prostanoids gave reduced background noise and separated the isobaric prostaglandin ions: PGE_2 and PGD_2. Separation of interconverting anomers, thromboxane B_2, was also achieved. The prostanoids exist at low concentrations in complex tissue matrices which require a reduction in background noise for a reliable measurement of inflammation. The method was developed as an alternative to time-consuming, complex chromatographic runs. Successful quantitation of the prostanoids was achieved with the addition of FAIMS.[59]

An investigation into the benefits offered by adding cylindrical FAIMS to LC-MS/MS for addressing the challenge of peptide isomers in proteomics by using a CV stepping method as gas-phase fractionation.[115] A 2-fold increase in the number of peptide assignments was observed with FAIMS compared to LC-MS/MS.

1.5 Overview of Thesis

The introduction to this thesis has discussed the principles of the differential mobility behaviour of ions in the gas phase and the application of technology for chemical detection in large number of fields. FAIMS is not only used to separate isobaric ions, but also offers chemical noise reduction and simplification of complex data. It is a quantitative technique that offers lower detection limits and faster run times when hyphenated with other existing

systems. The addition of FAIMS to existing analytical systems has already shown promise in improving analytical performance in many applications.

A miniaturised chip-based FAIMS device has been combined with a TOF mass spectrometer using relatively minor modifications to the electrospray source. The thesis presented here investigates the performance of the prototype FAIMS-MS system and evaluate the application of the technique for small molecule analysis.

1.6 Chapter One References

(1) Buryakov, I. A.; Krylov, E. V; Nazarov, E. G.; Kh, U. *Int. J. Mass Spectrom.* **1993**, *128*, 143–148.

(2) Guevremont, R. *Can. J. Anal. Sci. Spectrosc.* **2004**, *49*, 105–113.

(3) Brown, L. J.; Toutoungi, D. E.; Devenport, N. A.; Reynolds, J. C.; Kaur-Atwal, G.; Boyle, P.; Creaser, C. S. *Anal. Chem.* **2010**, *82*, 9827–34.

(4) Guevremont, R. *J. Chromatogr. A.* **2004**, *1058*, 3–19.

(5) McCooeye, M.; Ding, L.; Gardner, G. J.; Fraser, C. A.; Lam, J.; Sturgeon, R. E.; Mester, Z. *Anal. Chem.* **2003**, *75*, 2538–42.

(6) McCooeye, M. A.; Mester, Z.; Ells, B.; Barnett, D. A.; Purves, R. W.; Guevremont, R. *Anal. Chem.* **2002**, *74*, 3071–5.

(7) Hatsis, P.; Valaskovic, G.; Wu, J.-T. *Rapid Commun. Mass Spectrom.* **2009**, *23*, 3736–42.

(8) Coy, S. L.; Krylov, E. V; Schneider, B. B.; Covey, T. R.; Brenner, D. J.; Tyburski, J. B.; Patterson, A. D.; Krausz, K. W.; Fornace, A. J.; Nazarov, E. G. *Int. J. Mass Spectrom.* **2010**, *291*, 108–117.

(9) Barnett, D. A.; Purves, R. W.; Ells, B.; Guevremont, R. *J. Mass Spectrom.* **2000**, *35*, 976–80.

(10) Robinson, E. W.; Shvartsburg, A. A.; Tang, K.; Smith, R. D. *Anal. Chem.* **2008**, *80*, 7508–15.

(11) Creaser, C. S.; Griffiths, J. R.; Bramwell, C. J.; Noreen, S.; Hill, C. A.; Thomas, C. L. P. *Analyst*. **2004**, *129*, 984.

(12) Eiceman, G. A.; Karpas, Z.; Hill, H. H. *Ion Mobility Spectrometry*, Group, T. and F., Ed.; Third.; CRC Press: Boca Raton; 2013.

(13) Revercomb, H. E.; Mason, E. A. *Anal. Chem.* **1975**, *47*, 970–983.

(14) Kanu, A. B.; Dwivedi, P.; Tam, M.; Matz, L.; Hill, H. H. *J. Mass Spectrom.* **2008**, *43*, 1–22.

(15) Kolakowski, B. M.; Mester, Z. *Analyst*. **2007**, *132*, 842–64.

(16) Shvartsburg, A. A.; Smith, R. D.; Wilks, A.; Koehl, A.; Ruiz-Alonso, D.; Boyle, B. *Anal. Chem.* **2009**, *81*, 6489–95.

(17) Elistratov, A. A.; Shibkov, S. V; Nikolaev, E. N. *Eur. J. Mass Spectrom. (Chichester, Eng).* **2006**, *12*, 143–51.

(18) Schneider, B. B.; Covey, T. R.; Coy, S. L.; Krylov, E. V; Nazarov, E. G. *Int. J. Mass Spectrom.* **2010**, *291*, 108–117.

(19) Shvartsburg, A. A.; Tang, K.; Smith, R. D. *J. Am. Soc. Mass Spectrom.* **2005**, *16*, 1447–55.

(20) Shvartsburg, A. A.; Smith, R. D. *J. Am. Soc. Mass Spectrom.* **2008**, *19*, 1286–95.

(21) Tang, F.; Li, H.; Wang, X.; Yang, J.; Zhang, L.; Wang, F. *Sci. China Technol. Sci.* **2011**, *54*, 1407–1414.

(22) Guevremont, R.; Purves, R. W. *J. Am. Soc. Mass Spectrom.* **1999**, *10*, 492–501.

(23) Ruotolo, B. T.; McLean, J. A.; Gillig, K. J.; Russell, D. H. *J. Am. Soc. Mass Spectrom.* **2005**, *16*, 158–65.

(24) Eiceman, G. A.; Krylov, E. V; Tadjikov, B.; Ewing, R. G.; Nazarov, E. G.; Miller, R. A. *Analyst*. **2004**, *129*, 297–304.

(25) Eiceman, G. A.; Krylov, E. V; Krylova, N. S.; Nazarov, E. G.; Miller, R. A. *Anal. Chem.* **2004**, *76*, 4937–44.

(26) Krylov, E.; Nazarov, E. G.; Miller, R. A.; Tadjikov, B.; Eiceman, G. A. *J. Phys. Chem. A*. **2002**, *106*, 5437–44.

(27) Aksenov, A. A; Kapron, J.; Davis, C. E. *J. Am. Soc. Mass Spectrom.* **2012**, *23*, 1794–8.

(28) Spangler, G. E. *Int. J. Ion Mobil. Spectrom.* **2012**, *15*, 109–121.

(29) Xu, J.; Liu, Y. *Int. J. Ion Mobil. Spectrom.* **2009**, *12*, 149–156.

(30) Xu, J.; Han, F.; Li, H. *Int. J. Ion Mobil. Spectrom.* **2011**, *15*, 91–98.

(31) Krylov, E.; Coy, S.; Nazarov, E. *Int. J. Mass Spectrom.* **2009**, *279*, 119–125.

(32) Schneider, B. B.; Covey, T. R.; Coy, S. L.; Krylov, E. V; Nazarov, E. G. *Anal. Chem.* **2010**, *82*, 1867–80.

(33) Nazarov, E. G.; Coy, S. L.; Krylov, E. V; Miller, R. A.; Eiceman, G. A. *Anal. Chem.* **2006**, *78*, 7697–706.

(34) Krylova, N.; Krylov, E.; Eiceman, G. A.; Stone, J. A. *J. Phys. Chem. A*. **2003**, *107*, 3648–54.

(35) Levin, D. S.; Miller, R. A; Nazarov, E. G.; Vouros, P. *Anal. Chem.* **2006**, *78*, 5443–52.

(36) Shvartsburg, A. A.; Li, F.; Tang, K.; Smith, R. D. *Anal. Chem.* **2007**, *79*, 1523–8.

(37) Shvartsburg, A. A.; Bryskiewicz, T.; Purves, R. W.; Tang, K.; Guevremont, R.; Smith, R. D. *J. Phys. Chem. B*. **2006**, *110*, 21966–80.

(38) Shvartsburg, A. A.; Smith, R. D. *Anal. Chem.* **2012**, *84*, 7297–300.

(39) Kapron, J. T.; Jemal, M.; Duncan, G.; Kolakowski, B.; Purves, R. *Rapid Commun. Mass Spectrom.* **2005**, *19*, 1979–1983.

(40) Lu, Y.; Harrington, P. B. *Anal. Chem.* **2007**, *79*, 6752–9.

(41) Krylov, E. *Int. J. Mass Spectrom.* **2003**, *225*, 39–51.

(42) McCooeye, M.; Mester, Z. *Rapid Commun. Mass Spectrom.* **2006**, *20*, 1801–8.

(43) Purves, R. W.; Barnett, D. A.; Guevremont, R. *Int. J. Mass Spectrom.* **2000**, *197*, 163–177.

(44) Creese, A. J.; Shimwell, N. J.; Larkins, K. P. B.; Heath, J. K.; Cooper, H. J. *J. Am. Soc. Mass Spectrom.* **2013**, *24*, 431–43.

(45) Shvartsburg, A. A.; Li, F.; Tang, K.; Smith, R. D. *Anal. Chem.* **2006**, *78*, 3706–14.

(46) Mabrouki, R.; Kelly, R. T.; Prior, D. C.; Shvartsburg, A. A.; Tang, K.; Smith, R. D. *J. Am. Soc. Mass Spectrom.* **2009**, *20*, 1768–74.

(47) Purves, R. W. *Anal. Bioanal. Chem.* **2013**, *405*, 35–42.

(48) Staubs, A. E.; Matyjaszczyk, M. S. In *2008 IEEE Conference on Technologies for Homeland Security*; IEEE, 2008; pp. 199–204.

(49) Shvartsburg, A. A.; Tang, K.; Smith, R. D.; Holden, M.; Rush, M.; Thompson, A.; Toutoungi, D. *Anal. Chem.* **2009**, *81*, 8048–53.

(50) Wilks, A.; Hart, M.; Koehl, A.; Somerville, J.; Boyle, B.; Ruiz-Alonso, D. *Int. J. Ion Mobil. Spectrom.* **2012**, *15*, 199–222.

(51) Krylov, E. *Int. J. Ion Mobil. Spectrom.* **2012**, *15*, 85–90.

(52) Barnett, D. A.; Ouellette, R. J. *Rapid Commun. Mass Spectrom.* **2011**, *25*, 1959–71.

(53) Karpas, Z.; Berant, Z.; Shahal, O. *J. Am. Chem. Soc.* **1989**, *111*, 6015–6018.

(54) Krylov, E. V; Coy, S. L.; Vandermey, J.; Schneider, B. B.; Covey, T. R.; Nazarov, E. G. *Rev. Sci. Instrum.* **2010**, *81*, 024101.

(55) Shvartsburg, A. A.; Smith, R. D. *Anal. Chem.* **2011**, *83*, 9159–66.

(56) Karpas, Z.; Berant, Z. *J. Phys. Chem.* **1989**, *93*, 3021–3025.

(57) Shvartsburg, A. A.; Tang, K.; Smith, R. D. *Anal. Chem.* **2004**, *76*, 7366–74.

(58) Guddat, S.; Thevis, M.; Kapron, J.; Thomas, A.; Schänzer, W. *Drug Test. Anal.* **2009**, *1*, 545–53.

(59) Kapron, J.; Wu, J.; Mauriala, T.; Clark, P.; Purves, R. W.; Bateman, K. P. *Rapid Commun. Mass Spectrom.* **2006**, *20*, 1504–10.

(60) Shvartsburg, A. A; Creese, A. J.; Smith, R. D.; Cooper, H. J. *Anal. Chem.* **2011**, *83*, 6918–23.

(61) Creese, A. J.; Cooper, H. J. *Anal. Chem.* **2012**, *84*, 2597–601.

(62) Cui, M.; Ding, L.; Mester, Z. *Anal. Chem.* **2003**, *75*, 5847–53.

(63) Shvartsburg, A. A.; Smith, R. D. *Anal. Chem.* **2013**, *85*, 10–3.

(64) Blagojevic, V.; Chramow, A.; Schneider, B. B.; Covey, T. R.; Bohme, D. K. *Anal. Chem.* **2011**, *83*, 3470–6.

(65) Leblanc, Y.; Caraiman, D.; Aiello, M.; Ghobarah, H. *AB Sciex Technol.* **2011**, 1–5.

(66) Levin, D. S.; Vouros, P.; Miller, R. A; Nazarov, E. G.; Morris, J. C. *Anal. Chem.* **2006**, *78*, 96–106.

(67) Rorrer III, L. C.; Yost, R. A. *Int. J. Mass Spectrom.* **2010**, *300*, 173–181.

(68) Levin, D. S.; Vouros, P.; Miller, R. A.; Nazarov, E. G. *J. Am. Soc. Mass Spectrom.* **2007**, *18*, 502–11.

(69) Schneider, B. B.; Nazarov, E. G.; Covey, T. R. *Int. J. Ion Mobil. Spectrom.* **2012**, *15*, 141–150.

(70) Schneider, B. B.; Covey, T. R.; Nazarov, E. G. *Int. J. Ion Mobil. Spectrom.* **2013**, *16*, 207–216.

(71) Shvartsburg, A. A.; Smith, R. D. *Anal. Chem.* **2011**, *83*, 23–9.

(72) Gabryelski, W. *J. Am. Soc. Mass Spectrom.* **2003**, *14*, 265–277.

(73) Thomson, J. J. *Rays of Positive Electricity and their Application to Chemical Analysis*, 100th Anni.; American Society for Mass Spectrometry: Santa Fe; 1913.

(74) Hoffman, E. de; Stroobant, V. *Mass Spectrometry: Principles and Applications*, Third Edit.; John Wiley and Sons Ltd.: Chichester, West Sussex; 2007.

(75) Pitt, J. J. *Clin. Biochem. Rev.* **2009**, *30*, 19–34.

(76) Fenn, J. *J. Biomol. Tech. JBT*. **2002**, *9*, 411–22.

(77) Dole, M. *J. Chem. Phys.* **1968**, *49*, 2240.

(78) Fenn, J.; Mann, M.; Meng, C.; Shek, F.; Whitehouse, C. *Science* **1989**, *246*, 64–71.

(79) Yamashitat, M.; Fenn, J. B. *J. Phys. Chem.* **1984**, *434*, 4451–4459.

(80) Kebarle, P.; Verkerk, U. H. *Mass Spectrom. Rev.* **2009**, *28*, 898–917.

(81) Taylor, G. *Proc. R. Soc. A Math. Phys. Eng. Sci.* **1964**, *280*, 383–397.

(82) Kebarle, P. *J. Mass Spectrom.* **2000**, *35*, 804–17.

(83) Matuszewski, B. K.; Constanzer, M. L.; Chavez-Eng, C. M. *Anal. Chem.* **1998**, *70*, 882–9.

(84) Chen, H.; Venter, A.; Cooks, R. G. *Chem. Commun. (Camb).* **2006**, 2042–4.

(85) Law, W. S.; Wang, R.; Hu, B.; Berchtold, C.; Meier, L.; Chen, H.; Zenobi, R. *Anal. Chem.* **2010**, *82*, 4494–500.

(86) Orme, M. *Prog. Energy Combust. Sci.* **1997**, *23*, 65–79.

(87) Gallimore, P. J.; Kalberer, M. *Environ. Sci. Technol.* **2013**, *47*, 7324–31.

(88) Sleno, L.; Volmer, D. A. *J. Mass Spectrom.* **2004**, *39*, 1091–112.

(89) Sforza, S.; Ferroni, L.; Galaverna, G.; Dossena, A.; Marchelli, R. *J. Agric. Food Chem.* **2003**, *51*, 2130–5.

(90) Buré, C.; Gobert, W.; Lelièvre, D.; Delmas, a *J. Mass Spectrom.* **2001**, *36*, 1149–55.

(91) Hütteroth, A.; Putschew, A.; Jekel, M. *Int. J. Environ. Anal. Chem.* **2007**, *87*, 415–424.

(92) Es-Safi, N.-E.; Kerhoas, L.; Ducrot, P. H. *Spectrosc. Lett.* **2007**, *40*, 695–714.

(93) Guan, F.; Uboh, C.; Soma, L.; Luo, Y.; Driessen, B. *Anal. Chem.* **2004**, *76*, 5118–26.

(94) Swaim, C. L.; Smith, J. B.; Smith, D. L. *J. Am. Soc. Mass Spectrom.* **2004**, *15*, 736–49.

(95) Bristow, A. W. T.; Nichols, W. F.; Webb, K. S.; Conway, B. *Rapid Commun. Mass Spectrom.* **2002**, *16*, 2374–86.

(96) Wiley, W. C.; McLaren, I. H. *Rev. Sci. Instrum.* **1955**, *26*, 1150.

(97) Mamyrin, B. A. *Int. J. Mass Spectrom.* **2001**, *206*, 251–266.

(98) Bergmann, T.; Goehlich, H.; Martin, T. P.; Schaber, H.; Malegiannakis, G. *Rev. Sci. Instrum.* **1990**, *61*, 2585.

(99) Guilhaus, M.; Selby, D.; Mlynski, V. *Mass Spectrom. Rev.* **2000**, *19*, 65–107.

(100) March, R. E.; Hughes, R. J. *Theory of Quadrupole Mass Spectrometry, in Quadrupole Storage Mass Spectrometry*, Wiley Interscience: New York; 1989.

(101) Koppenaal, D. W.; Barinaga, C. J.; Denton, M. B.; Sperline, R. P.; Hieftje, G. M.; Schilling, G. D.; Andrade, F. J.; Barnes, J. H. *Anal. Chem.* **2005**, *77*, 418A–427A.

(102) Ells, B.; Barnett, D. A.; Froese, K.; Purves, R. W.; Hrudey, S.; Guevremont, R. *Anal. Chem.* **1999**, *71*, 4747–52.

(103) http://www.owlstonenanotech.com/ultrafaims/imsms-news/interactive-faims-ms-publications-and-citations-tool Date accessed 08/07/**2014**.

(104) Purves, R. W.; Guevremont, R.; Day, S.; Pipich, C. W.; Matyjaszczyk, M. S. *Rev. Sci. Instrum.* **1998**, *69*, 4094.

(105) Purves, R. W.; Guevremont, R. *Anal. Chem.* **1999**, *71*, 2346–2357.

(106) Li, J.; Purves, R. W.; Richards, J. C. *Anal. Chem.* **2004**, *76*, 4676–83.

(107) Smith, R. W.; Toutoungi, D. E.; Reynolds, J. C.; Bristow, A. W. T.; Ray, A.; Sage, A.; Wilson, I. D.; Weston, D. J.; Boyle, B.; Creaser, C. S. *J. Chromatogr. A.* **2013**, *1278*, 76–81.

(108) Gabryelski, W.; Froese, K. L. *Anal. Chem.* **2003**, *75*, 4612–23.

(109) Gabryelski, W.; Wu, F.; Froese, K. L. *Anal. Chem.* **2003**, *75*, 2478–86.

(110) Ells, B.; Barnett, D. A.; Purves, R. W.; Guevremont, R. *J. Environ. Monit.* **2000**, *2*, 393–397.

(111) Barnett, D. A.; Ells, B.; Guevremont, R.; Purves, R. W. *J. Am. Soc. Mass Spectrom.* **2002**, *13*, 1282–1291.

(112) Guevremont, R.; Barnett, D. A.; Purves, R. W.; Vandermey, J. *Anal. Chem.* **2000**, *72*, 4577–84.

(113) Xuan, Y.; Creese, A. J.; Horner, J. A.; Cooper, H. J. *Rapid Commun. Mass Spectrom.* **2009**, *23*, 1963–9.

(114) Tang, K.; Li, F.; Shvartsburg, A. A.; Strittmatter, E. F.; Smith, R. D. *Anal. Chem.* **2005**, *77*, 6381–8.

(115) Creese, A. J.; Smart, J.; Cooper, H. J. *Anal. Chem.* **2013**, *85*, 4836–43.

Chapter Two

Evaluation of the Effect of Experimental Conditions on FAIMS-MS Performance

2.1 Chapter Overview

An ESI-MS interface was modified to incorporate an miniaturised chip-based FAIMS device[1,2] at the capillary inlet orifice of the TOF MS. A central composite design (CCD) was used to explore the robustness and critical parameters of the FAIMS device for signal intensity across the full functioning range of the ESI source with liquid flow of up to 1 mL/min and using different solvent compositions. Critical parameters of the modified source were optimised using a test mixture of analytes varying in size, mass, charge and functionality. The performance of the miniaturised FAIMS was investigated using three different systems of isobaric, isomeric and near-mass ions where analysis by mass spectrometry without very high resolution or prior separation cannot be used to distinguish them. (i) The behaviour of methylmalonic acid (MMA) and interferant succinic acid (SA) ions formed by deprotonation ions and as adducts with group I metal ions has been studied. (ii) The quantitative determination of 6β-hydroxytestosterone (6β-HT) requires chromatographic separation from 2β-hydroxytestosterone (2β-HT), but this can be time-consuming when screening many potential drug candidates. The ability to distinguish between these hydroxytestosterone isomers by FAIMS and apply the approach as a rapid sample introduction method is investigated using different carrier gas temperatures and by adding water vapour to the carrier gas flow to achieve appropriate selectivity and sensitivity for rapid screening of potential drug candidates. The pharmaceutical excipients, 2-hydroxy-(4-octyloxy) benzophenone and PEG 400 (n = 7) were successfully isolated and subjected to in-source collision-induced dissociation (CID) for identification by characteristic fragment ions. Improved mass measurement accuracy and simplified product ion mass spectra were observed following FAIMS pre-selection and subsequent in-source CID of ions derived from pharmaceutical excipients, sufficiently close in *m/z* (17.7 ppm mass difference) that they could not be resolved by TOFMS alone.

2.2 Introduction

Earlier embodiments of FAIMS have been sensitive to change in operating conditions, such as peak position in CV spectra, so the first section of this chapter describes the systematic investigation of ESI source parameters on the CV transmission voltage and transmission. A central composite design (CCD) experiment was used to optimise the miniaturised FAIMS device and explore source conditions over the full functioning range to determine the functionality of the FAIMS device. The CCD required measurements at the minimum, mid-

point and maximum of the range of each parameter tested. The CCD program identifies the minimum number of experiments required to explore contributing effects of multiple parameters which are run in a random order. Parameters like liquid flow rate, liquid composition, source voltages and gas flows were investigated because these are likely to be changed during routine method development and maybe even within an analysis (like liquid composition), it is therefore critical for the peak position of an analyte ion in the FAIMS spectrum to be precise despite changes in source conditions. The CCD experiment was performed on the first ESI-FAIMS-TOF MS prototype device. Two prototype ESI-FAIMS-TOF MS prototypes are utilised for the experiments in this chapter.

FAIMS has been employed as an ion filter to select precursor ions prior to mass spectrometry analysis, because differential mobility is largely independent of *m/z* allowing orthogonal separations.[3] The ability to pre-select using FAIMS has been shown to simplify mass spectra by reducing background and isobaric ions.[4-7] The combination of FAIMS with tandem mass spectrometry (FAIMS-MS/MS) has also been reported for the structural and quantitative analysis of small molecules and peptides, with CID of mass-selected ions occurring in the collision cell located between the mass analysers of a Q-TOF or triple quadrupole spectrometer, or after mass isolation in an ion trap.[7-9]

The in-source fragmentation of ions in FAIMS-MS was reported by Guevremont *et al.*,[10] who observed a change in cluster distributions of leucine enkephalin of ions under low and high energy in an ESI ion source. It was concluded that fragmentation comparable to MS/MS analysis was induced under high energy conditions. Subsequent fragmentation studies were pursued using MS/MS of mass-selected ions in a triple quadrupole spectrometer rather than through in-source CID. Eiceman *et al.* also described fragmentation of chlorocarbon ions in the interface of an atmospheric pressure ionization mass spectrometer, which complicated the identification of FAIMS-selected ions.[11] Measurements were carried out under conditions designed to minimise rather than enhance ion decomposition in the mass spectrometer interface. The use of FAIMS with in-source CID and selected reaction monitoring MS/MS was used by Xia and Jemal to determine the location of source fragmentation in the analysis of ifetroban and its acylglucuronide metabolite.[12] FAIMS was used to transmit either the parent drug and its acylglucuronide, from which it was concluded that fragmentation, inducing the conversion of the acylglucuronide metabolite to the parent drug form occurred almost entirely after the inlet orifice of the mass spectrometer. The objective of this work was to minimize the effect of in-source CID on the LC-MS/MS with SRM for the quantitative

analysis of prodrugs and metabolites. The targeted use of in-source CID-MS using FAIMS to isolate ions from a mixture prior to fragmentation was reported by Coy and co-workers.[13] The separation of a simple mixture containing five isobaric model compounds (*m/z* 316) was achieved by direct infusion into the ESI source and differential mobility spectrometry. Ions were transmitted at their optimum CV and fragmentation induced by increasing the inlet cone voltage in the interface of a quadrupole MS.

The second section of this chapter describes an investigation of the ability of FAIMS to separate closely related ions using three model systems containing pairs of analytes that are isobaric, isomeric or sufficiently close in mass to be difficult to be separated by MS. The first of these pairs of analytes are succinic acid (SA) and methylmalonic acid (MMA). The latter is commonly used as a biochemical marker of vitamin B12 deficiency, partly due to MMA being a thousand times more concentrated in serum than vitamin B12 making it easier to measure accurately.[14,15] SA is an interferant typically removed from MMA using chromatography or derivatization prior to analysis by using mass spectrometry.[14,15] Analysis in positive ion mode of adducts formed with group I metals and in negative ion mode of deprotonated MMA and SA with corresponding fragments produced by in-source CID using ESI-FAIMS-MS is discussed in this chapter.

6β-hydroxytestosterone (6β-HT) is a major metabolite of testosterone through CYP3A4 action where testosterone is used as a substrate for measuring inhibition of the enzyme CYP3A4 when investigating drug-drug interactions for potential drug candidates. 2β-hydroxytestosterone (2β-HT) is another metabolite of testosterone whose formation is promoted when 6β-HT is inhibited which can prove problematic for the rapid determination of 6β-HT levels in the presence of 2β-HT without a time-consuming chromatographic step. Isomers 2β-HT and 6β-HT were analysed using ESI-FAIMS-MS and LC-ESI-FAIMS-MS to optimise separation by exploring different temperatures and water concentration of the carrier gas. Loop injections of the isomers were used to enable evaluation of combining fast sample introduction with a rapid FAIMS separation and MRM transition.

The final section of this chapter describes the development of generic FAIMS-in source CID-MS procedures (termed FISCID-MS). FISCID-MS exploits the ability to control the fragmentation of FAIMS-selected ions in the interface of the mass spectrometer, by combining the orthogonal separation characteristics of a miniaturised high field FAIMS device and in-source CID with time-of-flight mass spectrometry. The technique is shown to

provide major enhancements for the analysis of complex mixtures. FISCID-MS is demonstrated for the separation of pharmaceutical excipients: 2-hydroxy-(4-octyloxy) benzophenone and PEG 400 (n = 7).

2.3 Experimental

2.3.1 Chemicals

HPLC grade methanol (MeOH), acetonitrile (ACN), water and formic acid (FA) were purchased from Fisher Scientific (Loughborough, UK). The test mixture consisting of caffeine, MRFA, tetrapentylammonium bromide (TPAB), reserpine, insulin B chain and Vancomycin hydrochloride; MMA and SSA; and the two pharmaceutical excipients are 2-hydroxy-(4-octyloxy) benzophenone and PEG 400, were obtained from Sigma Aldrich (Gillingham, UK). 6β-HT and 2β-HT were supplied by Vertex Pharmaceuticals.

2.3.2 Sample Preparation

The test mixture was made up at different concentrations (Table 2.1) to give a similar response under standard infusion conditions in methanol/water (50:50) with 0.1 % FA. MMA and SA (30 μg/ml) were dissolved into methanol/water (50:50) with 0.2 mM ammonium acetate for negative ion mode and methanol/water (50:50) with either lithium chloride or potassium chloride (1 μg/ml) for positive ion mode. Stock solutions of 2β-HT and 6β-HT (100 μM in methanol) were diluted using methanol/water (50:50) with 0.1% formic acid (FA) to 5 μM for infusion studies and 0.1 μM for LC-FAIMS-MS experiments. Quantitation was pursued with 6β-HT in the range 0.1 μM – 5 μM in methanol/water (50:50) with 0.1 % FA. 2-hydroxy-(4-octyloxy) benzophenone and PEG 400 were prepared in methanol/water (50:50) with 0.1 % FA at respective concentrations of 5.1 and 104 pmol/μl (1:20 molar ratio).

Table 2.1 Concentrations of test mixture compounds

Test mixture component	Concentration /pmol/μl
Caffeine	167
MRFA	16.7
TPAB	0.167
Reserpine	8.3
Insulin B Chain	33.3
Vancomycin	167

2.3.3 Instrumentation

The FAIMS studies reported in this thesis were carried out under a collaboration with Owlstone Limited on the development of miniaturised chip-based FAIMS interfaces for mass spectrometry and an evaluation of applications in pharmaceutical and bioanalysis. Two prototype FAIMS chips were used in the evaluation and these are described in detail here. Both prototypes featured the miniaturised ultra-FAIMS device (Owlstone, Cambridge, UK) interfaced to an Agilent 6230 orthogonal acceleration time-of-flight mass spectrometer (Agilent Technologies, Santa Clara, CA, USA). The electrospray source of the ToF mass spectrometer was modified to accommodate the presence of the ultra-FAIMS chip within the spray shield (Figure 2.1). The first prototype device[16,17] consisted of 47 electrode pairs with an electrode gap of 35 μm, and a channel length of 300 μm. The FAIMS chip was connected to a field generator module, containing the electrical circuitry required to generate field asymmetric waveforms. The frequency of the applied asymmetric waveform was 25 MHz in a roughly 2:1 ratio of low field to high field. Comparative non-FAIMS data were acquired with analytes transmitted through the FAIMS chip with the DF and CV set to 0 kV/cm and 0 V, respectively.

The first prototype device has the voltages reversed compared to the conventional JetStream ESI source, in that the high voltage is applied to the nebuliser (~1.5 kV), and the spray shield, nozzle and counter electrode were connected at 400 V (Figure 2.1). The reason for this was that the silicon based chip was incompatible with the high voltages of the conventional design, the capillary voltage was set at a bias (-100 V to 100 V) to aid transmission. The units of the FAIMS parameters were kV/cm for DF and V for CV. The first prototype device was used for the analysis of HOBP and PEG, and for the CCD experiment.

The second prototype device featured a nickel-based chip with a 100 μm electrode gap and 700 μm channel length which enabled the standard voltage configuration of a JetStream ESI source of an Agilent 6230 TOF MS, where the nebuliser is grounded and the capillary voltages set to 3000-4000 V (Figure 2.2). The nozzle, spray shield and counter electrode were no longer connected. The chip housing was mounted onto the capillary in the same way as the earlier version. The units of the FAIMS parameters for this prototype were Td for DF and Td for CF. The second prototype was used for the experiments including: MMA, SA, 6β-HT and 2β-HT.

The ultraFAIMS A1 system is the most recent chip-based FAIMS interface and was fitted to a triple quadrupole mass spectrometer (Agilent Technologies 6460C). The quantitative experiments of the hydroxytestosterone isomers were performed using this system and with HPLC (Agilent Technologies, 1200 series) for loop injections of the isomers which were standard LC injections without a column in place. The voltages are the same as in the second prototype device but the design of the spray shield and the chip holder is different.

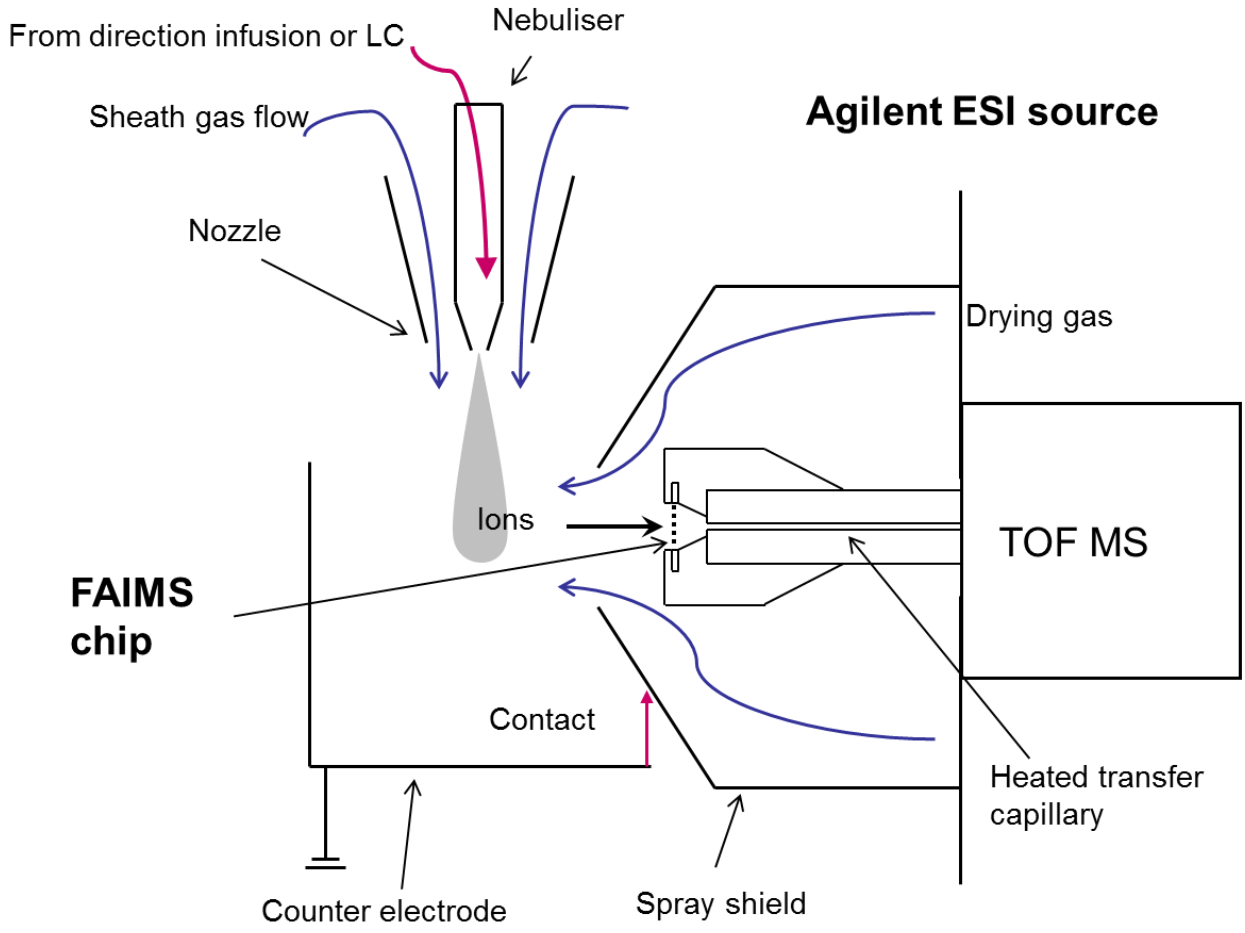

Figure 2.1 A schematic of ultra-FAIMS prototype device 1 interface with Agilent Jet Stream ESI for incorporating silicon-based chip

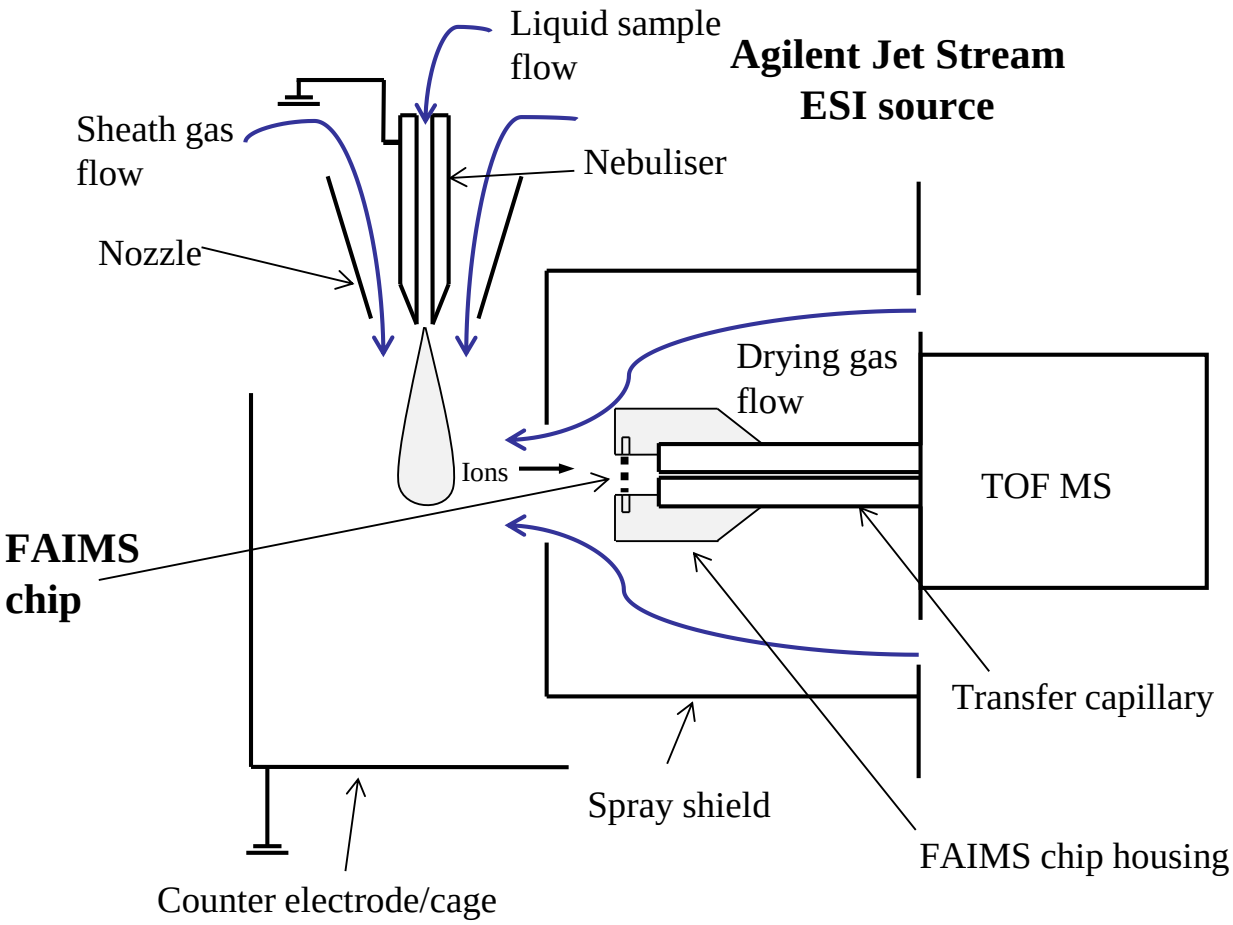

Figure 2.2 A schematic of ultra-FAIMS chip prototype device 2 interface with Agilent Jet Stream ESI for incorporating Nickel-based chip

Central Composite Design Experiment

A central composite design (CCD) using DOE PRO software (Microsoft Excel) was used to assess the critical source parameters on instrument performance and the stability of CV maximum values over a wide range of source conditions (Table 2.2 and 2.3). The CCD required measurements at the minimum, mid-point and maximum of range of each parameter tested. The CCD program identifies the minimum number of experiments required to explore contributing effects of multiple parameters.

The parameters investigated were: DI flow rates (10 – 50 µl/min) and LC flow rates (100 – 1000 µl/min), drying gas flow (4 – 12 l/min), nebuliser pressure (10 – 60 psig), sheath gas flow (4.6 – 12 l/min), capillary voltage (-100 - +40 V) and % organic solvent (10 – 90%); (Figure 1). The only organic solvent used for DI was methanol; methanol and acetonitrile were studied using LC flow rates. Other parameters including: fragmentor voltage, drying gas

temperature, sheath gas temperature, nozzle voltage and MS scan rate were kept constant throughout the experiment (Table 2.4). The dispersion field applied was 80% (48.8 kV/cm) of the maximum with a CV scan range -1 to +4 V. A 5-factor and 4-factor CCD was used for DI and LC flow rates respectively. Performance was monitored with a test mixture containing caffeine, MRFA, tetrapentylammonium bromide (TPAB), reserpine, insulin B chain and Vancomycin. Three replicates were recorded for each CCD row number.

Table 2.2 Conditions for direct infusion CCD experiment

Row#	Liquid flow µl/min	Capillary voltage V	Drying gas l/min	Sheath gas l/min	Nebulizer pressure psig
1	10	-100	4	5.5	60
2	10	-100	4	12	10
3	10	-100	12	5.5	10
4	10	-100	12	12	60
5	10	40	4	5.5	10
6	10	40	4	12	60
7	10	40	12	5.5	60
8	10	40	12	12	10
9	50	-100	4	5.5	10
10	50	-100	4	12	60
11	50	-100	12	5.5	60
12	50	-100	12	12	10
13	50	40	4	5.5	60
14	50	40	4	12	10
15	50	40	12	5.5	10
16	50	40	12	12	60
17	30	-30	8	8.75	35
18	30	-30	8	8.75	35
19	10	-30	8	8.75	35
20	50	-30	8	8.75	35
21	30	-100	8	8.75	35
22	30	40	8	8.75	35
23	30	-30	4	8.75	35
24	30	-30	12	8.75	35
25	30	-30	8	5.5	35
26	30	-30	8	12	35
27	30	-30	8	8.75	10
28	30	-30	8	8.75	60

Table 2.3 Conditions for liquid chromatography CCD experiment

Row#	Liquid Flow Rate	Nebuliser Pressure	Drying Gas Flow	% Organic Solvent
1	0.1	10	4	10
2	0.1	10	4	90
3	0.1	10	12	10
4	0.1	10	12	90
5	0.1	60	4	10
6	0.1	60	4	90
7	0.1	60	12	10
8	0.1	60	12	90
9	1	10	4	10
10	1	10	4	90
11	1	10	12	10
12	1	10	12	90
13	1	60	4	10
14	1	60	4	90
15	1	60	12	10
16	1	60	12	90
17	0.55	35	8	50
18	0.55	35	8	50
19	0.1	35	8	50
20	1	35	8	50
21	0.55	10	8	50
22	0.55	60	8	50
23	0.55	35	4	50
24	0.55	35	12	50
25	0.55	35	8	10
26	0.55	35	8	90

Table 2.4 Constant conditions for CCD experiment

TOF Settings	Value
Fragmentor voltage	175 V
Drying gas temperature	150 ˚C
Sheath gas temperature	250 ˚C
Nozzle voltage	400 V
TOF MS Scans	10 scans/s

FAIMS Settings	Value
CV Range	-1 to +4 V
D.F.	0 and 80 %
Scan rate	0.5 V/s
CV sweeps	2
CV scans	4 (10 s each)

FAIMS-MS analysis of isobaric, isomeric and near-mass ions

Methylmalonic acid (MMA) and Succinic acid (SA) were dissolved and diluted into a methanol/water (50:50) solution with either 0.1% formic acid, 1 µg/ml of either KCl or LiCl, sodium scavenged from glassware was used to produce sodiated ions for analysis in positive ion mode or with methanol/water (50:50) with 0.2 mM ammonium acetate for negative ion mode. Samples were infused individually into ESI-FAIMS-MS for investigating differential mobility behaviour of the different ions formed.

Separation of 6β-HT and 2β-HT was explored initially using infusion experiments on a TOF MS at different drying gas temperatures (50-150˚C) and with a modifier system (Bronkhorst controlled evaporator system) to introduce water (0.5 – 1.5 % v/v) with the drying gas temperature set to 150˚C. LC-FAIMS-MS used 0.55 ml/min with a 7 minute gradient run of water (0.1% formic acid) and acetonitrile (0.1% formic acid) and a 10 µl injection volume onto a C18 column (100 x 3.0 mm, Onyx Monolithic C18, CH0-8158, Phenomenex). The infusion method was transferred to a triple quadrupole mass spectrometer (Agilent 6460C) fitted with ultraFAIMS A1 device and separation conditions retested (DF 280 to 305 Td, water 0.75 to 1.5 %). Loop injections (10 µl) of hydroxytestosterone isomers (0.1 µM – 5 µM) using a mobile phase of acetonitrile (100%, 0.1% formic acid) at 0.2 ml/min without a column in place were used for quantitative studies. The triple quadrupole used an MRM transition was set to select 305.2 (Q1, unit resolution) and detect the product ion 269.4 (Q3, widest resolution) with collision energy set to 13 and dwell time 200 ms.

HOBP and PEG solutions were infused into the JetStream-ESI ion source at 50 µL/min and ionized using a voltage of 1.5 kV. Source conditions for all experiments were: nozzle voltage, spray shield and counter electrode, 400 V; skimmer voltage, 65 V; drying gas temperature, 150 °C; sheath gas temperature, 250 °C; nebulizer gas pressure, 25 psig. HOBP/PEG analysis was carried out with the inlet capillary voltage set to -29 V, the drying gas flow to 4.6 L/min and the sheath gas flow to 7 L/min. FAIMS separation was carried out at a 47 kV/cm DF, over a CV range of -1 V to +4 V at 0.5 V/s CV sweep rate. FAIMS-selected analytes were transmitted into the mass spectrometer interface by scanning a 0.1 V window around the optimum CV for transmission. The exact CV values and scan windows were experiment dependant and as such are indicated in the text where appropriate. FISCID-MS analysis was carried out in positive ion electrospray ionization mode with the fragmentor voltage set to 150 V for transmission of intact analytes without fragmentation and increased to 400 V to

induce in-source fragmentation by CID. Data were processed using Mass Hunter version B.01.03 (Agilent Technologies, Santa Clara, CA, USA) and Excel 2007 (Microsoft, Seattle, USA).

2.4 Results and Discussion

The robustness of FAIMS was determined over a wide range of ESI ion source conditions, including the use of different solvents and flow rates. The critical source parameters for optimising response and the transmission of ions over a range of *m/z* are discussed in this chapter. The separation of isobars, isomers and near-mass ions is demonstrated by investigating FAIMS spectra of methylmalonic acid (MMA) and succinic acid (SA), 2β-hydroxytestosterone (2β-HT) and 6β-hydroxytestosterone (6β-HT), and a PEG 400 (n=6) ion and 2-hydroxy-(4-octyloxy) benzophenone (HOBP).

2.4.1 Central Composite Design for Evaluating FAIMS Performance

A central composite design can be used to explore the individual and cumulative effect of multiple factors, making it an ideal method for evaluating and optimising the modified ESI source under the full range of conditions. The test mixture was adjusted to provide variation in size, functionality and mass range (*m/z* 195 to 1448) to investigate the effect of instrumental parameters of a wide range of analytes. Signal intensity was monitored for optimising sensitivity and the CV maximum recorded to evaluate stability of FAIMS performance.

The impact of the ion source parameters on the response showed that the major contributing parameters to the ion response were compound and charge-state dependent (Figure 2.3). Capillary voltage, liquid flow and nebuliser pressure have the greatest contribution to response while drying gas flow (the flow around the FAIMS chip) had the lowest. Optimum response was achieved with the sheath gas flow set to maximum (12 l/min). Critical parameters were observed to be similar whether the DF was switched on or off and the parameters observed to have a large effect on sensitivity are those known to affect ion generation in the ESI source. The CCD model generated optimum settings for each of the parameters for each compound and close agreement was found between predicted and experimental optimum conditions. Ion response was not investigated for LC-MS due to the nature of performing a FAIMS scan within a loop injection, where the position of the FAIMS

scan as the compounds eluted from the LC could not be controlled causing a large variation in intensity.

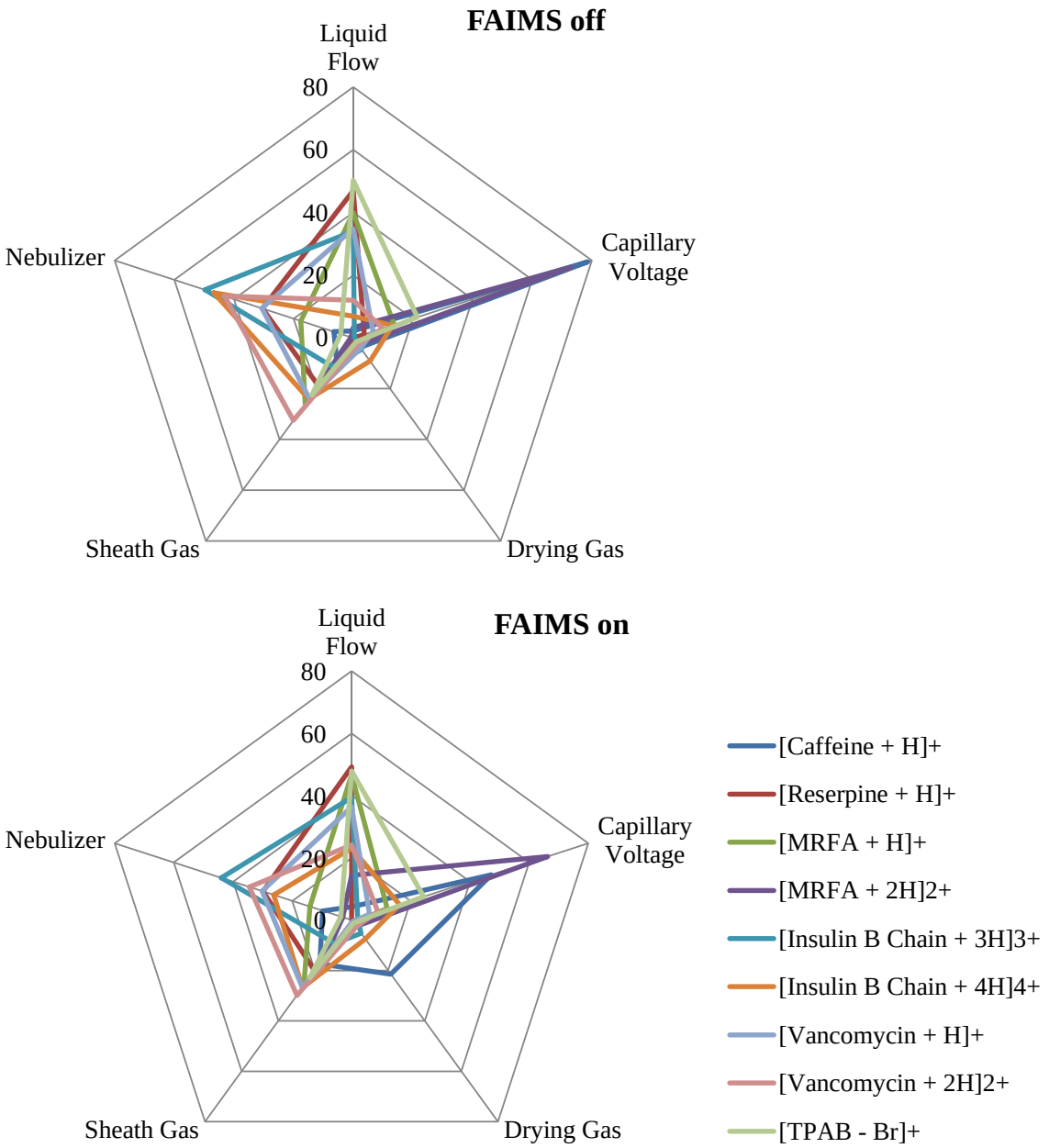

Figure 2.3 CCD parameter coefficients of contribution to response for each parameter

An important requirement of miniaturised FAIMS is to be able to adjust source parameters to optimise performance over a range of liquid flow rates or solvent compositions. The CCD explored gas and liquid flow rates at extreme and standard LC-MS conditions. The average CV peak maximum for each test mixture ion with direct infusion is shown in Table 2.5 and with LC injection in Table 2.6, where the latter has two data sets showing a mobile phase

with acetonitrile and water, and with methanol and water. Both Tables 2.5 and 2.6 show corresponding standard deviations to demonstrate precision for each test mixture ion. The average CV maximum value for each test mixture ion, when using direct infusion, is illustrated in Figure 2.4; CV is plotted against CCD experiment number where experiment conditions are changing between minimum, medium and maximum conditions for each parameter. It was found that the FAIMS chip remains stable even when subjected to extreme conditions of flow rates and different solvent compositions, even with a high (90%) aqueous mobile phase. The good stability of the FAIMS performance is critical if miniaturised FAIMS is to be used to for LC-FAIMS-MS analyses. Without good stability, every time the LC conditions are changed the FAIMS conditions would need to be re-optimised again which would not be possible in a gradient LC run. The reason for its high stability is likely due to the efficiency of desolvation in the ion source, where high temperatures and the drying gas reduce the number of neutral solvent molecules entering the FAIMS chip and prevent a modifier effect which would otherwise cause peaks to move in the CV spectrum.

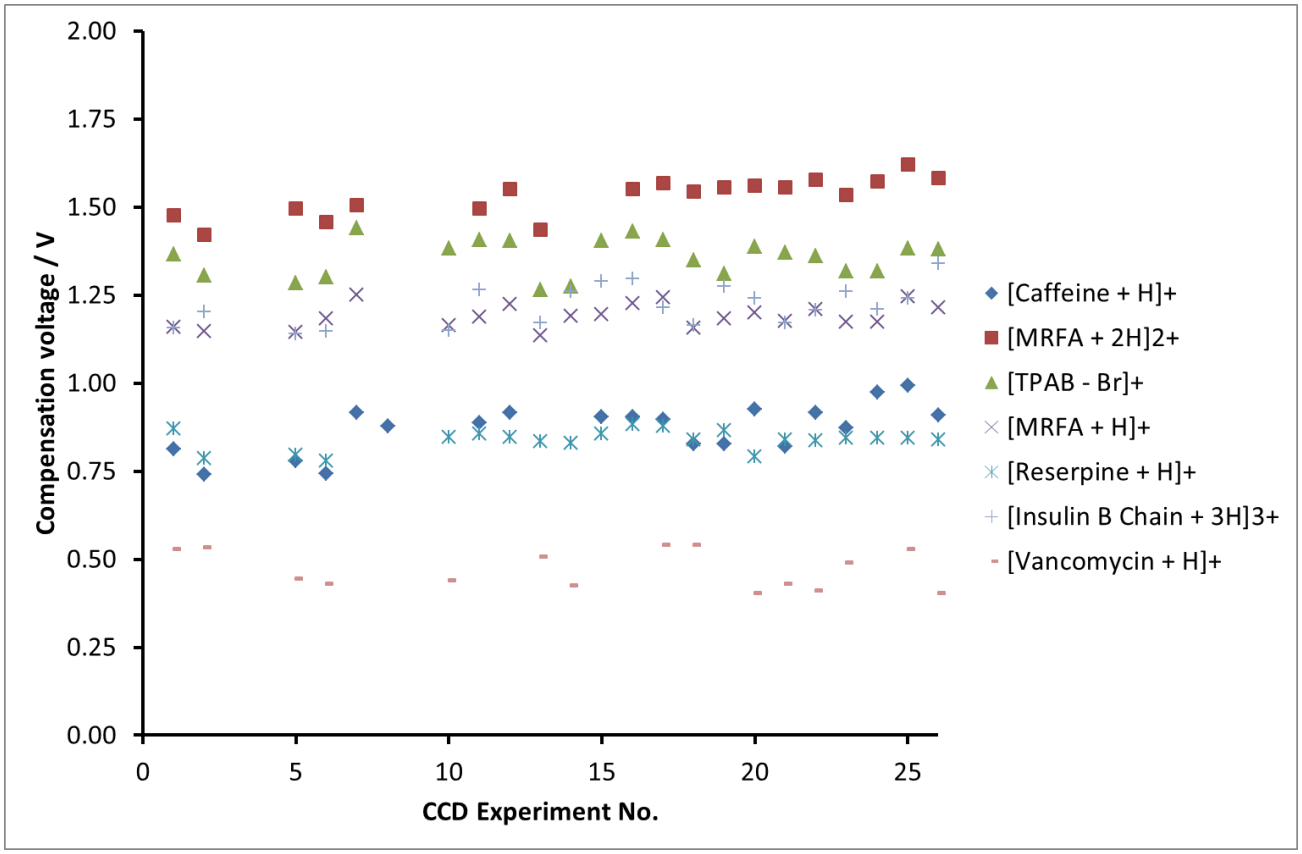

Figure 2.4 A plot of CV maximum against CCD experiment number (from Table 2.2) using direct infusion of the test mixture in methanol/water at DF 48.8 kV/cm (n=3)

Table 2.5 Peak position (CV) and standard deviation for test mixture compounds from the direct infusion FAIMS-MS CCD experiments with a methanol/water solvent

Ion	CV /V	St. Dev.
$[Caffeine + H]^+$	0.81	0.07
$[MRFA + 2H]^{2+}$	1.61	0.09
$[TPAB - Br]^+$	1.43	0.07
$[MRFA + H]^+$	1.25	0.05
$[Reserpine + H]^+$	0.90	0.04
$[Vancomycin + 2H]^{2+}$	1.32	0.08
$[Insulin\ B\ Chain + 4H]^{4+}$	1.51	0.08
$[Insulin\ B\ Chain + 3H]^{3+}$	1.37	0.05
$[Vancomycin + H]^+$	0.53	0.09

Table 2.6 Peak position (CV) and standard deviation for test mixture compounds from the LC-FAIMS-MS CCD experiments with methanol/water and acetonitrile/water solvents

Ion	Acetonitrile		Methanol	
	CV /V	Std Dev	CV /V	Std Dev
$[Caffeine + H]^+$	0.86	0.09	0.87	0.10
$[MRFA + 2H]^{2+}$	1.50	0.12	1.53	0.10
$[TPAB - Br]^+$	1.35	0.07	1.36	0.07
$[MRFA + H]^+$	1.19	0.08	1.19	0.05
$[Reserpine + H]^+$	0.84	0.06	0.84	0.05
$[Vancomycin + 2H]^{2+}$	1.22	0.07	1.23	0.05
$[Insulin\ B\ Chain + 3H]^{3+}$	1.17	0.08	1.22	0.09
$[Vancomycin + H]^+$	0.46	0.07	0.47	0.07

Under optimum conditions, a plot of % transmission of the test mixture ions at a DF of 48.8 kV/cm relative to a DF of 0 kV/cm against *m/z* is shown in Figure 2.5. There is a trend of increasing % transmission with higher *m/z*, this levels out at ~ *m/z* 600 Th but shown to be ~ 100% at *m/z* 1450 ($[Vancomyncin+H]^+$). Interestingly, the *m/z* 725 ($[Vancomycin+H]^{2+}$) ion

gives a % transmission of 67% at DF 48.8 kV/cm, suggesting that the trend observed here is not mass-dependant but also mass-to-charge dependant. Figure 2.5 shows that by applying a DF of 48.8 kV/cm, transmission of analyte ions is more critical for smaller ions (<500 Th) and should be considered during method development.

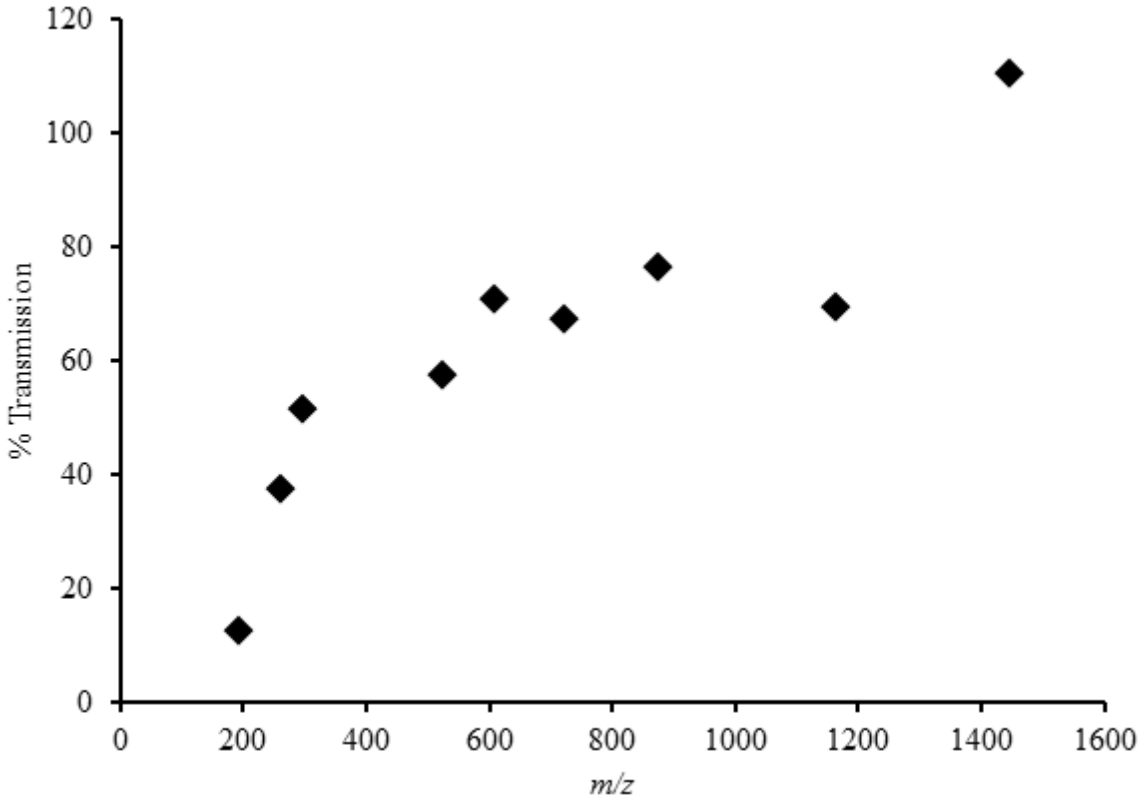

Figure 2.5 A plot of % transmission (from DF 0 to 80 % of maximum) against *m/z* (n=3)

2.4.2 Separation of isobaric, isomeric and near-mass ions

The presence of isobaric interferences can be problematic in mass spectrometry, but ion mobility has the ability to separate ions of the same mass or close in mass. In this section three examples of isobaric and isomeric systems were studied to evaluate the additional benefits FAIMS offers to mass spectral analysis.

2.4.2.1 Methylmalonic acid (MMA) and succinic acid (SA)

In negative ion mode, the deprotonated ions of MMA and SA (*m/z* 117.02) are readily formed by ESI under fragmention[18] both undergo the loss of carbon dioxide (*m/z* 117.02→73.02) due to in-source CID (Figure 2.6). The similarity of MMA and SA spectrum means that the analytes cannot be distinguished using mass spectrometry alone.

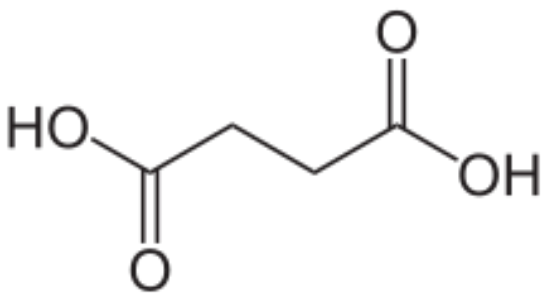

Succinic acid

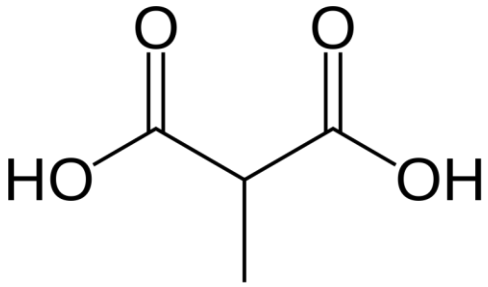

Methylmalonic acid

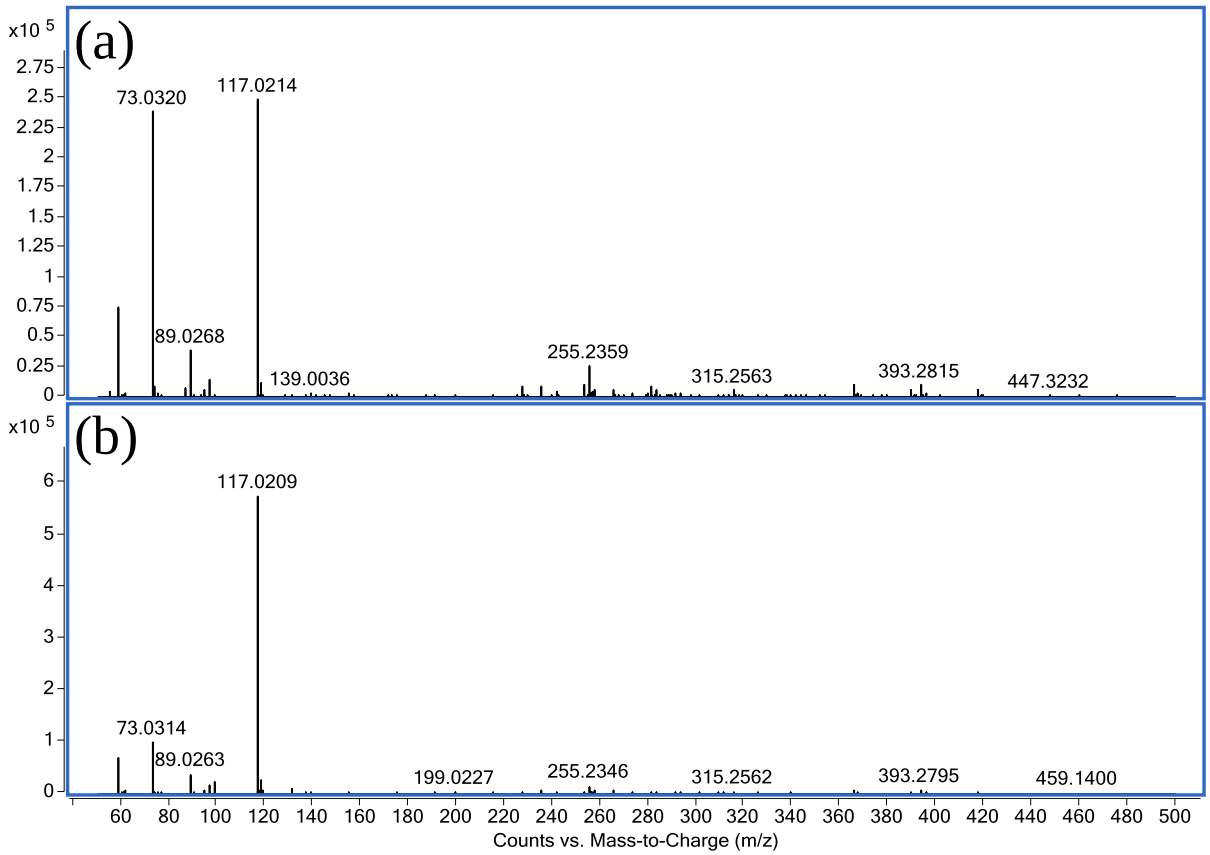

Figure 2.6 Negative ESI-MS of (a) MMA and (b) SA

FAIMS spectra of the $[M\text{-}H]^-$ and $[M\text{-}HCO_2]^-$ ions were acquired by running MMA and SA separately (Figure 2.7). The $[MMA\text{-}H]^-$ intensity is 2x lower than $[SA\text{-}H]^-$ (Figure 2.6) and Figure 2.7.a shows that with FAIMS spectra using the same signal intensity scale a much lower response of $[MMA\text{-}H]^-$ is observed when compared with the $[SA\text{-}H]^-$ ion peak. Plotting the data on a normalised scale allows the $[MMA\text{-}H]^-$ peak to be observed. The large loss of signal intensity when changing from a DF of 0 Td to 180 Td suggests the high electric fields of DF cause $[MMA\text{-}H]^-$ ion to fragment almost entirely before traversing the FAIMS device.

Interestingly a fragment peak of MMA is observed at CF -1.4Td whereas the fragment peak of SA is observed at CF -0.4 Td. The SA fragment overlaps almost exactly with the precursor SA ion, suggesting that the fragment is produced after the FAIMS device has transmitted $[SA\text{-}H]^-$ because it is highly unlikely that two separate ions will have exactly the same peak position throughout DF range 180 to 240 Td. The MMA fragment is fully resolved from the precursor MMA ion peak, suggesting that fragmentation to the product ion *m/z* 73.02 occurs prior to FAIMS separation. There is a small contribution where the $[MMA\text{-}CO_2\text{-}H]^-$ fragment peak overlaps with $[MMA\text{-}H]^-$ at CF -0.4 Td (640 counts) which is probably due to the poor transmission of the precursor ion (1286 counts). Increasing the DF above 180 Td causes the MMA fragment ion to shift in a positive direction bringing it closer to the SA fragment ion. In addition, the low mass of the fragment ion (*m/z* 73.02) means that transmission drops rapidly with DF (data not shown), making DF 180 Td the optimum DF for these isomers.

The unique positioning of FAIMS technology at the inlet of a mass spectrometer allows ions formed at different stages in the ESI-MS interface to be distinguished. In this case, MMA fragments produced prior to the FAIMS device are separated directly by the FAIMS device from the SA fragments that are produced after the FAIMS device has transmitted the SA precursor ion. Where the FAIMS device was unable to separate MMA and SA, it is able to distinguish between the isobars by separating isobaric fragments that are produced by in-source CID at different stages of the ESI source.

MMA and SA form adducts with group I metal ions Li^+, Na^+ and K^+ in a solution containing either lithium chloride or potassium chloride, sodium adducts were formed from sodium scavenged from glassware. Protonated molecules of MMA and SA were not investigated due to low abundances formed under acid conditions. The potential to separate the ions was investigated over the DF range 180 to 280 Td to determine the value of adduct formation. Discussion of adduct formation to improve FAIMS separation was described in Section 1.2.5.

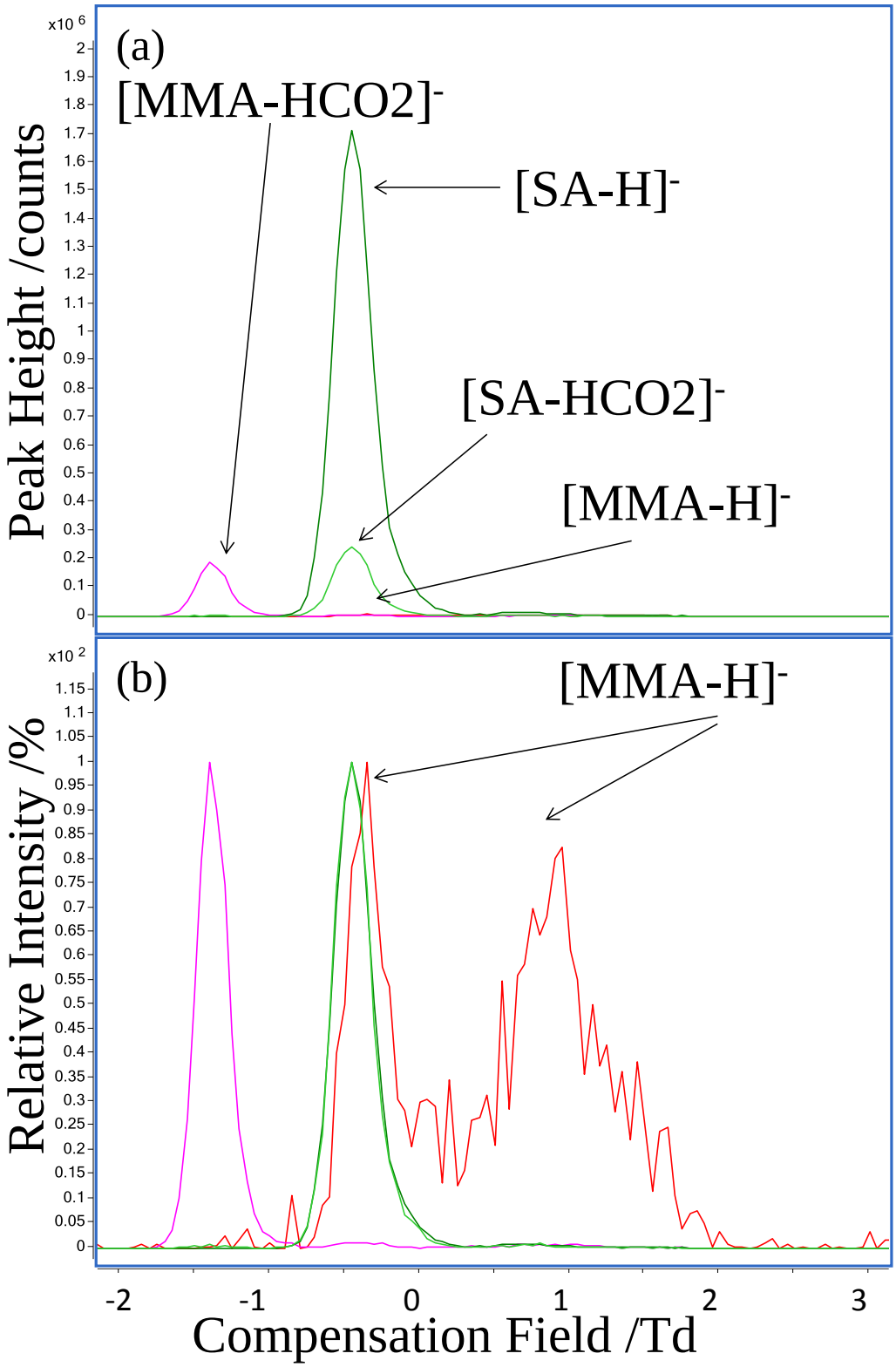

Figure 2.7 SIR (*m/z* 117.02 and 73.02) showing FAIMS spectra of $[MMA\text{-}H]^-$ (red), $[MMA\text{-}HCO_2]^-$ fragment (pink), $[SA\text{-}H]^-$ (dark green) and $[SA\text{-}HCO_2]^-$ fragment (light green) with (a) absolute intensities, and (b) normalised intensities (%); drying gas temperature was set to 75 ˚C, DF to 180 Td, Fragmentor to 150 V, negative ESI mode

FAIMS spectra of Li^+ and Na^+ adducts of MMA and SA are shown in Figure 2.8. The presence of lithium chloride results in two peaks for both isobars at DF 200 Td. The signal intensity of the main peaks of $[SA+Li]^+$ (CF -0.4Td) and $[MMA+Li]^+$ (CF -0.1 Td) decrease rapidly beyond 220 Td. The smaller peaks observed for both ions (CF = 1.2 Td) decrease rapidly in signal above DF 200 Td. Figure 2.8.a shows that at DF 200 Td there is no separation of the isobars and no improvement in separation was observed at higher DFs. A strong overlap of sodiated adducts was observed at 200 Td (CF = 0 Td, Figure 2.8.b). Investigation into higher DFs showed that signal decreased with increasing DF and were at baseline at DF 220 Td. It is possible that both sodiated and lithiated ions show a large loss in signal due the low *m/z* and a weak binding affinity to sodium and lithium ions. The low response and poor separation of these ions demonstrates that sodium and lithium cannot be used to distinguish between these isobaric ions.

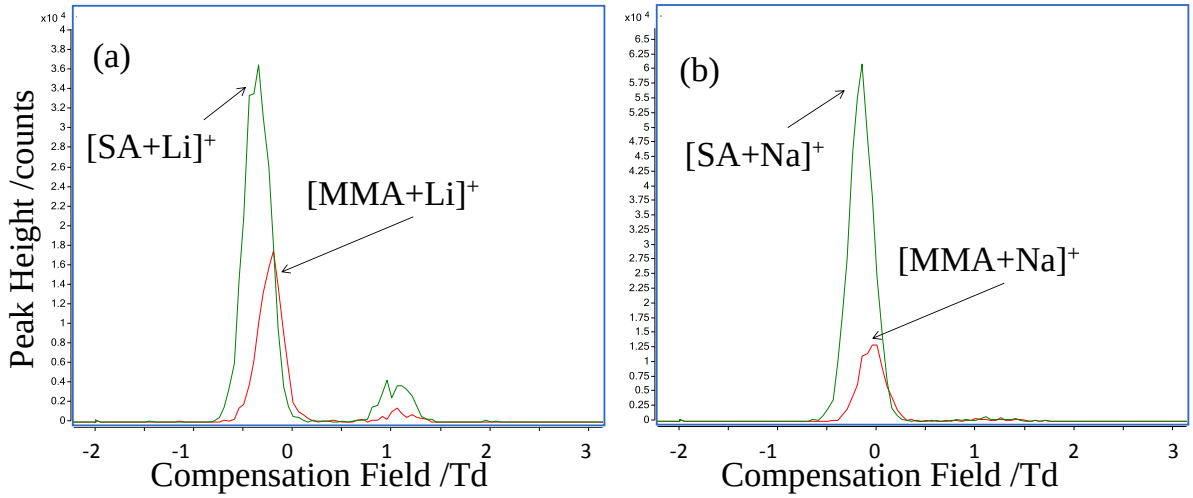

Figure 2.8 Selected ion response of lithiated (*m/z* 125.0421) and sodiated (*m./z* 141.0158) adducts of MMA and SA with (a) lithium chloride, and (b) scavenged sodium from glassware scanned at DF 200 Td with drying gas temperature set to 150 ˚C

Potassium chloride was used to promote adduct formation of MMA and SA with K^+, FAIMS spectra was acquired across a DF range of 180 to 280 Td at 100 ˚C and 150 ˚C to explore the behaviour of potassiated ions (shown in Figure 2.9). Regardless of DF and temperature, the intensity of the $[SA+K]^+$ ion peak does not significantly decrease with increasing DF as was observed with sodium and lithium. At DF 200 Td with dry gas temperature set to 100 ˚C, both $[SA+K]^+$ and $[MMA+K]^+$ overlap at CF 0.1 Td (Figure 2.9.a). Increasing DF to 220 Td causes $[SA+K]^+$ to shift to CF 0.2 Td and $[MMA+K]^+$ to shift to 0.6 Td (Figure 2.9.b). $[MMA+K]^+$ becomes better resolved at DF 240 Td with the CF maximum at 0.7 Td which is

between the main peak (CF 0.3 Td) and a small more shifted peak (CF 1.5 Td) (Figure 2.9.c). The source of the second small peak may be from a dimer fragmenting back to the potassiated adduct, although there is not a clear dimer peak in the mass spectra for either MMA (Figure 2.10.a) or SA (Figure 2.10.c) with potassium to support this theory. With the drying gas set to 150 ˚C and DF to 200 Td, $[SA+K]^+$ is at CF 0.1 Td and $[MMA+K]^+$ is at CF 0.5 Td (Figure 2.9.d) which is different to the overlapped peak observed with the same DF at 100 ˚C. Both $[SA+K]^+$ and $[MMA+K]^+$ shift with DF until at DF 240 Td the response for $[MMA+K]^+$ is reduce to baseline (Figure 2.9.e-f). The best separation was achieved at DF 240 Td with drying set to 100 ˚C with $[MMA+K]^+$ at CF 0.85 Td there is only 1.7 % interference from $[SA+K]^+$ despite a 2-fold reduction in $[MMA+K]^+$ response.

A comparison of mass spectra of MMA (Figure 2.10.a and b) and SA (Figure 2.10.c and d) using potassium shows that in both cases, FAIMS-selection of either $[MMA+K]^+$ or $[SA+K]^+$ results in making the FAIMS-selected ion (*m/z* 156.98, DF 240 Td, CF 0.3 and 0.85 Td respectively) the base peak in the mass spectrum (Figure 2.10.b and c) and mass spectra acquired without FAIMS-selection the potassiated adducts were at around 10% of the intensity of the base peak. The mass spectra shows that even with KCl in the sample, the sodiated ion (*m/z* 141.02) formed from scavenged sodium has a far higher response suggesting that these adducts are either more stable or more readily formed those formed with potassium. The change in peak position of analytes formed with group I metal ions shows the potential of forming different ions to improve separation and signal intensity compared to the more conventional protonated or deprotonated analyte ions.

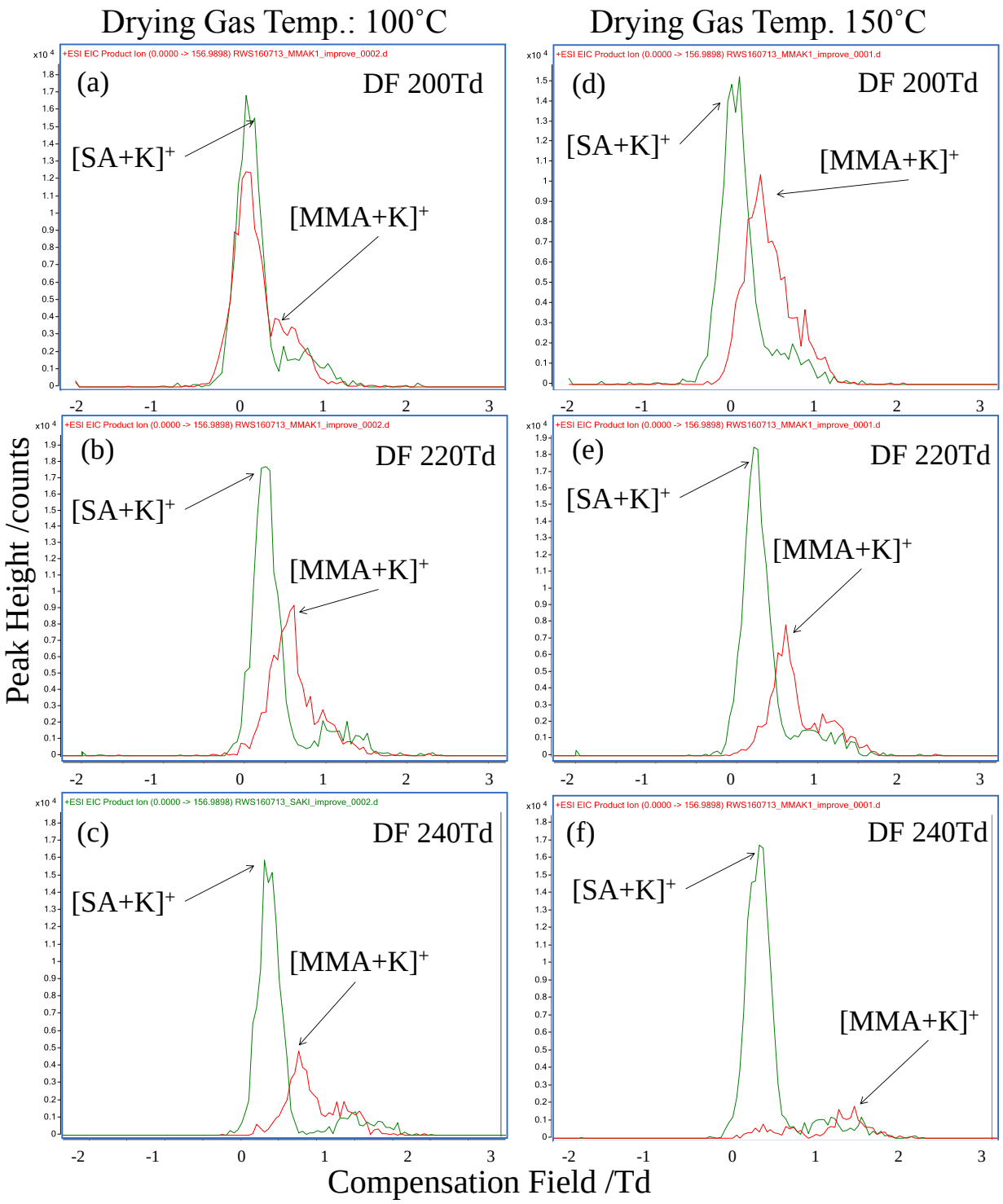

Figure 2.9 Selected ion response (*m/z* 156.9898) showing FAIMS spectra of $[MMA+K]^+$ and $[SA+K]^+$ at drying gas temperature 100 ˚C with DF set to (a) 200 Td, (b) 220 Td, (c) 240 Td; and at drying gas temperature 150 ˚C with DF set to (d) 200 Td, (e) 220 Td, and (f) 240 Td

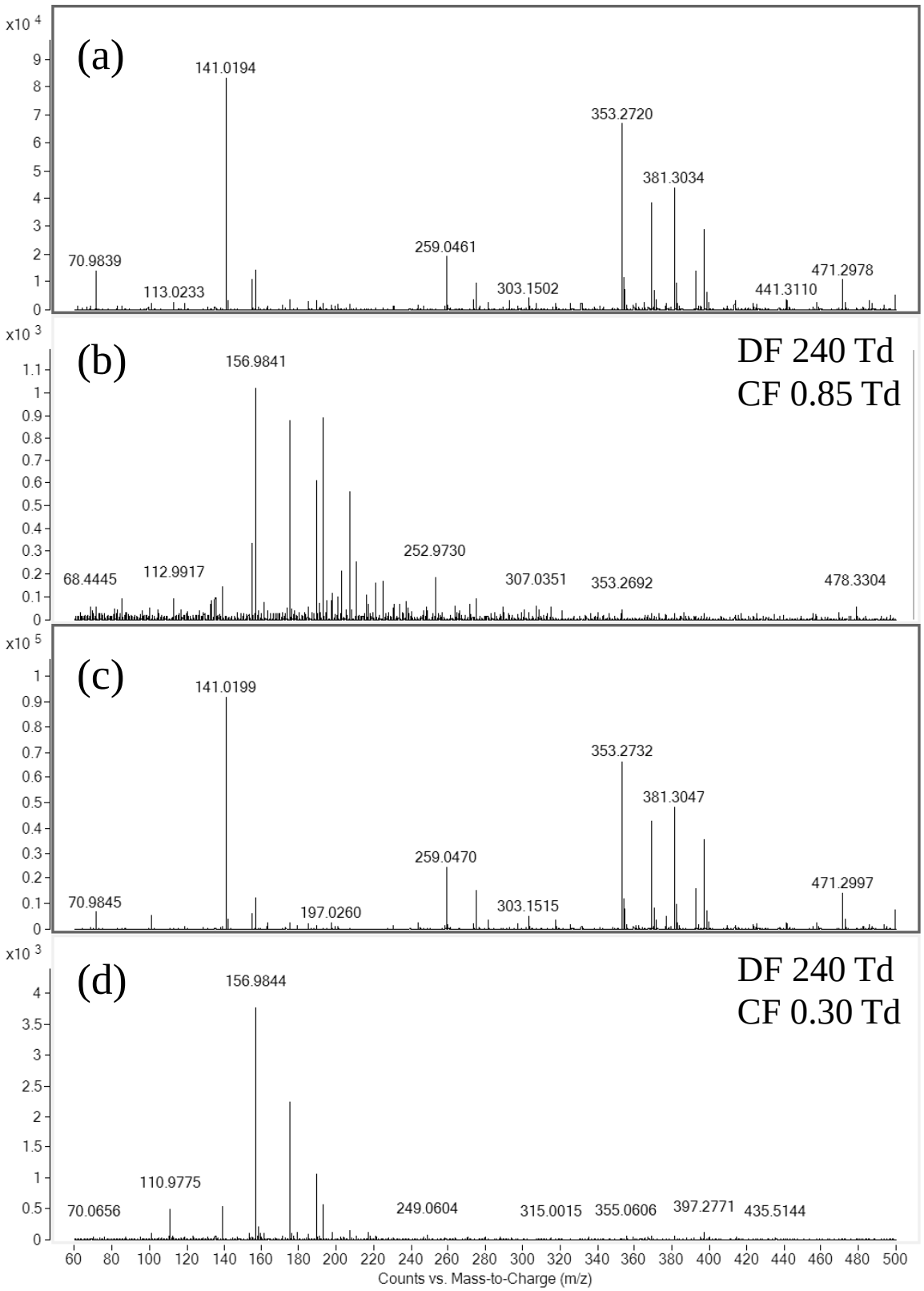

Figure 2.10 Mass spectra of MMA using (a) ESI-MS and (b) ESI-FAIMS-MS (DF 240 Td, CF 0.75 Td); and SA using (c) ESI-MS and (d) ESI-FAIMS-MS (DF 240 Td, CF 0.30 Td) with the drying gas set to 100 ˚C and with potassium chloride in solution to promote formation of potassium adducts

2.4.2.2 2β- and 6β-hydroxytestosterone

2β-hydroxytestosterone (2β-HT) and 6β-hydroxytestosterone (6β-HT) are isobaric anabolic steroids with no unique MRM transition making them challenging to determine by mass spectrometry without chromatographic separation. Currently chromatographic methods offer the desired selectivity, but the analysis time is increased because of the chromatographic separation. There is a need for faster, high-throughput methods for the determination of 6β-HT, particularly at the early stages of testing potential drug candidates. Rapid online-solid phase extraction (SPE) techniques offer a fast way to clean up samples prior to introduction into a mass spectrometer but do not separate 2β-HT and 6β-HT. FAIMS has the potential to offer a fast separation step that can filter ions before they enter the mass spectrometer and was investigated for 2β-HT and 6β-HT.

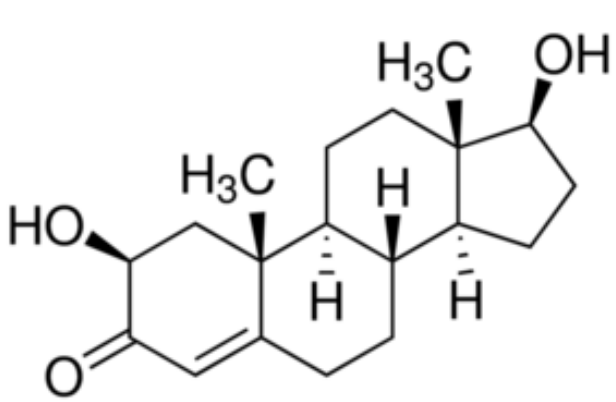

2β-hydroxytestosterone

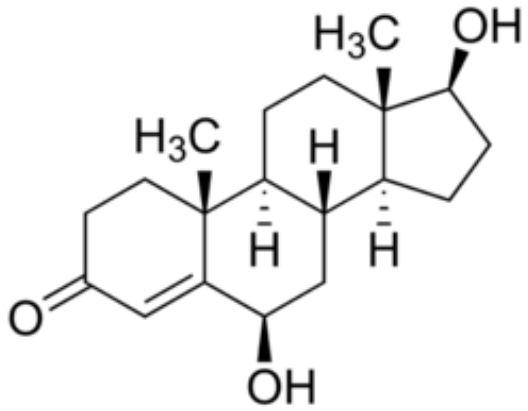

6β-hydroxytestosterone

The effect of temperature on peak location of the 2β-HT and 6β-HT isomers is shown in Figure 2.11.a-c. Peak height is highest at 150 ˚C but at 50 ˚C the two isomers are better resolved. The DF 240 Td is temperature adjusted in the FAIMS software, a positive shift for both isomers at lower temperature is observed and a better separation achievable at lower temperatures. The reason for the better resolution at 50 ˚C is that a lower temperature allows ions in the low-field stage of the asymmetric waveform to be more clustered making a greater difference between clustered and unclustered ions in the respective low and high field portions of the cycle. Optimum separation was determined to be at DF 232 Td with CF 1.9 Td for 2β-HT and CF 1.5 Td for 6β-HT with the drying gas set to 50 ˚C (Figure 2.12.a). FAIMS-MS was combined with LC to demonstrate the separation of the mixture. Injection of a mixture onto a C18 column and analysis by LC-MS shows two resolved peak for 6β-HT (RT = 4.4 mins) and 2β-HT (RT = 4.75 mins) (Figure 2.12.b). FAIMS selection of ions at a

CF of 1.9 Td results in the preferential selection of 6β-HT with only a baseline response for 2β-HT (Figure 2.12.c-d).

FAIMS separation may therefore be combined with off-line SPE for the selective determination of 6β-HT in the presence of 2β-HT. However, compatibility with online-SPE (featuring higher flow rates) requires the drying gas temperature to be at least 150˚C to prevent contamination of the ionisation source and aid desolvation to give sufficient signal for detection and low levels.

Initially, separation at a higher temperature (150˚C) was attempted but, at temperatures >100 ˚C the required selectivity (5%) was lost and even setting the DF to 280 Td does not give the required selectivity (Figure 2.13.a). An alternative approach of adding solvents to carrier gas of FAIMS device is described in detail in the next chapter (Chapter 3). The addition of a water vapour (1% v/v) resulted in an improvement in separation at the higher drying gas temperature (150 ˚C) with the DF set to 300 Td and the sheath gas set to 250 ˚C. The higher drying gas temperature will aid desolvation and help prevent contamination of the source. The sheath gas is a heated gas that surrounds the ESI ion beam and can improve sensitivity. Increasing the sheath gas from 250˚C to 350˚C increases the signal for 6β-HT by ~3-fold without loss of selectivity (Figure 2.13.c).

The FAIMS method was transferred to a triple quadrupole fitted with a miniaturised FAIMS chip, where the MRM transition *m/z* 305.2>269.4 will improve sensitivity. Optimising the FAIMS separation on the triple quadrupole MS, shows sufficient separation at DF 305 Td with 1.5 % water (Figure 2.14). At CF 1.65 Td and DF 305 Td (1.5 % water), there is a %RSD of 6.9% on the peak height of 6β-HT with 3.6% interference from 2β-HT, which is within the acceptable range (<5 %) for the quantitative determination of 6β-HT.

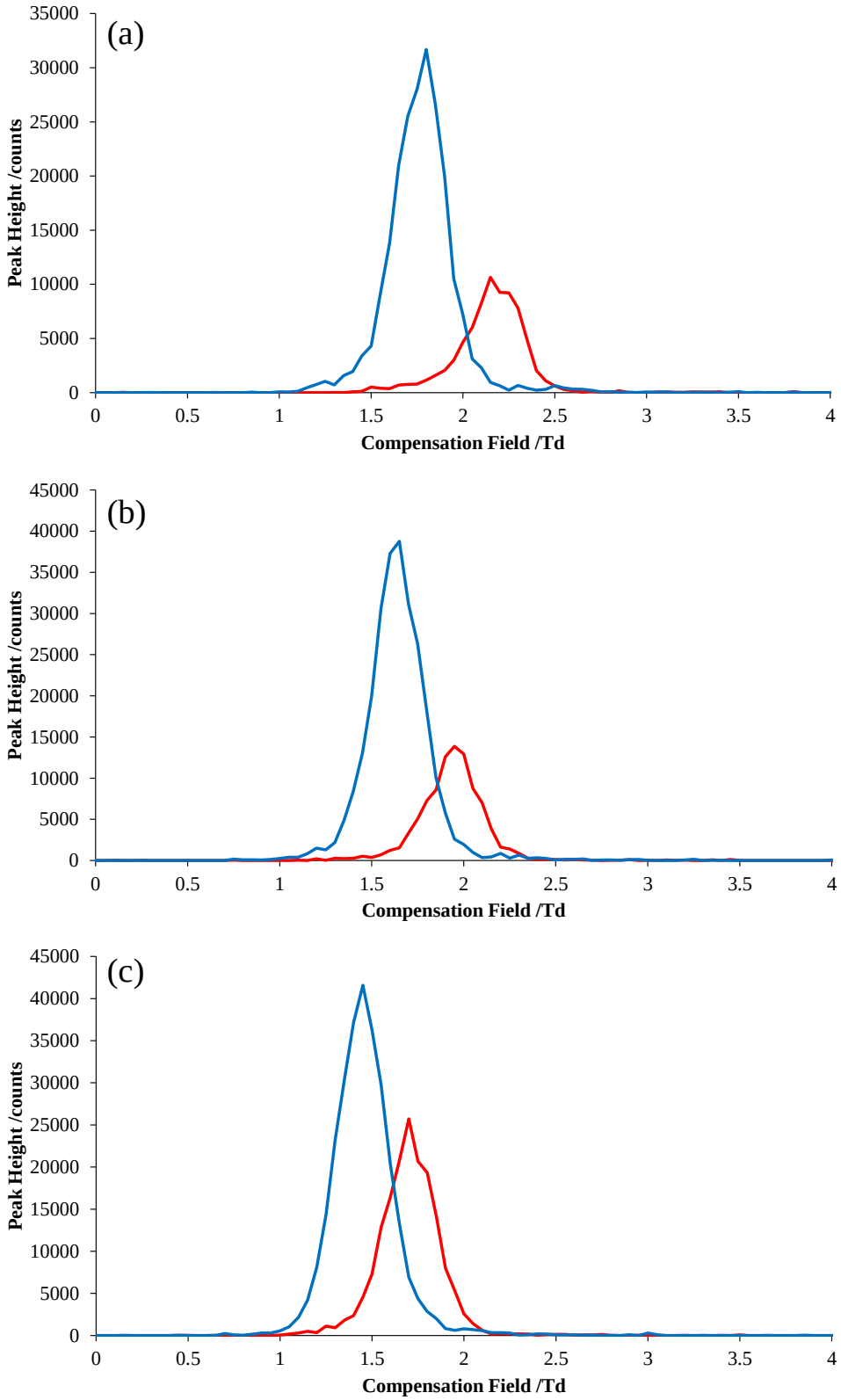

Figure 2.11 FAIMS spectra of 2β-HT (red) and 6β-HT (blue) at DF 240 Td with the drying gas set to (a) 50˚C, (b) 75˚C, and (c) 100˚C

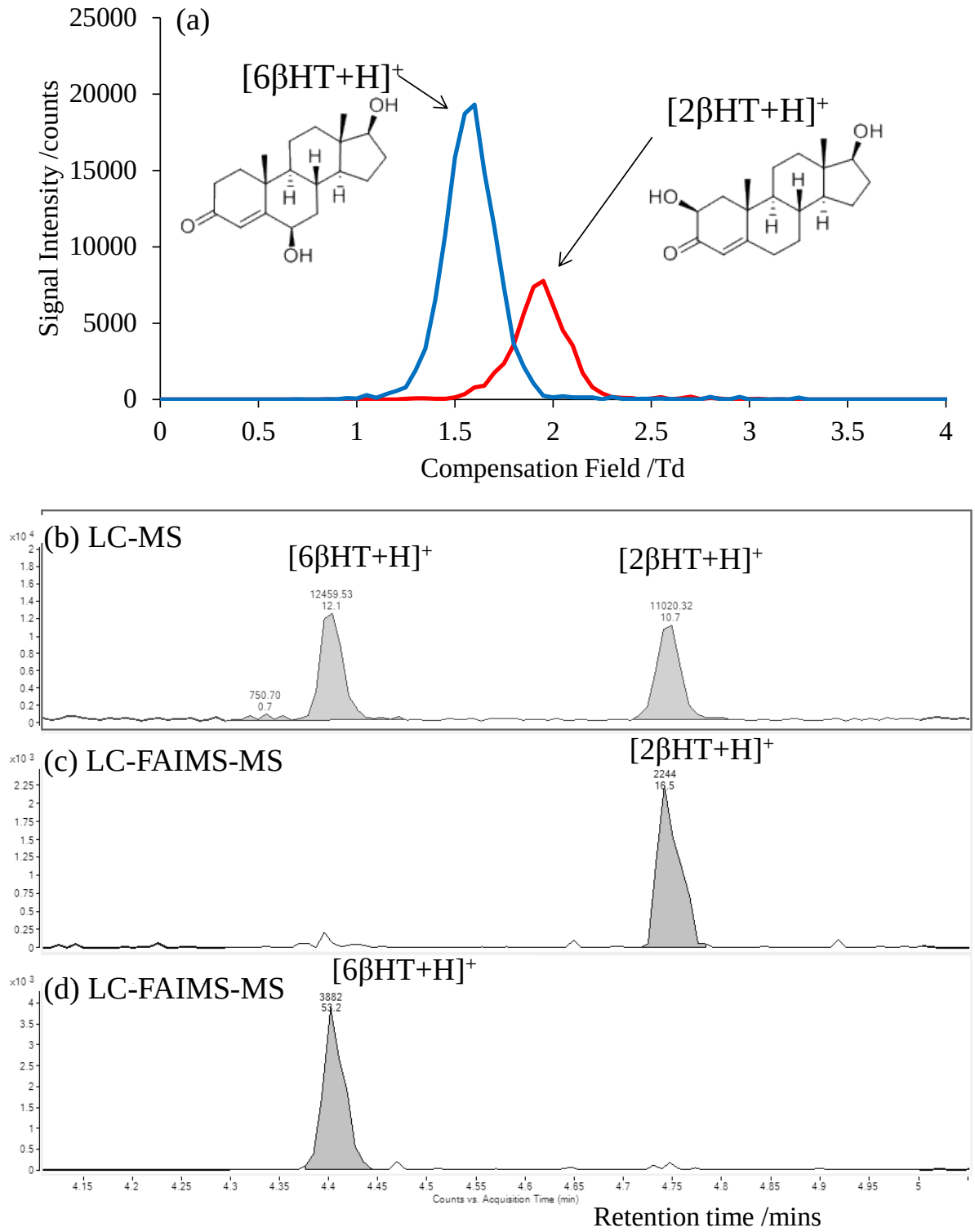

Figure 2.12 Selected ion response of 2β- and 6β-HT at 0.1μM (*m/z* 305.2111 ±0.02) with the drying gas set to 50˚C using (a) direct infusion-FAIMS-MS (DF 232 Td), (b) LC-MS (FAIMS off), (c) LC-FAIMS-MS (CF 1.9 Td, DF 232 Td), (c) LC-FAIMS-MS (CF 1.5 Td, DF 232 Td)

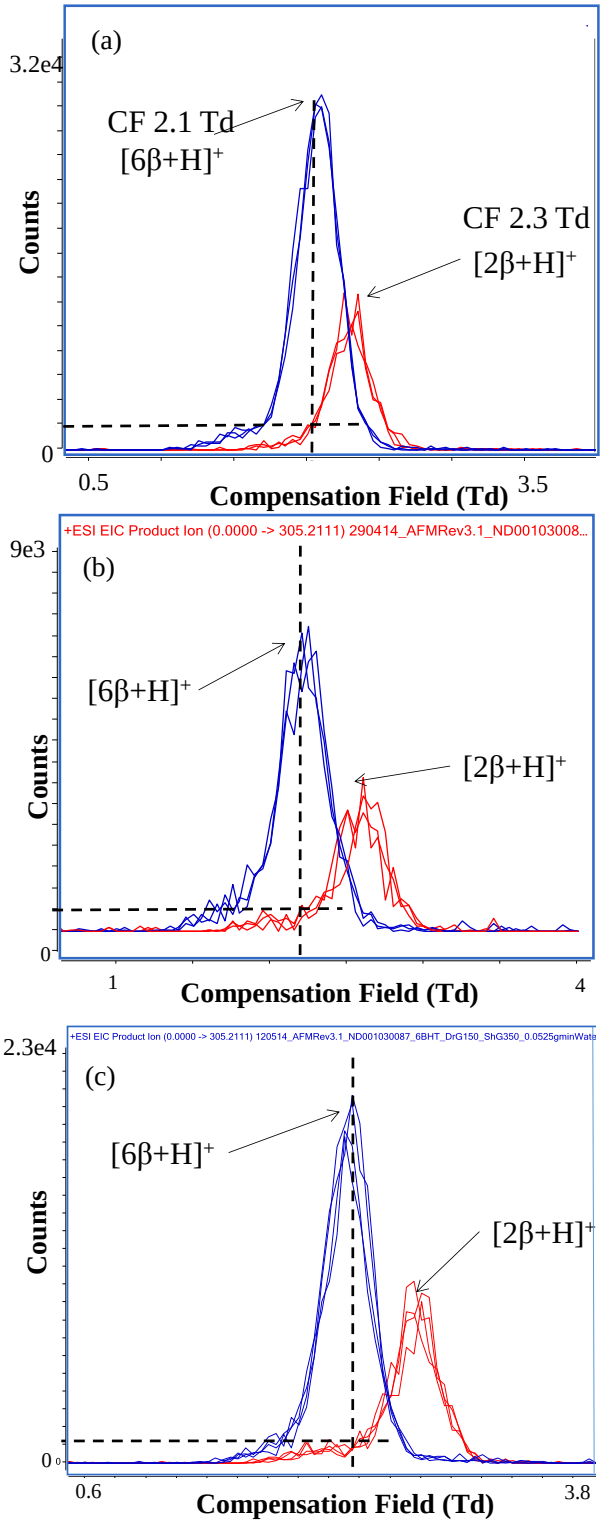

Figure 2.13 Selected ion response (*m/z* 305.2) showing FAIMS spectra of 2β-HT (red) and 6β-HT (blue) with the drying gas set to 150˚C with (a) dried nitrogen, DF 280 Td and sheath gas set to 250˚C; (b) 1% water (v/v) added to the drying gas, DF 300 Td and sheath gas set to 250˚C, and (c) 1% water (v/v) added to the drying gas, DF 300 Td and sheath gas set to 350˚C

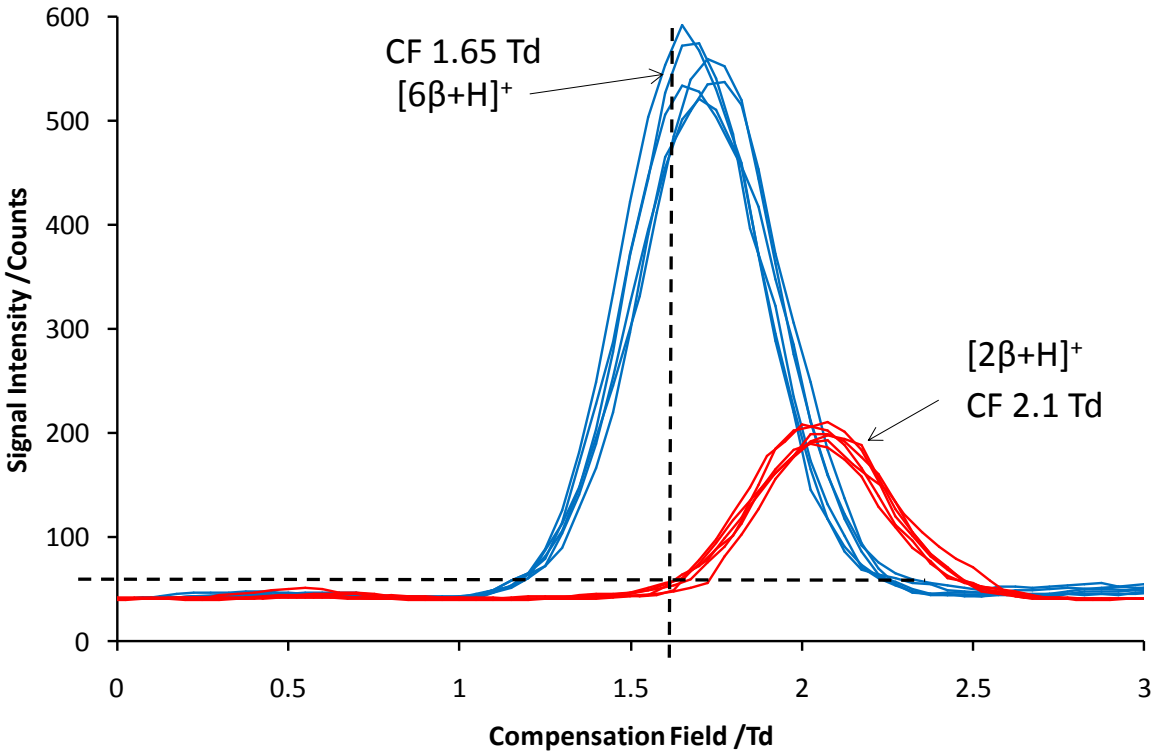

Figure 2.14 SRM (305.2>269.4) showing FAIMS spectra of 2β-HT (red) and 6β-HT (blue) at DF 305 Td with the drying gas set to 150˚C and sheath gas 350˚C with 1.5% water (v/v) added to the drying gas

Quantitative performance was evaluated by using loop injections to produce data similar to an online-SPE method. Standards of 2β-HT and 6β-HT were used to test the potential for the separation. Loop injections of 6β-HT alone and a mixture of the 6β-HT and 2β-HT (both at 1 µM) are shown in Figure 2.15. Without a FAIMS separation the peak is observed for 6β-HT when 2β-HT is absent from the sample (Figure 2.15.a). However with 2β-HT present the peak area is much higher (Figure 2.15.b) showing that there is a considerable amount of interference contributed by the presence of 2β-HT at equimolar concentration to 6β-HT. Figure 2.15.c and d show loop injections of 6β-HT in the absence of 2β-HT and 6β-HT with 2β-HT. The corresponding peak areas for the SRM transition (305.2>269.4) being 4123 and 4343 when setting the FAIMS to transmit 6β-HT selectively at 1.65 Td. Little difference is observed between the samples with and without 2β-HT present due to the significant reduction in interference from 2β-HT resulting from the FAIMS separation.

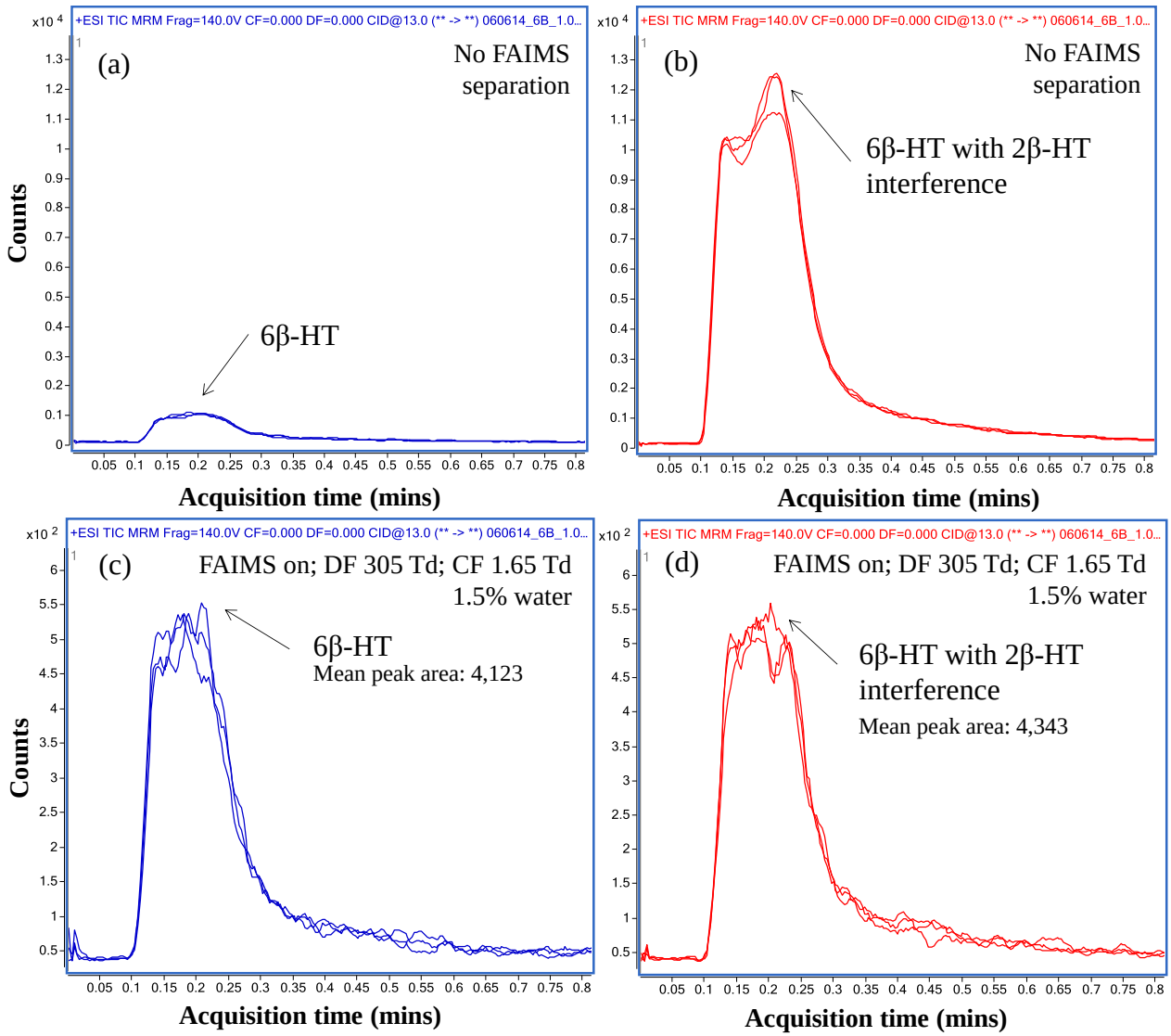

Figure 2.15 Loop injections-ESI-MS (no FAIMS) of (a) 6β-HT (1 μM), (b) 2β-HT and 6β-HT (1 μM); Loop injections-ESI-FAIMS-MS (DF 305 Td, CF 1.65 Td, 1.5% water) of (c) 6β-HT (1 μM), and (d) 2β-HT and 6β-HT (1 μM)

Setting FAIMS to transmit 6β-HT also reduces the absolute signal, particularly at high DF, but comparison of DF = 0Td and DF = 305 Td (Figure 2.16) shows that despite a 2-fold drop in signal, the signal-to-noise ratio is doubled with the DF set to 305 Td, demonstrating the advantage of noise reduction by FAIMS helping to improve low levels of quantitation even in the SRM transition 305.2>269.4.

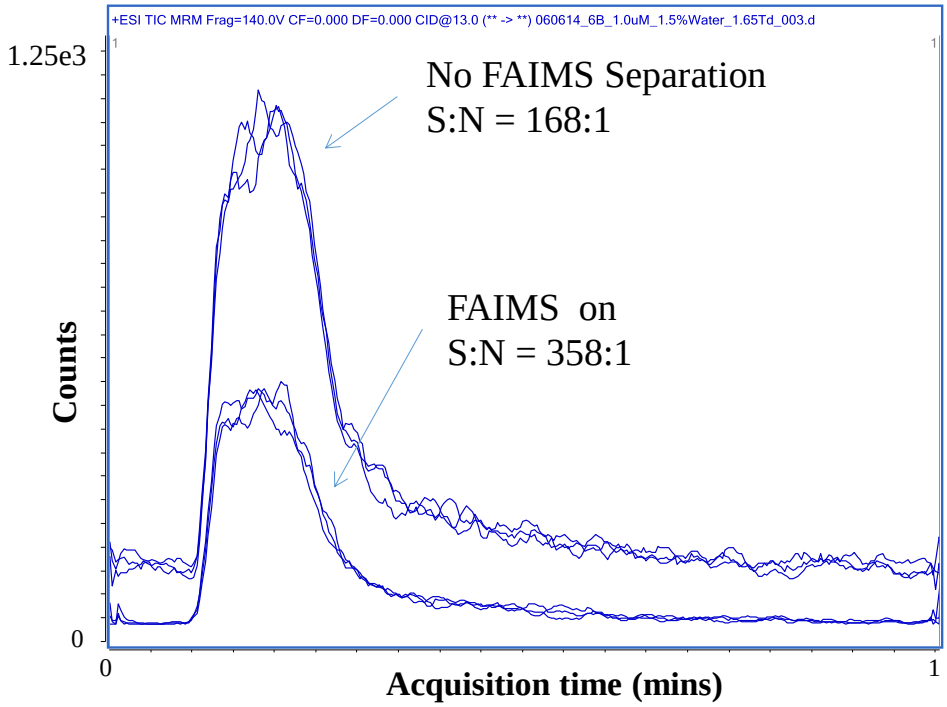

Figure 2.16 Selected ion response (m/z 305.2) of 6β-HT (1 µM) analysed using Loop injections-ESI-MS (no FAIMS) and Loop injections-ESI-FAIMS-MS (DF 305 Td, CF 1.65 Td, 1.5% water)

The use of a FAIMS separation for the quantitative determination of 6β-HT was further investigated by producing calibration plots using loop injections of 6β-HT and a mixture of 6β-HT and 2β-HT without FAIMS separation (Figure 2.17.a and b) and with DF set to 305 Td, CF set to 1.65 Td, with 1.5 % water added to the carrier gas to selectively transmit 6β-HT (Figure 2.17 c and d). Figures 2.17.a and 2.17.c show that for 6β-HT without 2β-HT present, both calibration plots produced with and without FAIMS are comparable, where good over the range 0.1 µM to 5 µM is observed. The lowest concentration used in Figure 2.17.c was used to estimate that the LOQ, which is below the required 0.17 µM, with a signal-to-noise at 0.1 µM of 34:1. The calibration plot of 6β-HT with 2β-HT interference present and without FAIMS selection show a loss in linearity and poor R^2 value of 0.465 (Figure 2.17.b) which could not be used for quantitative determination of 6β-HT even at high levels. The addition of FAIMS pre-selection of 6β-HT demonstrates that removal of 2β-HT regains the linear trend between peak area and concentration of 6β-HT with good precision (R^2 = 0.999). The potential for using FAIMS combined with a fast method of sample introduction is demonstrated and is advantageous where chromatographic separation is not available on the timescale required in the fast-paced drug discovery industry.

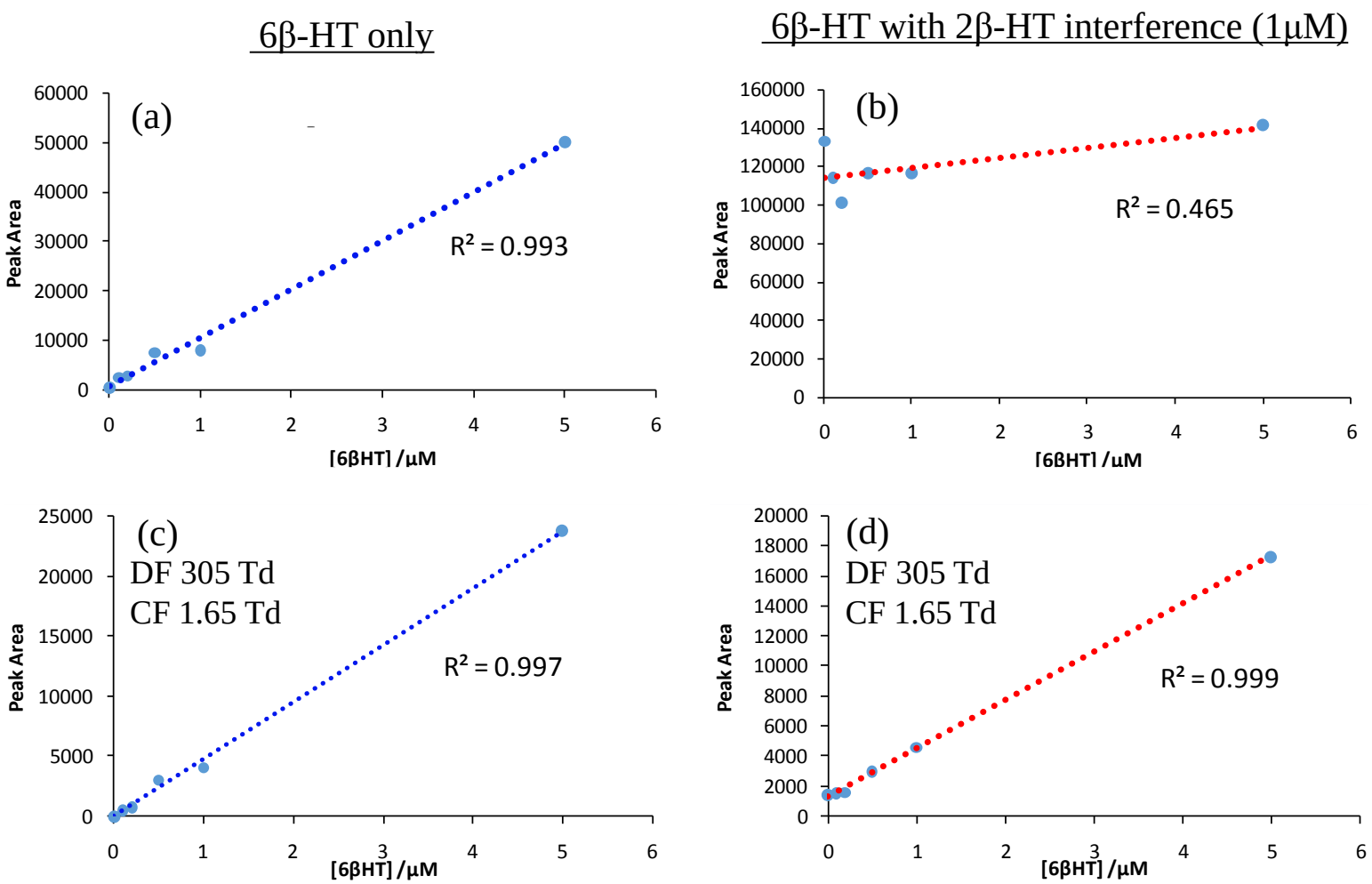

Figure 2.17 Calibration plots showing peak area against [6β-HT] using Loop injection-MS of (a) 6β-HT, (b) 6β-HT with 2β-HT (1μM); and using loop injection-FAIMS-MS (DF 305 Td, CF 1.65 Td, 1.5% water) of (a) 6β-HT, (b) 6β-HT with 2β-HT (1μM)

2.4.2.3 DI-FAIMS-MS and DI-FAIMS-in-source CID-MS Analysis of Pharmaceutical Excipients

Ions derived from the pharmaceutical excipients 2-hydroxy-4-octyloxybenzophenone (HOBP, m/z 327.1955) and PEG 400 were chosen as test analytes because the protonated HOBP and PEG n=7 oligomer (m/z 327.2013) are sufficiently close in mass (17.7 ppm mass difference) that these ions could not be resolved by the reflectron TOF mass analyser (resolving power required ~ 130K). Robust accurate mass measurement of these ions is therefore not possible without separation prior to mass analysis. The two components were analysed as a mixture containing a 20 fold molar excess of the PEG (Figure 2.18). CV sweeps (-1 to +4 V) with the DF set to 48 kV/cm were used to determine the optimum CV required for selected transmission of protonated HOBP and PEG, and subsequent in-source fragmentation. The selected ion response for m/z 327.2 (Figure 2.18) shows that the protonated PEG n=7 and HOBP ions are resolved by FAIMS.

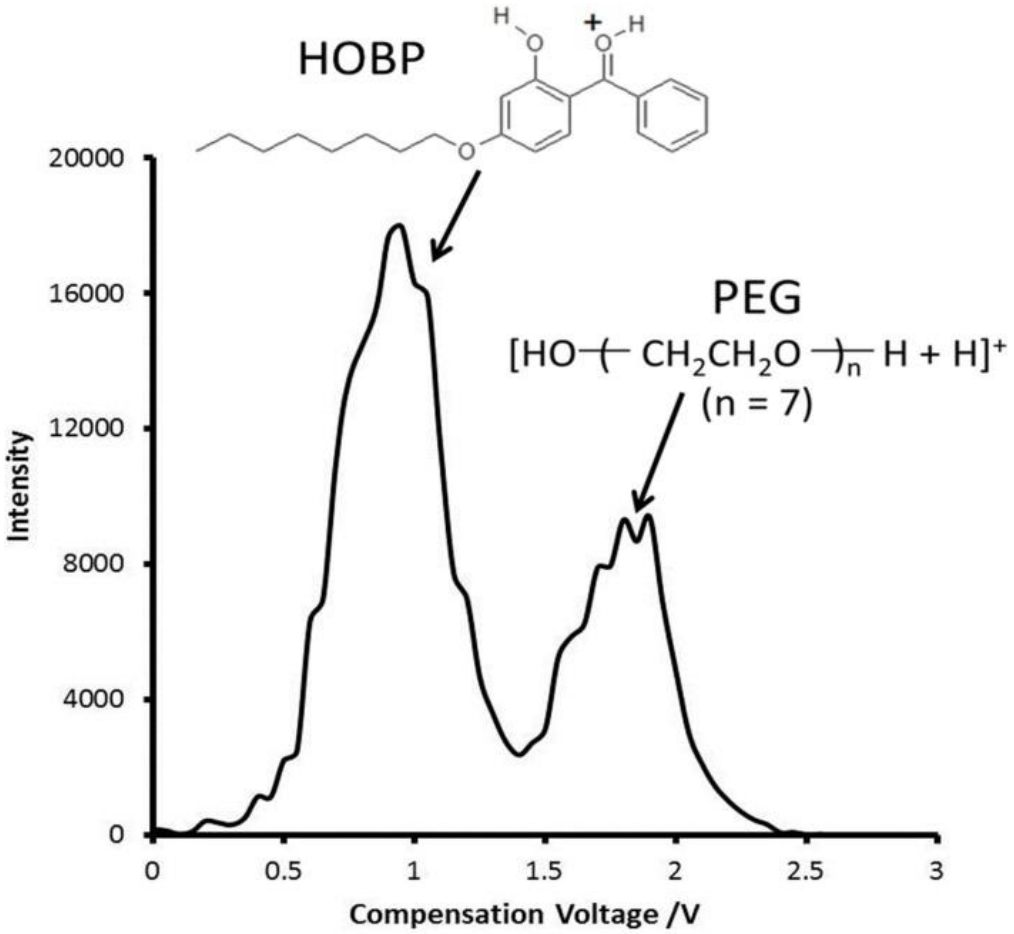

Figure 2.18 FAIMS-MS CV spectrum (m/z 327.2) of HOBP and PEG 400 at DF 48 kV/cm

The mass spectrum of the mixture without FAIMS separation (Figure 2.19.a) shows the typical polymer distribution of PEG ions, with the HOPB unresolved from the protonated PEG (n=7) ion. The measured mass of the overlapping peaks is m/z 327.1994, a mass difference of 11.9 and -5.8 ppm from HOBP and PEG respectively. In-source CID-MS of this mixture gives a complex product ion spectrum dominated by PEG fragment ions (Figure 2.19.b). Quasi-static FAIMS filtering (CV range 0.6– 0.7 V, DF 48 kV/cm) was used to transmit the HOPB ion selectively, which appears as the base peak in the resulting mass spectrum (Figure 2.19.c), with an observed mass of 327.1966 (3.3 ppm). The FISCID-MS product ion spectrum of the FAIMS-selected HOBP ion (Figure 2.19.d) shows the HOBP fragment ions free of interference from PEG fragment ion peaks, reducing the complexity of the mass spectrum and allowing unambiguous identification of the HOBP fragments.

These observations demonstrate the mass spectral enhancement possible using FISCID-MS, through the FAIMS pre-selection of a precursor ion in a complex mixture, on the basis of differential mobility, prior to in-source CID. FISCID-MS allows the unresolved ions to be separated and a clean product ion spectrum to be obtained for HOBP using a single mass analyser with only minor modification of the ion source to incorporate the miniaturized FAIMS device.

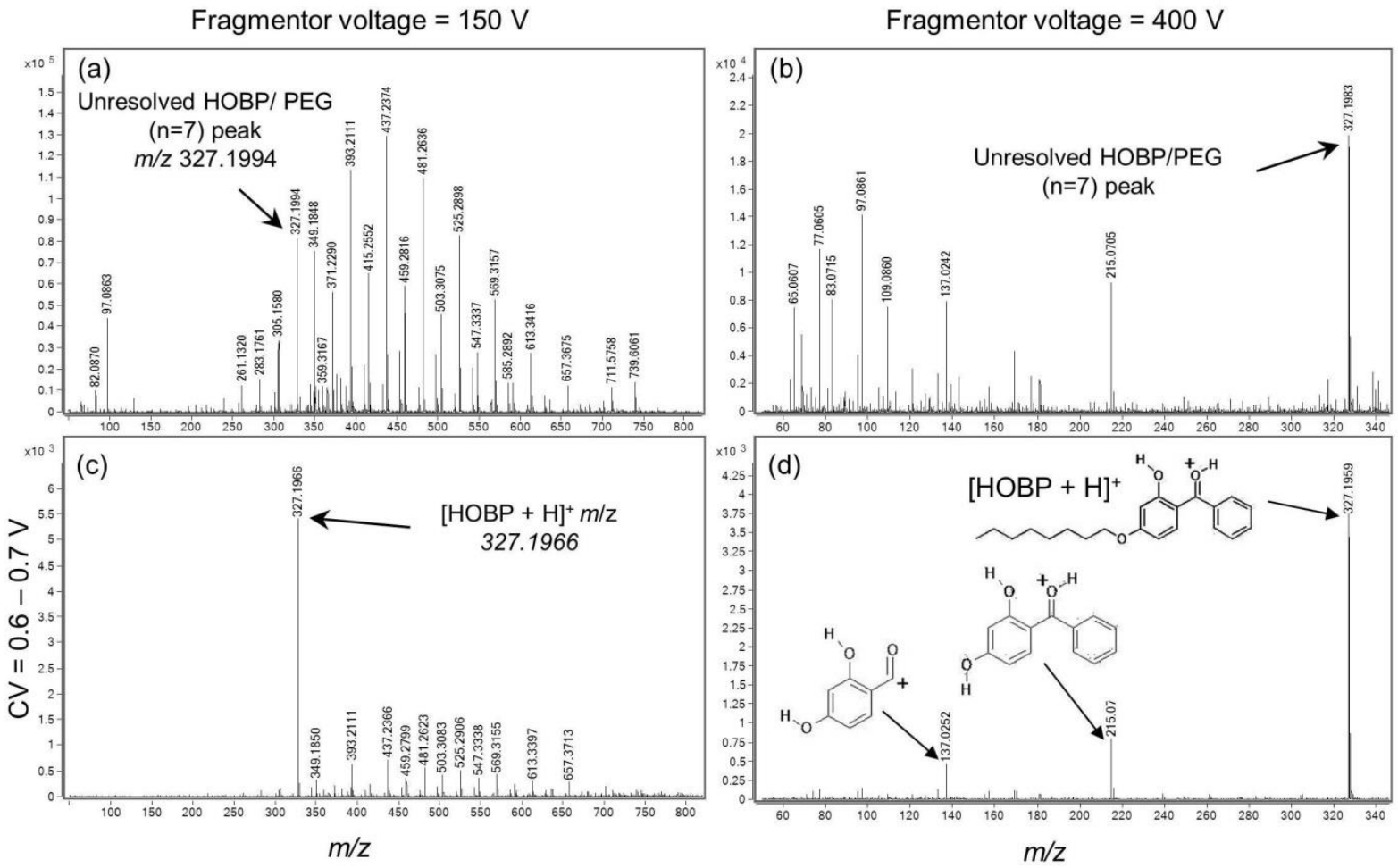

Figure 2.19 MS, FAIMS-MS and FISCID-MS mass spectra of a mixture of HOBP and PEG 400 (1:20 molar ratio): (a) without FAIMS separation or in-source CID, (b) In- source CID-MS without FAIMS separation, (c) FAIMS-selected HOBP ion (CV = 0.6–0.7 V) without in-source CID; (d) FISCID-MS product ion spectrum of the FAIMS-selected HOBP ion with in-source CID.

2.5 Conclusions

The CCD experiment shows the FAIMS device exhibits a stable CV over a range of conditions meaning that once optimum FAIMS conditions are established, the solvent composition and flow rate of the HPLC and source conditions can be changed without causing significant changes in FAIMS spectra. A plot of %transmission against *m/z* showed that transmission and higher DFs is more critical for smaller ions, ions higher than 500 Th experience less than 2-fold loss in transmission.

Separation of isobaric ions cannot always be achieved by increasing DF alone. The formation of deprotonated ions and adducts formed with group I metal ions and changing the temperature at the chip can potentially improve the separation of isobaric ions with similar functionality. However, whilst a lower temperature may offer an improvement in separation, higher temperatures are required for better desolvation. Adding water or other modifiers to the carrier gas may be an alternative for improving selectivity at higher gas temperatures. The potential to distinguish between isomers was not the only advantage observed when using FAIMS, reduction in chemical noise and simplification of mass spectra was also observed. Fragmentation mass spectra generated by in-source CID of FAIMS-selected ions provide enhanced selectivity for the qualitative and quantitative analysis of analytes in complex mixtures. FISCID-MS successfully separated pharmaceutical excipient ions that are too close in *m/z* value to be resolved by TOF-MS alone, providing improved accurate mass measurement and product ion spectrum free from interferences. FISCID-MS therefore offers significant improvements in selectivity for the mass spectrometric analysis of analytes using a single mass analyser, such as a TOF or quadrupole analyser, and has potential as an alternative to LC-MS/MS for qualitative and quantitative analysis, or for further enhancing selectivity using LC-FISCID-MS/MS routines.

2.6 References

(1) Staubs, A. E.; Matyjaszczyk, M. S. In *2008 IEEE Conference on Technologies for Homeland Security*; IEEE, 2008; 199–204.

(2) Shvartsburg, A. A.; Smith, R. D.; Wilks, A.; Koehl, A.; Ruiz-Alonso, D.; Boyle, B. *Anal. Chem.* **2009**, 81, 6489–95.

(3) Shvartsburg, A.A. Differential Ion Mobility Spectrometry: Nonlinear Ion Transport and Fundamentals of FAIMS, CRC Press, 2008.

(4) Barnett, D. A.; Ding, L.; Ells, B.; Purves, R. W.; Guevremont, R. *Rapid Commun. Mass Spectrom.* **2002**, 16, 676

(5) Rorrer III, L. C.; Yost, R. A. *Int. J. Mass Spectrom.* **2011**, 300, 173

(6) Barnett, D. A.; Purves, R. W.; Ells, B.; Guevremont, R. *J. Mass Spectrom.* **2000**, 35, 976

(7) Brown, L. J.; Toutoungi, D. E.; Devenport, N. A; Reynolds, J. C.; Kaur-Atwal, G.; Boyle, P.; Creaser, C. S. *Anal. Chem,* **2010**, 82, 9827.

(8) Wu, S. T.; Xia, Y. Q.; Jemal, M. *Rapid Commun. Mass Spectrom.* **2007**, 21, 3667

(9) Barnett, D. A.; Ells, B.; Guevremont R.; Purves, R. W. *J. Am. Soc. Mass Spectrom.* **2002**, 13, 1282

(10) Guevremont, R.; Purves, R. W. *J. Am. Soc. Mass Spectrom.* **1999**, 10, 492.

(11) Eiceman, G. A.; Krylov, E. V.; Tadjikov, B.; Ewing, R. G.; Nazarov, E. G.; Miller, R. A. *Analyst.* **2004**, 129, 297.

(12) Xia, Y.-Q.; Jemal, M. *Anal. Chem.* **2009**, 81, 7839.

(13) Coy, S. L.; Krylov, E. V.; Schneider, B. B.; Covey, T. R.; Brenner, D. J.; Tyburski, J. B.; Patterson, A. D.; Krausz, K. W.; Fornace, A. J.; Nazarov, E. G. *Int. J. Mass Spectrom.* **2010**, 291, 108.

(14) Magera, M. J.; Helgeson, J. K.; Matern, D.; Rinaldo, P. *Clin. Chem.* **2000**, 46, 1804–10.

(15) Kushnir, M. M.; Komaromy-Hiller, G.; Shushan, B.; Urry, F. M.; Roberts, W. L. *Clin. Chem.* **2001**, 47, 1993–2002.

(16) Shvartsburg, A. A.; Smith, R. D.; Wilks, A.; Koehl, A.; Ruiz-Alonso, D.; Boyle, B. *Anal. Chem.* **2009**, 81, 6489.

(17) Shvartsburg, A. A.; Tang, K.; Smith, R. D.; Holden, M.; Rush, M.; Thompson, A.; Toutoungi, D. *Anal. Chem.* **2009**, 81, 8048.

(18) Yuan, C.; Gabler, J.; El-Khoury, J. M.; Spatholt, R.; Wang, S. *Anal. Bioanal. Chem.* **2012**, 404, 133–40.

Chapter Three

Investigation of the Effect of Alcohol Gas Modifiers on Chip-Based FAIMS Separations of Peptides, Proteins and Small Molecules

3.1 Chapter Overview

This chapter describes the development of a method for introducing solvent modifiers into the FAIMS carrier gas with the aim of investigating the effect on ion separation and conformer distribution. A modifier system was constructed for the introduction of methanol and butanol modifiers (0.1-2% v/v) and evaluated using small molecules, peptides and proteins. The separation of the small molecules was strongly influenced by the DF, modifier type and modifier concentration. The CF spectra of the peptides investigated showed narrower peaks in the presence of modifiers than when alcohol modifiers were absent, where broad peaks were associated with changes in conformations or solvation of the peptide ions conformers. The narrower peaks aided in distinguishing between peptides with variations in amino acid sequence. Proteins ions also showed sharper CF peaks in the presence of alcohol modifiers and changes in charge distribution.

3.2 Introduction

A variety of methods have been utilised to improve FAIMS separations. These methods have included: changing the analyser gap width/geometry; temperature; waveform shape and frequency; ion residence time; and carrier gas composition which were all discussed in Chapter 1. Forming different adducts with group I metal ions was also shown to be effective in Chapter 2. The carrier gas typically consists of dried nitrogen or nitrogen/helium mixtures[1,2] and under these conditions sufficient separation cannot always be achieved by changing DF and temperature, and high consumption of helium can also prove expensive for routine use which has led to exploration of alternative methods. Changing the composition of the carrier gas by the addition of modifiers is an alternative approach to improving separations, where mixtures of gases and solvent vapour modifiers alter the alpha coefficient.[3,4] Using solvent vapour to modify the carrier gas of FAIMS analysers has been reported to significantly increase in selectivity[5] and lower costs associated with reducing the consumption of helium. Gas modifiers are neutral molecules that compete with the ion-dipole clustering/declustering mechanism of other molecules found in the nitrogen carrier gas. The non-covalent interaction between gas modifier and analyte ion makes it possible, in principle, to select a gas modifier based on these interactions to improve selectivity between analytes with different chemical properties.[5]

Methods for introducing liquid modifier vapours into the carrier gas have either used a bubbler system[6] or direct infusion of a liquid into a heated region through to the carrier gas.[4]

Gas modifiers compete with the clustering/declustering mechanism, changing the CCS of clustered ions, particularly in the low field portion of the asymmetric waveform and increase the difference between the clustered and partially, or fully declustered ion, potentially improving separation and analytical space.[7]

The effects of modifying the carrier gas of a miniaturised FAIMS device using different alcohol modifiers was investigated using small isobaric molecules (phthalic acid isomers), peptides and proteins. To date, studies with gas modifiers have been focussed on smaller molecules (<1000 Da), where clustering with gas modifiers creates a bigger difference between the low field and high field CCS and offer a greater chance of improving separation. The effect of modifiers on larger molecules (e.g. proteins) has not been described in the literature. These studies have the potential to provide new insight into the effect of alcohol modifiers on the FAIMS spectra of larger biomolecules.

3.3 Materials and Methods

3.3.1 Chemicals

Phthalic acid, isophthalic acid, terephthalic acid, bradykinin acetate, bombesin, MRFA, MFAR, cytochrome C, ammonium acetate, methanol (HPLC grade), water (HPLC grade), formic acid and 2-butanol were obtained from Sigma aldrich.

3.3.2 Sample Preparation

Phthalic acid solutions were prepared in methanol and diluted using methanol/water (90:10 with 0.2 mM ammonium acetate) to a concentration of 60 nmol/µl. Peptide and protein samples were dissolved in methanol/water (50:50, 0.1% formic acid) and diluted to 10 pmol/µl.

3.3.3 Instrumentation

ESI-FAIMS-MS analyses

The chip-based FAIMS prototype device 2 (Owlstone, Cambridge, UK), previously described in Section 2.3.3, was located in the modified Jet Stream ESI source of an Agilent 6230 TOF MS. The asymmetric waveform was supplied by the dispersion field (DF) feeder unit through a hole in the desolvation assembly. The FAIMS device used in these studies had a 100 µm gap between the electrodes arranged as multiple parallel channels with a 700 µm path length.

Dispersion fields (200-300Td) were applied with a 27 MHz frequency and compensation field (CF) scanned between -5 and + 5 Td. Nitrogen (99.5% Purity) was used as the carrier gas for the FAIMS device and ESI source. Solvent modifier vapour was introduced into the drying gas line (which supplied the carrier gas to the FAIMS chip), using a constructed interface described below (Figure 3.1). Samples were directly infused (10-15μL/min) into the ESI ion source which was operated in negative ion mode for the phthalic acids and positive ion mode for proteins and peptides. ESI-FAIMS-MS conditions were: sheath and drying gas flows, 9 and 7 L/min; sheath and drying gas temperatures, 250°C and 150°C; nebuliser pressure, 35 psig; spray shield, 2500 V; capillary voltage and nozzle voltage, 3000 V and 2000 V respectively. Fragmentor voltage was varied between 150 and 300 V, MS acquisition rate was set to 10 scan/s.

Solvent Delivery System

The solvent delivery system was constructed in-house to enable introduction of aliphatic alcohol gas modifiers (up to 3% v/v) into the nitrogen carrier gas flow (Figure 3.1). Liquid solvent was introduced using either a syringe pump or a HPLC binary pump (Agilent 1200 series) at flow rates in the range 10-1000 μl/min using a standard PEEK union and tubing, connected to a stainless steel pipe (0.8 mm O.D., 0.6 mm I.D., 37.9 mm length, Swagelok) which passed through the tee-union (1/8 inch) and to the end of the nebuliser where it protruded (2.2 mm) from a piece of stainless tubing (1/16 inch O.D., 0.045 inch I.D., 123.1 mm length) fitted to the opposite end of the tee-union. PTFE tubing (1/4 inch) was fitted to the outlet of the drying gas line where it was connected to stainless steel tubing (1/8 inch) which formed a circle before connecting the tee-union. The gas would pass through the tee-union and around the stainless steel liquid line to provide gas (nitrogen) at the tip of the nebuliser. The interface was heated with heating cord (HTC-060, Omega Ltd), temperature controlled using a thermocouple (type K, RS Components Ltd.) in the range 80 ˚C - 120 ˚C, below the 150 ˚C of the drying gas to prevent temperature fluctuations in the FAIMS device, but high enough so that vapours would not condense before reaching the FAIMS device. The solvent delivery system was insulated to keep the temperature constant. Solvent vapour from the nebuliser passes through the stainless steel tubing (1/4 inch) to the drying gas inlet of the ESI source.

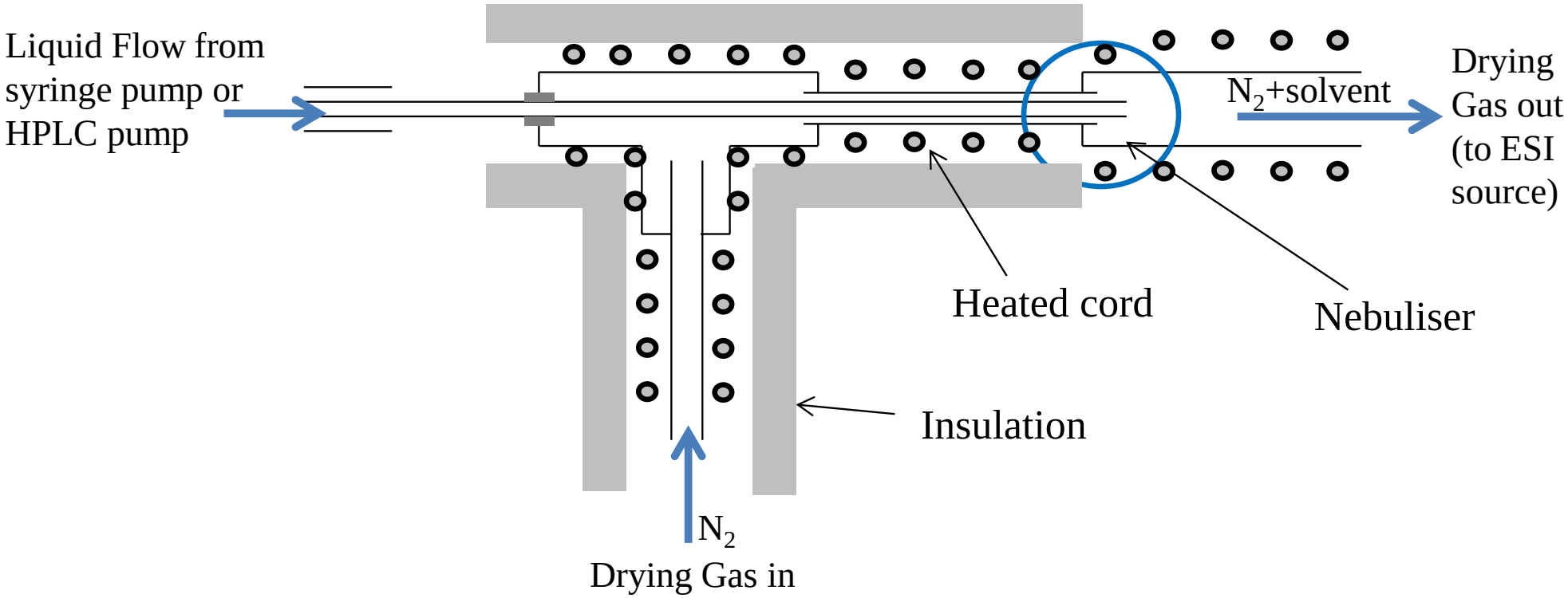

Figure 3.1 Schematic of solvent delivery system for introduction of solvent vapour modifiers into the drying gas, featuring a nebuliser and heating to the drying gas going in and to the modified drying gas going out for improving evaporation of the liquid solvent

3.4 Results and Discussion

The solvent vapour delivery system was constructed to introduce organic modifiers into the nitrogen carrier gas stream. The modifier interface was capable of vaporising a range of solvents including water, low molecular weight alcohols and acetonitrile to generate modifier concentrations up to 2 % (v/v) in nitrogen. Phthalic acid isomers were used initially as test compounds to evaluate effects of methanol and butanol modifiers on small molecules analysed by the miniaturised FAIMS. The effect of gas modifiers on larger molecules, such as proteins is also discussed in this section.

3.4.1 Solvent Vapour Clusters in the Mass Spectrum

The nebuliser solvent delivery system was assembled and tested externally from the mass spectrometer to assess if it could produce solvent vapour doped nitrogen. PTFE tubing was attached at the outlet of the nebuliser system to help assess whether a droplet free vapour was formed by visual inspection. Water was used to test the system because it is a more challenging solvent to evaporate than the aliphatic alcohols used for this study, due to its higher boiling point. Initially, a LC pump was used to introduce water (0.1-1 ml/min) to the nebuliser system. A mist of droplets was observed a short distance from the outlet of the nebuliser system as a result of incomplete desolvation of the water droplets. Heating cord (set to 100 ˚C) was used to heat the solvent delivery interface and nebuliser and pre-heat the gas to aid in the initial evaporation step. Heating the interface resulted in a clear, mist-free flow of modified nitrogen gas. Once a reliable system for evaporating liquids was established, the effect of introducing solvent vapours to the drying gas flow of the TOF mass spectrometer could be investigated.

Methanol vapour was initially introduced to the drying gas using methanol/water (50:50, 0.1% FA) ESI solution. Figure 3.2.a shows that when 1% (v/v) methanol vapour was added to the carrier gas, both singly protonated and sodiated clusters of methanol were observed in the mass spectrum with the n = 4 cluster of protonated methanol being the base peak. The peaks associated with methanol clusters were not observed in the absence of a methanol vapour. 2-butanol also produced several clusters with $[(BuOH)_3+H]^+$ being the base peak (Figure 3.2.b). I think that it is most likely that the observation of protonated $[(MeOH)_n+H]^+$ and $[(BuOH)_n+H]^+$ clusters (in the presence of methanol and butanol modifiers) arise as a result of proton transfer from protonated water clusters formed in the ESI source because of

the higher proton affinities of 2-butanol (815 kJ/mol) and methanol (761 kJ/mol) compared to water (697 kJ/mol).

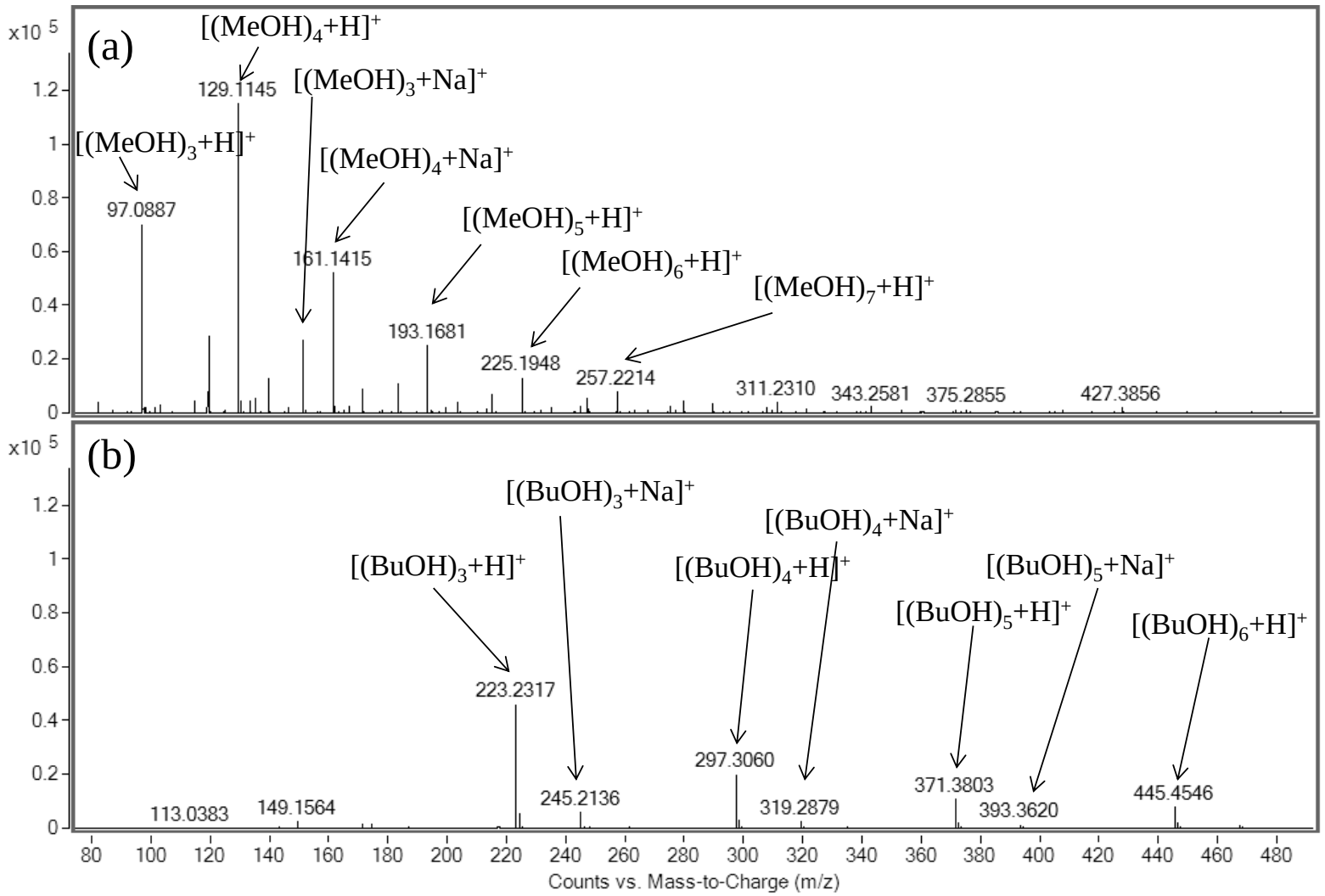

Figure 3.2 Mass spectra showing ESI-MS of methanol:water (50:50, 0.1% formic acid) analysed with (a) 1% methanol (v/v), and (b) 1 % 2-butanol added to the drying gas

3.4.2 Application of Gas Modifiers to Improve Separation of Phthalic Acid positional isomers

Separation of deprotonated isomeric o-, m- and p-phthalic acid is challenging using mass spectrometry alone and requires chromatographic or other pre-separation for them to be distinguished. Some differences are observed when using electron ionisation (EI) although this is not sufficient at low levels.[8] Infusion of each phthalic acid into the ESI-FAIMS-MS source was used to explore the potential for separation using FAIMS in dried nitrogen. The selected ion responses (SIR) of *m/z* 165 show that the phthalic acid isomers do not separate at DF 230 Td when using dried nitrogen as the carrier gas, although the location of CF maxima does vary for each isomer (Figure 3.3). Higher DFs do not improve the separation between the isomers.

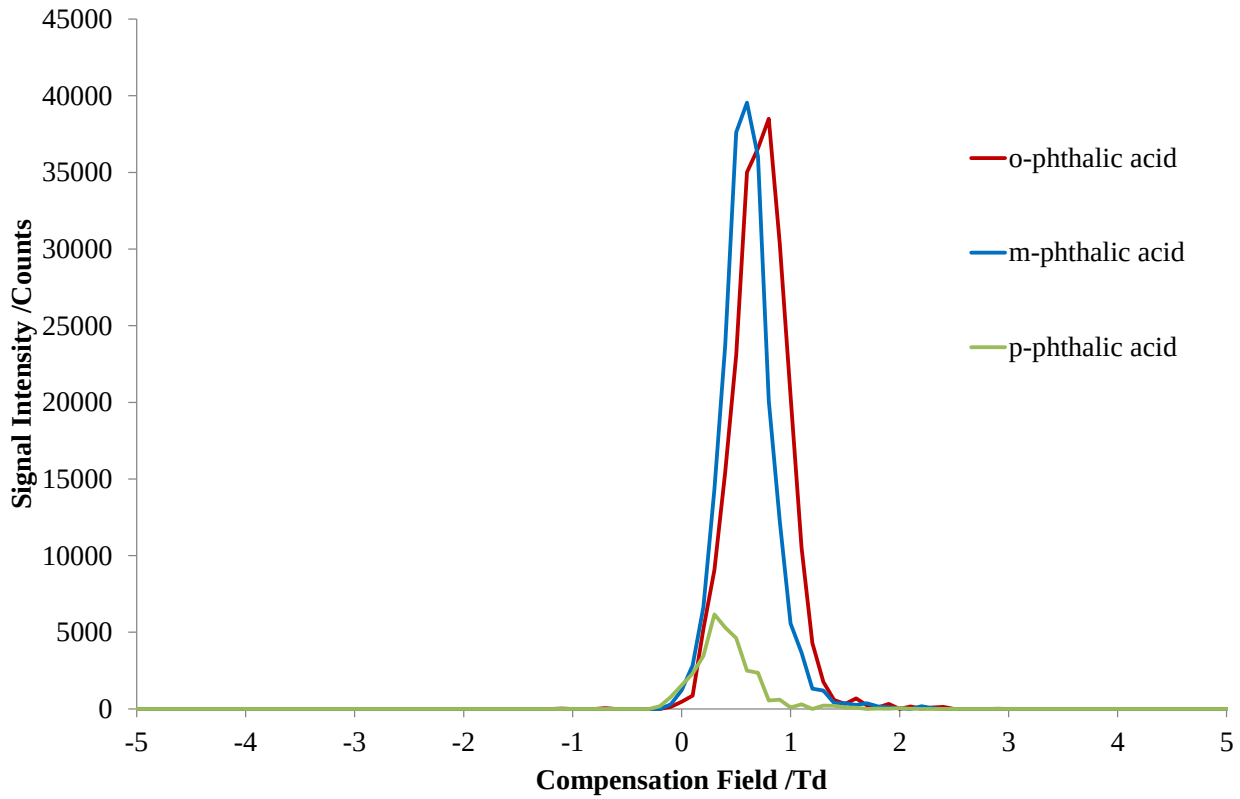

Figure 3.3 FAIMS spectra of o-phthalic acid (red), m-phthalic acid (blue) and p-phthalic acid (green) using a dried nitrogen carrier gas with the FAIMS device set to DF 230 Td

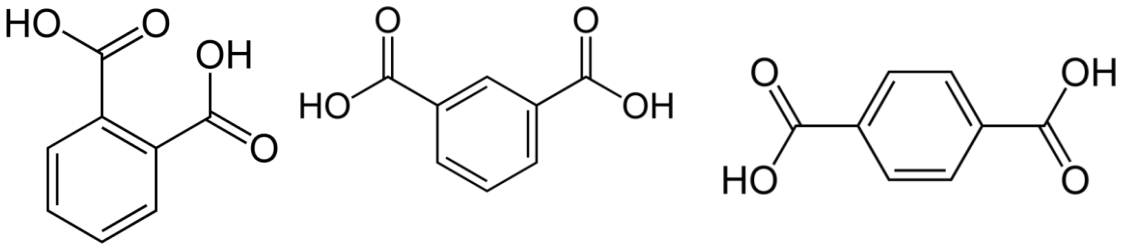

o-phthalic acid m-phthalic acid p-phthalic acid

The effect of methanol and 2-butanol modifiers was investigated over a range of concentrations and DF (200 to 300 Td). Methanol was increased from 0.01 % (v/v) methanol to 3 % methanol (v/v) No significant shift was observed up to 0.1 % but at higher modifier concentration all of the phthalic acid peaks began to shift towards a negative CF as shown in Figure 3.4 for deprotonated p-phthalic acid. At 0.1 % and 0.5 %, there is an initial increase in signal. It seems that for smaller ions, a small amount of modifier improves response, which could be a result of the methanol clustering with the small ions and giving it a bigger *m/z*, reducing its loss to diffusion because losses are greater for smaller *m/z* ions. At 1 % and above, the signal decreases rapidly, which may result from energetic collisions or due to ion scattering at higher modifier concentration.

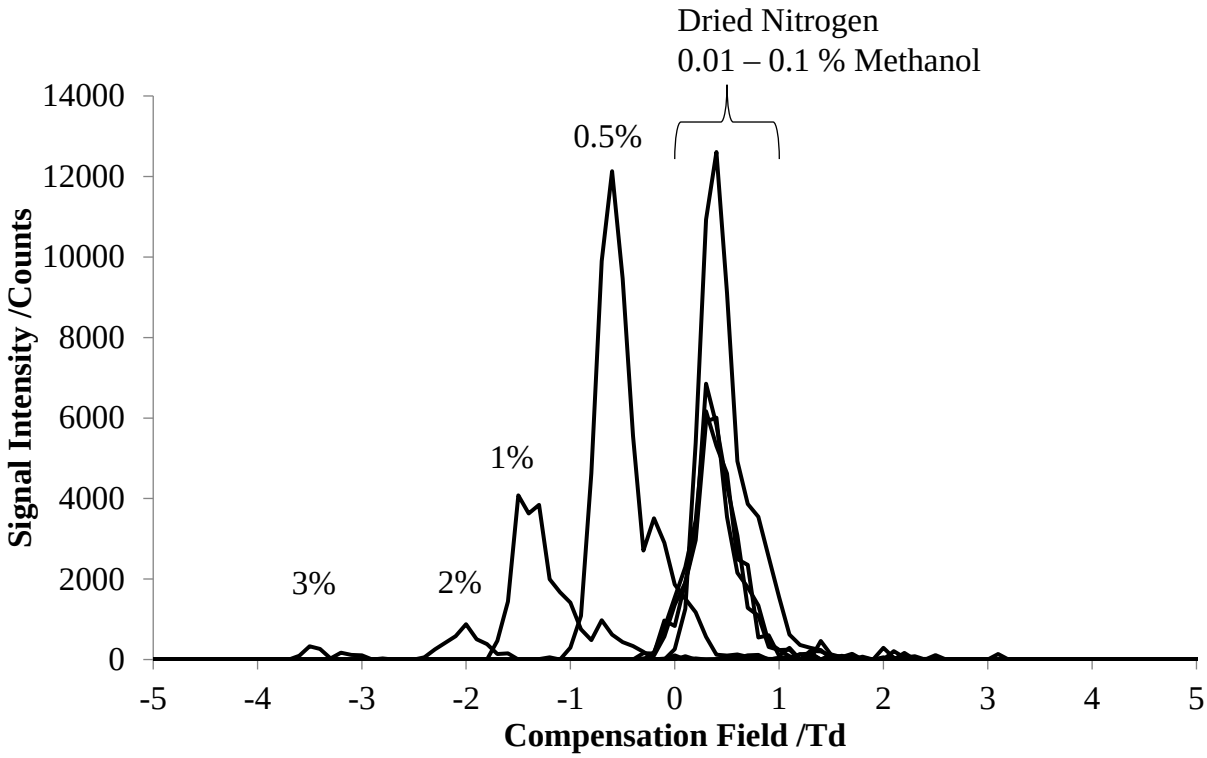

Figure 3.4 FAIMS spectra (SIR 165.0193) showing the effect of peak position of deprotonated p-phthalic acid in the presence of methanol (0-3 % v/v) at DF 230 Td

Phthalic acid isomers were selected as a model for testing the constructed modifier system and the effect of modifiers with chip-based FAIMS because behaviour of the compounds with FAIMS was discussed in the literature. Depending on the modifier type, the isomers change the order in which they appear in the FAIMS spectrum.[9] A comparison of the effect of DF on the CF peak location of each phthalic acid with dried nitrogen, 1% methanol and 1% 2-butanol is shown in Figure 3.5. In dried nitrogen, the phthalic acids shift in a positive direction, there is little separation and the isomers do not change in order. The addition of 1% methanol reduces the positive shift and instead the CF fluctuates between positive and negative shifts with increasing DF (Figure 3.5.a). The phthalic acid peaks are further apart with methanol than they are with dried nitrogen. Adding 2-butanol to the carrier gas seems to magnify the effect observed with methanol. The positive shift with DF using dried nitrogen is now a negative shift for m-phthalic acid and p-phthalic acid. Interestingly o-phthalic acid has the most negative CF shift (-1.7 Td) at DF 200 Td but shifts towards the positive CF resulting in a different order in the FAIMS spectrum depending on the DF applied (Figure 3.5.b). The order of the phthalic acids in dried nitrogen and 1% methanol is the same above DF 240 Td. m-Phthalic acid and p-phthalic acid remain close and in the same order at all DFs studied.

The change in peak positions with DF and change in order in the FAIMS spectrum of the isomers suggests that the solvent modifiers added to the chip region are influencing the clustering/declustering mechanism and that a true modifier effect is occurring with miniaturised FAIMS when using a nebuliser to introduce solvent vapours. It is likely that the phthalic acid ions and modifier molecules are interacting through hydrogen bonding. The reason for o-phthalic acid behaving differently to m- and p-phthalic acids may be due to the adjacent position of the acid groups of o-phthalic acid resulting in intramolecular hydrogen bonding. Internal hydrogen bonding will not occur with m-phthalic acid or p-phthalic acid because the acid groups are positioned too far apart, resulting in little difference between them. There are two possibilities for o-phthalic acid changing from type A to type C, discussed previously in Section 1.2.1, effective temperature (T_{eff}) and collisional cross section (CCS). In the event of a decreasing mobility (K) with increasing DF (type C), the CCS is either smaller in the low field portion or bigger in the high field portion. It is possible that without the internal H-bonding occurring in the m- and p-phthalic acids, the 2-butanol molecules form a stronger H-bond that is difficult to break in the high-field portion so a clustered ion is retained, decreasing the high field mobility. The internal bonding of o-phthalic acid reduces the number of 2-butanol molecules that can H-bond to its acid groups as

for m- and p-phthalic acids, so the ion will become more declustered in the high field than m- and p-phthalic acids and have increasing mobility with increasing DF (Type A). A recent study on predicting CV of alkyl benzoic acids in the presence of alcohol modifiers showed that despite good accuracy between predicted and experimental values, ions that changed from type A to type B ions prevented prediction.[10]

Not only have the peak positions of the isomers changed but peak heights are also affected by methanol concentration and DF dependent. Figure 3.6.a shows that o-phthalic has the highest intensity at DF 250 Td with 1% methanol, however the intensity decreases when the DF is increased to 290 Td, where m-phthalic acid has the highest intensity (Figure 3.6.b). Despite the big increase in DF, the peak locations of the isomers are almost unchanged. These conditions allow the p-phthalic acid to be selectively transmitted by FAIMS; however the other o- and m-phthalic acid isomers cannot be clearly distinguished. Increasing the concentration of methanol vapour causes a bigger shift but a large loss in intensity was also observed (Figure 3.4). An alternative to increasing concentration is to explore different modifiers, Figure 3.5.b shows that 2-butanol offers greater peak shifts and alters the peak order throughout the DF range 200 to 300 Td giving the potential for gaining selectivity between the isomers where methanol could not.

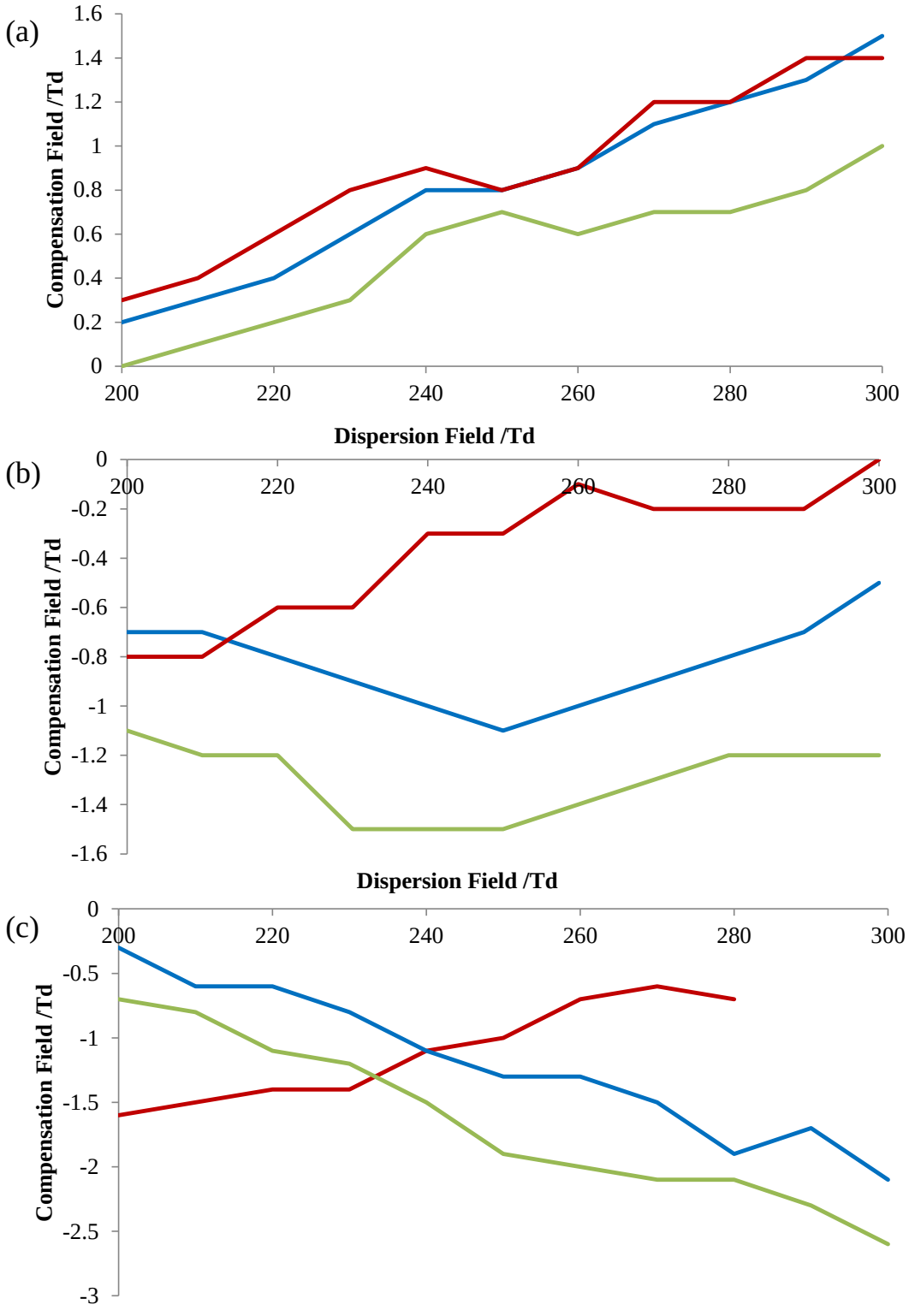

Figure 3.5 Peak location (n=3) of o-phthalic acid (red), m-phthalic acid (blue) and p-phthalic acid (green) with (a) dried nitrogen, (b) 1% methanol, and (c) 1% 2-butanol

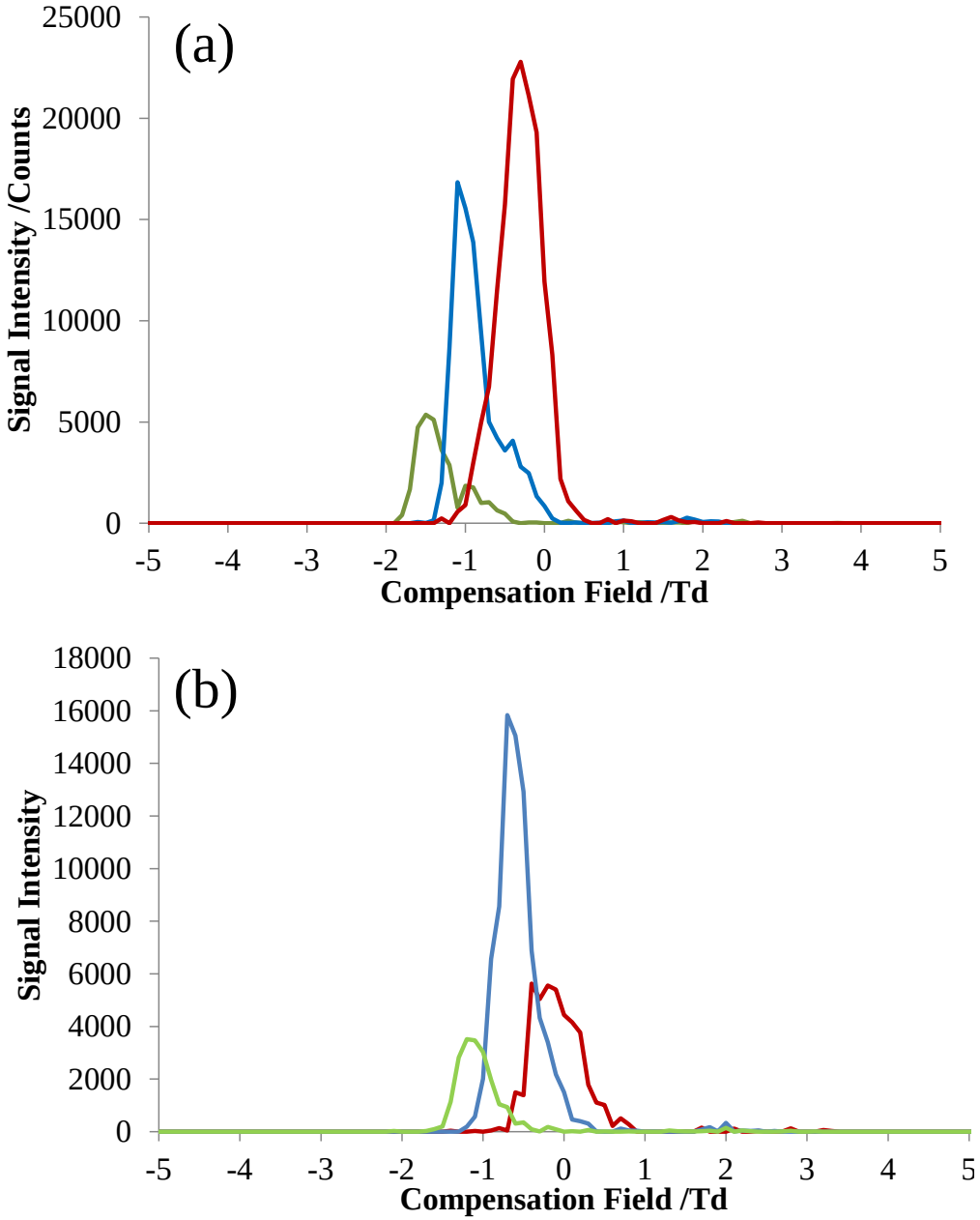

Figure 3.6 FAIMS spectra of o-phthalic acid (red), m-phthalic acid (blue) and p-phthalic acid (green) with 1% methanol set to (a) 250 Td, (b) 290 Td

A comparison of FAIMS spectra of the phthalic acid isomers at two different 2-butanol concentrations and DFs is shown in Figure 3.7. At 1% v/v 2-butanol, DF 290 Td gave the best separation (Figure 3.7.a). Increasing the 2-butanol concentration to 2% v/v 2-butanol resulted in a reduction to noise level at DF 290 Td due to either a combination of suppression of analytes at higher modifier concentration or loss in transmission typically seen at high DF. However, 2% 2-butanol and a DF of 210 Td, where little separation was observed with 1% 2-butanol, resulted in a big improvement in separation of the isomers (Figure 3.7.b).

Interestingly, if the DF had been set to 290 Td (based on the separation achieved with 1% 2-butanol) during the investigation of the effect of changing 2-butanol concentration, the separation at 210 Td with 2% 2-butanol would have been missed. These data demonstrate that when exploring the use of modifiers to optimise selectivity and sensitivity the combined influence of modifier type, modifier concentration and DF on FAIMS behaviour of ions needs to be explored. The effect of temperature also needs to be considered as it may influence the differential mobility of ions in the presence of a modifier.

Resolution was calculated for the phthalic acids in dried nitrogen, 1% 2-butanol at DF 290 Td and 2% 2-butanol at DF 210 Td using equation 3.1 to determine which conditions offer the best separation. The CF peak maximum and width at half maximum height for the phthalic acid are shown in Table 3.1. The presence of 2-butanol results in a slightly greater peak width with 1% 2-butanol and a narrower width at 2% for o-phthalic acid compared to dried nitrogen. Peak width decreased with 1% and 2% 2-butanol for the m- and p-phthalic acids. Peak location and width at half maximum was used to calculated resolution between each pair of isomers, shown in Table 3.2. Dried nitrogen gives the worst resolution in all cases. The resolution of m-phthalic acid and p-phthalic acid is best at 1% 2-butanol. Resolution between o-phthalic acid and p-phthalic acid is also best at 1% 2-butanol, but resolution between o-phthalic acid and m-phthalic acid is best at 2% 2-butanol. Figure 3.7 shows that there are additional peak features at around 10% relative intensity in the response of 2% 2-butanol (Figure 3.7.b). The identity of these ions is not known. FAIMS can be used as a filter and 'hop' between static CF/DF values to transmit FAIMS-selected analyte ions. At 1% 2-butanol, there is considerably less isomer interference when selecting the CF maximum for each isomer than if isomers were being selected with 2% 2-butanol, where interference is close to 10%. Based on this observation, 1% 2-butanol with DF set to 290 Td would be the optimum conditions to use to analyse each of the phthalic acid isomers.

$$\frac{2(CF_2 - CF_1)}{w_{0.5\,(2)} + w_{0.5\,(1)}}$$ Equation 3.1

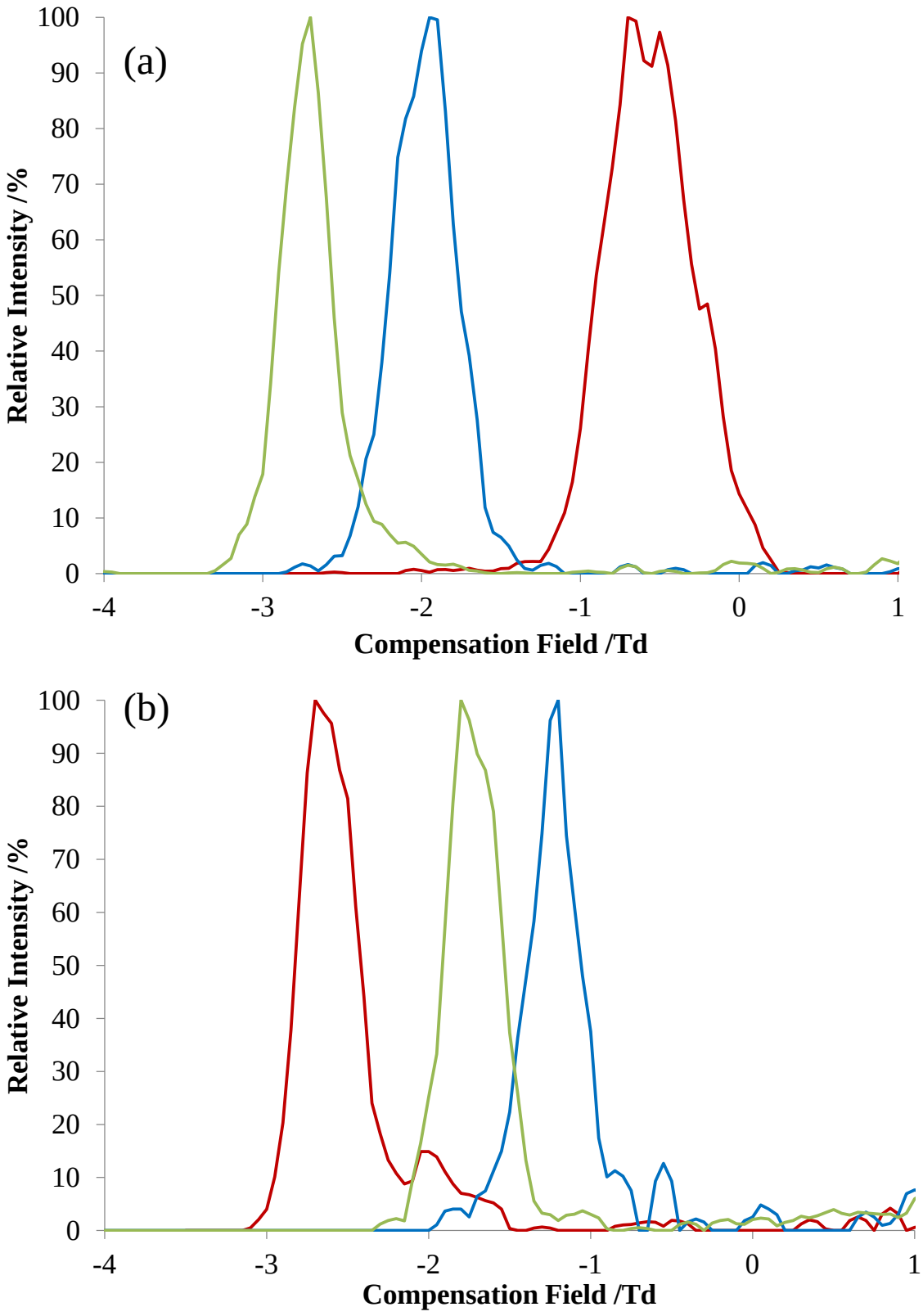

Figure 3.7 FAIMS spectra of o-phthalic acid (red), m-phthalic acid (blue) and p-phthalic acid (green) with (a) 1% 2-butanol set to 290 Td, and (b) 2% 2-butanol set to 210 Td

Table 3.1 Peak maximum (CF) and peak width and half maximum height ($w_{0.5}$) of o-, m- and p-phthalic acid with dried nitrogen and 1% 2-butanol

Carrier Gas	o-phthalic		m-phthalic		p-phthalic	
	CF /Td	$w_{0.5}$ /Td	CF /Td	$w_{0.5}$ /Td	CF /Td	$w_{0.5}$ /Td
Dry N2 (DF 290 Td)	1.7	0.53	1.5	0.53	1	0.6
1% 2-BuOH (DF 290 Td)	-0.5	0.65	-1.9	0.47	-2.7	0.34
2% 2-BuOH (210 Td)	-2.7	0.4	-1.2	0.3	-1.8	0.4

Table 3.2 Peak resolution between each phthalic acid pair, calculated from width at half maximum height

Carrier Gas	Resolution		
	o- and m-phthalic acid	m- and p-phthalic acid	o- and p-phthalic acid
Dry N2 (DF 290 Td)	0.22	0.52	0.73
1% 2-BuOH (DF 290 Td)	1.47	1.16	2.61
2% 2-BuOH (210 Td)	2.5	1.0	1.3

3.4.3 Exploring the Effect of Gas Modifiers on Peptides and Proteins

The nebuliser-based solvent modifier system was used in the previous section to demonstrate that small ions can be shifted in FAIMS spectra when adding solvent vapours to the gas flow that primarily contributes to the carrier gas flow of the FAIMS analyser. However, there is little reported evidence of the effect of solvent vapours (or gas modifiers) on larger ions, like peptides and proteins. In this section, the effect of solvent vapours on the FAIMS spectra and mass spectra of peptides and proteins is discussed.

Bombesin and Bradykinin in dried nitrogen and 2-butanol

The effect of 2-butanol on doubly charged bradykinin (Bk) and bombesin (Bo) was initially explored. The peak shape of the $[Bk+2H]^{2+}$ ion suggests that multiple partially resolved conformers may be present when analysed with dried nitrogen carrier gas (Figure 3.8.a). This is consistent with reported drift-tube and FAIMS spectrum of this ion.[11,12] The addition of 2-butanol (0.25%) results in the broad peak becoming narrower (Figure 3.8.b), but must involve the collapse of several distinct conformers to a single conformer, or a narrow range of conformers in the presence of 2-butanol vapour. The intensity for $[Bk+2H]^{2+}$ at CF 1.2 Td is reduced, enabling the selective transmission of $[Bo+2H]^{2+}$ with less interference from $[Bk+2H]^{2+}$ (Figure 3.8.i and ii). $[Bk+2H]^{2+}$ has a negative CF shift at higher levels of 2-butanol, becoming more overlapped with $[Bo+2H]^{2+}$ (data not shown).

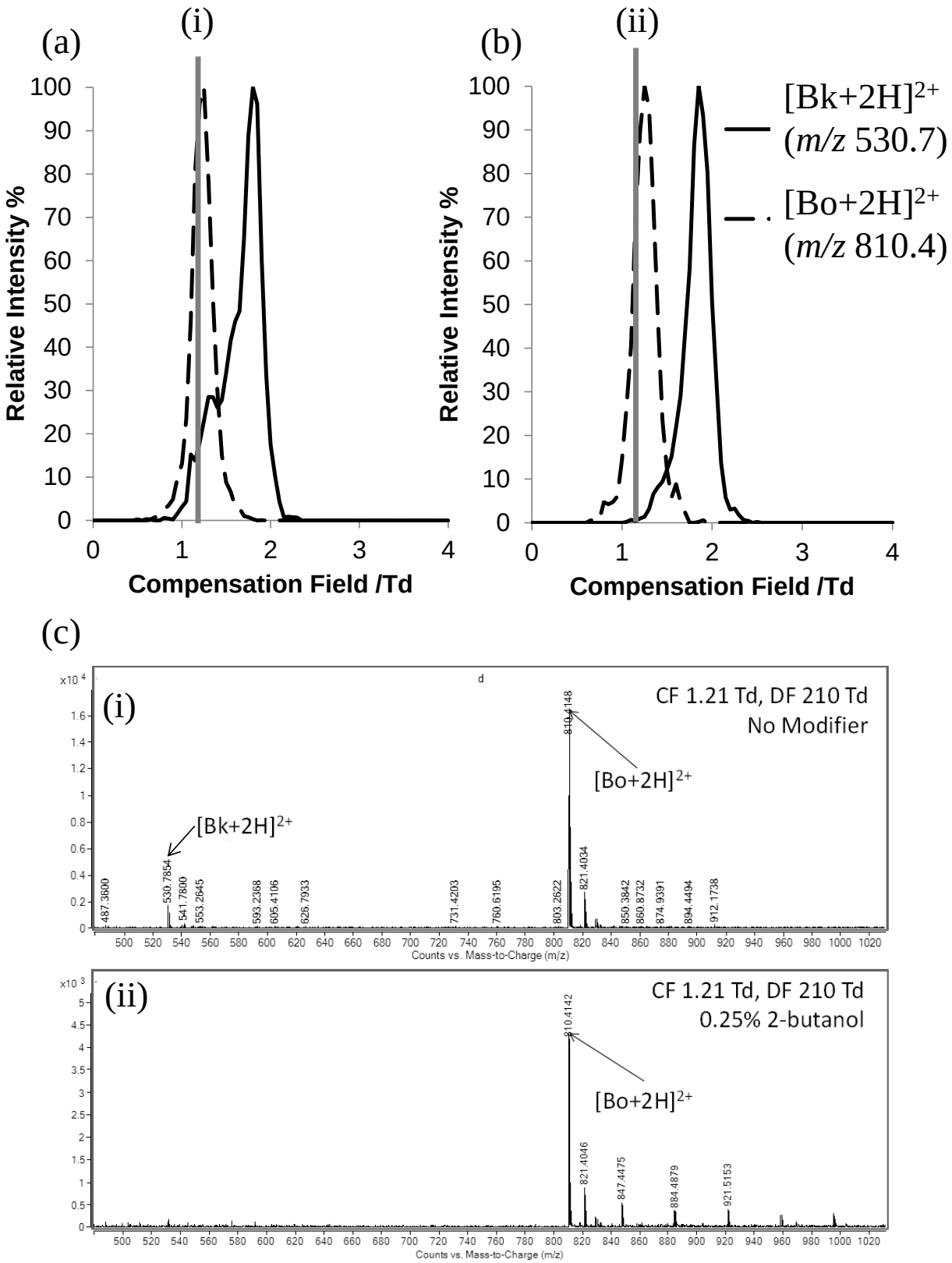

Figure 3.8 CF spectra of $[Bo+2H]^{2+}$ (SIR *m/z* 810) and $[Bk+2H]^{2+}$ (SIR *m/z* 530) at DF 210 Td with: (a) dried nitrogen and (b) 0.25% 2-butanol; and (c) mass spectra from CF spectra (indicated by grey line) using: (i) dried nitrogen, and (ii) 0.25% 2-butanol

MRFA and MFAR

Earlier in this section, the separation of phthalic acids demonstrated that small ions with little structural differences could be distinguished using FAIMS-MS by the addition of 2-butanol to the carrier gas. Consequently, the possibility of applying this method to peptide ions that differ only in amino acid sequence was investigated. The potential for separating sequence isomers MRFA and MFAR using FAIMS was explored using dried nitrogen, methanol and 2-butanol at the 1% v/v level as the carrier gas. Figure 3.9.a demonstrates that the protonated ions could not be resolved using only dried nitrogen at DFs up to 300 Td, but the location of the peak maximum for the peptides does differ with protonated MFAR at CF 2.6 Td and protonated MRFA at CF 3.1 Td. The presence of either methanol or 2-butanol results in a negative CF shift compared to the peak location in dried nitrogen (Figure 3.9.b-c). Protonated MFAR shifts from CF 2.6 Td to 2.3 Td by the addition of methanol and to CF 1.4 Td when in the presence of 2-butanol (both at 1% v/v). Protonated MRFA also shifted negatively, from CF 3.1 Td to 2.7 Td by adding methanol to the carrier gas, and to CF 1.9 with 2-butnaol. Despite the negative shift, the protonated peptides retain positive CF values unlike the negative CF values observed with the phthalic acids, which suggests that the magnitude of the modifier effect is dependent on size or mass. The difference between the peak maxima is affected by the addition of alcohols to the carrier gas, in fact 2-butanol addition resulted in the peak maximum of MRFA and MFAR being closer (0.4 Td) than when in the absence of alcohol (0.5 Td difference). However, even though the peaks get closer, the protonated MRFA peak is narrower with the addition of 2-butanol, due to the asymmetry on the left hand side of the MRFA peak being removed. This results in a partial separation of MRFA and MFAR in the presence of 1% v/v 2-butanol modifier which means that MFAR could be transmitted by selecting a point CF of ~1.2 Td which would remove most of the MRFA interference.

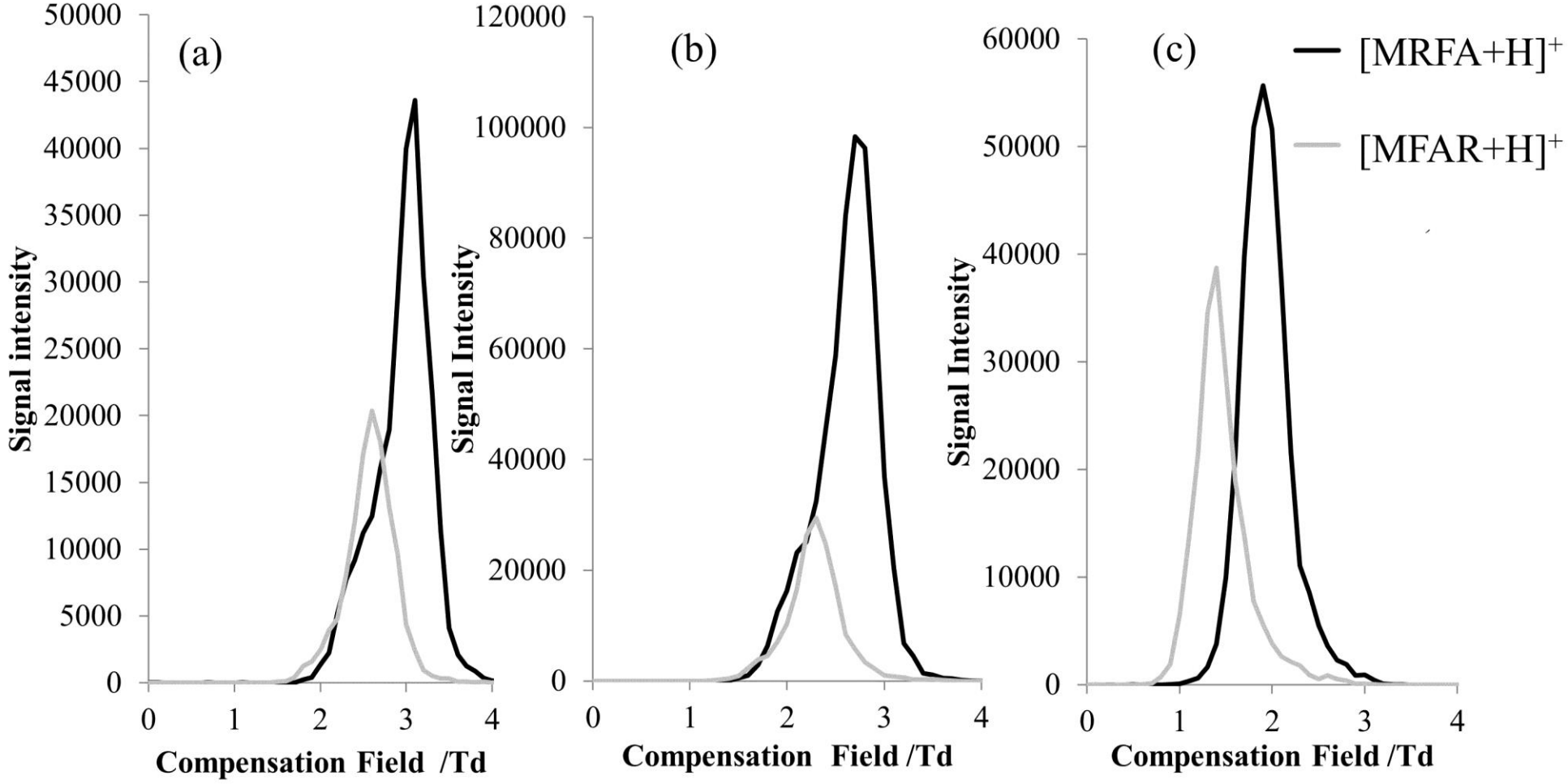

Figure 3.9 CF spectra of SIR *m/z* 524.1 at DF 300 Td with: (a) dried nitrogen; (b) 1% methanol; (c) 1% 2-butanol

Proteins: Cytochrome C

The effect of gas modifiers on proteins has not previously been explored so cytochrome c was selected as it is a commonly used model protein.[13] Denatured cytochrome C was introduced into the ESI source with different drying gas compositions. Dried nitrogen results in multiple peaks which could be associated with different conformers or different levels of hydration of the protein. The number of peaks present is dependent on charge stage, with +12 giving 2 peaks and +19 3 defined peaks (Figure 3.10). The addition of methanol vapour reduces the number of peaks observed at higher charge states (Figure 3.10.b-c) whereas lower charge states (e.g. +12) there is no change in the number of peaks seen in the FAIMS spectrum (Figure 3.10.a) and no shift in peak location that would usually be observed with smaller ions.

The +20, +21 and +22 charge states of cytochrome C were observed in the mass spectrum only under dried nitrogen conditions, but were reduced to baseline by addition of 1% methanol modifier (Figure 3.11). The higher charge states produce more peaks in the FAIMS spectrum which appear on the negative side of the peaks that exist at lower charge states, suggesting that it is the unfolded conformers that are being removed or modified by the addition of methanol. The higher charge states that are suppressed are likely to be more unfolded conformations than the lower charge states that are much less affected by methanol vapour. For cytochrome C to produce fewer peaks in the FAIMS spectrum, it could be hypothesised that methanol is either causing a charge state reduction/stripping effect or a change in conformation. In these preliminary studies, the existing higher charge states lose peaks associated with unfolded conformers at lower concentrations before there is a reduction in the more folded conformers (Figure 3.10.b) which may suggest that either the unfolded conformers are more exposed for charge stripping or that the protein is favouring a more folded conformation. A study of alcohol modifiers suggested loss of ions may be due to charge exchange to a modifier with a higher proton affinity.[10] More experiments are needed to further understand the cause of the effect that is seen with cytochrome C in the presence of modifiers.

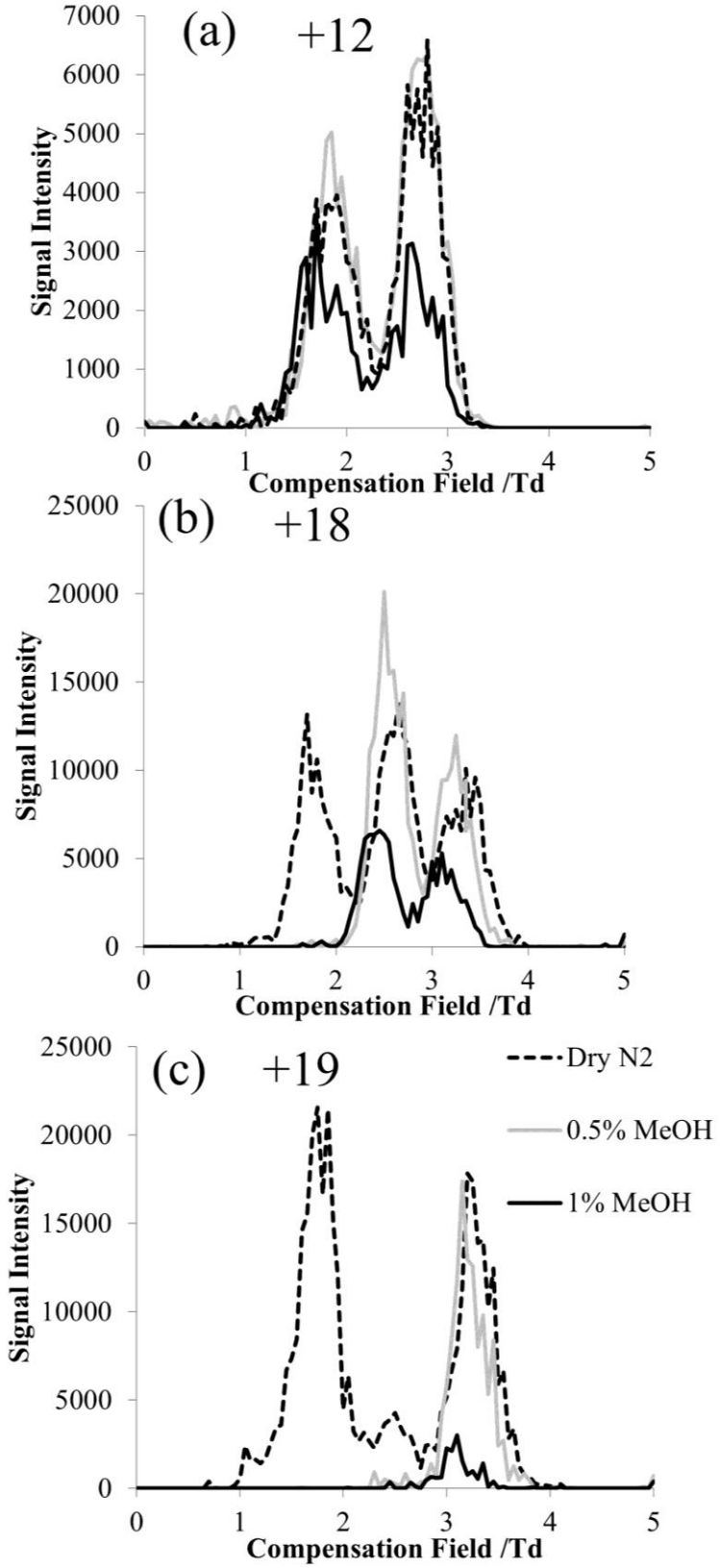

Figure 3.10 CF spectra of Cytochrome c charge states: (a) +12 (*m/z* 1030.9), (b) +18 (*m/z* 687.6), (c) +19 (*m/z* 651.5); at DF 300 Td with dried nitrogen (dashed line), 0.5% methanol (grey line) and 1% methanol (black line)

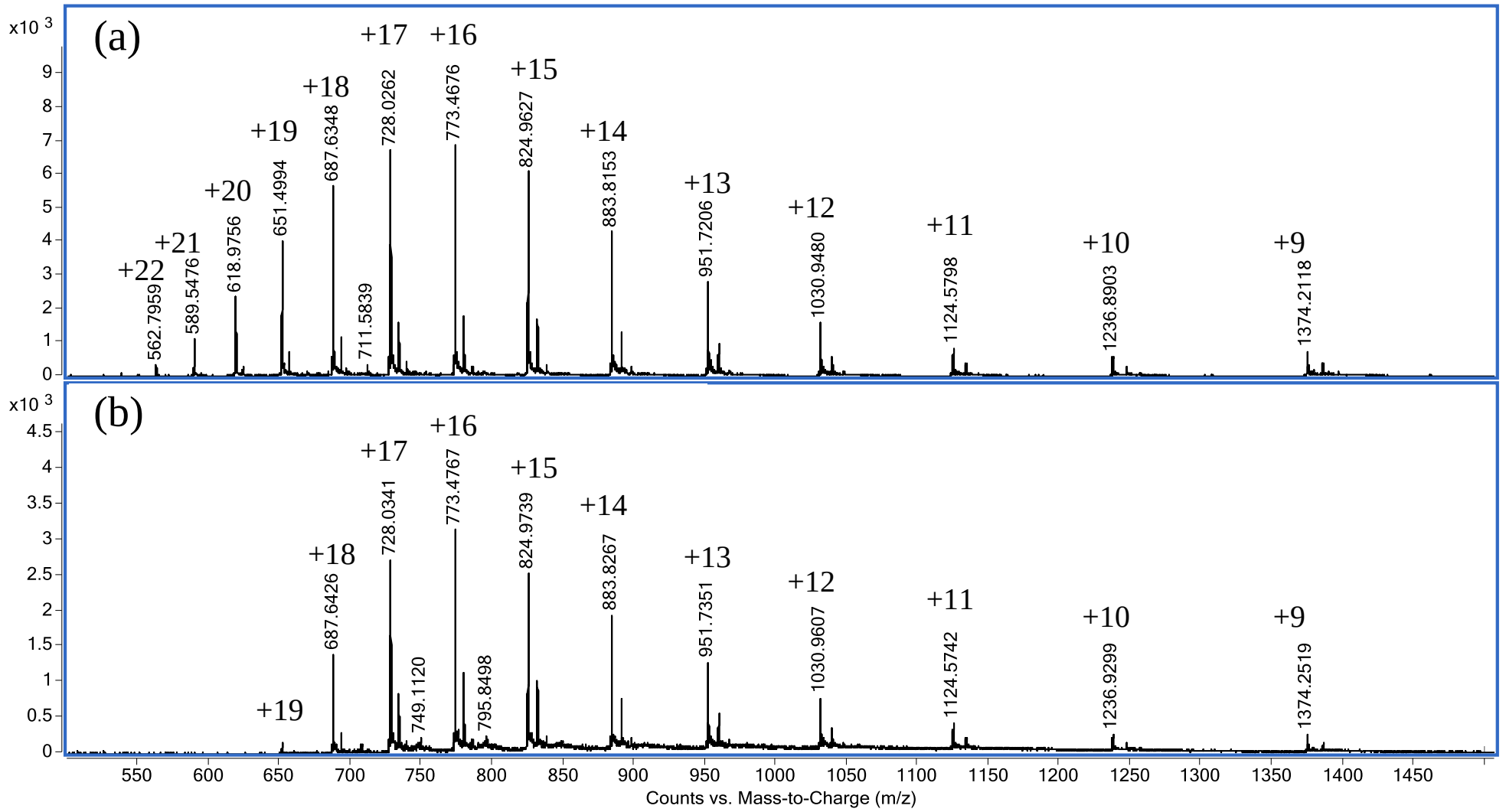

Figure 3.11 Mass spectra of Cytochrome C with (a) dried nitrogen, and (b) 1% methanol; without FAIMS separation

3.5 Conclusion

Significant shifts in CF peak maxima were observed for small molecules with % level modifiers. Positional isomers of phthalic acids could be selectively transmitted through the FAIMS device depending on the DF, choice of modifier and modifier concentration. The CF spectra of peptides and proteins produced fewer peaks in the CF spectrum when alcohol modifiers were introduced into the carrier gas, showing a preference for some conformers. CF peak shifts with the addition of a modifier are greater for small molecules, where the difference between clustered and declustered ions is larger. Separation, selectivity and signal intensity of analytes are influenced by the choice of modifier, the modifier concentration and the applied dispersion field.

3.6 Chapter Three References

(1) Kolakowski, B. M.; Mester, Z. *Analyst*. **2007**, *132*, 842–64.

(2) Barnett, D. A.; Ouellette, R. J. *Rapid Commun. Mass Spectrom.* **2011**, *25*, 1959–71.

(3) Eiceman, G. A.; Krylov, E. V; Krylova, N. S.; Nazarov, E. G.; Miller, R. A. *Anal. Chem.* **2004**, *76*, 4937–44.

(4) Schneider, B. B.; Nazarov, E. G.; Covey, T. R. *Int. J. Ion Mobil. Spectrom.* **2012**, *15*, 141–150.

(5) Schneider, B. B.; Covey, T. R.; Nazarov, E. G. *Int. J. Ion Mobil. Spectrom.* **2013**, *16*, 207–216.

(6) Ross, S. K.; McDonald, G.; Marchant, S. *Analyst*. **2008**, *133*, 602–7.

(7) Levin, D. S.; Vouros, P.; Miller, R. a; Nazarov, E. G.; Morris, J. C. *Anal. Chem.* **2006**, *78*, 96–106.

(8) Karasek, F.W.; Kim, S.H. *Anal. Chem.* **1975**, 47, 1166-1168.

(9) Rorrer III, L. C.; Yost, R. A. *Int. J. Mass Spectrom.* **2010**, *300*, 173–181.

(10) Auerbach, D.; Aspenleiter, J.; Volmer, D.A. *J. Am. Soc. Mass Spectrom.* **2014**, 25, 1610-1621

(11) Brown, L.J.; Toutoungi, D.E.; Devenport, N.A.; Reynolds, J.C.; Kuar-Atwal G.; Boyle, P.; Creaser, C.S. *Anal. Chem.* **2010**, 82, 9827-9834

(12) Pierson, N.A.; Chen, L.; Valentine, S.J.; Russell, D.H.; Clemmer, D.E. *J. Am. Soc. Chem.* **2011**, 133, 13810-13813

(13) Purves, R. W.; Ells, B.; Barnett, D. A.; Guevremont, R. *Can. J. Chem.* **2005**, *83*, 1961–1968.

Chapter 4

Direct Analysis of Pharmaceutical Impurities by Direct Infusion and Thermal Desorption combined with Field Asymmetric Waveform Ion Mobility Spectrometry-Mass Spectrometry

4.1 Chapter Overview

The first part demonstrates the rapid, direct determination of N-methyl pyrrolidine (NMP), an impurity in the cephalosporin antibiotic cefepime, by direct infusion ESI combined with field asymmetric waveform ion mobility spectrometry-mass spectrometry (ESI-FAIMS-MS). The addition of a chip-based FAIMS separation prior to detection by time-of-flight mass spectrometry enables selective transmission of NMP in the presence of cefepime without interference from NMP formed by in-source CID. The limits of detection and quantification of NMP in cefepime were well below the 0.3% (w/w) threshold concentration for NMP in cefepime.

The second part of this chapter shows thermal desorption in combination with FAIMS-MS for the rapid, direct analysis of isobaric potentially genotoxic impurities (PGIs) in a surrogate active pharmaceutical ingredient. PGI vapours released by thermal desorption were ionized by extractive electrospray ionization. FAIMS-selected PGIs were detected below the 1 ppm threshold of toxicological concern.

4.2 Part A: Cefepime and its impurity N-methyl pyrrolidine

4.2.1 Introduction

Cefepime (I) is a fourth-generation cephalosporin antibiotic that was developed as a broad range activity antibiotic in the 1990s.[1,2] Cefepime was found to be particularly effective against pseudomonas aeruginosa strains which exhibited resistance against other cephalosporin antibiotics, such as ceftazidime and cefotaxime.[3] Cefepime has greater activity against Gram-negative bacteria compared to other cephalosporins,[4] and is used to treat a wide degree of infectious diseases.[5] However, cefepime is unstable and slowly degrades over time. The degradation rate is greatly increased at higher temperatures (25-37 ˚C) and in an aqueous solution, the loss affects the antibiotic activity significantly enough that it is recommended cefepime not be used for clinical use in aqueous conditions at >25 ˚C for more than a few hours.[6]

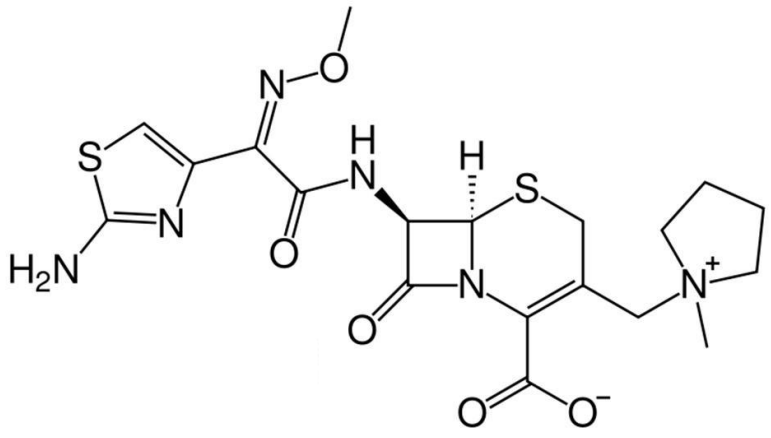

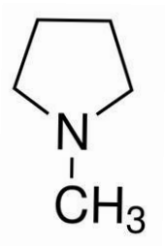

I II

The impurity N-methyl pyrrolidine (NMP, II) may be present in cefepime samples as a result of degradation of the drug. NMP has been reported as having unknown toxicity by the US Environmental Protection Agency,[7] and the potential for toxicity to patients receiving the drug is yet to be determined. An experimental study performed on monkeys, in which NMP (50 mg/kg) was administered over 28-30 consecutive days resulted in them developing esotropia and ataxia.[8] The dosage of NMP used in the study was much greater than the amount expected to be received in a daily dose of cefepime (~6g) administered to patients, but the presence of the potentially harmful impurity is still undesirable. It has been reported that an increase in the NMP level is proportional to the decline in the antibiotic potency of cefepime.[9,10] Monitoring the level of NMP in cefepime is, therefore, important for ensuring drug quality for clinical use and a threshold concentration of NMP in cefepime has been set at 0.3 % (w/w).

The determination of NMP in cefepime presents an analytical challenge because of the rapid degradation of cefepime to NMP in aqueous solution above 4 ˚C and outside the pH range 4-6, resulting in the presence of higher levels of NMP in solution than are present in the solid cefepime sample. At present, there are four main techniques that have been employed for NMP determination: high performance liquid chromatography (HPLC), ion chromatography (IC), capillary electrophoresis (CE) and gas chromatography (GC).[5,6,9-11] There are limitations associated with all these techniques. The HPLC method requires a mobile phase of pH 2 and the IC method uses a column temperature of 40 ˚C; both of these conditions could lead to degradation of cefepime and reduce measurement accuracy. Poor detection and quantification limits for CE and the use of a solvent with high toxicity, pyridine, to extract NMP for the GC

technique makes these methods less desirable for routine analysis of NMP. The preparation of a cefepime sample for analysis therefore requires either the extraction of the NMP from the cefepime matrix to minimise the contribution from NMP produced by degradation in solution prior to analysis, or rapid analysis of the sample solution before significant degradation occurs.[12]

A further challenge in the determination of NMP in cefepime is that the singly and doubly protonated cefepime generated by electrospray mass spectrometry (ESI-MS) are readily fragmented in the mass spectrometer interface by 'in-source' collision-induced dissociation (in-source CID) to form protonated NMP. The NMP generated by in-source CID interferes with response from the protonated NMP formed from NMP present in the cefepime sample, since NMP resulting from the sample and *via* in-source CID cannot be distinguished by mass spectrometry alone.

In this chapter, the potential for combining a miniaturised FAIMS device with direct infusion-ESI-MS to remove interference from NMP fragment ions generated by in-source CID, enabling the determination of NMP in cefepime is demonstrated and the quantitative performance evaluated.

4.2.2 Materials and Methods

4.2.2.1 Chemicals

Cefepime was obtained from Orchid Chemicals and Pharmaceuticals Limited (Chennai, India). N-methyl pyrrolidine was supplied by Sigma-Aldrich Limited (Gillingham, UK).

4.2.2.2 Sample Preparation

NMP standards

A stock solution of NMP (1 mg/ml) was prepared in methanol/water (50:50). The stock was subsequently diluted to 1 μg/ml with methanol/water (50:50) + 0.1% formic acid. A series of dilutions in the range 0.01 – 1 μg/ml (2-fold at each step) were used for standard addition experiments.

Cefepime samples

Fresh solutions of cefepime (5 mg/ml) were prepared in methanol 10 minutes prior to analysis. A single 100-fold dilution of the cefepime solution (to 50 μg/ml, 10μl) in

methanol/water (50:50) + 0.1% formic acid (990 µl), or NMP solution (500 µl + 490 µl diluent) for the standard additions calibration, was performed immediately before analysis. NMP solution and methanol/water (50:50) + 0.1% formic acid portions were combined before preparation of cefepime samples so that weighing cefepime, dissolving cefepime, and transferring a 10 µl aliquot of cefepime solution to the diluted NMP solution were the only steps performed between each acquisition.

4.2.2.3 Instrumentation

Sample solutions and standards were infused (15 µl/min) using a syringe pump into the JetStream ESI source of an Agilent 6230 TOF MS (Agilent Technologies, UK) operated in positive ion mode. The ESI source was operated with a grounded nebuliser pressure of 35 psig, a nozzle voltage of 2000 V, a sheath gas temperature of 250 ˚C at a flow of, 8 L/min, a drying gas temperature of 150 ˚C at a flow of 7 L/min and a spray shield voltage of 2500 V.

The second prototype chip-based FAIMS device (Owlstone Ltd., Cambridge, UK) was fitted at the inlet to the mass spectrometer for the analysis of cefepime samples. The MS inlet transfer capillary was operated at 3000 V with a nebulizer voltage of 2000 V. The chip-based FAIMS consists of multiple parallel electrode gaps (100 µm) with a short path length (700 µm), as described previously in Section 2.3.3. The fragmentor voltage applied at the TOF inlet and was varied between 75 and 375 V (25 V steps), but set to 200 V for quantitative measurements. The MS acquisition rate was set to 10 scans/s for FAIMS scanning experiments and 1 scan/s for quantification using static FAIMS.

Scanning FAIMS experiments were carried out in the range CF -2 to 5 Td (scan speed 0.5 Td/s) at each DF, which was incremented in the range 180-230 Td in 5 Td steps to determine optimum conditions to separate NMP from cefepime. Static FAIMS experiments used a fixed CF (0 Td) and DF (180 Td) to pre-select NMP generated in the ESI ion source. Cefepime solutions were infused into the source and data acquired for 2 min/sample. Data were acquired using Agilent MassHunter Acquisition B.05.00 and processed using Agilent MassHunter Qualitative Analysis B.05.00. Microsoft Excel 2010 was used to produce CF plots.

4.2.3 Results and Discussion

Cefepime degrades rapidly in solution, so the time between preparing a cefepime solution for analysis and acquiring data for the determination of NMP can potentially influence the

accuracy of the quantification of NMP in the original cefepime sample. Sample preparation and analysis time therefore needs to be minimised, making the direct infusion of the sample into the ESI source of a mass spectrometer a potentially rapid alternative to conventional approaches for NMP determination. However, the conditions used for ESI-MS may lead to fragmentation of cefepime ions to protonated NMP in the mass spectrometer interface, which will increase the NMP response. The potential of FAIMS to separate the response for NMP in the original cefepime sample from NMP generated by in-source CID was therefore investigated.

4.2.3.1 ESI-MS of cefepime: in-source CID

ESI-MS analysis of a cefepime solution spiked with NMP (0.1% w/w), shows the presence of intense doubly (*m/z* 241) and singly (*m/z* 481) protonated cefepime peaks in the spectrum, with a relatively weak response for protonated NMP (*m/*z 86; Figure 4.1). The voltage applied to a lens in the mass spectrometer interface affects transmission of ions into the mass spectrometer and can also cause in-source collision-induced dissociation (in-source CID).[2,3] The response for NMP in Figure 4.1 may therefore be attributed to contributions from NMP in the cefepime sample and from in-source CID of protonated cefepime. Optimising the lens voltage (termed the fragmentor voltage for the mass spectrometer used in this study) is important for the analysis because it has a significant impact on the analyte response. The effect of fragmentor voltage on the intensity of the NMP (*m/z* 86) and cefepime (*m/z* 481) ions was investigated to determine the extent of cefepime fragmentation by in-source CID. NMP and cefepime were infused separately into the ESI source and the fragmentor voltage varied in the range 75-375 V (Figure 4.2). The maximum response for transmission of the NMP ion was at a fragmentor voltage of 200 V (Figure 4.2.a). However, infusion of a cefepime standard also resulted in a response for NMP, which increased at fragmentor voltages above 200 V as a result of in-source CID at all fragmentor voltages studied (Figure 4.2.b). The NMP response in the cefepime sample directly infused into the ESI source therefore arises from a combination of the NMP in the cefepime sample and in-source CID of the cefepime ion generated by ESI, preventing the direct determination of NMP by ESI-MS.

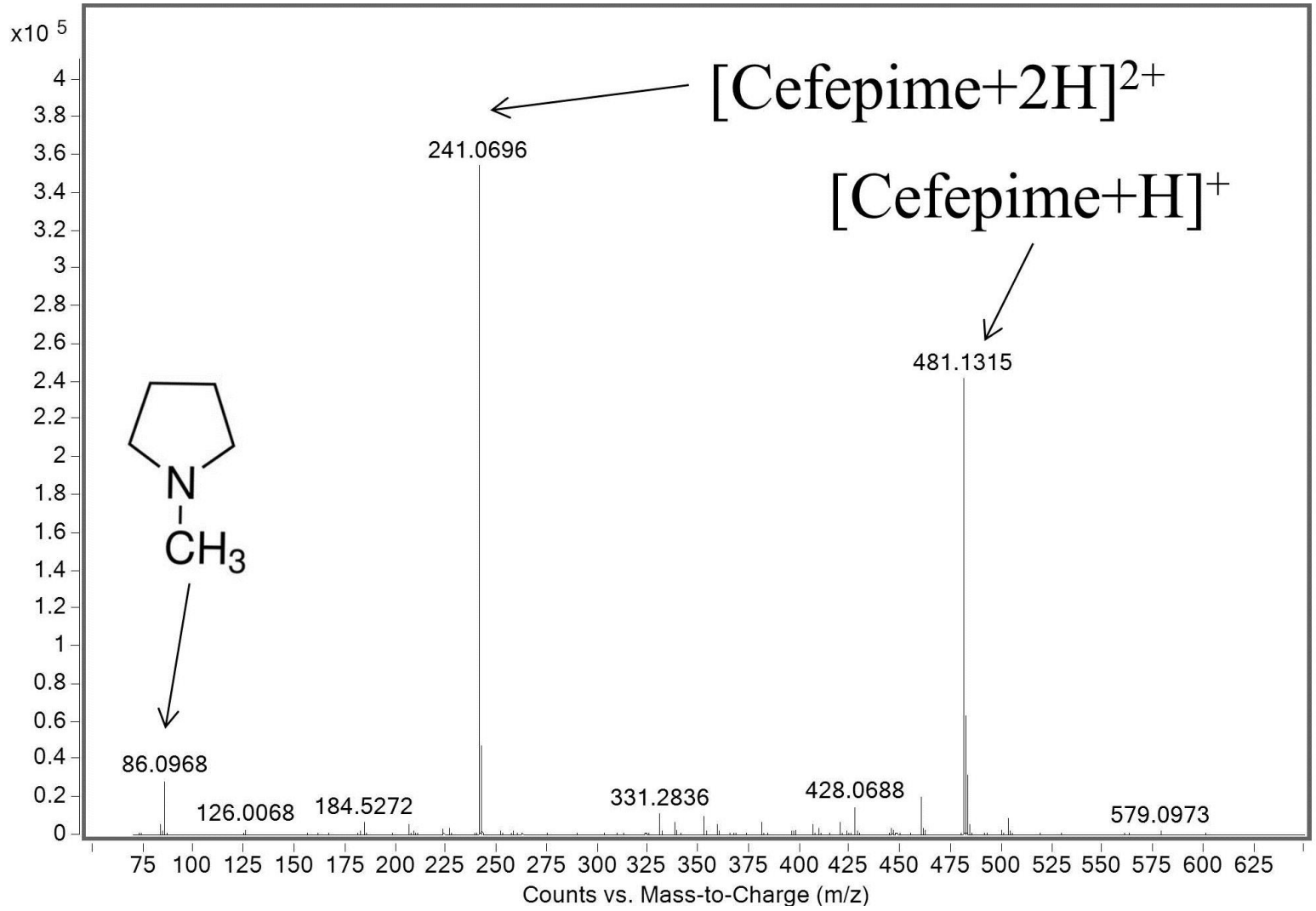

Figure 4.1 Electrospray mass spectrum of cefepime sample with NMP spiked at 0.1% (w/w).

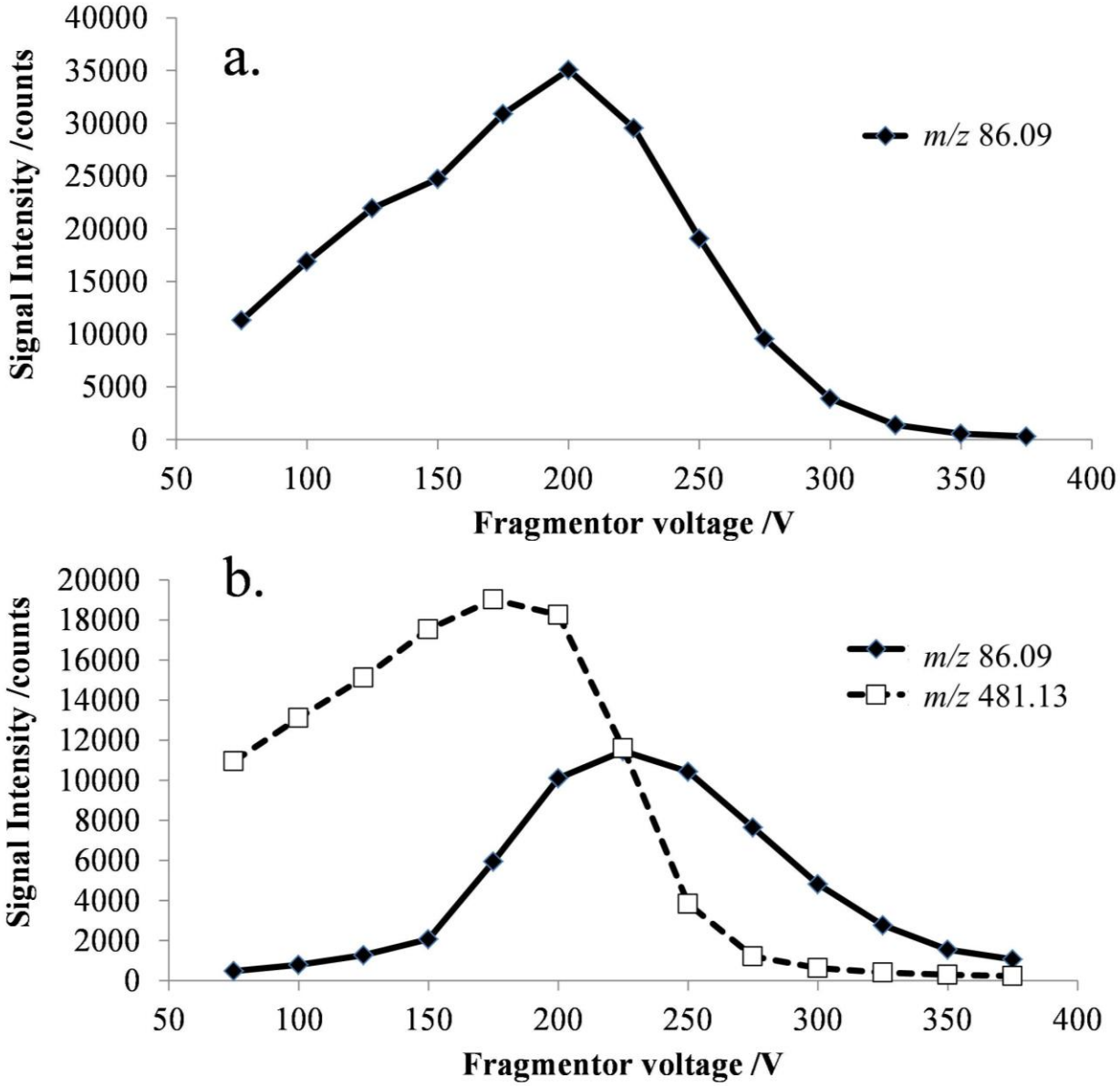

Figure 4.2 Selected ion responses for $[NMP+H]^+$ (*m/z* 86) and $[Cefepime+H]^+$ (*m/z* 481) at 25 V increments of the fragmentor voltage (75-375 V), (a) NMP standard; and (b) Cefepime standard

4.2.3.2 Direct infusion ESI-FAIMS-MS studies

The FAIMS dispersion field (DF) and compensation field (CF) characteristics of protonated cefepime and NMP were investigated to determine whether these ions could be separated on the basis of differences in their high field and low field mobility. Figure 4.3 shows the mass-selected ion responses for cefepime (*m/z* 241 and 481, solid grey and dashed line) and NMP (*m/z* 86, solid black line) in the FAIMS compensation field (CF) spectrum (-1.5 – 2 Td) of a solution of cefepime containing 0.1 % (w/w) NMP. A DF stepping experiment was used to determine the optimum DF (180 Td) for the separation of NMP and cefepime. The protonated NMP selected ion response shows two peaks at CF 0 Td and at CF 0.7 Td. The first peak (CF 0 Td, Figure 4.3 insert) matches the CF spectrum of an NMP standard without cefepime in the sample (data not shown) indicating that this peak arises from the NMP ions produced in the ESI source. The second peak (CF 0.7 Td) is associated with NMP formed by in-source CID of the protonated cefepime in the mass spectrometer interface after transmission of the intact cefepime ion through the FAIMS, which therefore appears in the FAIMS spectrum at the same CF as cefepime. Separation of NMP (0 Td) and cefepime (0.7 Td) with NMP at 0.1% (w/w) demonstrates the effectiveness of FAIMS to transmit NMP in the presence of a 1000 fold excess of cefepime.

The mass spectrum extracted from the FAIMS CF scan at a CF of 0 Td shows the protonated NMP to be the base peak in the mass spectrum (Figure 4.4). There is a weak response from the protonated cefepime at this CF, because of the 1000 fold excess of the drug, but this is small compared to the relative responses for NMP and cefepime in the absence of a FAIMS separation (Figure 4.4). The FAIMS device is therefore able to transmit the NMP generated in the ESI source from the original cefepime solution selectively, with no contribution from the NMP formed by in-source CID, making it possible to determine NMP in cefepime by direct ESI-FAIMS-MS without prior chromatographic separation.

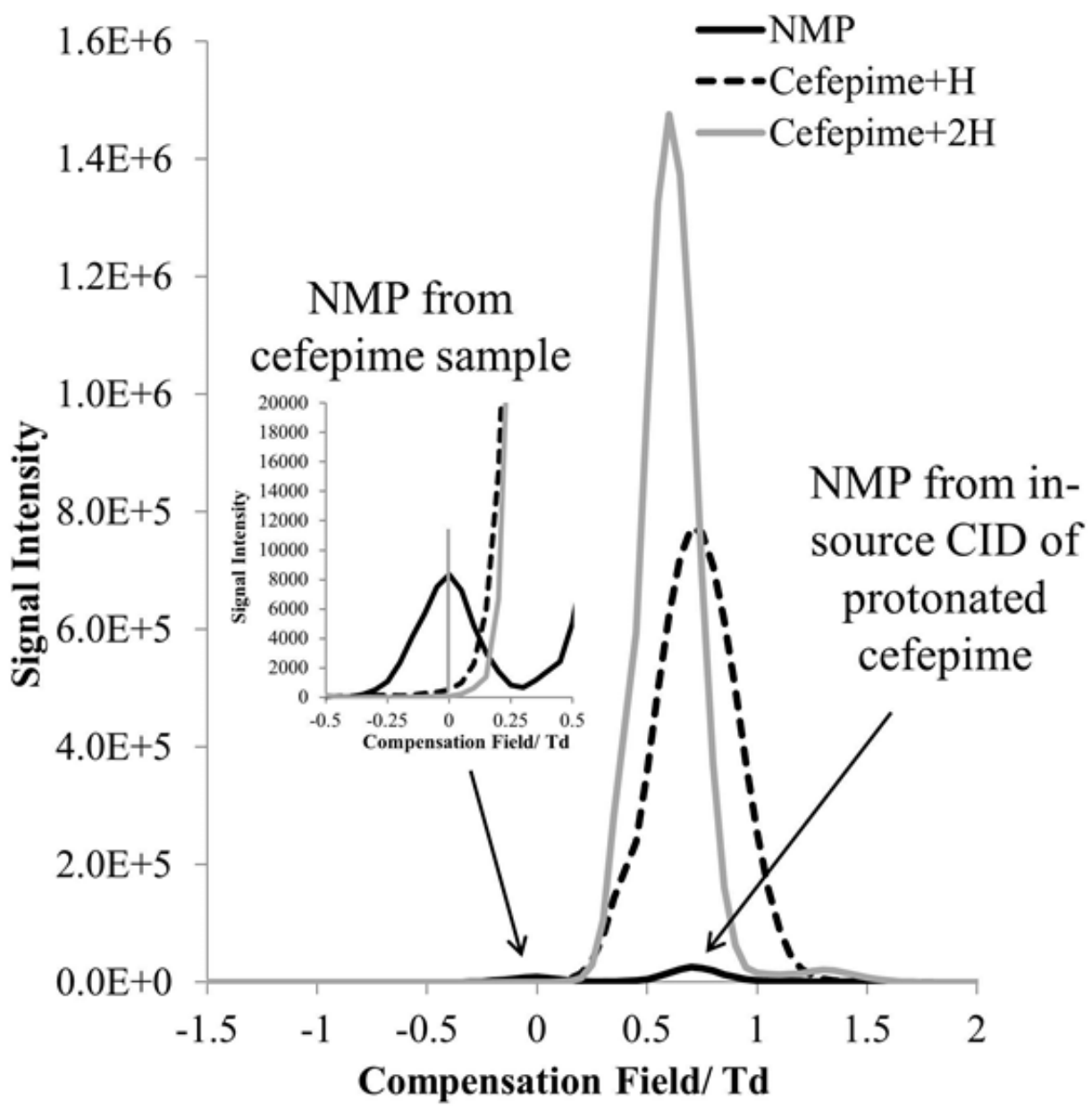

Figure 4.3 CF spectra showing selected ion response (SIR) of $[NMP+H]^+$ (*m/z* 86) and $[Cefepime+H]^+$ (*m/z* 481) at a 1:1000 ratio (w/w) at DF 180 Td

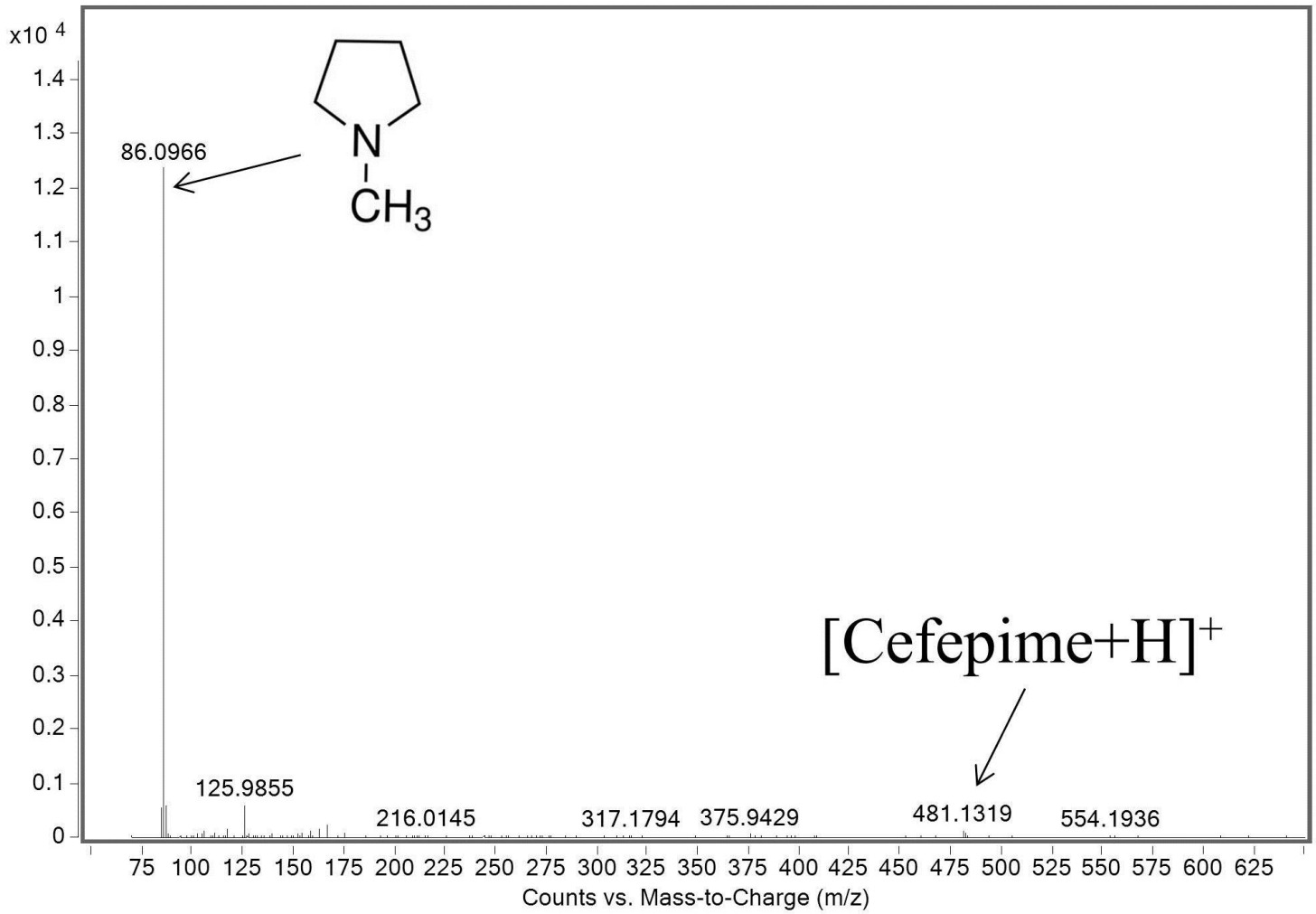

Figure 4.4 Mass spectrum of an infused sample of Cefepime spiked with NMP at 0.1% (w/w) obtained by ESI-FAIMS-MS (DF 180 Td; CF 0 Td)

The FAIMS was operated in static mode (CF 0.1 Td, DF 180 Td) to selectively transmit NMP generated in the ESI ion source through the device for the determination of NMP in cefepime. Cefepime solutions were infused into the source and data acquired for 2 min/sample. The limit of detection for NMP was estimated to be 0.011% (w/w), giving a limit of quantitation 0.036% (w/w), which is well below the 0.3% threshold concentration for NMP in cefepime. The %RSD for replicate samples was 3.85% (n=6, 0.37 µg/ml) for NMP, with good linearity (R^2 0.9979) for standard additions of NMP in the range 0.005 – 0.5 µg/ml (Figure 4.5). The level of NMP in this cefepime was calculated from the calibration plot and found to be 0.32 µg/ml (0.64 %), which is higher than the 0.3 % limit as a result of degradation over time during storage. These preliminary quantitative data demonstrate the potential of direct ESI-FAIMS-MS for the determination of NMP in cefepime at, and below, the threshold concentration, subject to full validation of the method.

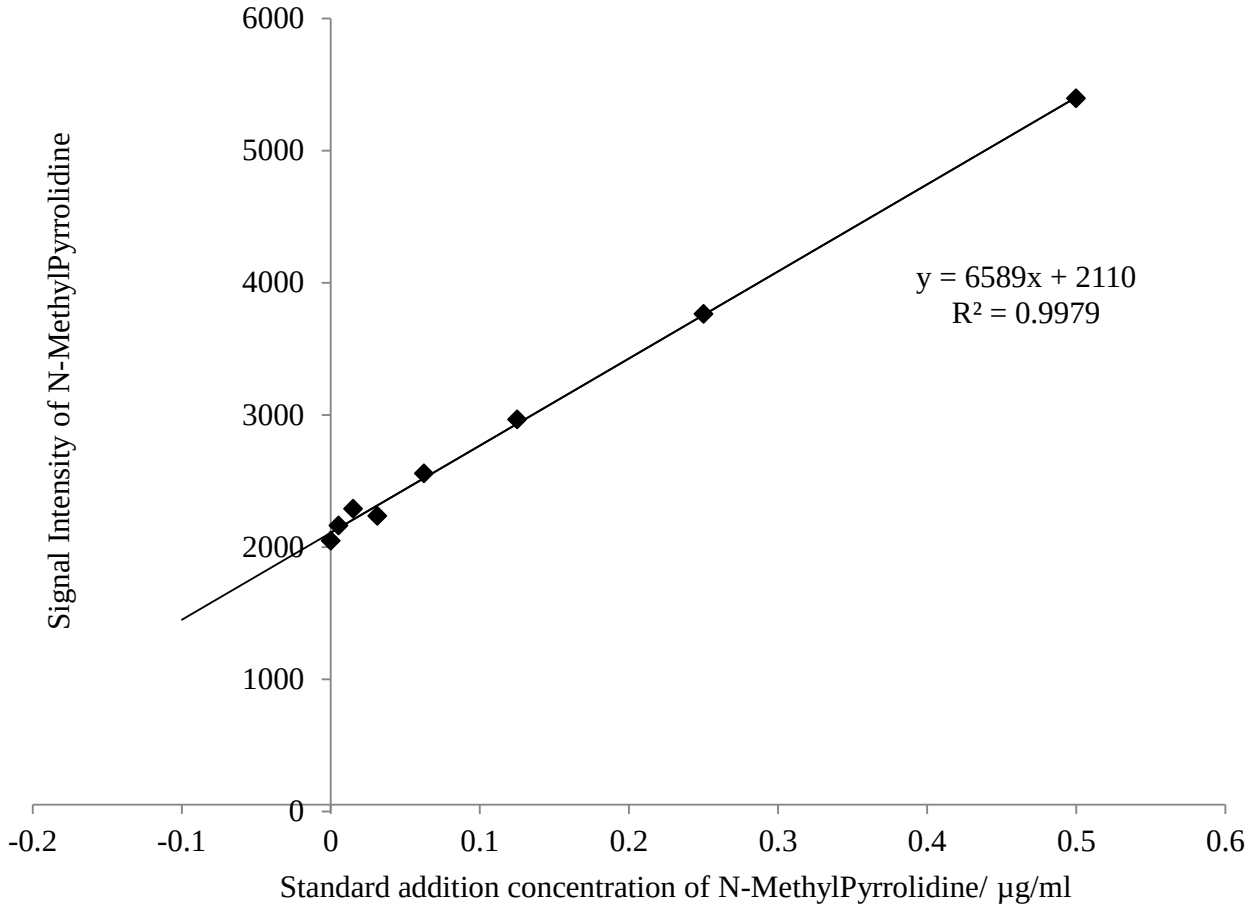

Figure 4.5 Standard addition calibration plot of NMP (0.005 – 0.5 µg/ml) in cefepime (50 µg/ml)

4.3 Part B: Potentially genotoxic impurities

4.3.1 Introduction

Potentially genotoxic impurities (PGIs) have characteristic structures that may exhibit carcinogenicity.[13,14] PGIs need to be monitored during the production of active pharmaceutical ingredients (APIs) to ensure that their concentrations remain below the threshold value of toxicological concern (TTC) required by the European Medicines Agency;[15,16] which is typically ~1.5 μg/day, equivalent to 1.5 ppm assuming a 1 g/day dose. Gas chromatography-mass spectrometry (GC-MS) and high performance liquid chromatography-mass spectrometry (LC-MS) are widely used techniques for monitoring the levels of PGI compounds in APIs. However, these conventional pharmaceutical analysis methods require lengthy sample preparation and/or chromatographic separation. Consequently, there is a need for new analytical strategies to meet the fast-paced pharmaceutical research and discovery environment.[17,18]

Thermal desorption is an extraction technique, where an analyte is transferred into the gas phase from a solid or liquid. The technique requires minimal sample preparation and is often interfaced with gas chromatography-mass spectrometry.[19] Desorbed PGIs have been ionised *via* extractive electrospray in an electrospray ionisation source (ESI) and detected by mass spectrometry.[5,20] Thermal desorption has also been interfaced with drift tube ion mobility-mass spectrometry (IM-MS) for the analysis of breath samples collected on solid adsorbents, with the ion mobility separation adding selectivity to the analyses.[21]

This section describes a rapid method for the determination of the isobaric PGIs, 2,4,6-trimethylaniline (III) and N,N-dimethyl-*m*-toluidine (IV) by thermal desorption from a surrogate API with a FAIMS separation prior to detection using mass spectrometry. Good precision was observed at the 1 ppm level for the FAIMS pre-selected PGIs, with a limit of quantification established well below the required TTC.

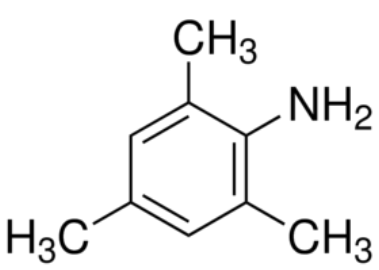

(III)

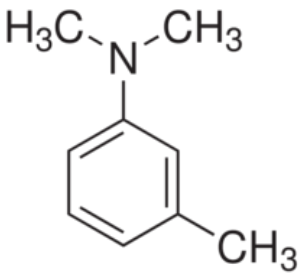

(IV)

4.3.2 Materials and Methods

4.3.2.1 Chemicals

2,4,6-trimethylaniline (2,4,6-TMA), N,N-dimethyl-*m*-toluidine (N,N-DMT), starch, and HPLC grade acetonitrile, methanol, water and formic acid were obtained from Sigma Aldrich (Gillingham, UK).

4.3.2.2 Sample Preparation

Standard solutions of 2,4,6-TMA (50 ng/ml) and N,N-DMT (50 ng/ml) were prepared in methanol/water (50:50) with 0.1% formic acid for infusion studies and in acetonitrile for thermal desorption studies. The PGI mixture (4 μL, 2.5 μg/mL) was added to a surrogate API, starch (10 mg) which was immediately inserted into a thermal desorption tube between two pieces of Siltek Deactivated Wool (Borosilicate, Markes Int.), as shown in Figure 4.2. The concentration of each of the PGIs in the starch was 1 ppm (w/w).

4.3.2.3 Instrumentation

TD-ESI-FAIMS-MS analyses were carried out using a Markes UNITY1 thermal desorption unit (Markes International, Swansea, UK) combined with an Agilent 6230 TOFMS (Agilent technologies, U.K.) fitted with the prototype chip-based FAIMS device. The experimental arrangement is shown schematically in Figure 4.6. 2,4,6-TMA and N,N-DMT were desorbed from the surrogate API (starch) at 230 °C for 2 min onto a cold trap (Tenax, -10 °C) and then rapidly desorbed from the trap (250 °C, >40 °C/s, 2 mins). The thermal desorption cycle time was ~10 minutes. The heated transfer line from the thermal desorber, containing a fused silica capillary (0.25 mm i.d.) was maintained at 200°C and introduced into the JetStream ESI of the TOFMS by removing the glass from a viewing window in the source housing. The tip of the fused silica capillary was positioned in the source at an angle of approximately 55˚ to the nebuliser, but set back ~10 mm to give the maximum response. Extractive electrospray and direct infusion electrospray were carried out in positive ion mode using a 10 μL/min infusion of methanol/water (50:50) with 0.1% formic acid. The ESI spray nebuliser pressure was set to 30 psig with an 8 L/min sheath gas flow at 250 °C. The nozzle voltage was set to 2000 V; the transfer capillary, spray shield and counter electrode were set to 3000 V and the drying gas flow to 6 L/min at 150 °C.

The miniaturised chip-based FAIMS prototype device 2 (Owlstone Ltd, Cambridge), consisting of multiple parallel electrode gaps (100 μm) with a short path length (700 μm),[22-24] was used for the analysis. Scanning FAIMS-MS experiments were carried out by direct infusion of 2,4,6-TMA and N,N-DMT individually to evaluate the potential for separation of these isobaric compounds. The DF was stepped (10 Td) from 200 to 300 Td and the CF was scanned from -2 to +5 Td to determine optimum separation conditions. The mass spectrometer fragmentor voltage was set to 175 V for FAIMS-selected transmission experiments. The MS scan rates were 10 scans/s and 1 scan/s in the mass range *m/*z 70-1000 for direct infusion and thermal desorption experiments respectively.

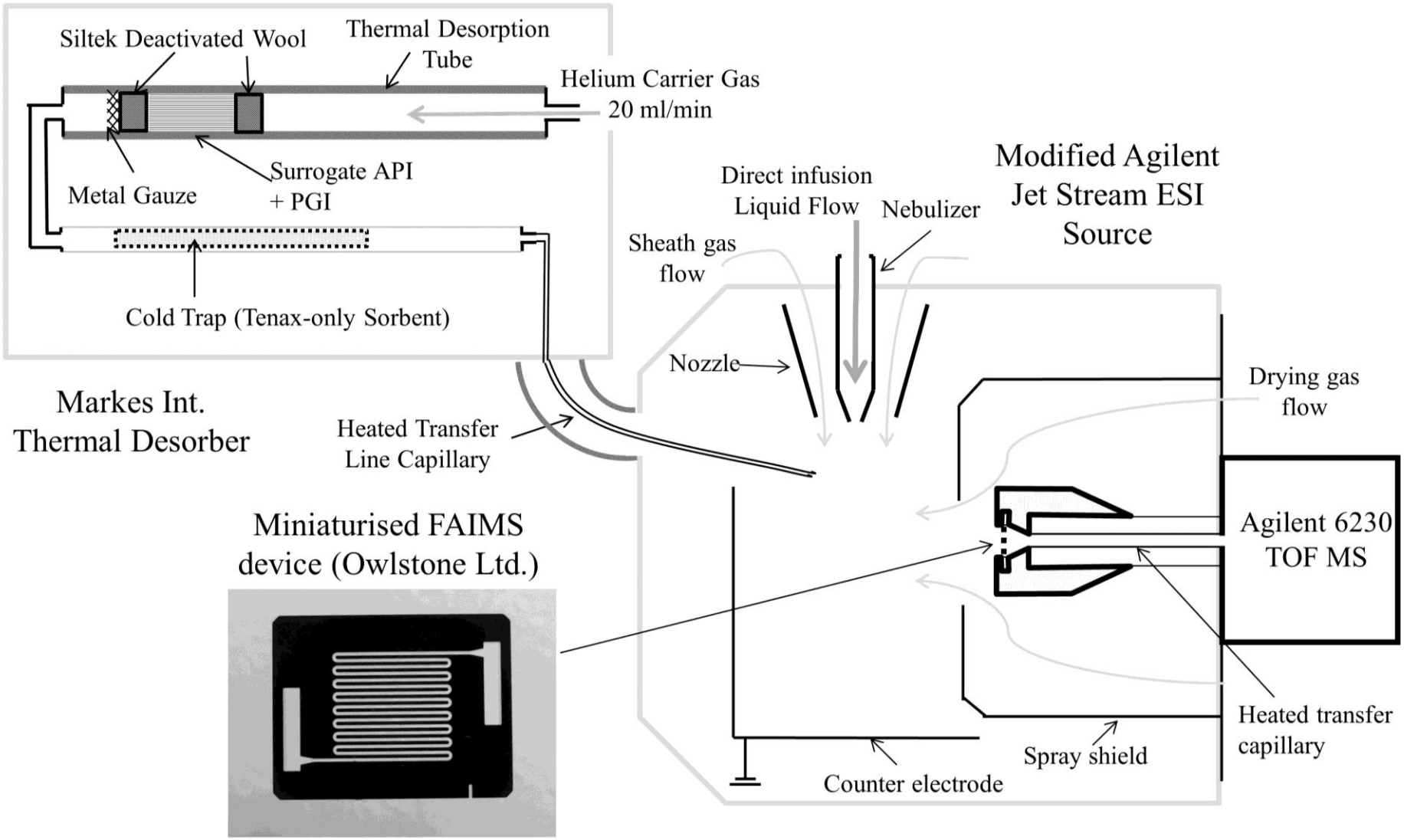

Figure 4.6 A schematic diagram of the thermal desorber interfaced to the ESI-FAIMS-MS ion source

4.3.3 Results and Discussion

The thermal desorption of volatile compounds from a less volatile solid sample, such as an API, has the potential to speed up analysis by removing time consuming sample preparation and chromatographic separation steps. Furthermore, there is an even greater potential advantage in that such approaches are matrix independent and can be applied to the analysis of a wide range of PGI/API combinations. Increasing sample throughput is important for efficient quality control, but selectivity may be compromised to reduce analysis times, particularly for isobaric analytes that cannot be distinguished by mass spectrometry.[25,26] Miniaturised, chip-based FAIMS into the ion source of a time-of-flight mass spectrometer (FAIMS-MS), was therefore investigated for the separation of the isobaric PGIs 2,4,6-trimethylaniline (2,4,6-TMA) and N,N-dimethyl-*m*-toluidine (N,N-DMT).

4.3.3.1 Direct infusion FAIMS-MS studies

The two substituted anilines, 2,4,6-TMA and N,N-DMT, were introduced by direct infusion into the ESI-FAIMS-MS to explore the potential for a rapid separation step which would be compatible with the thermal desorption of these analytes. A DF stepping experiment, with the CF scanned at each DF, was used to determine the optimum DF for maximum separation without compromising sensitivity.[27] The CF spectrum obtained at the optimum DF, which was determined to be 230 Td, is shown in Figure 4.7. The spectrum contains two peaks corresponding to 2,4,6-TMA and N,N-DMT centered at a CF at 1.0 and 1.5 Td respectively. There is also a small peak at CF 2 Td in Figure 4.7, which is assigned to the protonated dimer of 2,4,6-TMA. The N,N-DMT peak lies between the 2,4,6-TMA monomer and dimer peaks where there is no significant interference from either. 2,4,6-TMA and N,N-DMT were sufficiently resolved at a DF of 230 Td to enable the selective transmission of each without significant interference from the other.

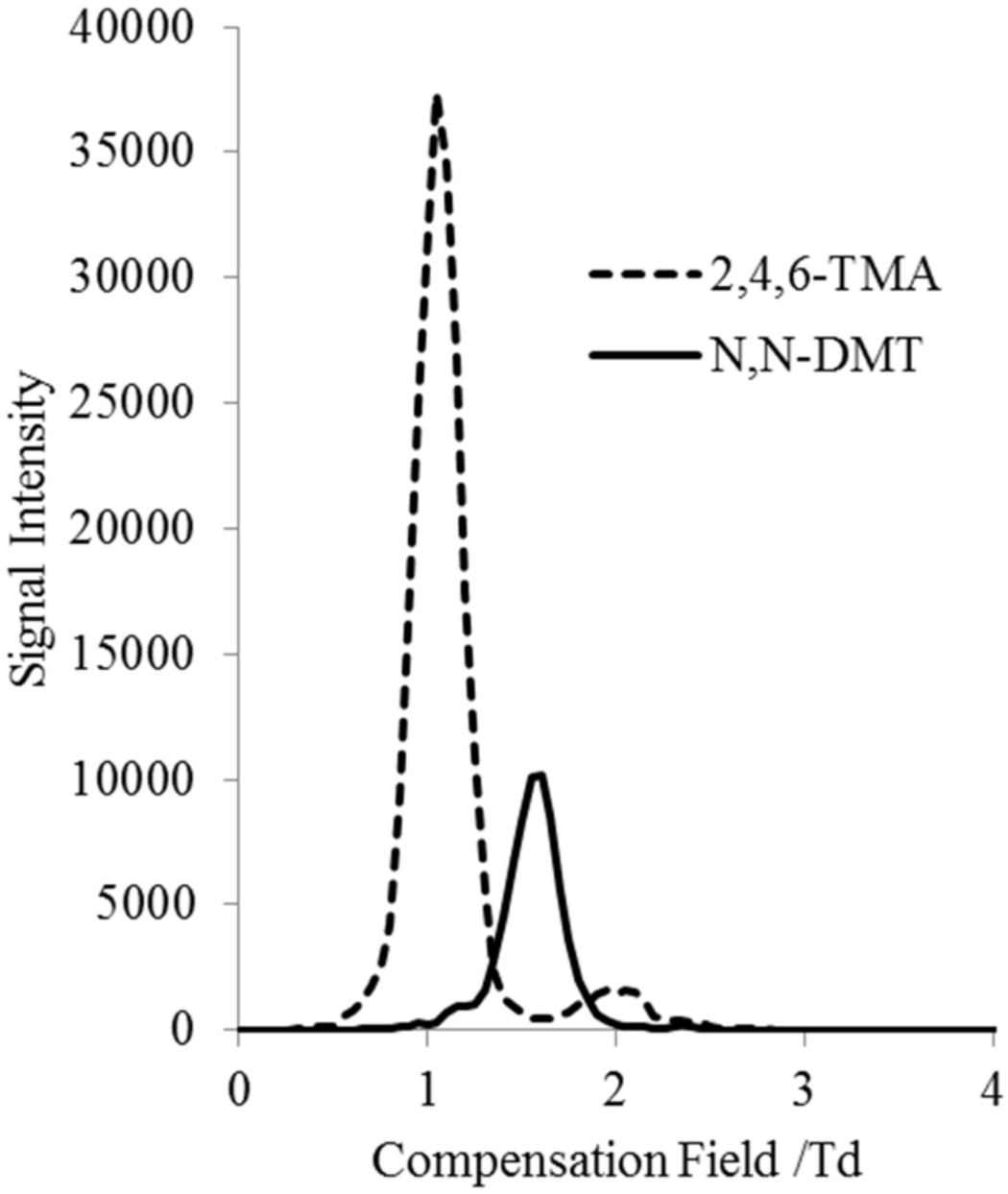

Figure 4.7 FAIMS CF scan of 2,4,6-TMA (dashed) and N,N-DMT (solid) with DF set to 230 Td

4.3.3.2 TD-FAIMS-MS analysis of 2,4,6-TMA and N,N-DMT

2,4,6-TMA and N,N-DMT are sufficiently volatile to be thermally desorbed from a surrogate API (starch) and transferred to the ESI source *via* a heated transfer line. The desorbed molecules were ionised using extractive electrospray (EESI) and detected using FAIMS-time-of-flight mass spectrometry (TOF MS). The FAIMS CF was set to transmit either 2,4,6-TMA (CF 1.0 Td) or N,N-DMT (CF 1.5 Td) selectively at a DF of 230 Td following ionization.

Figure 4.8 shows typical thermal desorption profiles (*m/z* 136) for the FAIMS pre-selected 2,4,6-TMA and N,N-DMT, spiked as a mixture into a surrogate API (starch) at 1 ppm (w/w). A good peak shape for the thermal desorption profile of each PGI was achieved by using a single sorbent (Tenax) in the desorber cold trap. The time axis corresponds to the mass spectrometry acquisition time, which was started 1 minute before the heating of the cold trap. Figure 4.8.a and 4.8.b inserts show mass spectra corresponding to the maximum point of the thermal desorption profiles of FAIMS-selected 2,4,6-TMA and N,N-DMT respectively, showing the protonated ions at *m/z* 136. The use of a FAIMS separation at the appropriate DF and CF determined from the direct infusion studies, adds selectivity to the analysis by discriminating between N,N-DMT and 2,4,6-TMA.

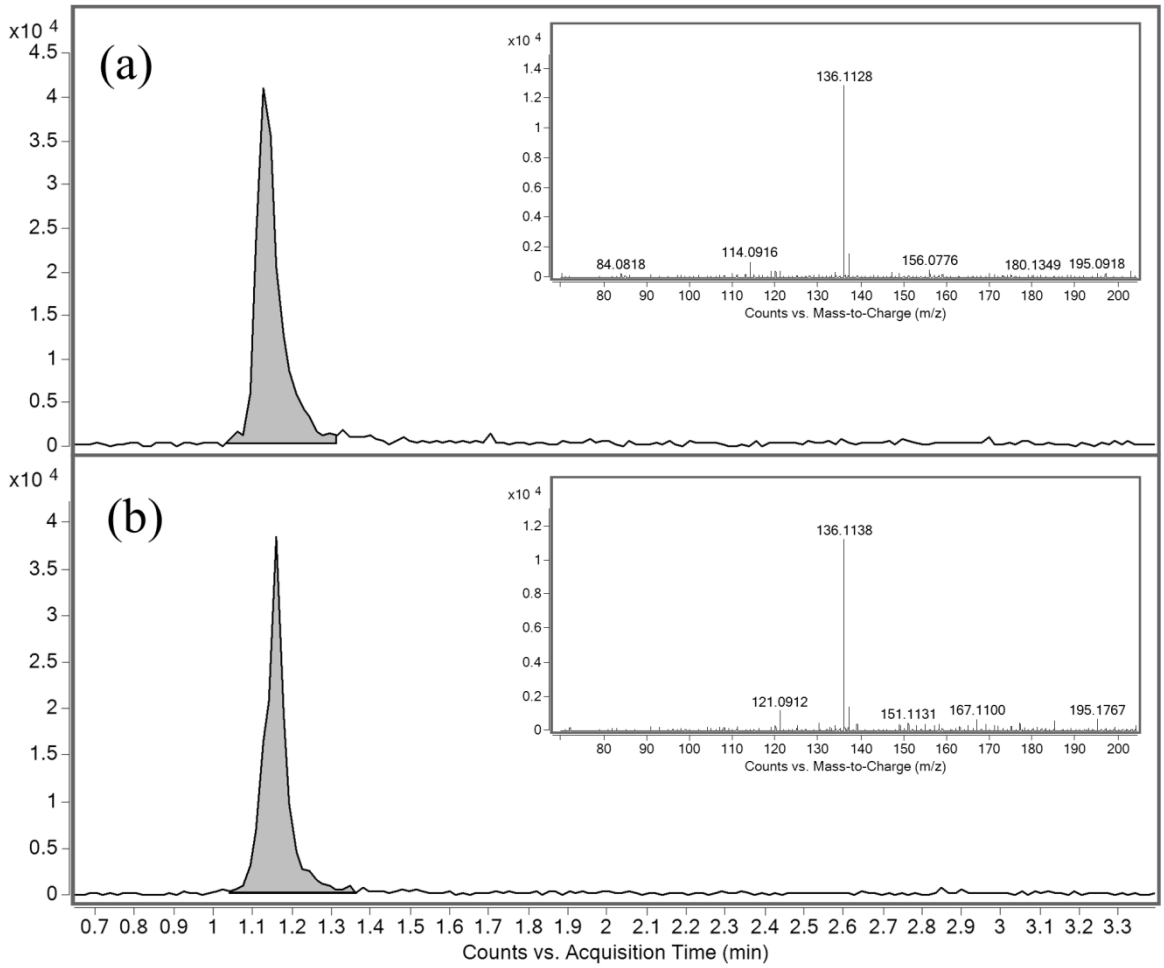

Figure 4.8 TD-ESI-FAIMS-MS selected ion profiles (*m/z* 136.1) of (a) 2,4,6-trimethylaniline (CF = 1 Td, DF 230 Td); and (b) N,N-dimethyl-*m*-toluidine (CF = 1.5 Td, DF 230 Td), desorbed directly from starch at 1 ppm (w/w). Inset are the corresponding mass spectra at the desorption peak maxima.

The quantification limits and precision were evaluated to test performance of the prototype TD-FAIMS-MS analysis (Table 4.1). The limit of quantification (LOQ) was determined to be 0.19 ppm and 0.13 ppm for the FAIMS pre-selected 2,4,6-TMA and N,N-DMT respectively (10:1 signal: noise), spiked as a mixture into 10 mg of the surrogate API. These LOQs are approximately an order of magnitude below 1.5 ppm, the TTC limit assuming a 1 g/day dose (European Medicines Agency). However, detection of PGIs at 'as low as reasonably possible' (the so-called ALARP concept) levels[13,14] is encouraged, but not essential, for unusually toxic impurities where detection below the TTC may be required. This requirement is easily met using TD-FAIMS-MS, as well as reducing sample preparation and analysis times.

Table 4.1 Quantitative determination of 2,4,6-TMA and N,N-DMT by TD-FAIMS-MS

Compound	LOQ /ppm	RSD /%
2,4,6-trimethylaniline	0.19	8.4
N,N-dimethyl-*m*-toluidine	0.13	7.5

4.4 Conclusion

Chip-based FAIMS combined with TOF MS has been used for the rapid determination of the isobaric PGIs 2,4,6-TMA and N,N-DMT, without the need for a chromatographic separation. The ability to filter ions based on differential mobility, an orthogonal technique to mass spectrometry, provides an added dimension of separation to the TD-MS analysis. Direct thermal desorption of 2,4,6-TMA and N,N-DMT from a solid matrix was demonstrated at 1 ppm, below the TTC, with good precision (< 8.4%). The combination of good reproducibility and limits of quantification almost an order of magnitude below the TTC, shows that TD-FAIMS-MS has the potential as a rapid, quantitative screening method for monitoring volatile PGIs in active pharmaceutical ingredients. Other API matrices would need to be investigated to demonstrate the ubiquity of this technique. The approach may also be used for the analysis of volatile organic compounds in other solid matrices

The solution degradation and in-source CID of cefepime to NMP presents an analytical challenge for the determination of NMP in cefepime. The use of a FAIMS separation of NMP and cefepime ions prior to mass spectrometric analysis allows NMP in a cefepime sample to be distinguished from NMP ions generated by in-source CID in the mass spectrometer interface. Direct infusion of a cefepime solution using ESI-FAIMS-MS is shown to be a rapid, selective method for the quantitative determination of NMP in cefepime with an LOQ well below the required 0.3 % threshold and good precision. The method reported here for NMP in cefepime has potential for generic application to the direct determination of impurities present in other active pharmaceutical ingredients which fragment to yield the impurity ion by in-source CID.

4.6 References

1. R. H. Barbhaiya, S. T. Forgue, C. R. Gleason, C. A. Knupp, K. A. Pittman, D. J. Weidler, H. Movahhed, J. Tenney, and R. R. Martin, *Antimicrob. Agents Chemother.*, 1992, **36**, 552–557.

2. P. Van Der Auwera and P. Santella, *J. Antimicrob. Chemother.*, 1993, **32**, 103–115.

3. J. Fung-Tomc, E. Huczko, M. Pearce, and R. E. Kessler, *Antimicrob. Agents Chemother.*, 1988, **32**, 1443–1445.

4. P. F. Sprauten, P. M. Beringer, S. G. Louie, T. W. Synold, and M. A. Gill, *Antimicrob. Agents Chemother.*, 2003, **47**, 1991–1994.

5. N. Baririan, H. Chanteux, E. Viaene, H. Servais, P.M. Tulkens, *J. Antimicrob. Chemother.*, 2003, **51**, 651–658.

6. E. Viaene, H. Chanteux, and P. M. Tulkens, *Antimicrobial Agents and Chemotherapy*, 2002, **46**, 2327–2332.

7. *Off. Prev. Pestic. toxic Subst. United States Environ. Prot. agency, Washington, DC*, 2009, 8.

8. T. McGovern, D. Jacobson-Kram, *Trend. Anal. Chem.*, 2006, **25**, 790-795

9. S. J. Prasanna, H. K. Sharma, K. Mukkanti, V. J. Kumar, G. Raja, and M. Sivakumaran, *J. Chromatogr. Sci.*, 2010, **48**, 830–834.

10. M. A. Farajzadeh, L. Goushjuii, and Y. Bashour, *J. Sep. Sci.*, 2010, **33**, 3767–3773.

11. N. H. Subramanian, S. Thyagarajan, P. Manigandan, R. G. Jeevan, and G. Radhakrishnan, *J. Chromatogr. Sci.*, 2009, **47**, 549–552.

12. N. Page, R. Stevenson, M. Powell, *Anal. Methods*, 2014, 6, 1248-1253.

13. L. Muller, R.J. Mauthe, C.M. Riley, M.M. Andino, D.D. Antonis, C. Beels, J. DeGeorge, A.G.M. De Knaep, D. Ellison, J.A. Fagerland, R. Frank, B. Fritschel, S. Galloway, E. Harpur, C.D.N. Humfrey, A.S. Jacks, N. Jagota, J. Mackinnon, G. Mohan, D.K. Ness, M.R. O'Donovan, M.D. Smith, G. Vudathala, L. Yotti, *Regul. Toxicol. Pharm.*, 2006, **44**, 198-211

14. *Genotoxic Impurities: Strategies for Identification and Control*, A. Teasdale, John Wiley and Sons Inc., New Jersey, 2010

15. http://www.ema.europa.eu/docs/en_GB/document_library/Scientific_guideline/2009/09/WC5 00002903.pdf, accessed on 16/11/2012

16. http://www.fda.gov/downloads/Drugs/.../Guidances/ucm079235.pdf, accessed on 16/11/2012

17. B.A. Olson, B.C. Castle, D.P. Myers, *Trend. Anal. Chem.*, 2006, **25**, 796-805

18. J.F. Pankow, W. Luo, L.M. Isabelle, D.A. Bender, R.J. Baker, *Anal. Chem.*, 1998, **70**, 5213-5221

19. J. Ding, S. Yang, D. Liang, H. Chen, Z. Wu, L. Zhang, Y. Ren, *Analyst*, 2009, **134**,2040-2050

20. N.A. Devenport, L.C. Sealey, F.H. Alruways, D.J. Weston, J.C. Reynolds, C.S. Creaser, *Anal. Chem.*, 2013, **85**, 6224-6227

21. J.C. Reynolds, G.J. Blackburn, C. Guallar-Hoyas, V.H. Moll, V. Bocos-Bintintan, G. Kaur-Atwal, M.D. Howdle, E.L. Harry, L.J. Brown, C.S. Creaser, C.L.P. Thomas, *Anal. Chem.*, 2010, **82**, 2139-2144

22. L.J. Brown, D.E. Toutoungi, N.A. Devenport, J.C. Reynolds, G. Kaur-Atwal, B. Boyle and C.S. Creaser, *Anal. Chem.*, 2010, **82**, 9827-9834

23. A.A. Shvartsburg, R.D. Smith, A. Wilks, A. Koehl, D. Ruiz-Alonso, P. Boyle, *Anal. Chem.*, 2009, **81**, 6489-6495

24. A.A. Shvartsburg, K. Tang, R.D. Smith, M. Holden, M. Rush, A. Thompson, D. Toutoungi, *Anal. Chem.*, 2009, **81**, 8048-8053

25. M.E. Kugler-Steigmeier, U. Friederich, U. Graf, P. Maier, C. Schlatter, *Arch. Toxicol., Suppl.*, 1998, **12**, 337-340

26. G. Vanhoenacker, E. Dumont, F. David, A. Baker, P. Sandra, *J. Chrom. A*, 2009, **1216**, 3563-3570

27. R.W. Smith, D.E. Toutoungi, J.C. Reynolds, A.W.T. Bristow, A. Ray, A. Sage, I.D. Wilson, D.J. Weston, B. Boyle, C.S. Creaser, *J. Chromatogr. A*, 2013, **1278**, 76-81

Chapter 5

Enhanced Performance in the Determination of Ibuprofen 1-β-O acyl glucuronide in Urine by Combining High Field Asymmetric Waveform Ion Mobility Spectrometry with Liquid Chromatography-Time-of-Flight Mass Spectrometry

5.1 Chapter Overview

The incorporation of a chip-based high field asymmetric waveform ion mobility spectrometry (FAIMS) separation in the ultra (high)-performance liquid chromatography-high resolution mass spectrometry (UHPLC-HRMS) determination of the (R/S) ibuprofen 1-β-O acyl glucuronide metabolite in urine has been investigated. UHPLC-FAIMS-HRMS reduced matrix chemical noise, improved the limit of quantitation approximately two-fold and increased the linear dynamic range compared to the determination of the metabolite without FAIMS separation. A quantitative evaluation of the prototype UHPLC-FAIMS-HRMS system showed better reproducibility for the drug metabolite (%RSD 2.7%) at biologically relevant concentrations in urine. In-source collision induced dissociation of the FAIMS-selected deprotonated metabolite was used to fragment the ion prior to mass analysis, enhancing selectivity by removing co-eluting species and aiding the qualitative identification of the metabolite by increasing the signal-to-noise ratio of the fragment ions.

5.2 Introduction

The performance of a liquid chromatographic separation is determined both by the on-column separation and by the selectivity of the detector. UHPLC can significantly reduce chromatographic run times, but the use of selective detection, such as mass spectrometry, is required if the highest sensitivity, selectivity and throughput is to be achieved. Tandem mass spectrometry using a triple quadrupole mass spectrometer capable of mass-selecting precursor ions for selected reaction monitoring is widely used in the quantitative chromatographic determination of drugs and metabolites. However, recent years have seen the emergence of high resolution mass spectrometry (HRMS), using TOF or Orbitrap mass analysers, as an alternative to triple quadrupole instruments.[1,2] The advantage of coupling UHPLC with HRMS is that HRMS provides both robust quantification and qualitative analysis using a single mass spectrometer platform. However, HRMS may lack the selectivity and sensitivity of selected reaction monitoring on a tandem mass spectrometer.

One approach to enhancing the selectivity of LC-MS analyses is the incorporation of a rapid gas-phase separation by ion mobility (IM) spectrometry between the LC and the mass spectrometer. Two ion mobility approaches are currently utilised: drift tube-ion mobility spectrometry, which separates ions based on time taken to traverse a drift tube,[3] and field asymmetric waveform ion mobility spectrometry (FAIMS), or differential mobility

spectrometry.[4] The details of these techniques were discussed in detail in Section 1.1. Drift-tube IM has been interfaced with ultra (high)-performance liquid chromatography-mass spectrometry (UHPLC-IM-MS) to enhance the quantitative determination of drugs and metabolites in urine by removing co-eluting interferences.[5,6] However, incorporation of a drift-tube ion mobility separation can significantly reduce the linear dynamic range (LDR) compared to LC-MS alone.[7-10]

FAIMS separation is orthogonal to MS and acts as an on-line filter for ions entering the MS because ions are pre-selected by FAIMS based upon their differential ion mobility. The compensation field (CF) for transmission of an ion in FAIMS is a characteristic of ion structure and is scanned at a fixed DF to determine the optimum CF at which the ion is preferentially transmitted, whilst other interfering ions are neutralised and filtered out.[4,11] FAIMS devices interfaced with MS can improve analytical selectivity by providing a differential mobility separation prior to MS detection of small molecules, metabolites and peptides.[12-14]

Fragmentation of ions using a single mass analyser can be achieved by increasing voltages in the interface region between the ESI source and the vacuum of the mass spectrometer, called in-source CID (Section 1.5), which will fragment all co-eluting ions generated in the ESI source.[15] However, the production of fragments from multiple precursors, without ion pre-selection, complicates fragmentation spectra making identification difficult. The effect of in-source CID on the analysis of glucuronide metabolites in biological matrices has been explored.[16] A comparison between in-source CID and collision cell CID using a triple quadrupole mass spectrometer for characterising microcystins in water samples showed that even though in-source CID proved to be more sensitive, CID of a mass-selected precursor ion in a collision cell was found to be more selective for analyte identification. Fragmentation patterns were found to be similar for the two techniques.[17] Combining FAIMS-selection with in-source CID, referred to FISCID-MS (Section 2.2), has been used for the identification of an active pharmaceutical ingredient in a common pharmaceutical excipient and the qualitative and quantitative analysis of peptides in plasma by LC-FISCID-MS and was described in Section 2.4.2.3.

This chapter reports an investigation into the potential of FAIMS for enhancing performance of a UHPLC-MS analysis of the drug metabolite (R/S) ibuprofen 1-β-O acyl glucuronide,

IAG (Figure 5.1, I), in urine. The analysis was carried out without prior sample clean-up, by the incorporation of a FAIMS separation using the prototype chip-based FAIMS device. FAIMS pre-selection of the metabolite is shown to improve the limit of quantification, linear dynamic range and reproducibility, and allow a shorter chromatographic run time compared to UHPLC-MS by reducing chemical/matrix interference. The FAIMS device was also used to pre-select IAG for UHPLC-FISCID-MS, enhancing the qualitative identification of the metabolite.

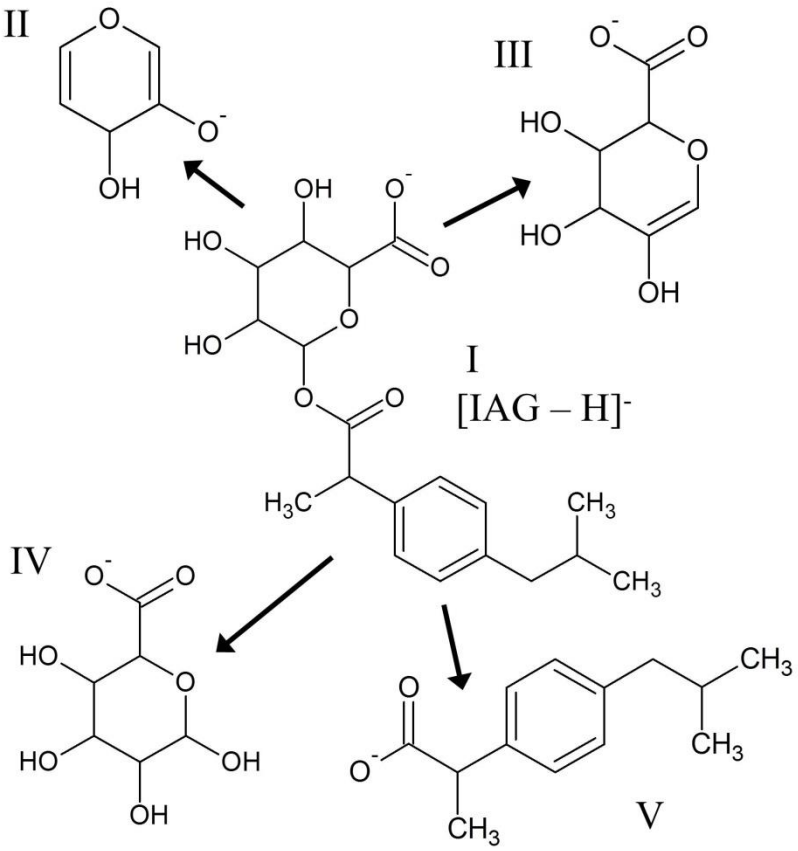

Figure 5.1 Fragments produced from $[IAG - H]^-$ (I) by CID: decarboxylated di-dehydrated glucuronate (II); dehydrated glucuronate (III); glucuronate (IV); and aglycone (V).[20]

5.3 Experimental

5.3.1 Chemicals

HPLC grade methanol (MeOH), acetonitrile (ACN), water, formic acid (FA) and ammonium acetate were purchased from Fisher Scientific (Loughborough, UK). (R/S) Ibuprofen 1-β-O-acyl glucuronide was supplied by AstraZeneca (Alderley Park, UK). Ibuprofen was extracted into methanol from an ibuprofen tablet (200 mg).

5.3.2 Sample Preparation

Aliquots of urine (5 ml) from healthy adult males (x2) and females (x2) (AstraZeneca, UK) was pooled (20 ml) and filtered (0.45 μm), diluted (2x) with a solution of the IAG metabolite (0.055 to 44 μg/ml in 50:50 acetonitrile:aqueous ammonium acetate (10 mM) at pH 3) and with diluent to include a urine blank (to check for any existing IAG in the urine), corresponding to IAG urine concentrations in the range 0.028 to 22 μg/ml.

5.3.3 Instrumentation

UHPLC-FAIMS-MS and UHPLC-FISCID-MS analyses of IAG were carried out using an Agilent 1200 series HPLC interfaced with an Agilent 6230 time-of-flight mass spectrometer fitted with a JetStream ESI source operated in negative ion mode (Agilent Technologies, Santa Clara, CA, USA). The chip-based FAIMS prototype device 2 (Owlstone, Cambridge, UK) has been previously described in Section 2.3.3 and was located in front of the transfer inlet capillary, behind a modified spray shield within a Jet Stream ESI source. FAIMS devices with a 100 μm electrode gap and a depth of 700 μm were used for the analysis. The FAIMS electrodes were arranged as multiple parallel channels, linked by a serpentine channel with trench lengths of 51.7, 78.1 and 97.0 mm. Dispersion fields in the range 200 to 300 Td were applied at a 27 MHz frequency with an approximate low to high field ratio of 2:1. Nitrogen (99.5 % purity) was used as the carrier gas for the FAIMS system and for the ESI source and mass spectrometer interface.

Samples were introduced into the ESI source either by direct infusion at a flow rate of 15 µl/min or from the liquid chromatograph. UHPLC separation was carried out, with a 5 µl

sample injection volume on a Zorbax C18 column (2.1 x 50 mm, 1.8 μm, Agilent Technologies) with an isocratic 0.2 ml/min flow of 50:50 acetonitrile:aqueous ammonium acetate (10 mM) at pH 3. The scan rate of the TOF MS was 10 scans/sec for scanning FAIMS-MS experiments and 1 scan/sec for UHPLC-FAIMS-MS and UHPLC-FISCID-MS experiments. Data were acquired with the instrument mode set to extended dynamic range (2 GHz) at a resolution of 5700. Source conditions for LC experiments were: nozzle voltage, 2000 V; sheath gas temperature and flow, 350 °C and 11 L/min; drying gas temperature and flow, 150°C and 10 L/min; nebuliser pressure, 25 psig; transfer capillary, 4000 V; skimmer voltage, 65 V; fragmentor voltage, -150 V and -250 V for transmission and in-source CID respectively. Data were processed using Mass Hunter Qualitative Software B.04.00 (Agilent Technologies, Santa Clara, CA, USA) and Microsoft Excel 2010 (Microsoft, Seattle, USA).

5.4 Results and Discussion

5.4.1 Direct Infusion FAIMS analysis of IAG and ibuprofen

Direct infusion of ibuprofen and the IAG metabolite (0.65 μg/ml) was used to optimise the microscale FAIMS conditions for separation and sensitivity. FAIMS compensation field (CF) spectra of the $[M-H]^-$ ions of the analytes obtained at a dispersion field (DF) of 200, 230 and 260 Td are shown in Figure 5.2. The IAG response is separated from that of the parent drug ibuprofen as a result of structural differences between the two ions with IAG showing a greater CF shift at all DFs. The separation of IAG and the parent drug improved with increased DF. A decrease in the absolute intensity of IAG was observed when the DF was increased from 200 to 260 Td, but with a significant increase in the response relative to ibuprofen, which falls sharply with increasing DF. A decrease in ion intensity with DF is commonly observed for low mass ions as a result of losses by diffusion, where diffusion increases with DF.[4] The optimum CF for transmission of IAG was at 2.2 Td with a DF of 260 Td, based on the best separation without significant loss of signal intensity for IAG, and these conditions were used in the high resolution UHPLC-FAIMS-MS analyses.

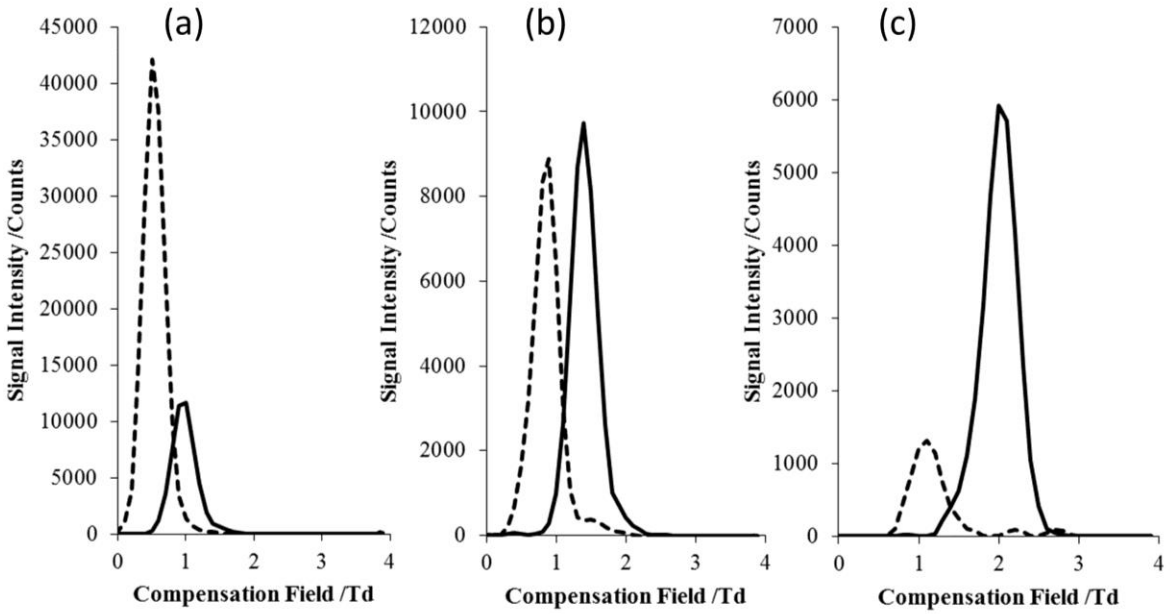

Figure 5.2 FAIMS CF spectra of ibuprofen, *m/z* 205, (dashed line) and IAG, *m/z* 381 (solid line) at DF: (a) 200 Td, (b) 230 Td and (c) 260 Td.

The FAIMS devices with different serpentine channel lengths of 51.7, 78.1 and 97.0 mm were investigated to determine the most suitable for the analysis. The CF spectra in Figure 5.3.a-c shows that the peak width for IAG decreases with increasing trench length. The exact peak widths are shown in Table 5.1; the corresponding full width at half maximum (FWHM) demonstrate improvement in FWHM with increasing trench length. The most likely hypothesis for peak widths becoming smaller for larger trench length is that the ion residence time is higher in the FAIMS chip with a large trench length. This is because the flow through the chip is slower when the trench length is longer, and that a smaller trench length results in a higher flow with a lower ion residence time. The vacuum pump of the MS pulls the carrier gas flow through the FAIMS chip which determines the carrier gas flow rate; a longer trench length effectively creates a larger cross section tube resulting in a lower flow rate just as a shorter trench length creates a smaller cross section giving a higher flow rate. The flow/ion residence time of an ion in the FAIMS device changes the width of the peak but also results in a change in ion intensity, where longer ion residence times increase signal loss due to diffusion. Figure 5.4 shows that trench length has a far greater impact on peak area of deprotonated ibuprofen than on IAG. The peak area of ibuprofen is reduced by ~5 times compared to ~3 times for IAG when changing from 51.7 mm to 78.1 mm trench length. The chip with a trench length of 78.1 mm was selected for quantitative studies because it offers a good compromise between small peak widths and acceptable transmission. The option of FAIMS chips with different trench lengths means that FAIMS devices can be selected to be better suited for an analysis that either requires greater transmission or narrower peak widths.

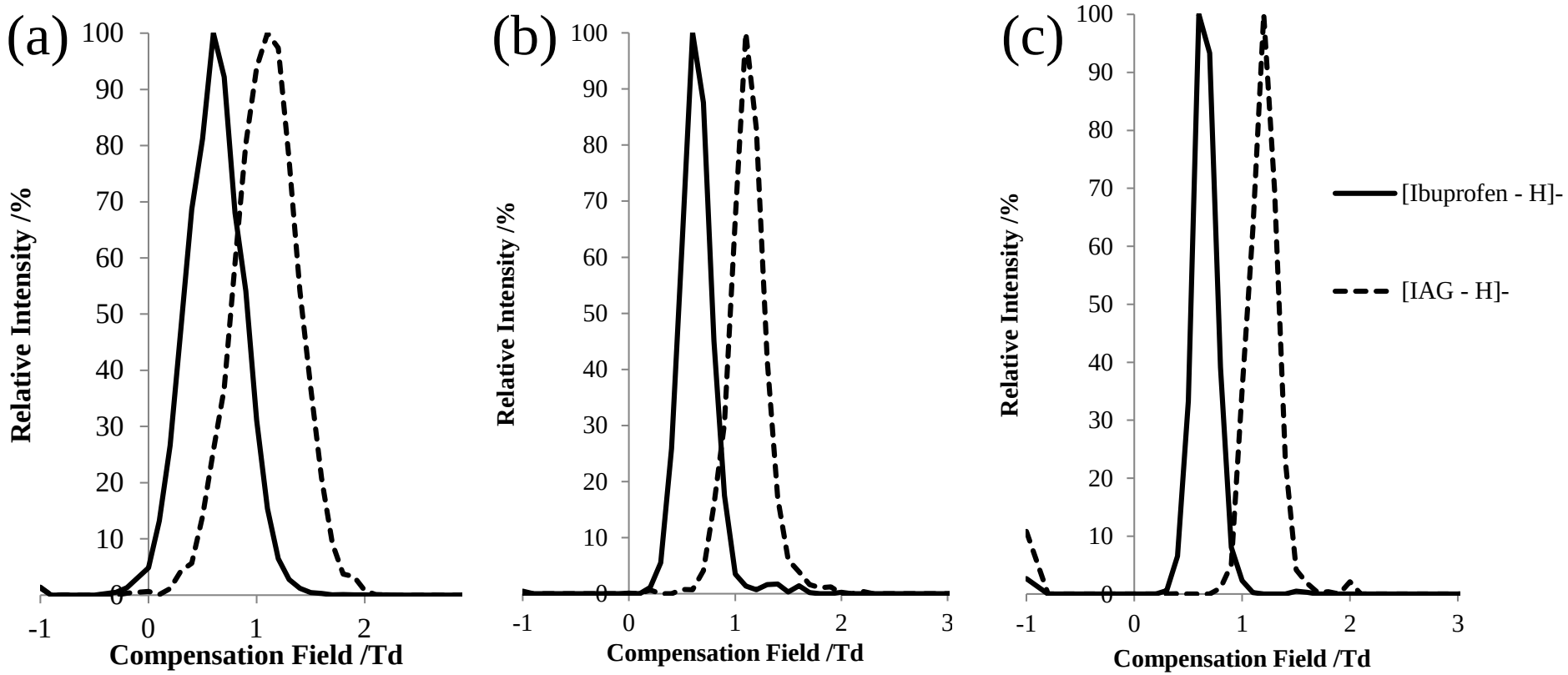

Figure 5.3 FAIMS CF spectra of ibuprofen, *m/z* 205, (dashed line) and IAG, *m/z* 381 (solid line) at DF 220 Td using FAIMS chips with different trench lengths: (a) 51.7 mm, (b) 78.1 mm and (c) 97.0 mm

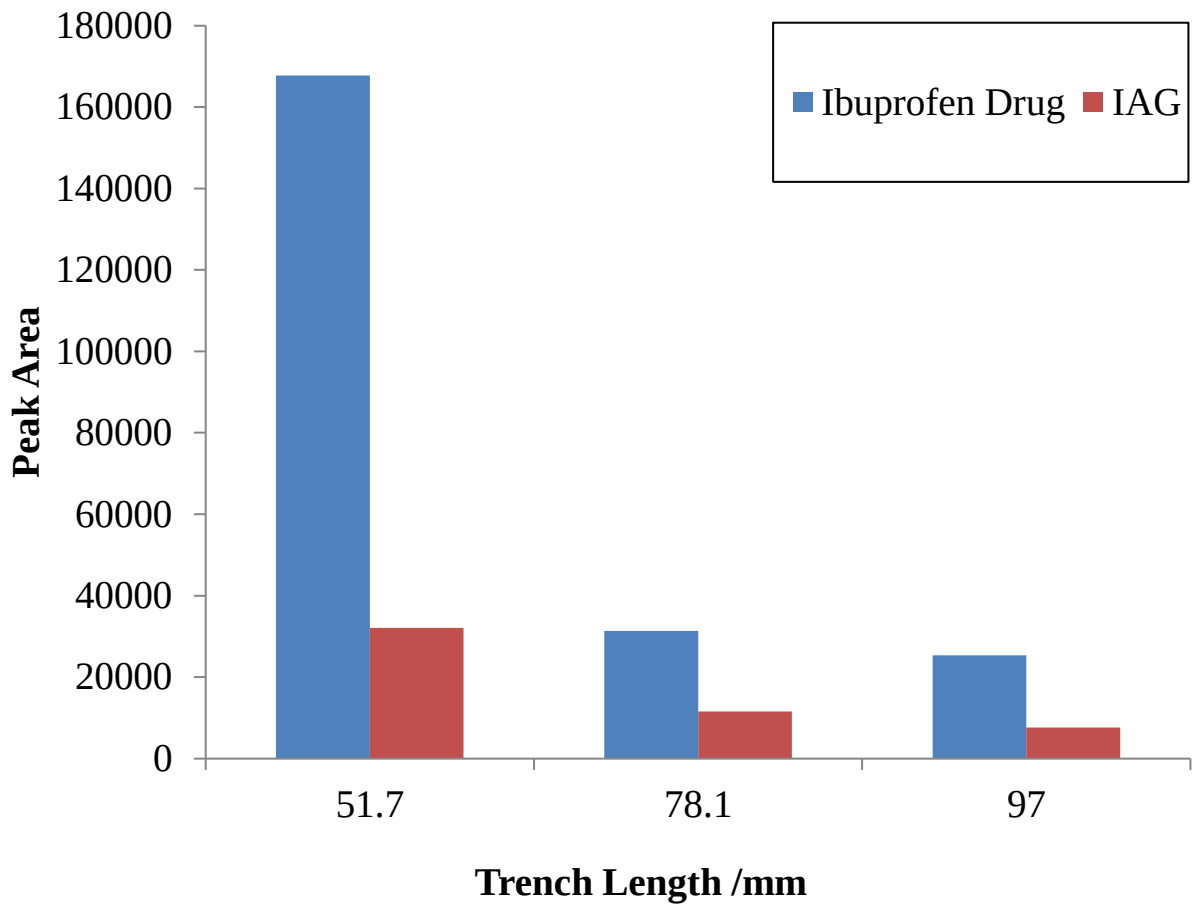

Figure 5.4 Bar chart showing peak area of ibuprofen (blue) and IAG (red) against trench length

Table 5.1 The effect of different FAIMS chip trench lengths on peak width at half height and resolution of IAG peak

Trench Length /mm	Peak width at half height	Resolution
51.7	0.66	1.7
78.1	0.32	3.4
97.0	0.28	3.9

5.4.2 Determination of IAG by UHPLC-FAIMS-TOF-MS

The UHPLC-MS (FAIMS off) and UHPLC-FAIMS-MS (FAIMS on) selected ion chromatograms ($[M-H]^-$; *m/z* 381) obtained for the analysis of IAG spiked into urine with a high resolution mass window of *m/z* 381±0.02 (±50 ppm) is shown in Figure 5.5.a. The UHPLC gradient was adjusted to minimise the run time for the IAG, but this resulted in a significant overlap between the IAG peak and urine matrix components. The observed co-elution of IAG with matrix components could be reduced by changing the UHPLC conditions to separate the metabolite from the urine matrix, but at the cost of a significantly increased chromatographic run time. A narrower mass window, *m/z* 381±0.008 (±20 ppm) was therefore investigated to determine whether this would improve selectivity without extending the chromatographic run time. The absolute intensity of the IAG peak, with the FAIMS switched off, is reduced by a factor of two if the mass window is narrowed from ±50 ppm to ±20 ppm (Figure 5.5.b), but there is no additional discrimination against the chemical noise from the urine matrix at the mass resolution used in the analysis (5700 FWHM).

The advantage of the incorporation of the FAIMS separation is demonstrated by a significant reduction in the co-eluting chemical noise from the urine matrix (Figure 5.5.c and d), whilst maintaining a rapid elution time. Ionization suppression in the ESI source was not determined, but was the same in both FAIMS on and FAIMS off modes, allowing an evaluation of the improvement in the chromatographic performance offered by FAIMS. The removal of chemical noise resulted in a better signal-to-noise ratio and peak integration with FAIMS on, even though the absolute intensity of the IAG peak was reduced because of ion losses in the device. FAIMS pre-selection of IAG removes matrix ions to baseline for both the *m/z* 381 ±0.02 and ±0.008 mass windows, but at a cost of lower sensitivity and signal-to-noise ratio for the narrower window. The ±0.02 mass window was therefore used in subsequent studies.

Setting the mass window to 381 ±0.5 instead of the narrower mass windows associated with TOF mass spectra can be used to mimic the selected ion chromatograms that would be produced if using a low resolution (e.g. single quadruple) mass analyser (Figure 5.6). The intensity of the IAG peak is higher with the wider mass window than when using a mass window of ±0.02 or ±0.008, although the benefit of the higher intensity is negated by the presence of greater chemical interference in the chromatogram (Figure 5.6.a). The high mass

resolution possible when using the narrow mass range of the TOF mass analyser reduced some of the interference observed in the ±0.5 mass window, although the overall matrix profile is similar for all three mass windows. However, effective removal of chemical interference was again achieved by using FAIMS-selective transmission of the IAG ion (Figure 5.6.b). These observations emphasise the orthogonality of the FAIMS and MS separations and demonstrate the potential of FAIMS to enhance quantitative performance of both low and high resolution mass analysers.

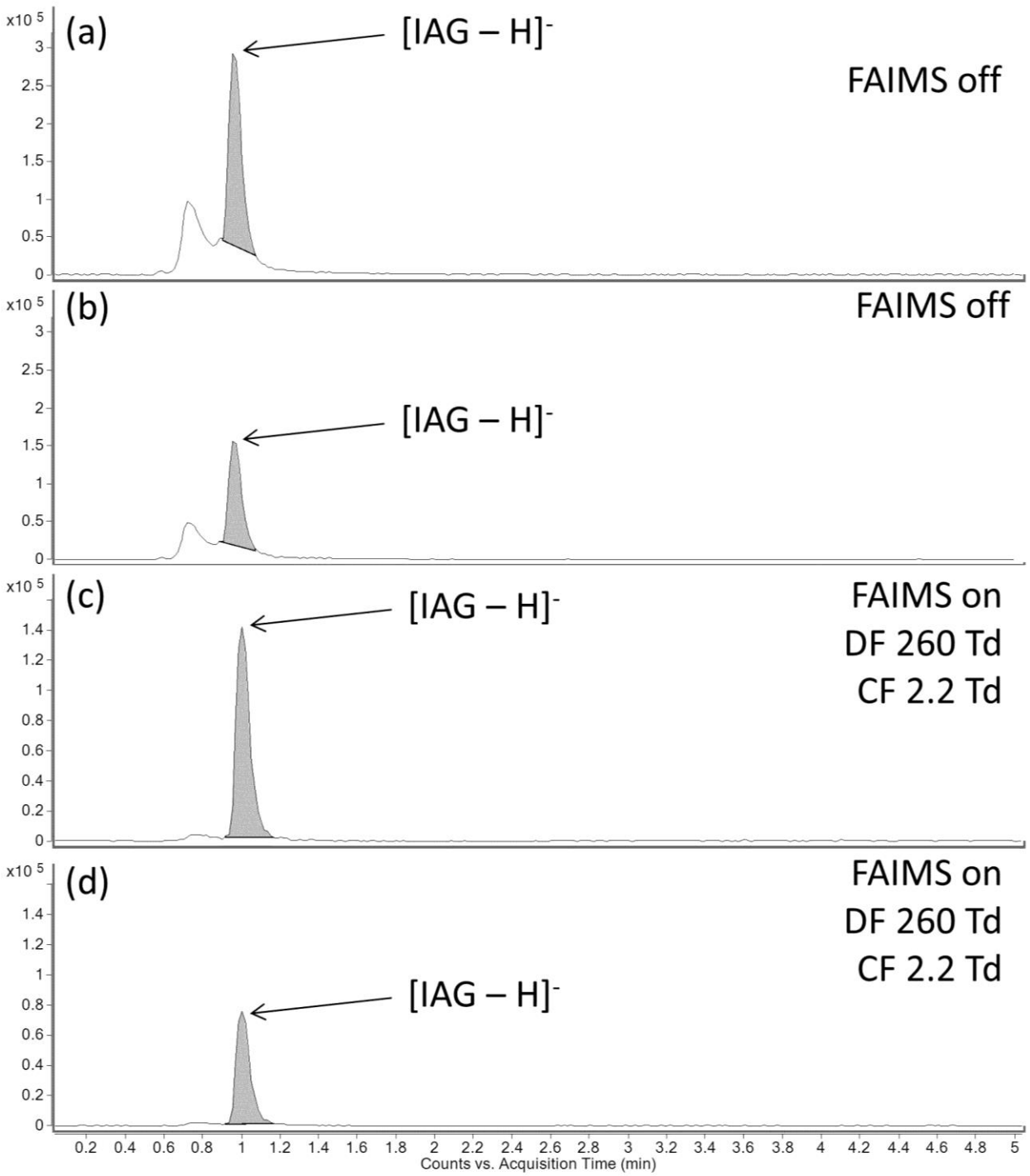

Figure 5.5 Selected ion chromatograms (*m/z* 381) for IAG (highlighted) spiked into urine (0.55 μg/ml) analysed by UHPLC-MS (FAIMS off) using a mass window of (a) *m/z* 381±0.02 and (b) *m/z* 381±0.008; and by UHPLC-FAIMS-MS (FAIMS on) with selective transmission of IAG (DF 260 Td, CF 2.2 Td) using a mass window of (c) *m/z* 381±0.02 and (d) *m/z* 381±0.008

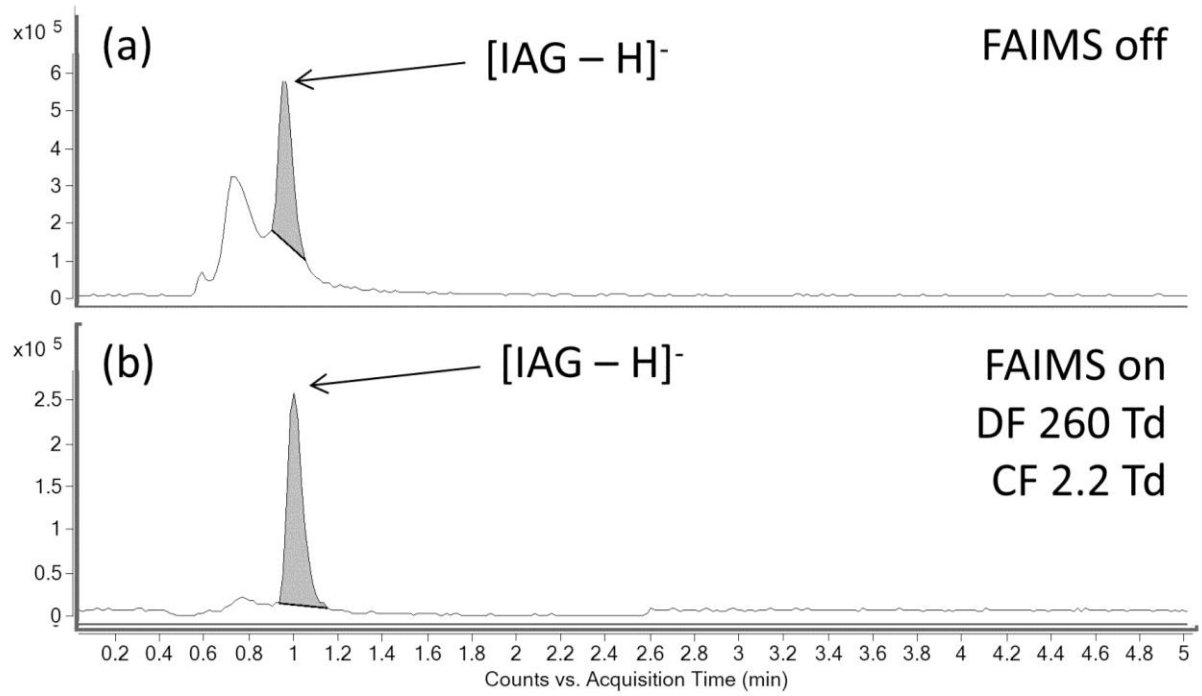

Figure 5.6 Selected ion chromatograms (*m/z* 381) for IAG (highlighted) spiked into urine (0.55 μg/ml) analysed by UHPLC-MS (FAIMS off) using a mass window of (a) *m/z* 381±0.5; and by UHPLC-FAIMS-MS (FAIMS on) with selective transmission of IAG (DF 260 Td, CF 2.2 Td) using a mass window of (c) *m/z* 381±0.5

The mass spectrum taken from the IAG UHPLC peak with FAIMS off (Figure 5.7.a) showed IAG (*m/z* 381.1570; -3.9 ppm) to be a minor peak in a complex mass spectrum. The effect of the FAIMS selection of IAG across a wide mass range is apparent from the mass spectrum for IAG with FAIMS on (Figure 5.7.b) which is simplified compared to FAIMS off, with IAG as the base peak in the mass spectrum (*m/z* 381.1553; 0.52 ppm), as a result of discrimination against interferences from urine matrix.

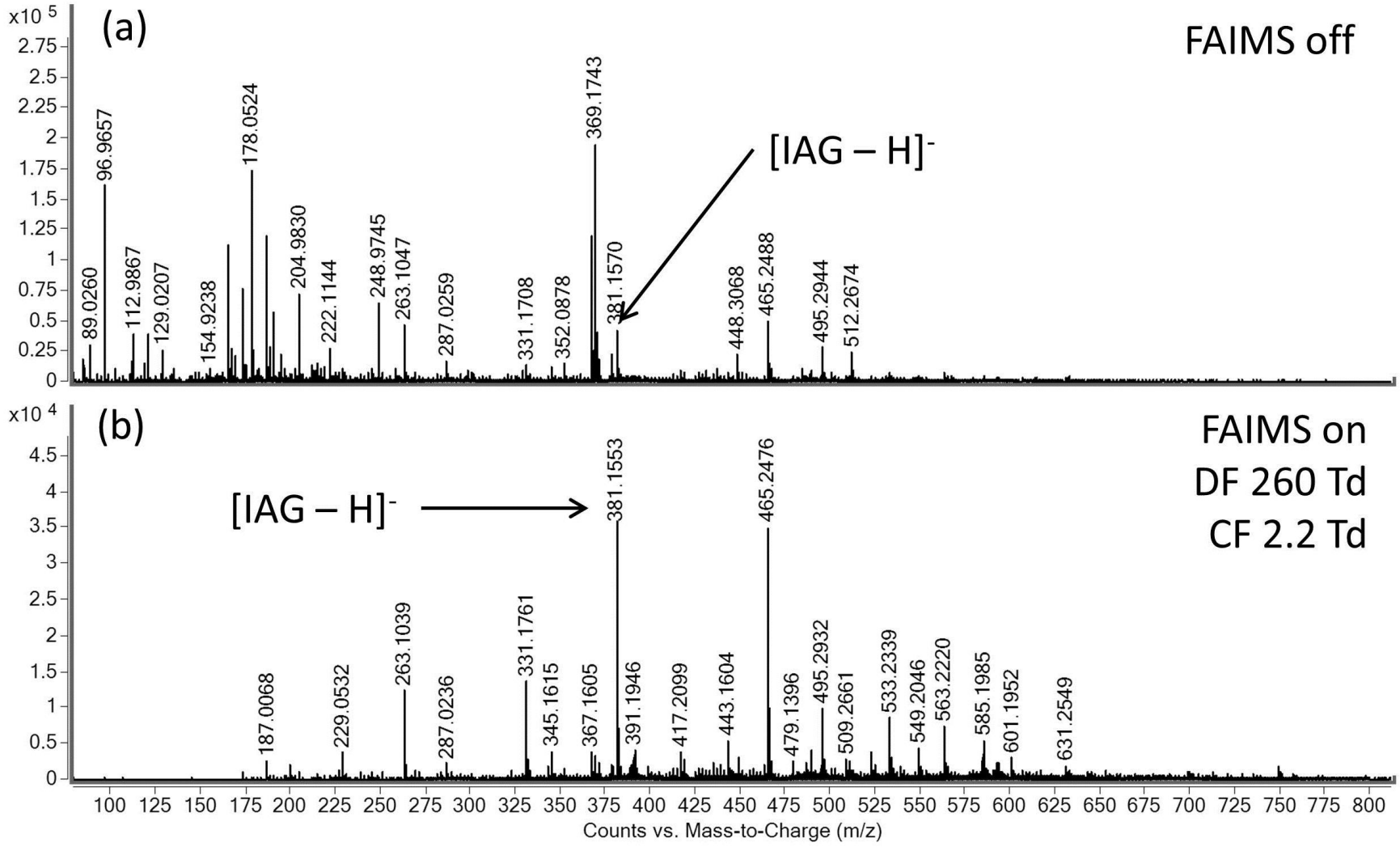

Figure 5.7 Mass spectra at retention time (RT) 0.98-1.02 mins with (a) FAIMS off, and (b) FAIMS on (DF 260 Td, CF 2.2 Td)

Figure 5.8 and Table 5.2 compare the quantitative performance of the UHPLC-MS and UHPLC-FAIMS-MS methods for the determination of IAG in urine. The limit of quantitation (LOQ; signal-to-noise 10:1) for IAG was reduced from 18 ng/ml (FAIMS off) to 10 ng/ml (FAIMS on), based on the selected ion peak areas of IAG (*m/*z 381 ±0.02) using UHPLC-FAIMS-MS. Calibration graphs for the IAG spiked into urine and analysed by UHPLC-MS with FAIMS off (Figure 5.8.a) and FAIMS on (Figure 5.8.b) are shown in Figure 5.8. The upper limit of the linear dynamic range (LDR) was the same in both FAIMS off and on modes, giving an increased LDR of >3 orders of magnitude for the miniaturised FAIMS-MS as a result of the lower LOQ, in contrast to a LDR of ~2 orders of magnitude with cylindrical FAIMS-MS [18,19] and <2.5 orders of magnitude for drift tube IM-MS.[5,6] The intra-day reproducibility of the prototype UHPLC-FAIMS-MS system was compared with UHPLC-MS by analysing IAG spiked into urine (15.5 μg/ml) and running FAIMS in on and off modes respectively (Table 5.2). %RSDs, sufficient for good quantification, were obtained for both UHPLC-MS (5.0%) and UHPLC-FAIMS-MS (2.7%), with the UHPLC-FAIMS-MS showing better reproducibility. These data demonstrate that the FAIMS device enhances quantitative performance compared to high resolution UHPLC and MS analysis.

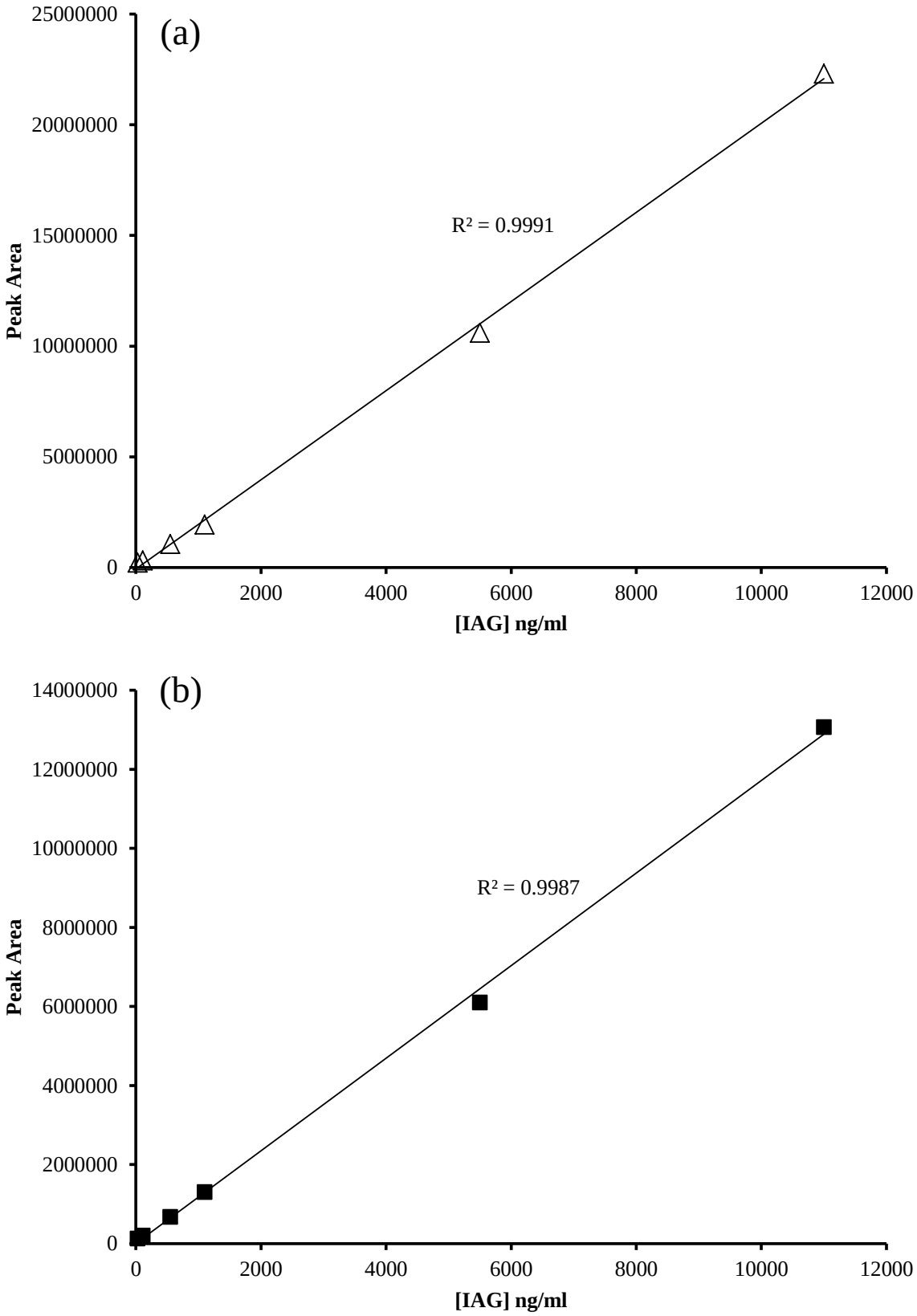

Figure 5.8 Calibration plots of IAG spiked into urine analysed by (a) UHPLC-MS (FAIMS off, unshaded triangle); and by (b) UHPLC-FAIMS-MS (FAIMS on, black square) with selective transmission of IAG (DF 260 Td, CF 2.2 Td)

Table 5.2 A comparison of LOQ; LDR (R^2) and intra-day reproducibility for the determination of IAG spiked into urine (15.5 μg/ml, n=5)

	UHPLC-MS	UHPLC-FAIMS-MS
LOQ (µg/ml)	0.018	0.010
LDR (µg/ml)	0.018-11	0.010-11
R^2	0.9991	0.9987
Intra-day (% RSD)	5.0	2.7

5.4.3 Qualitative identification of IAG by UHPLC-FISCID-MS

The in-source CID fragmentation of IAG ion was used to assess the improvement offered by the UHPLC-FISCID-MS technique for the qualitative identification of IAG. The FAIMS-selected $[M-H]^-$ ion of IAG was subjected to in-source CID to produce the characteristic fragments of the ion (Figure 5.1). A comparison of the selected ion chromatograms of the aglycone fragment (*m/z* 205.1234) for a urine sample spiked with IAG (3.9 μg/ml), with and without FAIMS pre-selection prior to in-source CID, was used to define the level of isobaric chemical interference present in the sample spiked with IAG (Figure 5.9.a and b). Peak integration of the UHPLC-FISCID-MS data was more reliable than UHPLC-MS data because chemical interference was reduced almost to baseline.

Mass spectra extracted from the aglycone peaks (Figure 5.10) shows the effect of applying the FAIMS separation to the UHPLC-CID-MS analysis of IAG. Four diagnostic fragment ions for IAG are observed in the production mass spectrum (Figure 5.1):[20] decarboxylated di-dehydrated glucuronate (II, *m/z* 113); dehydrated glucuronate (III, *m/z* 175); glucuronate (IV, *m/z* 193); and the aglycone (V, *m/z* 205). In Figure 5.10, these fragments are difficult to locate due to the complexity of the mass spectrum and poor signal to noise as a result of other ions in the matrix. Pre-selecting IAG using FAIMS before in-source CID reduced the intensity of interfering ions, increasing the relative intensity of the IAG (Figure 5.10.b). The signal-to-noise ratios for the fragment ions increased by approximately 2-fold with FAIMS

on (Table 5.3), enhancing the response of the IAG fragments relative to other interfering peaks to aid identification.

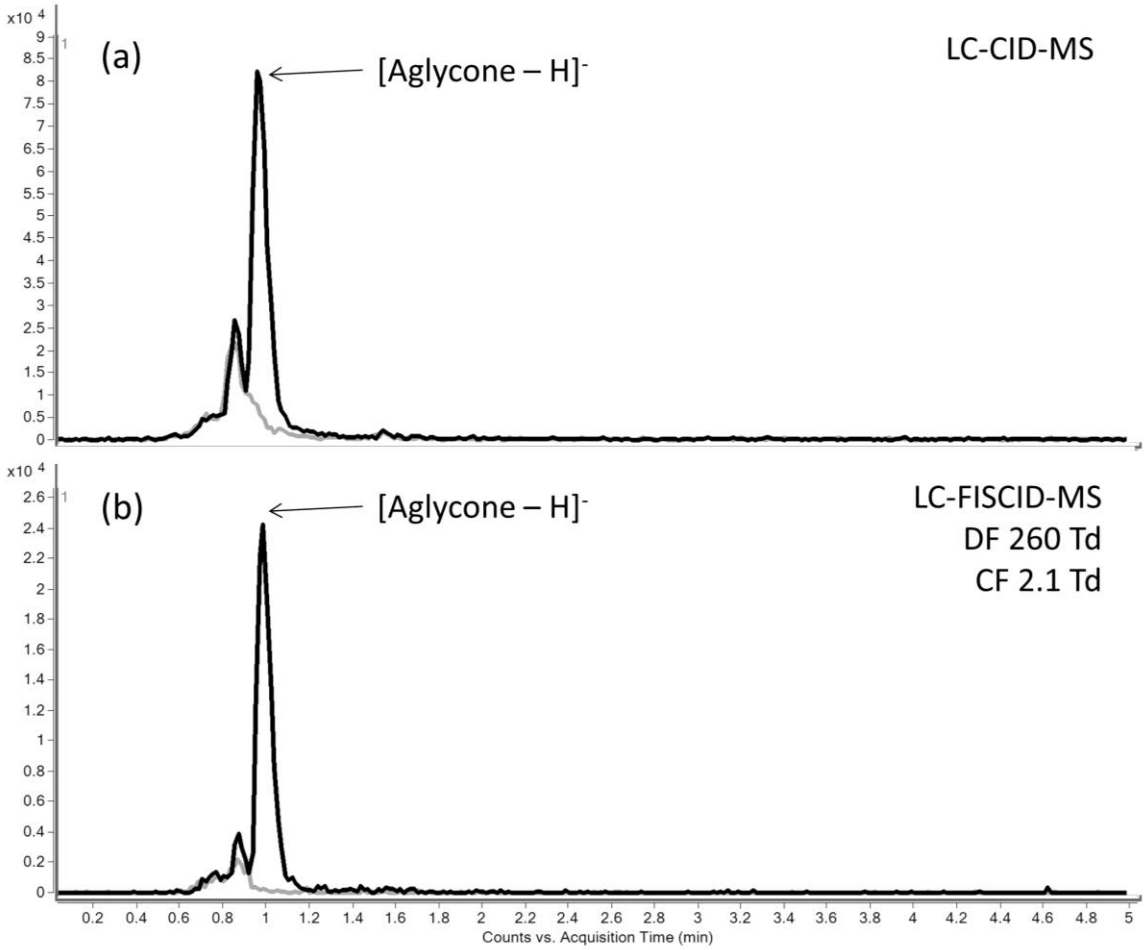

Figure 5.9 Selected ion chromatograms (*m/z* 205 ±0.02) of the [Aglycone – H]$^-$ for the urine blank (grey) and IAG (black) spiked into urine (3.9 μg/ml) by (a) UHPLC-CID-MS and (b) UHPLC-FISCID-MS

Table 5.3 A comparison of signal-to-noise ratios for in-source CID generated IAG fragment ions from the analysis of a spiked urine sample with FAIMS off and FAIMS on

Fragments	S:N Ratio (FAIMS off)	S:N Ratio (FAIMS on)
II	14.9	33.0
III	17.5	34.0
IV	13.9	31.6
V	8.6	16.4

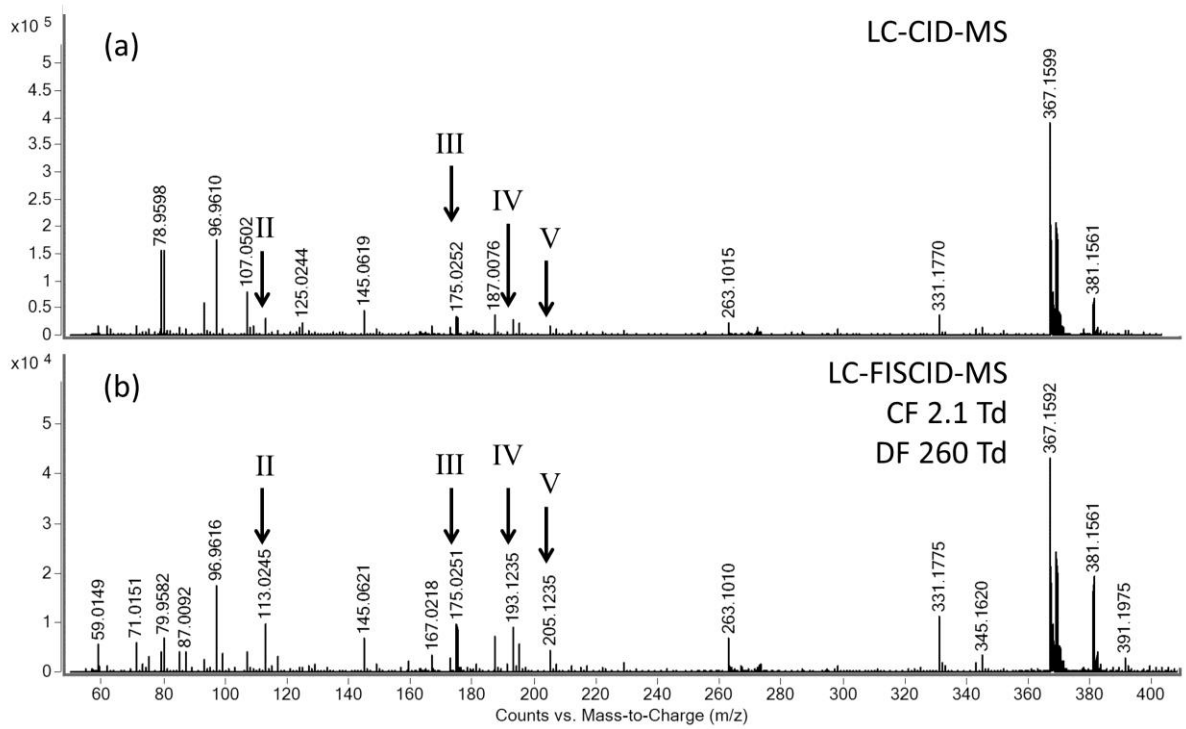

Figure 5.10 Mass spectra at RT 0.97-1.02 mins with (a) UHPLC-CID-MS, and (b) UHPLC-FISCID-MS

5.5 CONCLUSIONS

The incorporation of the chip-based FAIMS in the ESI source of the UHPLC-TOF spectrometer is shown to be a novel approach for improving the qualitative and quantitative performance of the chromatographic analysis of IAG by reducing co-eluting chemical interference from the urine matrix. UHPLC-FAIMS-HRMS showed a lower LOQ, increased LDR and better reproducibility, compared to UHPLC-HRMS without a FAIMS separation. The FAIMS device was able to distinguish IAG from ibuprofen, preventing interference from the drug when observing the aglycone fragment. The UHPLC-FISCID-MS technique removed interference from urine in the chromatogram for IAG and enhanced the qualitative identification of fragments of IAG by reducing the relative response of interfering peaks from the urine. An important conclusion from this study is that the orthogonality of the FAIMS and MS separations can provide reductions in chemical noise that cannot be achieved by increased mass resolution. This suggests that low resolution LC-MS analysers would also benefit from the use of FAIMS.

5.6 References

(1) Rochat, B. *Bioanalysis* **2012**, 4, 1709.

(2) Ramanathan, R.; Jemal, M.; Ramagiri, S.; Xia, Y.-Q.; Humphreys, W.G.; Olah, T.; Korfmacher, W.A.; *J. Mass Spectrom.* **2011**, 46, 595.

(3) Creaser, C.S.; Griffiths, J.R.; Bramwell, C.J.; Noreen, S.; Hill, C.A.; Thomas, C.L.P.; *Analyst* **2004**, 129, 984.

(4) Shvartsburg, A.A.; Differential Ion Mobility Spectrometry: Nonlinear Ion Transport and Fundamentals of FAIMS, CRC Press, Boca Raton, **2008**.

(5) Devenport, N.A.; Reynolds, J.C.; Parkash, V.; Cook, J.; Weston, D.J.; Creaser, C.S.; *J. Chrom. B* **2011**, 279, 3797.

(6) Kaur-Atwal, G.; Reynolds, J.C.; Mussell, C.; Champarnaud, E.; Knapman, T.W.; Ashcroft, A.E.; O'Connor, G.; Chrisrtie, S.D.R.; Creaser, C.S. *Analyst* **2011**, 136, 3911.

(7) Cui, M.; Ding, L.; Mester, Z. *Anal. Chem*. **2003**, 75, 5847.

(8) Kanu, A.B.; Dwivedi, P.; Tam, M.; Matz, L.; Hill Jr. H.H.; *J. Mass Spectrom.* **2008**, 43, 1.

(9) Barnett, D.A.; Ells, B.; Guevremont, R. *J. Am. Soc. Mass Spectrom.* **2000**, 11, 563.

(10) Purves, R.W.; Guevremont, R.; Day, S.; Pipich, C.W.; Matyjaszczyk, M.S.; *Rev. Sci. Instrum.* **1998**, 69, 4094.

(11) Buryakov, I.A.; Krylov, E.V.; Nazarov, E.G.; Rasulev, U.Kh. *Int. J. Mass Spectrom. Ion Processes* **1993**, 128, 143.

(12) Brown, L.J.; Smith, R.W.; Toutoungi, D.E.; Reynolds, J.C.; Bristow, A.W.T.; Ray, A.; Sage, A.; Wilson, I.D.; Weston, D.J.; Boyle, B.; Creaser, C.S. *Anal. Chem.* **2012**, 84, 4095.

(13) Hall, A.B.; Coy, S.L.; Nazarov, E.; Vouros, P. *Int J. Ion Mobil. Spec.* **2012**, 15, 151.

(14) Brown, L.J.; Toutoungi, D.E.; Devenport, N.A.; Reynolds, J.C.; Kaur-Atwal, G.; Boyle, P.; Creaser, C.S. *Anal. Chem.* **2010**, 82, 9827.

(15) McLuckey, S.A. *J. Am. Soc. Mass Spectrom*. **1992**, 3, 599.

(16) Yan, Z.; Caldwell, G.W.; Jones, W.J.; Masucci, J.A. *Rapid Commun. Mass Spectrom.* **2003**, 17, 1433.

(17) Kubwabo, C.; Vais, N.; Benoit, F.M. *Rapid Commun. Mass Spectrom*. **2005**, 19, 597.

(18) Barnett, D.A.; Ells, B.; Purves, R.W.; Guevremont, R. *J. Am. Soc. Mass Spectrom*. **1999**, 10, 1279.

(19) Purves, R.W.; Guevremont, R. *Anal.Chem.* **1999**, 71, 2346.

(20) Johnson, C.H.; Karlsson, E.; Sarda, S.; Iddon, L.; Iqbal, M.; Meng, X.; Harding, J.R.; Stachulski, A.V.; Nicholson, J.K.; Wilson, I.D.; Lindon, J.C. *Xenobiotica* **2010**, 40, 9.

Chapter 6

Conclusions and Future Work

6.1 Thesis Overview

The performance of a miniaturised field asymmetric waveform ion mobility spectrometry device combined with mass spectrometry (FAIMS-MS) has been studied and is reported in this thesis. In the following sections, each chapter is summarised and proposals for future research are discussed.

6.2.1 Summary of Chapter One

Chapter one discussed the principles of differential mobility spectrometry and mass spectrometry along with parameters that are important in determining FAIMS performance. The benefits of the addition of FAIMS to mass spectrometry systems for chemical analysis were reviewed with reference to the relevant literature, demonstrating the potential for the separation of isobaric ions that using FAIMS offers. FAIMS was also shown to offer improvements in detection limits, reduction in chemical noise, faster run times and simplification of complex data.

6.2.2 Summary of Chapter Two

The effect of changing experimental conditions in the ion source and FAIMS-MS interface on the performance of the prototype miniaturised FAIMS device was studied using a test mixture of small molecules and peptides in Chapter two. The CV was found to be stable over the full functioning range of the electrospray source, meaning that optimised FAIMS conditions did not change significantly when optimising source conditions, solvent composition or liquid flow rate (up to 1 ml/min). Transmission of ions with a lower *m/z* was found to be reduced at higher DFs whereas for ions with a higher *m/z* where there was little change in transmission with increasing DFs.

An investigation of three different systems including pairs of isobaric, isomeric and near-mass ions showed that miniaturised FAIMS has the ability to distinguish between analytes that are challenging to separate by mass spectrometry. The FAIMS separation of decarboxylated acids using deprotonated ions fragment ions and adducts formed with group I metal ions showed that the choice of ion is important in FAIMS separations, as are the effects of DF and temperature on the FAIMS spectra. The addition of a modifier to the carrier gas was also shown to improve separation, particularly where higher temperatures are required for desolvation. Signal loss of FAIMS-selected analytes is compensated for by reductions in chemical noise and the simplification of complex spectra. Combining FAIMS-selection of

analytes in tandem with fragmentation by in-source CID (FISCID-MS) enables the acquisition of FAIMS-selected fragment ions on a single mass analyser, where in-source CID alone produces complex spectra from multiple precursors. The FAIMS-MS analysis of the isomers 2β- and 6β-hydroxytestosterone showed relatively small structural changes may be sufficient to allow FAIMS separation.

The results reported in this chapter provide insight into the capabilities and limitations of miniaturised FAIMS. Further studies using a larger database of analytes, including series of homologous compounds, would be useful for further understanding the capabilities of miniaturised FAIMS combined with mass spectrometry. This study would also need to be expanded to different temperatures and analytes formed as adducts with other metal ions, including metals from different groups and with different charge states.

The separation of the hydroxytestosterone isomers demonstrates proof of principle, where the 6β-hydroxytestosterone was transmitted using FAIMS without significant interference from 2β-hydroxytestosterone. The next step is to combine FAIMS with a rapid method of sample clean up, such as off-line or on-line SPE, for the analysis of mixtures of the isomers spiked into human liver microsomes, in order to evaluate the sensitivity and selectivity of FAIMS-MS when presented with a more challenging sample matrix. Success at this step could be followed by testing real samples used in drug screening assays as an alternative to current LC-MS methods in a high-throughput environment.

6.2.3 Summary of Chapter Three

The effects of adding solvent vapour gas modifiers to the carrier gas of the miniaturised FAIMS were explored in Chapter three. A heated nebuliser-based vapour generator was constructed to introduce solvent vapours into the carrier gas to investigate the effect of alcohol modifiers on the performance of FAIMS-MS using small molecules, peptides and proteins. The results show that for small molecules, large shifts in the CF spectra are observed in the presence of modifiers and that modifier type and concentration combined with DF influences the order of the ions appear in the CF spectrum. In this study, only methanol and 2-butanol were used as modifiers, but the effect of other aliphatic alcohol modifiers (including primary, secondary and tertiary alcohols) should be further investigated along with other solvents with different functionality. The aim of studying other modifiers with other analytes that also vary in functionality would be to better understand analyte and modifier molecule interactions by focussing on physical properties, including functionality,

polarity and solubility. A comprehensive study could allow an analyst to predict the most appropriate solvents for a FAIMS-MS analysis.

Peptides exhibited a small shift in CF, but the smaller peak widths observed in the presence of modifiers improved the selectivity between sequence isomers and doubly protonated peptides. Proteins in the presence of modifiers showed a reduction in number of peaks, where multiple peaks are associated with different conformations or solvation states; a CF shift with alcohol modifiers was not observed for proteins. It would be interesting to explore if there is a size trend, where large molecules (like proteins) show little or no change in CF maxima position in the presence of modifiers, but smaller molecules show large CF shifts, and if this trend of size is related to type of modifier. Further investigation into the effect of modifiers on proteins is also important to better understand the selective reduction of other protein peaks while others remain.

There may be potential to explore the kinetics of clustering and declustering of solvent molecules to analytes using FAIMS, where temperature and modifier concentration may give insight to the interaction of each solvent molecule with analyte ion. This may also help explain the phenomenon observed with peptides and proteins in the presence of modifiers.

6.2.4 Summary of Chapter Four

Chapter four reported an investigation of the advantages of combining a fast FAIMS separation with TOF MS to analyse two systems of nitrogen-containing pharmaceutical impurities. The direct FAIMS-MS analysis of a degradation product of an antibiotic drug and of potentially genotoxic impurities in a surrogate active pharmaceutical excipient were investigated. The former system presents an analytical challenge due to the antibiotic drug fragmenting readily by in-source CID to form the same ion as the degradation product. The unique positioning of the FAIMS device at the inlet of the mass spectrometer enabled FAIMS-selection of the in-source generated degradation product, preventing interference from in-source CID of the antibiotic drug. Further experiments should include full validation of the quantitative FAIMS-MS analysis of the degradation product. It would also be beneficial to automate the sample preparation to shorten the run time and reduce solution degradation.

Thermal desorption was used to evaporate potentially genotoxic impurities from a surrogate active pharmaceutical ingredient into the electrospray source of the FAIMS-MS spectrometer

to allow the PGIs to be ionized by extractive electrospray (EESI). Sufficient selectivity and precision was observed for the direct analysis of the PGIs at the threshold of toxicological concern by TD-FAIMS-EESI-MS. At present, the method requires manual loading of samples to the thermal desorber and automation could significantly improve run time. There are commercially available thermal desorbers with integrated autosamplers, and it would be interesting to combine these techniques with FAIMS-MS to increase the sample throughput.

6.2.5 Summary of Chapter Five

Chapter five reports the development of a UHPLC-FAIMS-MS method for the quantitative determination of a drug metabolite in urine. Initially, infusion studies of the drug ibuprofen and its glucuronide metabolite explored DF and chip trench lengths for optimum selectivity and sensitivity. The UHPLC-FAIMS-MS analysis was carried out without sample clean-up and used a shorter chromatographic run time for rapid elution of the metabolite which without FAIMS co-eluted with chemical/matrix interference. The FAIMS conditions were transferred to the UHPLC-MS method and found to offer significant reduction in co-eluting chemical noise, whereas narrowing the mass windows without FAIMS offered no improvement in signal-to-noise. FAIMS pre-selection of the metabolite simplified the mass spectra and improved signal-to-noise by 2-fold. The improvement in signal-to-noise gives lower limits of quantitation, which combined with no loss in linearity at the top end resulted in an improvement in the linear dynamic range. UHPLC-FISCID-MS also showed an increase in signal-to-noise for fragments of the FAIMS-selected metabolite.

The data in this chapter demonstrate that the quantitative and qualitative performance for determination of the drug metabolite in urine is enhanced by the addition of a FAIMS separation. The orthogonality of the FAIMS and MS separations provide reductions in chemical noise that cannot be achieved by increased mass resolution, this suggests that low resolution LC-MS analysers would also benefit from the addition of a FAIMS device. It would be interesting to transfer the FAIMS method to a lower resolution LC-MS and assess the improvement in both qualitative and quantitative aspects for determination of urinary drug metabolites. Future work should also include an evaluation of lifetime of the FAIMS chip when subjected to routine analysis of urine samples without sample clean up to determine how robust the FAIMS device is with challenging sample matrices.

6.3 Summary of Thesis

This thesis investigates the potential of using miniaturised chip-based FAIMS in combination with mass spectrometry for the analysis of a variety of compounds in different sample matrices. Exploration of carrier gas properties and adduct formation showed that FAIMS is a selective spectrometer that is highly orthogonal to mass spectrometry and has been shown to enhance sensitivity and selectivity of rapid analyses. There is a paradigm shift towards high resolution mass spectrometry and high throughput mass spectrometry to answer the requirement for analyses to be faster[1] and provide more information with good quantitation.[2] Miniaturised FAIMS is shown to be rapid, selective and sensitive for samples that are challenging to high resolution and high-throughput mass spectrometry, this complementary technology has the potential to have a key position alongside modern mass spectrometry.

6.4 References

(1) Hopfgartner, G.; Bourgogne, E. *Mass Spectrom. Rev.* **2003**, 22, 195-210

(2) Rochat, B.; Kottelat, E.; McMullen, J. *Bioanalysis* **2012**, 4, 2939-2958

Appendices

Appendix 1: Conference presentations

Posters:

- BMSS 2011 32nd annual meeting 'From Atoms to Biomolecules', and winner of the Bordoli Poster Prize 'Optimisation of ultra-FAIMS-MS Parameters using a Central Composite Design'

- Research Network Meeting 2012 at Loughborough University 'Determination of a Urinary Drug metabolite using LC-FAIMS-MS and LC-FAIMS-In Source CID-MS'

- ASMS Annual Meeting 2012: 'Determination of a urinary drug metabolite using liquid chromatography combined with FAIMS-MS and FAIMS-in source CID-MS'. Presented by Prof. C.S. Creaser.

- ISIMS 2012: 'Direct Analysis of Potentially Genotoxic Impurities in Active Pharmaceutical Ingredients using Miniaturized Field Asymmetric Waveform Ion Mobility Spectrometry'. Presented by Dr. J.C. Reynolds.

- IMSC 2012: 'Evaluation of the performance of microscale FAIMS for the enhancement of the quantitative analysis of metabolites and peptides'. Presented by Dr. D.E. Toutoungi.

- ASMS Annual Meeting 2013: Exploring the effects of carrier gas modifiers using chip-based field asymmetric waveform ion mobility spectrometry combined with mass spectrometry'

- BMSS Annual Meeting 2013: 'The Effect of Alcohol Carrier Gas Modifiers on Chip-based FAIMS-Mass Spectrometry Analysis of Small Molecules, Peptides and Proteins'

- BMSS Annual Meeting 2013: 'Determination of N-methylpyrrolidine in cefepime hydrochloride using field asymmetric waveform ion mobility spectrometry combined with mass spectrometry'. Presented by Prof. C.S. Creaser

Oral Presentations:

- BMSS 2012 April 'Determination of a Urinary Drug Metabolite using LC-FAIMS-MS and LC-FAIMS in-source CID-MS'

- IMS Special Interest Group BMSS 2013 June 'Enhancing Structural Studied by Incorporating Chip-based Field Asymmetric Waveform Ion Mobility Spectrometry with Mass Spectrometry'

- ASMS 2014 Annual Meeting: 'Fast separation of hydroxytestosterone isomers using chip-based FAIMS combined with mass spectrometry for high-throughput drug assays'

- IMS Special Interest Group BMSS 2014: 'Use of chip-based FAIMS to remove isomeric interferences for high-throughput measurement of drug-drug interactions'

Article:

- Article published in BMSS Mass Matters (67, April 2012): 'Optimisation of a miniaturised FAIMS-MS System with a Central Composite Design'

- Article published in International Labmate/Labmate Asia (39, January/February 2014): 'Enhancing Mass Spectrometric Performance with Field Asymmetric Waveform Ion Mobility Spectrometry'

Appendix 2: Peer review publications

- 'Enhanced Analyte Detection Using In-Source Fragmentation of Field Asymmetric Waveform Ion Mobility Spectrometry-Selected Ions in Combination with Time-of-Flight Mass Spectrometry', Brown, L.J.; Smith, R.W.; Toutoungi, D.E.; Reynolds, J.C.; Bristow, A.W.; Ray, A,; Sage, A.; Wilson, I.D.; Weston. D.J.; Boyle, B.; Creaser, C.S.; Analytical Chemistry, 2012, 84, 4095-4103

- 'Enhanced performance in the determination of ibuprofen 1-β-O-acyl glucuronide in urine by combining high field asymmetric waveform ion mobility spectrometry with liquid chromatography-time-of-flight mass spectrometry', Smith, R.W.; Toutoungi, D.E.; Reynolds,

J.C.; Bristow, A.W.; Ray, A.; Sage, A.; Wilson, I.D.; Weston, D.J.; Boyle, B.; Creaser, C.S.; Journal of Chromatography, 2013, 1278, 76-81

- 'Direct analysis of potentially genotoxic impurities by thermal desorption-field asymmetric waveform ion mobility spectrometry-mass spectrometry', Smith, R.W.; Reynolds, J.C.; Lee, S-.L; Creaser, C.S.; Analytical Methods, 2013, 5, 3799-3802

- 'Rapid Determination of N-Methylpyrrolidine in Cefepime by Combining Direct Infusion Electrospray Ionisation-Time-of-Flight Mass Spectrometry with Field Asymmetric Waveform Ion Mobility Spectrometry', Smith, R.W.; Cox, L.B.; Yudin, A.; Reynolds, J.C.; Powell, M.; Creaser, C.S.; Submitted for publication at Analytical Methods, 29/08/2014

analytical chemistry

Article

pubs.acs.org/ac

Enhanced Analyte Detection Using In-Source Fragmentation of Field Asymmetric Waveform Ion Mobility Spectrometry-Selected Ions in Combination with Time-of-Flight Mass Spectrometry

Lauren J. Brown,[†] Robert W. Smith,[†] Danielle E. Toutoungi,[‡] James C. Reynolds,[†] Anthony W. T. Bristow,[§] Andrew Ray,[§] Ashley Sage,[⊥] Ian D. Wilson,[¶] Daniel J. Weston,[¶] Billy Boyle,[‡] and Colin S. Creaser*,[†]

[†]Centre for Analytical Science, Department of Chemistry, Loughborough University, Leicestershire, LE11 3TU, United Kingdom

[‡]Owlstone Ltd, 127 Cambridge Science Park, Cambridge, CB4 0GD, United Kingdom

[§]Pharmaceutical Development, AstraZeneca, Macclesfield, SK10 2NA, United Kingdom

[⊥]Agilent Technologies, Lakeside, Cheadle Royal Business Park, Stockport, SK8 3GR, United Kingdom

[¶]DMPK Innovative Medicines, AstraZeneca R&D, Alderley Park, Cheshire, SK10 4TG, United Kingdom

ABSTRACT: Miniaturized ultra high field asymmetric waveform ion mobility spectrometry (FAIMS) is used for the selective transmission of differential mobility-selected ions prior to in-source collision-induced dissociation (CID) and time-of-flight mass spectrometry (TOFMS) analysis. The FAIMS-in-source collision induced dissociation-TOFMS (FISCID-MS) method requires only minor modification of the ion source region of the mass spectrometer and is shown to significantly enhance analyte detection in complex mixtures. Improved mass measurement accuracy and simplified product ion mass spectra were observed following FAIMS preselection and subsequent in-source CID of ions derived from pharmaceutical excipients, sufficiently close in m/z (17.7 ppm mass difference) that they could not be resolved by TOFMS alone. The FISCID-MS approach is also demonstrated for the qualitative and quantitative analysis of mixtures of peptides with FAIMS used to filter out unrelated precursor ions thereby simplifying the resulting product ion mass spectra. Liquid chromatography combined with FISCID-MS was applied to the analysis of coeluting model peptides and tryptic peptides derived from human plasma proteins, allowing precursor ion selection and CID to yield product ion data suitable for peptide identification via database searching. The potential of FISCID-MS for the quantitative determination of a model peptide spiked into human plasma in the range of 0.45−9.0 μg/mL is demonstrated, showing good reproducibility (%RSD < 14.6%) and linearity (R^2 > 0.99).

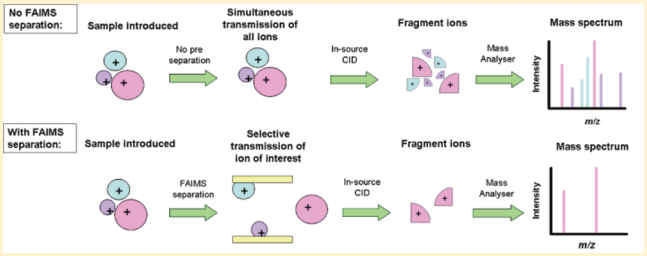

Collision-induced dissociation in the intermediate pressure region between an atmospheric pressure ion source and the vacuum of a mass analyzer, commonly referred to as in-source collision-induced dissociation (CID) or cone voltage fragmentation, may be used to induce fragmentation of ions passing through the interface.[1] The use of elevated interface voltages in the mass spectrometer interface allows product ion spectra to be generated for structural analysis of intact protonated molecules generated by electrospray ionization.[2] However, in the absence of precursor ion preselection, this can result in a complex mass spectrum containing overlapping precursor and product ions, which presents a challenge for spectral interpretation. Information regarding the relationship between precursor and product ions may also be lost because different precursor ions are fragmented simultaneously. Tandem mass spectrometry (MS/MS), in which a precursor ion is first selected on the basis of mass-to-charge (m/z) ratio and then subjected to CID with the resulting fragment ions identified by a second mass analyzer, is therefore the method of choice for obtaining fragmentation data for elucidation of structure and quantitative analysis. An alternative approach is to combine mass spectrometry analysis with the separation of gas-phase ions by ion mobility spectrometry or field asymmetric waveform ion mobility spectrometry (FAIMS).[3−7]

Field asymmetric waveform ion mobility spectrometry (FAIMS) is a gas-phase atmospheric pressure separation technique that exploits the difference in the mobility of an ion in alternating low and high electric fields.[8,9] The alternating electric fields are generated in the gap between two closely spaced electrodes by the application of an asymmetric RF waveform, causing ions to oscillate between the electrodes. Ions with different mobilities under low and high field conditions accumulate a net drift toward an electrode eventually resulting

Received: January 20, 2012
Accepted: March 28, 2012
Published: March 28, 2012

   dx.doi.org/10.1021/ac300212r | *Anal. Chem.* 2012, 84, 4095−4103

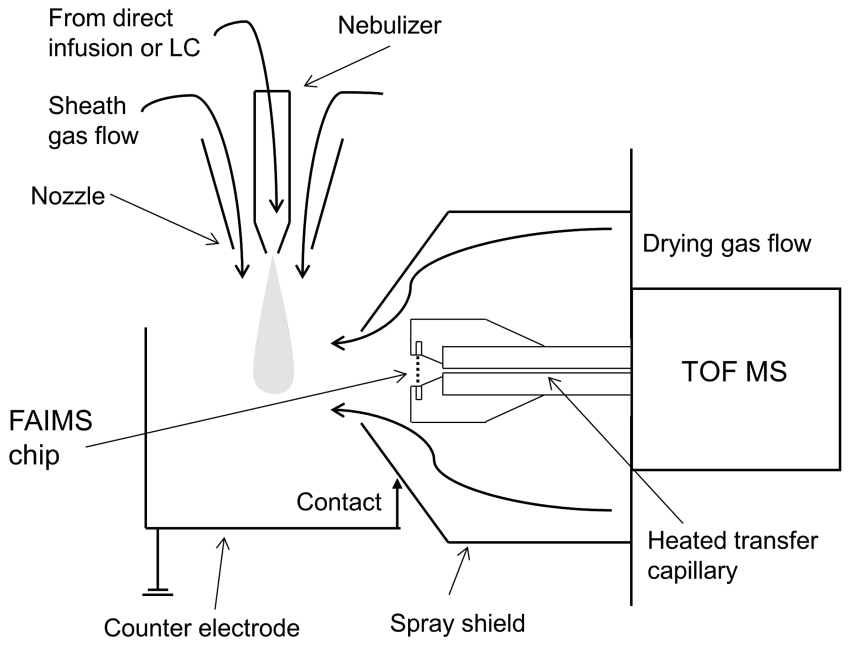

Figure 1. Schematic diagram of the FAIMS-MS interface.

in collision and neutralization. A small DC voltage is applied to one of the electrodes to reverse the drift of the ion so that collision with the electrode is avoided.[5] This is termed the compensation voltage (CV)[8] and allows ions to pass between the electrodes and be detected. The CV for ion transmission is compound specific, resulting from the difference in mobility in high and low fields.

FAIMS has been employed as an ion filter to select precursor ions prior to mass spectrometry analysis, because differential mobility is largely independent of m/z allowing orthogonal separations.[9] The ability to preselect using FAIMS has been shown to simplify mass spectra by reducing background and isobaric ions.[10−13] The combination of FAIMS with tandem mass spectrometry (FAIMS-MS/MS) has also been reported for the structural and quantitative analysis of small molecules and peptides, with CID of mass-selected ions occurring in the collision cell located between the mass analysers of a Q-time of flight (Q-TOF) or triple quadrupole spectrometer or after mass isolation in an ion trap.[13−15]

The in-source fragmentation of ions in FAIMS-MS was reported by Guevremont et al.,[16] who observed a change in cluster distributions of leucine enkephalin ions under low and high energy in an electrospray ionization (ESI) ion source. It was concluded that fragmentation comparable to MS/MS analysis was induced under high energy conditions. Subsequent fragmentation studies were pursued using MS/MS of mass-selected ions in a triple quadrupole spectrometer rather than through in-source CID. Eiceman et al. also described fragmentation of chlorocarbon ions in the interface of an atmospheric pressure ionization mass spectrometer, which complicated the identification of FAIMS-selected ions.[17] Measurements were carried out under conditions designed to minimize rather than enhance ion decomposition in the mass spectrometer interface. The use of FAIMS with in-source CID and selected reaction monitoring MS/MS was used by Xia and Jemal to determine the location of source fragmentation in the analysis of ifetroban and its acylglucuronide metabolite.[18] FAIMS was used to transmit either the parent drug or its acylglucuronide, from which it was concluded that fragmentation inducing the conversion of the acylglucuronide metabolite to the parent drug form occurred almost entirely after the inlet orifice of the mass spectrometer. The objective of this work was to minimize the effect of in-source CID on the LC-MS/MS with selected reaction monitoring (SRM) for the quantitative analysis of prodrugs and metabolites. The targeted use of in-source CID-MS using FAIMS to isolate ions from a mixture prior to fragmentation was reported by Coy and co-workers.[19] The separation of a simple mixture containing five isobaric model compounds (m/z 316) was achieved by direct infusion into the ESI source and differential mobility spectrometry. Ions were transmitted at their optimum CV and fragmentation induced by increasing the inlet cone voltage in the interface of a quadrupole MS.

Here, we describe the development of generic FAIMS-in source CID-MS procedures (which we term FISCID-MS) that exploit the ability to control the fragmentation of FAIMS-selected ions in the interface of the mass spectrometer, by combining the orthogonal separation characteristics of a miniaturized high field FAIMS device and in-source CID with time-of-flight mass spectrometry. The technique requires only minor modification of the ion source region of the mass spectrometer to incorporate the FAIMS device but is shown to provide major enhancements for the analysis of complex mixtures. FISCID-MS is demonstrated for the separation of pharmaceutical excipients[20] and for the qualitative and quantitative analysis of model and tryptic peptides derived from human plasma.

EXPERIMENTAL SECTION

Chemicals and Reagents. HPLC grade methanol (MeOH), acetonitrile (ACN), water, and formic acid (FA) were purchased from Fisher Scientific (Loughborough, UK). Leucine enkephalin (YGGFL), bradykinin (RPPGFSPFR), bombesin (EQRLGNQWAVGHLM), lutenizing hormone releasing hormone (EHWSYGLRPG), and the tetrapeptide MRFA were obtained from Sigma Aldrich (Gillingham, UK). All peptide standards were prepared at a concentration of 10

dx.doi.org/10.1021/ac300212r | Anal. Chem. 2012, 84, 4095−4103

pmol/μL in 50/50 (v/v) methanol/water containing 0.1% FA. 2-Hydroxy-(4-octyloxy) benzophenone and polyethylene glycol (PEG) 400, obtained from Sigma Aldrich (Gillingham, UK), were prepared in 50/50 (v/v) methanol/water with 0.1% FA at respective concentrations of 5.1 and 104 pmol/μL (1:20 molar ratio).

Sample Preparation. Human blood samples were collected from volunteers in lithium heparin tubes (BD, Oxford, UK) and centrifuged at 1500*g* for 15 min at 4 °C. ACN (400 μL) was added to an aliquot of the collected plasma (200 μL) before being vortex-mixed for 30 s and sonicated for 10 min to precipitate the proteins. The supernatant was removed, and proteins were reconstituted in 2 mL of water. Trypsin Gold Mass Spectrometry grade (100 μg; Promega, Southampton, UK) was dissolved in 100 mM ammonium bicarbonate, and 6 μL was added to the plasma extract. The sample was digested overnight at 37 °C. The reaction was quenched with 200 μL of 1% trifluoroacetic acid (TFA) solution (Sigma Aldrich, Gillingham, UK) in water, and the digested plasma was prepared for LC analysis via solid phase extraction (SPE) using 3 mL volume Oasis C_{18} solid phase microextraction cartidges (Waters, Manchester, UK). The cartridge was conditioned with 3 mL of 50% ACN in water and equilibrated with 3 mL of 0.1% TFA in water. Peptides generated by protein digestion and retained on the SPE cartridge were washed with 2 mL of 0.1% TFA in water. The retained peptides were then eluted in 200 μL of 20:80 water/ACN (v/v) with 0.1% FA. The eluate was dried down under argon and reconstituted in 90:10 water/ACN (v/v) with 0.1% FA. Standard solutions of Gramicidin S (cyclo(VOLDFP)$_2$) were prepared for quantitative analysis in 10:90 water/ACN (v/v) with 0.1% FA at concentrations in the range of 5−500 ng/μL. Aliquots (20 μL) of these standards were spiked into 200 μL of the plasma tryptic digest to give concentrations of 0.45−45 μg/mL.

Instrumentation. FISCID-MS analysis was carried out in positive ion electrospray ionization mode using a prototype miniaturized FAIMS device (Owlstone, Cambridge, UK), interfaced to an Agilent 6230 orthogonal acceleration time-of-flight mass spectrometer (Agilent Technologies, Santa Clara, CA, USA). The electrospray source of the TOF mass spectrometer was modified to accommodate the presence of the FAIMS chip within the spray shield (Figure 1). The FAIMS chip has been described in detail elsewhere[21,22] and consists of 47 electrode pairs with a channel width of 35 μm and a channel length of 300 μm. The FAIMS chip was connected to a field generator module, containing the electrical circuitry required to generate field asymmetric waveforms. The frequency of the applied asymmetric waveform was 25 MHz in a roughly 2:1 ratio of low field to high field. Comparative non-FAIMS data were acquired with analytes transmitted through the FAIMS chip with the dispersion field (DF) and CV set to 0 kV/cm and 0 V, respectively. FAIMS separation was carried out at a 47 kV/cm DF, over a CV range of −1 V to +4 at 0.5 V/s CV sweep rate. For LC-FISCID-MS analysis, FAIMS-selected analytes were transmitted into the mass spectrometer interface by scanning a 0.1 V window around the optimum CV for transmission. The exact CV values and scan windows were experiment dependent and as such are indicated in the text where appropriate. Data were processed using Mass Hunter version B.01.03 (Agilent Technologies, Santa Clara, CA, USA) and Excel 2007 (Microsoft, Seattle, USA).

TOF spectral acquisitions were performed at a rate of 10 spectra/s for the analysis of peptide standards and 2 spectra/s for the analysis of plasma samples. Analytes were infused into the JetStream-ESI ion source at 50 μL/min and ionized using a voltage of 1.5 kV. Source conditions for all experiments were nozzle voltage, spray shield, and counter electrode, 400 V; skimmer voltage, 65 V; drying gas temperature, 150 °C; sheath gas temperature, 250 °C; nebulizer gas pressure, 25 psig. HOBP/PEG analysis was carried out with the inlet capillary voltage set to −29 V, the drying gas flow set to 4.6 L/min, and the sheath gas flow set to 7 L/min. Peptide analysis was carried out with the inlet capillary voltage set to −15 V, the drying gas flow set to 10 L/min, and the sheath gas flow set to 12 L/min. The fragmentor voltage was set to 150 V for transmission of intact analytes without fragmentation and increased to the region of 350−400 V in order to induce in-source fragmentation by CID. The fragmentor voltage was compound dependent and is indicated in the text where appropriate.

LC separation of peptide standards was carried out using an XBridge C_{18} 5 μm column, with dimensions 2.1 × 50 mm, 5 μm (Waters, Manchester, UK), operated at a flow rate of 0.2 mL/min using an isocratic mobile phase of 30:70 water/ACN (v/v) with 0.1% FA, with a run time of 3 min and a 2 μL injection volume. Analysis of the spiked plasma tryptic digest was carried out using a Poroshell 300SB-C_{18} column, with dimensions 2.1 × 7.5 mm, 5 μm (Agilent, Santa Clara, CA, USA), at a flow rate of 0.4 mL/min with a 20 μL injection volume. The gradient elution program consisted of a linear increase from 95:5 water/ACN (v/v) to 60:40 water/ACN (v/v) in 10 min and then to 10:90 water/ACN (v/v) in 2 min. The gradient was then returned to the initial conditions giving a total run time of 15 min.

RESULTS AND DISCUSSION

The control of fragmentation of FAIMS-selected ions in the interface of a TOF mass spectrometer yields product ion information on the selected precursor ions. The potential of this FAIMS-in-source CID-MS (FISCID-MS) approach to enhance the analysis of complex mixtures using a single mass analyzer has been evaluated for the separation of pharmaceutical excipients and for peptide sequencing and quantification.

Separation of Pharmaceutical Excipients. Ions derived from the pharmaceutical excipients 2-hydroxy-4-octyloxybenzophenone (HOBP, *m/z* 327.1955) and PEG 400 were chosen as test analytes because the protonated HOBP and PEG *n* = 7 oligomer (*m/z* 327.2013) are sufficiently close in mass (17.7 ppm mass difference) that these ions could not be resolved by the reflectron TOF mass analyzer (resolving power required ∼130K). Robust accurate mass measurement of these ions is therefore not possible without separation prior to mass analysis. The two components were analyzed as a mixture containing a 20-fold molar excess of the PEG (Figure 2). CV sweeps (−1 to +4 V) with the DF set to 48 kV/cm were used to determine the optimum CV required for selected transmission and subsequent in-source fragmentation. The selected ion response for *m/z* 327.2 (Figure 2) shows that the protonated PEG *n* = 7 and HOBP ions are resolved by FAIMS.

The mass spectrum of the mixture without FAIMS separation (Figure 3a) shows the typical polymer distribution of PEG ions, with the HOPB unresolved from the protonated PEG (*n* = 7) ion. The measured mass of the overlapping peaks is *m/z* 327.1994, a mass difference of 11.9 and −5.8 ppm from HOBP and PEG, respectively. In-source CID-MS of this

dx.doi.org/10.1021/ac300212r | *Anal. Chem.* 2012, 84, 4095−4103

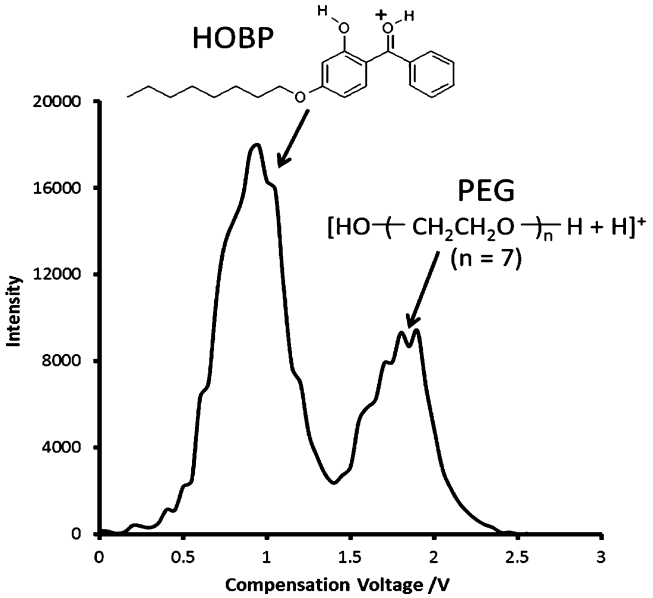

Figure 2. FAIMS-MS CV spectrum (m/z 327.2) of HOBP and PEG 400.

mixture gives a complex product ion spectrum dominated by PEG fragment ions (Figure 3b). Quasi-static FAIMS filtering (CV range 0.6−0.7 V) was used to transmit the HOPB ion selectively, which appears as the base peak in the resulting mass spectrum (Figure 3c), with an observed mass of 327.1966 (3.3 ppm). The FISCID-MS product ion spectrum of the FAIMS-selected HOBP ion (Figure 3d) shows the HOBP fragment ions free of interference from PEG fragment ion peaks, reducing the complexity of the mass spectrum and allowing unambiguous identification of the HOBP fragments. These observations demonstrate the mass spectral enhancement possible using FISCID-MS, through the FAIMS preselection of a precursor ion in a complex mixture, on the basis of differential mobility, prior to in-source CID. FISCID-MS allows the unresolved ions to be separated and a clean product ion spectrum to be obtained for HOBP using a single mass analyzer with only minor modification of the ion source to incorporate the miniaturized FAIMS device.

Isolation of Peptide Ions for Sequence Analysis. The FISCID-MS method was applied to the analysis of a mixture of peptide standards, MRFA, bradykinin, luteinizing hormone releasing hormone peptide (LHRH), leucine enkephalin, and bombesin (Figure 4a). The mixture was first infused directly into the ESI source of the mass spectrometer without FAIMS separation, producing a mass spectrum containing the $[M + H]^+$ ions of the four peptides, the $[M + 2H]^{2+}$ ions of bradykinin, LHRH, and bombesin, and the $[M + 3H]^{3+}$ ion of bradykinin, resulting in a complex mass spectrum (Figure 4a). FISCID-MS of the peptide mixture using a fragmentor voltage of 350 V without FAIMS preselection results in a complex product ion spectrum (Figure 4b) with a predominance of singly changed ions which do not readily fragment. FAIMS selection of singly charged peptide ions to generate a pseudo-peptide mass fingerprint for protein identification has been

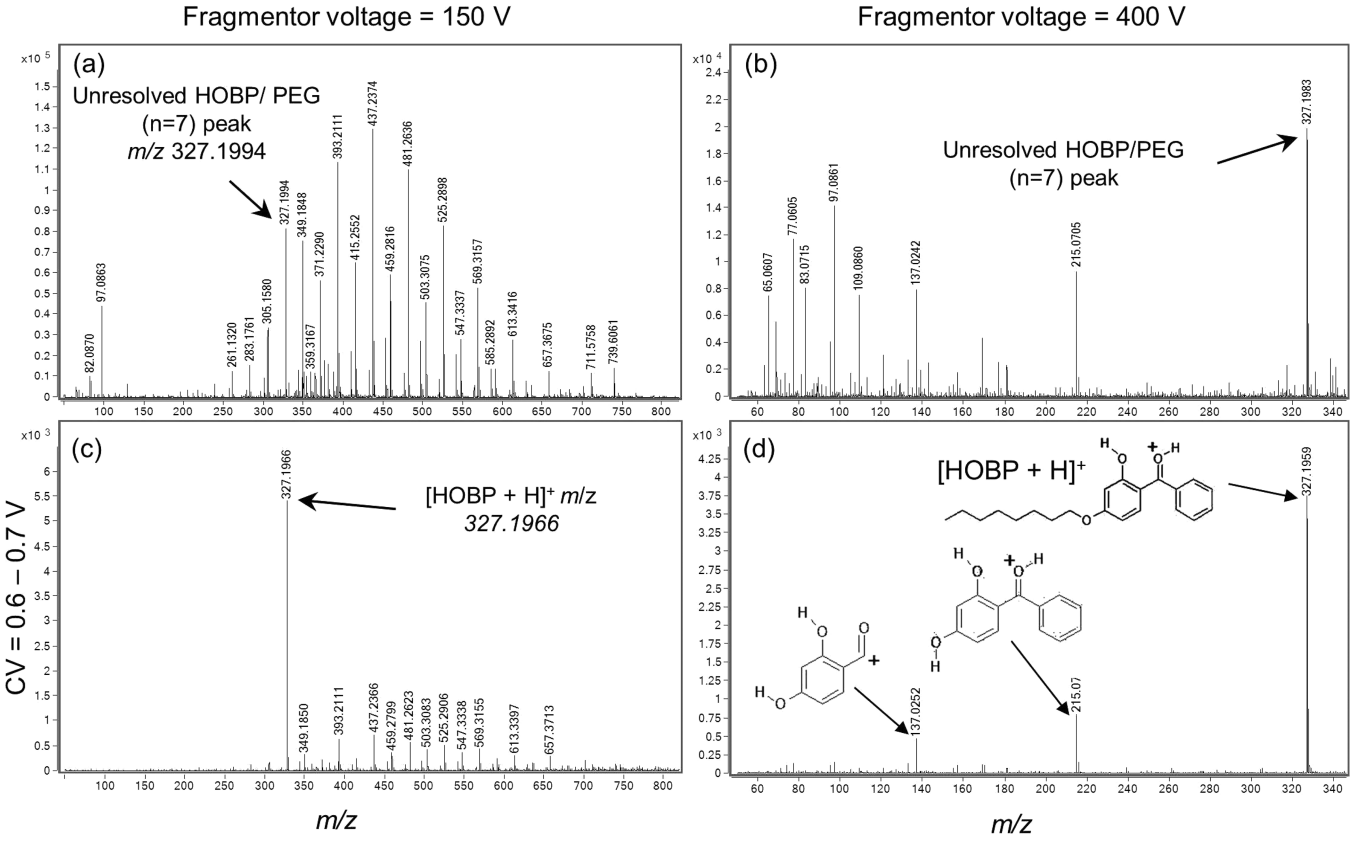

Figure 3. MS, FAIMS-MS, and FISCID-MS mass spectra of a mixture of HOBP and PEG 400 (1:20 molar ratio): (a) without FAIMS separation or in-source CID, (b) in-source CID-MS without FAIMS separation, and (c) FAIMS-selected HOBP ion (CV = 0.6−0.7 V) without in-source CID; (d) FISCID-MS product ion spectrum of the FAIMS-selected HOBP ion with in-source CID.

dx.doi.org/10.1021/ac300212r | Anal. Chem. 2012, 84, 4095−4103

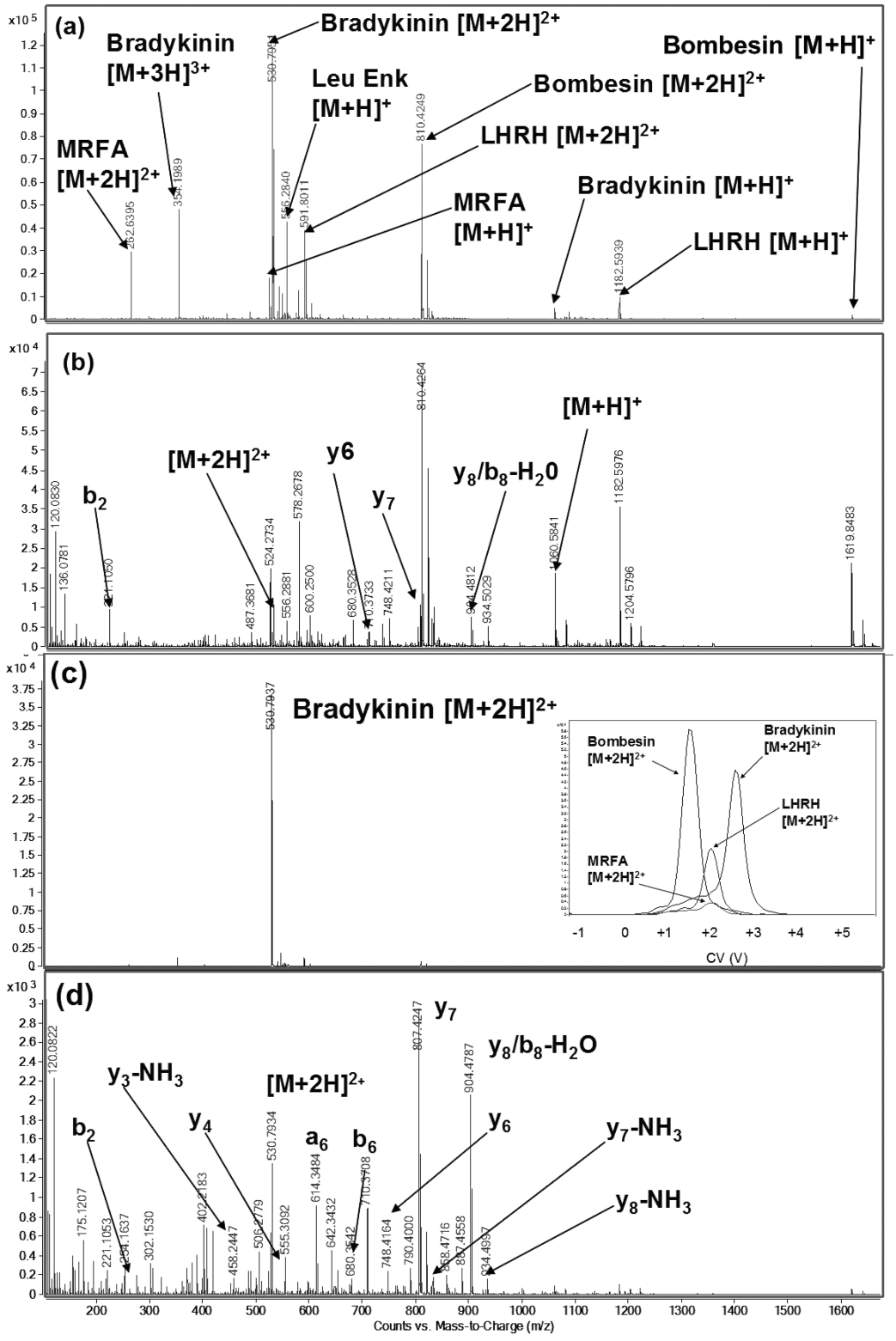

Figure 4. MS, FAIMS-MS, and FISCID-MS analysis of a peptide mixture: mass spectrum (a) without FAIMS selection or in-source CID, (b) in-source CID-MS (350 V) without FAIMS selection, and (c) FAIMS-selection of the $[M + 2H]^{2+}$ bradykinin ion (CV = 2.6−2.7 V) with (inset) mass-selected CV spectra; (d) FISCID-MS product ion spectrum of the $[M + 2H]^{2+}$ bradykinin ion (CV = 2.6−2.7 V, fragmentor voltage 350 V).

reported previously,[13] but higher charge state ions are preferred for sequence analysis by CID. A FAIMS CV spectrum was obtained by scanning the CV voltage in the range of 0 to +4 V with a DF of 48 kV/cm, and the selected ion responses for the $[M + 2H]^{2+}$ ions were extracted from the total ion response. The FAIMS device was then programmed to the appropriate CV for transmission of each of the $[M + 2H]^{2+}$ species. The isolation of the $[M + 2H]^{2+}$ bradykinin ion from the other singly and multiple charged peptide ions by FAIMS at a CV of +2.6−2.7 V is shown in Figure 4c. Using FAIMS to transmit the

dx.doi.org/10.1021/ac300212r | Anal. Chem. 2012, 84, 4095−4103

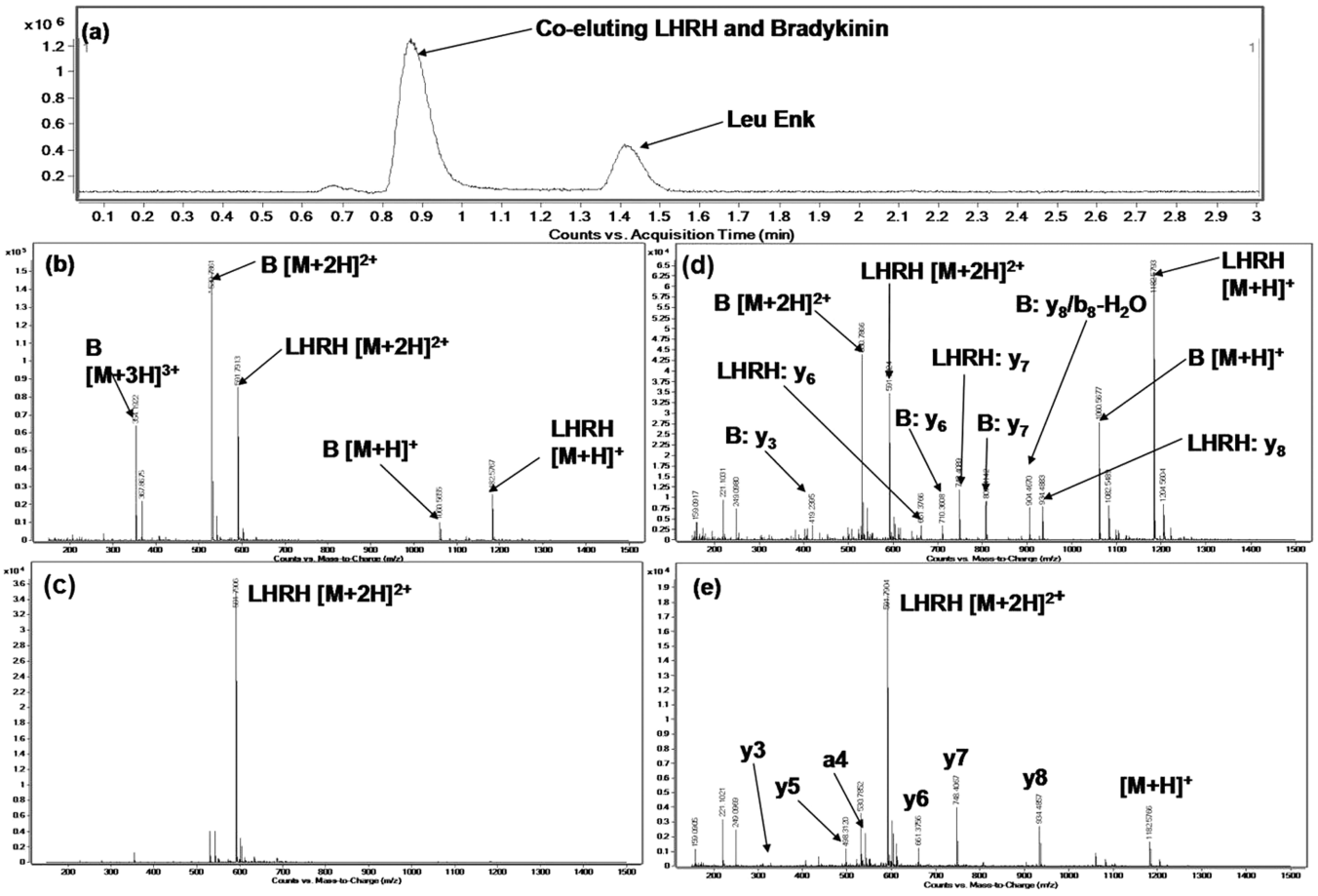

Figure 5. LC-MS and LC-FISCID-MS analysis of a peptide mixture: (a) TIC of peptide mixture; mass spectrum of (b) LC peak at ~0.9 min without FAIMS selection or in-source CID and (c) FAIMS preselection of LHRH $[M + 2H]^{2+}$ ion from coeluting peptides (CV = 1.8−1.9 V); (d) in-source CID-MS (fragmentor voltage 350 V) product ion spectrum without FAIMS preselection; (e) FISCID-MS product ion spectrum (CV = 1.8−1.9 V, fragmentor voltage 350 V) of FAIMS-selected LHRH $[M + 2H]^{2+}$ ion from coeluting peptides.

bradykinin $[M + 2H]^{2+}$ ion selectively in a FISCID-MS analysis filtered out unrelated precursor ions producing a product ion mass spectrum containing the characteristic fragments of bradykinin (Figure 4d). A comparison of peak lists generated by the TOFMS software identified 21 characteristic bradykinin fragment ions using the FISCID-MS method, compared to just 6 without FAIMS separation, enhancing confidence in the identification of bradykinin, based on sequence coverage.

FISCID-MS was then combined with an LC preseparation to evaluate the potential of FAIMS to aid the identification of coeluting peptides. The coeluting bradykinin and LHRH peptide (RT 0.88 min; Figure 5a) produced a mass spectrum containing singly and multiply charged peptide ions from both peptides (Figure 5b). The $[M + 2H]^{2+}$ ion of LHRH was isolated from the other peptide ions by applying a CV of 1.7−1.8 V (Figure 5c). The complex, overlapping LC-in-source CID-MS spectrum of the coeluting peptides without FAIMS separation (Figure 5d) is simplified by FAIMS preselection of the LHRH $[M + 2H]^{2+}$ ion enhancing the detection of the characteristic product ions of LHRH (Figure 5e).

The LC-FISCID-MS method was applied to the analysis of a complex mixture of tryptic peptides derived from human plasma proteins. The plasma tryptic digest was initially analyzed by LC-MS without FAIMS separation or in-source fragmentation (Figure 6a). The complex nature of the sample resulted in the coelution of several tryptic peptides, even after LC separation. One such example was m/z 480.7889, observed at a retention time of 3.5 min. The selected ion chromatograms obtained in the retention time range of 3.4−3.6 min without FAIMS-selection shows overlap with other coeluting peptide ions (Figure 6b). This can be seen on the corresponding mass spectrum (Figure 6c) averaged across the m/z 480 LC peak at half height. The mass spectrum, acquired with the FAIMS programmed to the optimum CV (2.5−2.6 V) for transmission of the m/z 480 peptide ions, is shown in Figure 6d. By applying a FAIMS preselection, the coeluting m/z 564, m/z 707, and other ions are filtered out, with the m/z 480 ion preferentially transmitted, resulting in a much simpler mass spectrum (Figure 6d). In order to evaluate whether spectral quality could be enhanced by FAIMS-selected ion transmission prior to in-source CID, the peptides were subjected to a fragmentor voltage of 340 V to induce fragmentation of the coeluting peptides from the LC-MS analysis with and without FAIMS separation. A complex product ion spectrum is obtained without FAIMS selection (Figure 6e), compared to the product ion mass spectrum observed using LC-FISCID-MS with FAIMS selection at a CV of 2.5−2.6 V (Figure 6f).

The prominent peaks in the LC-FISCID-MS product ion spectrum (Figure 6f) suggested the data acquired would be suitable for database searching to identify the unknown plasma peptides from the observed b and y fragments. Peptide identification was carried out via the MASCOT search engine,[23]

dx.doi.org/10.1021/ac300212r | Anal. Chem. 2012, 84, 4095−4103

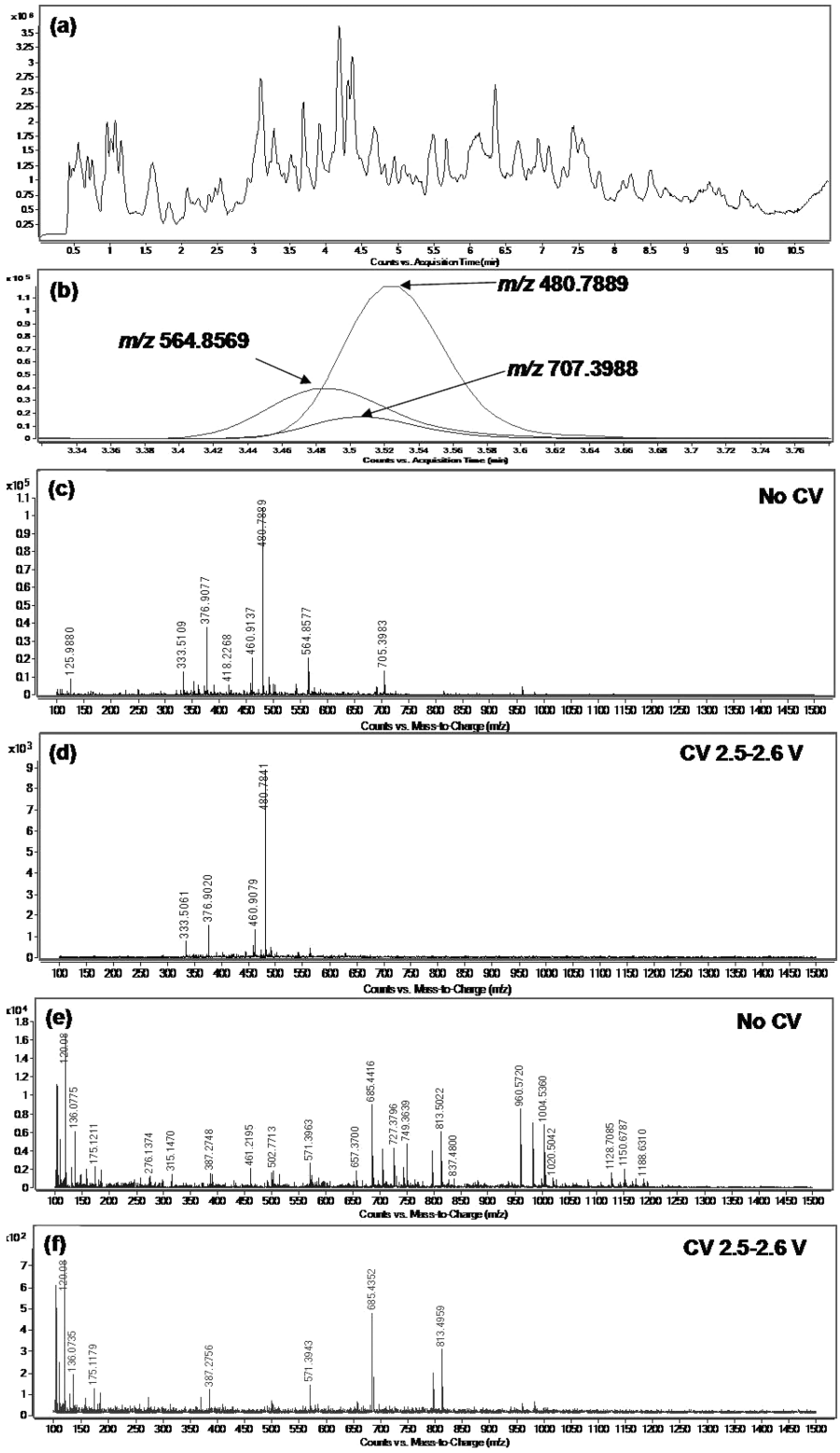

Figure 6. LC-MS and LC-FISCID-MS analysis of human plasma tryptic digest: (a) TIC, (b) selected ion chromatograms at 3.4−3.6 min, (c) LC-MS spectrum of peaks at 3.52 min without FAIMS separation, (d) LC-FAIMS-MS spectrum with FAIMS selection of the m/z 480 ion (CV of 2.5−2.6 V), (e) LC-in-source CID-MS spectrum without FAIMS selection, and (f) LC-FISCID-MS spectrum with FAIMS selection of the m/z 480 ion and in-source CID (CV 2.5−2.6 V, fragmentor voltage 340 V).

and all ions with intensities greater than 10% of the base peak were included in the peak list generated by the TOF-MS software for the data obtained both with and without FAIMS filtering. The peak list was searched against the SwissProt protein database. With no FAIMS separation, the LC-CID-MS method yielded no significant hits on the database, and therefore, no protein was identified. However, with the CV set to 2.5−2.6 V, human serum albumin (HSA) was identified as the top hit, the only significant match, with a confidence score of 34 (where 27 or above was deemed statistically significant at

dx.doi.org/10.1021/ac300212r | Anal. Chem. 2012, 84, 4095−4103

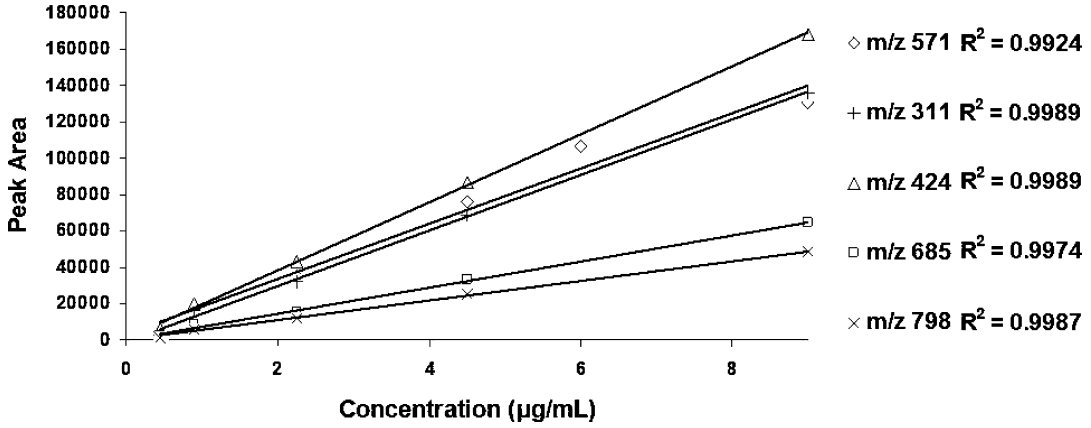

Figure 7. Calibration graphs for the quantitative LC-FISCID-MS analysis of the FAIMS-selected (CV 1.75−1.85 V) $[M + 2H]^{2+}$ precursor ion (m/z 571) and four product ions (m/z 311, 424, 685, and 798) of gramicidin S spiked in human plasma tryptic digest.

a 95% confidence interval), based on the fragmentation of the doubly charged FQNALLVR tryptic fragment (m/z 480.7854).

Peptide Quantification. The quantitative characteristics of LC-FISCID-MS were evaluated for the determination of a peptide spiked into human plasma. The peptide gramicidin S was chosen as a test compound, as it is not present in plasma and is therefore unaffected by natural fluctuations in abundance between plasma samples. A reproducibility study was performed using aliquots of human plasma tryptic digest spiked with 9 ng on column mass (0.45 μg/mL) of gramicidin S to determine the stability of LC-FISCID-MS for replicate injections of plasma. The % relative standard deviation (%RSD) for the peak area of the FAIMS-selected (CV +1.75−1.85 V) $[M + 2H]^{2+}$ precursor ion (m/z 571) without in-source fragmentation was 5.1% (n = 6). LC-FISCID-MS peak area precision for the fragment ions at m/z 311, m/z 424, m/z 685, and m/z 798, generated by in-source fragmentation of the FAIMS-selected m/z 571 precursor ion gave %RSDs (n = 6) of 13.3%, 14.6%, 13.1%, and 8.2% respectively, demonstrating good reproducibility of LC-FISCID-MS for quantitative measurement at this concentration.

Calibration graphs for the LC-FAIMS-MS analysis of the gramicidin precursor ion (m/z 571) and the LC-FISCID-MS analysis of the four product ions (m/z 311, 424, 685, and 798) were prepared by spiking the plasma tryptic digest with different concentrations of gramicidin S. A linear response (R^2 > 0.99) was observed in the range of 0.45−9.0 μg/mL for the precursor ion and all four product ions (Figure 7). The enhanced selectivity, reproducibility, and linear response to the spiked peptide in the plasma extract suggest that LC-FISCID-MS has the potential to offer significant benefits compared to the use of a single mass analyzer. This approach may also be an alternative to LC-MS/MS with SRM for quantitative analysis, while still being able to perform qualitative structural characterization and elemental formula analyses in the same experiment. This potential paradigm shift mirrors current trends within the pharmaceutical industry, where time-efficient use of one high-resolution mass analyzer for quantitative bioanalysis and qualitative metabolite characterization is receiving much attention.[24,25]

CONCLUSIONS

FAIMS preselection of precursor ions using a miniaturized high field FAIMS device followed by in-source CID-MS requires only minor modification of the ion source region of the mass spectrometer but provides enhanced selectivity for the qualitative and quantitative analysis of analytes in complex mixtures. Thus, FISCID-MS successfully separated pharmaceutical excipient ions that are too close in m/z value to be resolved by TOF-MS alone, providing improved accurate mass measurement and a product ion spectrum free from interferences. Transmission of FAIMS-selected peptide ions from a mixture on the basis of differential mobility facilitated peptide identification by enhancing the characteristic fragment ions of the selected precursor ion in the FAIMS-selected product ion spectrum. The LC-FISCID-MS analysis of these model peptides and a human plasma tryptic digest reduced the mass spectral complexity of coeluting peptides. The product ion spectra obtained via LC-FISCID-MS enabled the identification of plasma proteins with high confidence that could not otherwise be identified without FAIMS selection of the precursor ion, because of the presence of unrelated fragment ions in the mass spectrum. The quantitative potential of LC-FISCID-MS has also been demonstrated for the determination of a FAIMS-selected peptide in a spiked plasma tryptic digest sample. FISCID-MS therefore offers significant improvements in selectivity for analyses conducted using a mass spectrometer with a single mass analyzer, such as a TOF or quadrupole analyzer, and has potential as an alternative to LC-MS/MS for qualitative and quantitative analysis or for further enhancing selectivity using LC-FISCID-MS/MS routines.

AUTHOR INFORMATION

Corresponding Author

*E-mail: C.S.Creaser@lboro.ac.uk.

Notes

The authors declare no competing financial interest.

ACKNOWLEDGMENTS

The authors thank Loughborough University, Agilent Technologies, and Owlstone Limited for financial support.

REFERENCES

(1) McLuckey, S. A. *J. Am. Soc. Mass Spectrom.* **1992**, *3*, 599.
(2) Bure, C.; Lange, C. *Curr. Org. Chem.* **2003**, *7*, 1613.
(3) Creaser, C. S.; Griffiths, J. R.; Bramwell, C. J.; Noreen, S.; Hill, C. A.; Thomas, C. L. P. *Analyst* **2004**, *129*, 984.
(4) Kanu, A. B.; Dwivedi, P.; Tam, M.; Matz, L.; Hill, H. H., Jr. *J. Mass Spectrom.* **2008**, *43*, 1.

(5) Barnett, D. A.; Ells, B.; Guevremont, R. *J. Am. Soc. Mass Spectrom.* **2000**, *11*, 563.
(6) Purves, R. W.; Guevremont, R.; Day, S.; Pipich, C. W.; Matyjaszczyk, M. S. *Rev. Sci. Instrum.* **1998**, *69*, 4094.
(7) Hoaglund-Hyzer, C. S.; Clemmer, D. E. *Anal. Chem.* **2001**, *73*, 177.
(8) Buryakov, I. A.; Krylov, E. V.; Nazarov, E. G.; Rasulev, U.Kh. *Int. J. Mass Spectrom. Ion Processes* **1993**, *128*, 143.
(9) Shvartsburg, A. A. *Differential Ion Mobility Spectrometry: Nonlinear Ion Transport and Fundamentals of FAIMS*; CRC Press: Boca Raton, 2008.
(10) Barnett, D. A.; Ding, L.; Ells, B.; Purves, R. W.; Guevremont, R. *Rapid Commun. Mass Spectrom.* **2002**, *16*, 676.
(11) Rorrer, L. C., III; Yost, R. A. *Int. J. Mass Spectrom.* **2011**, *300*, 173.
(12) Barnett, D. A.; Purves, R. W.; Ells, B.; Guevremont, R. *J. Mass Spectrom.* **2000**, *35*, 976.
(13) Brown, L. J.; Toutoungi, D. E.; Devenport, N. A; Reynolds, J. C.; Kaur-Atwal, G.; Boyle, B.; Creaser, C. S. *Anal. Chem.* **2010**, *82*, 9827.
(14) Wu, S. T.; Xia, Y. Q.; Jemal, M. *Rapid Commun. Mass Spectrom.* **2007**, *21*, 3667.
(15) Barnett, D. A.; Ells, B.; Guevremont, R.; Purves, R. W. *J. Am. Soc. Mass Spectrom.* **2002**, *13*, 1282.
(16) Guevremont, R.; Purves, R. W. *J. Am. Soc. Mass Spectrom.* **1999**, *10*, 492.
(17) Eiceman, G. A.; Krylov, E. V.; Tadjikov, B.; Ewing, R. G.; Nazarov, E. G.; Miller, R. A. *Analyst* **2004**, *129*, 297.
(18) Xia, Y.-Q.; Jemal, M. *Anal. Chem.* **2009**, *81*, 7839.
(19) Coy, S. L.; Krylov, E. V.; Schneider, B. B.; Covey, T. R.; Brenner, D. J.; Tyburski, J. B.; Patterson, A. D.; Krausz, K. W.; Fornace, A. J.; Nazarov, E. G. *Int. J. Mass Spectrom.* **2010**, *291*, 108.
(20) Pifferi, G.; Restani, P. *Il Farmaco* **2003**, *58*, 541.
(21) Shvartsburg, A. A.; Smith, R. D.; Wilks, A.; Koehl, A.; Ruiz-Alonso, D.; Boyle, B. *Anal. Chem.* **2009**, *81*, 6489.
(22) Shvartsburg, A. A.; Tang, K.; Smith, R. D.; Holden, M.; Rush, M.; Thompson, A.; Toutoungi, D. *Anal. Chem.* **2009**, *81*, 8048.
(23) Mascot search engine, http://www.matrixscience.com, date accessed: 27/10/2011.
(24) Korfmacher, W. A. *Bioanalysis* **2011**, *3*, 1169.
(25) Weston, D. J.; Beattie, I. G. *Bioanalysis* **2011**, *3*, 1795.

Journal of Chromatography A, 1278 (2013) 76–81

Contents lists available at SciVerse ScienceDirect

Journal of Chromatography A

journal homepage: www.elsevier.com/locate/chroma

Enhanced performance in the determination of ibuprofen 1-β-O-acyl glucuronide in urine by combining high field asymmetric waveform ion mobility spectrometry with liquid chromatography-time-of-flight mass spectrometry

Robert W. Smith[a], Danielle E. Toutoungi[b], James C. Reynolds[a], Anthony W.T. Bristow[c], Andrew Ray[c], Ashley Sage[d], Ian D. Wilson[e], Daniel J. Weston[e], Billy Boyle[b], Colin S. Creaser[a,*]

[a] Centre for Analytical Science, Department of Chemistry, Loughborough University, Leicestershire, LE11 3TU, UK
[b] Owlstone Ltd, 127 Cambridge Science Park, Cambridge, CB4 0GD, UK
[c] Pharmaceutical Development, AstraZeneca, Macclesfield, SK10 2NA, UK
[d] Agilent Technologies, Lakeside, Cheadle Royal Business Park, Stockport, SK8 3GR, UK
[e] DMPK Innovative Medicines, AstraZeneca R&D, Alderley Park, Cheshire, SK10 4TG, UK

ARTICLE INFO

Article history:
Received 7 October 2012
Received in revised form
13 December 2012
Accepted 23 December 2012
Available online 8 January 2013

Keywords:
UHPLC
FAIMS
Mass spectrometry
Metabolite
Urine

ABSTRACT

The incorporation of a chip-based high field asymmetric waveform ion mobility spectrometry (FAIMS) separation in the ultra (high)-performance liquid chromatography–high resolution mass spectrometry (UHPLC–HRMS) determination of the (R/S) ibuprofen 1-β-O-acyl glucuronide metabolite in urine is reported. UHPLC–FAIMS–HRMS reduced matrix chemical noise, improved the limit of quantitation approximately two-fold and increased the linear dynamic range compared to the determination of the metabolite without FAIMS separation. A quantitative evaluation of the prototype UHPLC–FAIMS–HRMS system showed better reproducibility for the drug metabolite (%RSD 2.7%) at biologically relevant concentrations in urine. In-source collision induced dissociation of the FAIMS-selected deprotonated metabolite was used to fragment the ion prior to mass analysis, enhancing selectivity by removing co-eluting species and aiding the qualitative identification of the metabolite by increasing the signal-to-noise ratio of the fragment ions.

1. Introduction

The performance of a liquid chromatographic separation is determined both by the on-column separation and by the selectivity of the detector. UHPLC has significantly reduced chromatographic run times, but the use of selective detection, such as mass spectrometry, is required if the highest throughput is to be achieved. Tandem mass spectrometry using a triple quadrupole mass spectrometer capable of mass-selecting precursor ions for selected reaction monitoring is widely used in the quantitative chromatographic determination of drugs and metabolites. However, recent years have seen the emergence of high resolution mass spectrometry (HRMS), using TOF or Orbitrap mass analysers, as an alternative to triple quadrupole instruments [1,2]. The advantage of coupling UHPLC with HRMS is that HRMS provides both robust quantification and qualitative analysis using a single mass spectrometer platform. However, HRMS may lack the selectivity and sensitivity of selected reaction monitoring.

One approach to enhancing the selectivity of LC–MS analyses is the incorporation of a rapid gas-phase separation by ion mobility (IM) spectrometry between the LC and the mass spectrometer. Two ion mobility approaches are currently utilised: drift tube-ion mobility spectrometry, which separates ions based on time taken to traverse a drift tube [3], and field asymmetric waveform ion mobility spectrometry (FAIMS), also known as differential mobility spectrometry [4]. Drift-tube IM has been interfaced with ultra (high)-performance liquid chromatography-mass spectrometry (UHPLC–IM–MS) to enhance the quantitative determination of drugs and metabolites in urine by removing co-eluting interferences [5,6]. However, incorporation of a drift-tube ion mobility separation significantly reduces the linear dynamic range (LDR) compared to LC–MS alone [7–10].

FAIMS separation is orthogonal to MS and acts as an on-line filter for ions entering the MS. Ions are pre-selected by FAIMS based upon their differential ion mobility – the difference in mobility under low and high electric fields. In FAIMS, a dispersion field (DF) with an asymmetric waveform alternating between low and high fields is applied across the gap between two parallel electrodes, causing ions to oscillate between the electrodes. If high and low field mobilities are different, ions drift towards one of the electrodes as

* Corresponding author. Tel.: +44 01509 222552; fax: +44 01509223925.
E-mail address: C.S.Creaser@lboro.ac.uk (C.S. Creaser).

0021-9673/$ – see front matter © 2013 Elsevier B.V. All rights reserved.
http://dx.doi.org/10.1016/j.chroma.2012.12.065

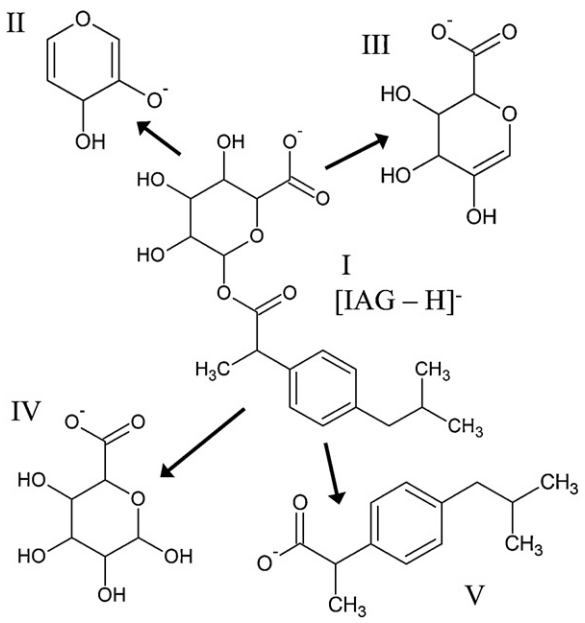

Fig. 1. Fragments produced from $[IAG-H]^-$ (I); decarboxylated di-dehydrated glucuronate (II); dehydrated glucuronate (III); glucuronate (IV); and aglycone (V).

they are carried through the electrode gap by a flow of nitrogen buffer gas at atmospheric pressure. The drift will result in a neutralising collision with one of the electrodes unless compensated for by a compensation field (CF). The CF for transmission of an ion is a characteristic of ion structure and is scanned at a fixed DF to determine the optimum CF at which the ion is preferentially transmitted, whilst other interfering ions are neutralised and filtered out [4,11]. FAIMS devices have been interfaced with MS to improve analytical selectivity by providing a differential mobility separation prior to MS detection of small molecules, metabolites and peptides [12–14].

Fragmentation of ions using a single mass analyser can be achieved by increasing voltages in the interface region between the ESI source and the vacuum of the mass spectrometer, called in-source CID, which will fragment all co-eluting ions generated in the ESI source [15]. The production of fragments from multiple precursors, without ion pre-selection, complicates fragmentation spectra making identification difficult. The effect of in-source CID on the analysis of glucuronide metabolites in biological matrices has been explored [16]. A comparison between in-source CID and collision cell CID using a triple quadrupole mass spectrometer for characterising microcystins in water samples showed that even though in-source CID proved to be more sensitive, CID in a collision cell was found to be more selective for identification. Fragmentation patterns were found to be similar for the two techniques [17]. Combining FAIMS with in-source CID, referred to FISCID–MS, has been used for the identification of an active pharmaceutical ingredient in a common pharmaceutical excipient and the qualitative and quantitative analysis of peptides in plasma by LC–FISCID–MS [12].

In this paper, we report enhanced chromatographic performance in the UHPLC–MS analysis of the drug metabolite (R/S) ibuprofen 1-β-O-acyl glucuronide, IAG (Fig. 1, I), in urine, without sample clean-up, by the incorporation of a FAIMS separation using a prototype chip-based FAIMS device. FAIMS pre-selection of the metabolite is shown to improve the limit of quantification, linear dynamic range and reproducibility, and allow a shorter chromatographic run time compared to UHPLC–MS by reducing chemical/matrix interference. The FAIMS device was also used to pre-select IAG for UHPLC–FISCID–MS, enhancing the qualitative identification of the metabolite.

2. Experimental

2.1. Chemicals

HPLC grade methanol (MeOH), acetonitrile (ACN), water, formic acid (FA) and ammonium acetate were purchased from Fisher Scientific (Loughborough, UK). (R/S) Ibuprofen 1-β-O-acyl glucuronide was supplied by AstraZeneca (Alderley Park, UK). Ibuprofen was extracted into methanol from an ibuprofen tablet (200 mg).

2.2. Sample preparation

Aliquots of urine (5 ml) from healthy adult males (2×) and females (2×) (AstraZeneca, UK) was pooled (20 ml) and filtered (0.45 μm), diluted (2×) with a solution of the IAG metabolite (0.055–44 μg/ml in 50:50 acetonitrile:aqueous ammonium acetate (10 mM) at pH 3), corresponding to urine concentrations in the range 0.028–22 μg/ml.

2.3. Instrumentation

UHPLC–FAIMS–MS and UHPLC–FISCID–MS analyses of IAG were carried out using an Agilent 1200 series HPLC interfaced with an Agilent 6230 time-of-flight mass spectrometer fitted with a JetStream ESI source operated in negative ion mode (Agilent Technologies, Santa Clara, CA, USA). The prototype chip-based FAIMS device (Owlstone, Cambridge, UK) has been previously described elsewhere [12] and was located in front of the transfer inlet capillary, behind a modified spray shield within a Jet Stream ESI source. The dispersion field (DF) feeder supplied asymmetric waveforms to the FAIMS device through a hole in the desolvation assembly. The FAIMS device has a 100 μm electrode gap and a depth of 700 μm with the FAIMS electrodes arranged as multiple parallel channels, linked by a serpentine channel – trench length (50–100 mm). Dispersion fields in the range 200–300 Td were applied at a 27 MHz frequency with an approximate low to high field ratio of 2:1. Nitrogen (99.5% purity) was used as the carrier gas for the FAIMS system and for the ESI source and mass spectrometer interface.

Samples were introduced into the ESI source either by direct infusion or from the liquid chromatograph. UHPLC separation was carried out, with a 5 μl sample injection volume on a Zorbax C18 column (2.1 mm × 50 mm, 1.8 μm) with an isocratic 0.2 ml/min flow of 50:50 acetonitrile:aqueous ammonium acetate (10 mM) at pH 3. The scan rate of the TOF MS was 10 scans/s for scanning FAIMS–MS experiments and 1 scan/s for UHPLC–FAIMS–MS and UHPLC–FISCID–MS experiments. Data were acquired with the instrument mode set to extended dynamic range (2 GHz) at a resolution of 5700. Source conditions for LC experiments were nozzle voltage, 2000 V; sheath gas temperature and flow, 350 °C and 11 L/min; drying gas temperature and flow, 150 °C and 10 L/min; nebuliser pressure, 25 psig; transfer capillary, 4000 V; skimmer voltage, 65 V; fragmentor voltage, −150 V and −250 V for transmission and in-source CID respectively. Data were processed using Mass Hunter Qualitative Software B.04.00 (Agilent Technologies, Santa Clara, CA, USA) and Microsoft Excel 2010 (Microsoft, Seattle, USA).

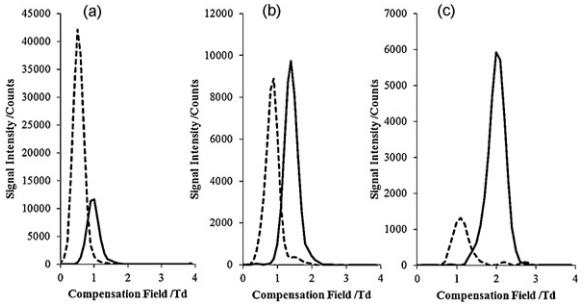

Fig. 2. FAIMS CF spectra of ibuprofen, m/z 205, (dashed line) and IAG, m/z 381 (solid line) at DF: (a) 200 Td, (b) 230 Td and (c) 260 Td.

3. Results and discussion

3.1. Direct infusion FAIMS analysis of IAG and ibuprofen

Direct infusion of ibuprofen and the IAG metabolite (0.65 μg/ml) was used to optimise the microscale FAIMS conditions for separation and sensitivity. FAIMS compensation field (CF) spectra of the $[M-H]^-$ ions of the analytes obtained at a dispersion field (DF) of 200, 230 and 260 Td are shown in Fig. 2. The IAG response is separated from that of the parent drug ibuprofen as a result of structural differences between the two ions. The separation of IAG and the parent drug improves with increased DF. A decrease in the absolute intensity of IAG was observed when the DF was increased from 200 to 260 Td, but with a significant increase in the response relative to ibuprofen, which falls sharply with increasing DF. The optimum CF for transmission of IAG was at 2.2 Td with a DF of 260 Td, based on the best separation without significant loss of signal intensity for IAG, and these conditions were used in the high resolution UHPLC–FAIMS–MS analyses.

3.2. Determination of IAG by UHPLC–FAIMS–TOF-MS

The UHPLC–MS (FAIMS off) and UHPLC–FAIMS–MS (FAIMS on) selected ion chromatograms ($[M-H]^-$; m/z 381) obtained for the analysis of IAG spiked into urine with a high resolution mass window of m/z 381 ± 0.02 (±50 ppm) is shown in Fig. 3a. The UHPLC gradient was adjusted to minimise the run time for the IAG, but this resulted in a significant overlap between the IAG peak and urine matrix components. The observed co-elution of IAG with matrix components could be reduced by changing the UHPLC conditions to separate the metabolite from the urine matrix, but at the cost of a significantly increased chromatographic run time. A narrower mass window, m/z 381 ± 0.008 (±20 ppm) was therefore investigated to

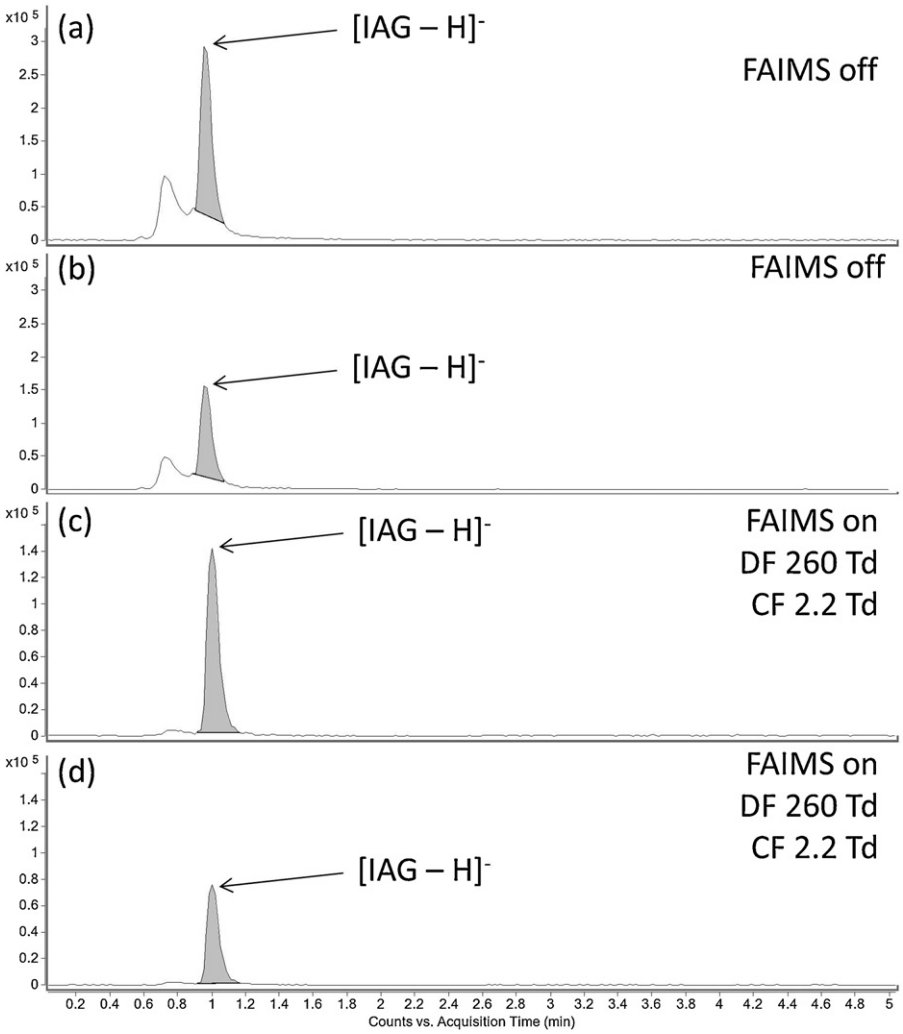

Fig. 3. Selected ion chromatograms (m/z 381) for IAG (highlighted) spiked into urine (0.55 μg/ml) analysed by UHPLC–MS (FAIMS off) using a mass window of (a) m/z 381 ± 0.02 and (b) m/z 381 ± 0.008; and by UHPLC–FAIMS–MS (FAIMS on) with selective transmission of IAG (DF 260 Td, CF 2.2 Td) using a mass window of (c) m/z 381 ± 0.02 and (d) m/z 381 ± 0.008.

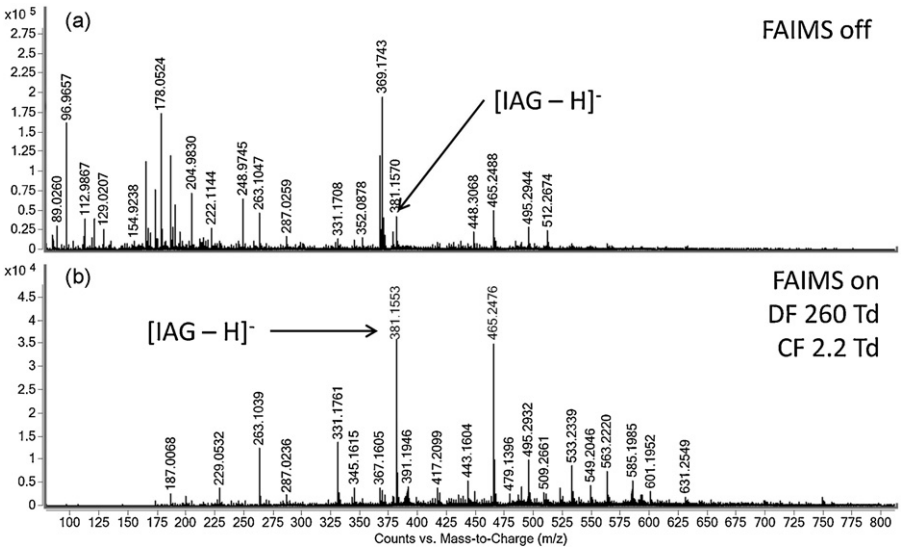

Fig. 4. Mass spectra at retention time (RT) 0.98–1.02 min with (a) FAIMS off, and (b) FAIMS on.

determine whether this would improve selectivity without extending the chromatographic run time. The absolute intensity of the IAG peak, with the FAIMS switched off, is reduced by a factor of two if the mass window is narrowed from ±50 ppm to ±20 ppm (Fig. 3b), but there is no additional discrimination against the chemical noise from the urine matrix at the mass resolution used in the analysis (5700 FWHM).

The advantage of the incorporation of the FAIMS separation is demonstrated by a significant reduction in the co-eluting chemical noise from the urine matrix (Fig. 3c and d), whilst maintaining a rapid elution time. Ionisation suppression in the ESI source was not determined, but was the same in both FAIMS on and FAIMS off modes, allowing an evaluation of the improvement in the chromatographic performance offered by FAIMS. The removal of chemical noise resulted in an improvement in signal-to-noise ratio and better peak integration with FAIMS on, even though the absolute intensity of the IAG peak was reduced because of ion losses in the device. FAIMS pre-selection of IAG removes matrix ions to baseline for both the m/z 381 ±0.02 and ±0.008 mass windows, but at a cost of lower sensitivity and signal-to-noise ratio for the narrower window. The ±0.02 mass window was therefore used in subsequent studies.

The mass spectrum taken from the IAG UHPLC peak with FAIMS off (Fig. 4a) showed IAG (m/z 381.1570; −3.9 ppm) to be a minor peak in a complex mass spectrum. The mass spectrum for IAG with FAIMS on (Fig. 4b) was simplified, with IAG as the base peak in the mass spectrum (m/z 381.1553; 0.52 ppm), as a result of discrimination against interferences from urine matrix.

Table 1 compares the quantitative performance of the UHPLC–MS and UHPLC–FAIMS–MS methods for the determination of IAG. The limit of quantitation (LOQ; signal-to-noise 10:1) for IAG was reduced from 18 ng/ml (FAIMS off) to 10 ng/ml (FAIMS on), based on the selected ion peak areas of IAG (m/z 381 ± 0.02) using UHPLC–FAIMS–MS. The upper limit of the linear dynamic range (LDR) was the same in both FAIMS off and on modes, giving an increased LDR of >3 orders of magnitude for the miniaturised FAIMS–MS, in contrast to ∼2 orders of magnitude with cylindrical FAIMS–MS [18,19] and <2.5 orders of magnitude for drift tube IM–MS [5,6]. The intra-day reproducibility of the prototype UHPLC–FAIMS–MS system was compared with UHPLC–MS by analysing IAG spiked into urine (15.5 μg/ml) and running FAIMS in on and off modes respectively (Table 1). %RSDs, sufficient for good quantification, were obtained for both UHPLC–MS (5.0%) and UHPLC–FAIMS–MS (2.7%), with the UHPLC–FAIMS–MS showing better reproducibility. These data demonstrate that the FAIMS device enhances quantitative performance compared to high resolution UHPLC and MS analysis.

Table 1
A comparison of LOQ; LDR (R^2) and intra-day reproducibility for the determination of IAG spiked into urine (15.5 μg/ml, $n = 5$).

	UHPLC–MS	UHPLC–FAMS–MS
LOQ(μg/ml)	0.018	0.010
LDR(μg/ml)	0.018–11	0.010–11
R^2	0.9991	0.9987
Intra-day (%RSD)	5.0	2.7

3.3. Qualitative identification of IAG by UHPLC–FISCID–MS

The in-source CID fragmentation of IAG ion was used to assess the improvement offered by the UHPLC–FISCID–MS technique for the qualitative identification of IAG. The FAIMS-selected $[M-H]^-$ ion of IAG was subjected to in-source CID to produce the characteristic fragments of the ion (Fig. 1). A comparison of the selected ion chromatograms of the aglycone fragment (m/z 205.1234) for a urine sample spiked with IAG (3.9 μg/ml), with and without FAIMS pre-selection prior to in-source CID, was used to define the level of isobaric chemical interference present in the sample spiked with IAG (Fig. 5a and b). Peak integration of the UHPLC–FISCID–MS data was more reliable than UHPLC–MS data because chemical interference was reduced almost to baseline.

Mass spectra extracted from the aglycone peaks (Fig. 6) shows the effect of applying the FAIMS separation to the UHPLC–CID–MS analysis of IAG. Four diagnostic fragment ions for IAG are observed in the production mass spectrum (Fig. 1) [20]: decarboxylated dehydrated glucuronate (II, m/z 113); dehydrated glucuronate (III, m/z 175); glucuronate (IV, m/z 193); and the aglycone (V, m/z 205). In Fig. 6a, these fragments are difficult to locate due to the complexity of the mass spectrum and poor signal to noise as a result of other ions in the matrix. Pre-selecting IAG using FAIMS before in-source CID reduced the intensity of interfering ions, increasing the relative intensity of the IAG (Fig. 6b). The signal-to-noise ratios for the fragment ions increased by approximately 2-fold with FAIMS on (Table 2), enhancing the response of the IAG fragments relative to other interfering peaks to aid identification.

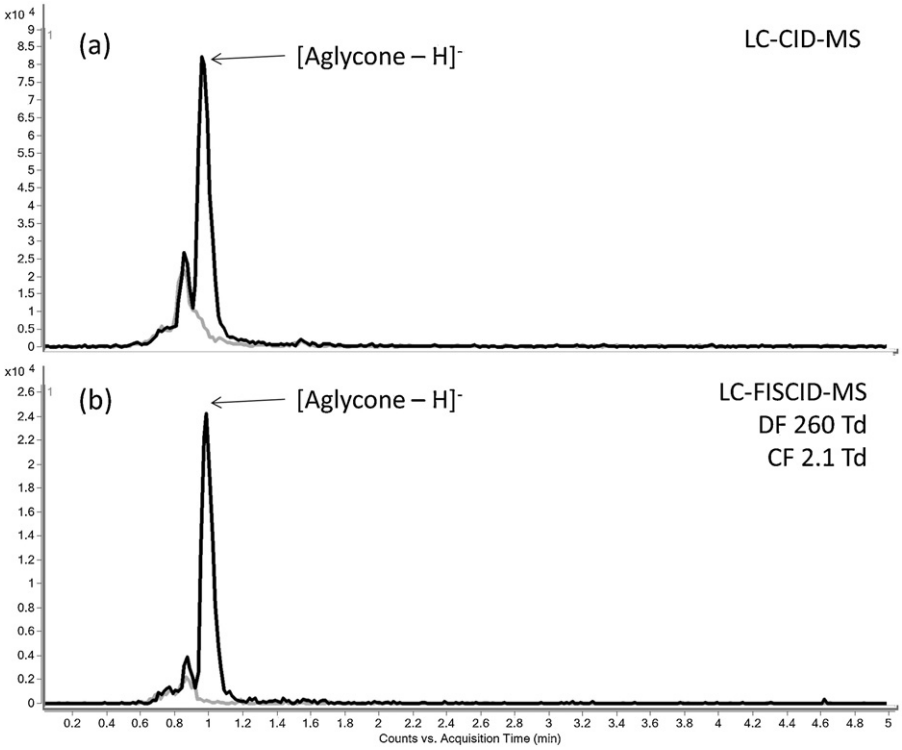

Fig. 5. Selected ion chromatograms (m/z 205 ± 0.02) of the [Aglycone−H]$^-$ for the urine blank (grey) and IAG (black) spiked into urine (3.9 μg/ml) by (a) UHPLC–CID–MS and (b) UHPLC–FISCID–MS.

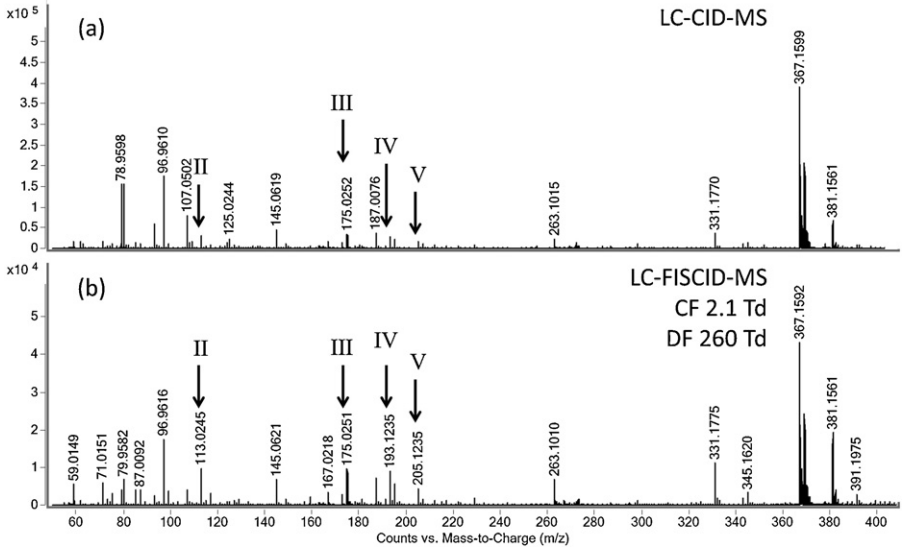

Fig. 6. Mass spectra at RT 0.97–1.02 min with (a) UHPLC–CID–MS, and (b) UHPLC–FISCID–MS.

Table 2
A comparison of signal-to-noise ratios for in-source CID generated IAG fragment ions from the analysis of a spiked urine sample with FAIMS off and FAIMS on.

Fragments	S:N ratio(FAIMS off)	S:N ratio(FAIMS on)
II	14.9	33.0
III	17.5	34.0
IV	13.9	31.6
V	8.6	16.4

4. Conclusions

The incorporation of the chip-based FAIMS in the ESI source of the UHPLC-TOF spectrometer is a novel approach for improving the qualitative and quantitative performance of the chromatographic analysis of IAG by reducing co-eluting chemical interference from the urine matrix. UHPLC–FAIMS–HRMS showed a lower LOQ, increased LDR and better reproducibility, compared to UHPLC–HRMS without a FAIMS separation. The FAIMS device was able to distinguish IAG from ibuprofen, preventing interference from the drug when observing the aglycone fragment. The UHPLC–FISCID–MS technique removed interference from urine in

the chromatogram for IAG and enhanced the qualitative identification of fragments of IAG by reducing the relative response of interfering peaks from the urine.

Acknowledgements

The authors thank Loughborough University, Agilent Technologies, Owlstone Limited and AstraZeneca for financial and technical support and supplying chemicals.

References

[1] B. Rochat, Bioanalysis 4 (2012) 1709.
[2] R. Ramanathan, M. Jemal, S. Ramagiri, Y.-Q. Xia, W.G. Humphreys, T. Olah, W.A. Korfmacher, J. Mass Spectrom. 46 (2011) 595.
[3] C.S. Creaser, J.R. Griffiths, C.J. Bramwell, S. Noreen, C.A. Hill, C.L.P. Thomas, Analyst 129 (2004) 984.
[4] A.A. Shvartsburg, Differential Ion Mobility Spectrometry: Nonlinear Ion Transport and Fundamentals of FAIMS, CRC Press, Boca Raton, 2008.
[5] N.A. Devenport, J.C. Reynolds, V. Parkash, J. Cook, D.J. Weston, C.S. Creaser, J. Chromatogr. B 879 (2011) 3797.
[6] G. Kaur-Atwal, J.C. Reynolds, C. Mussell, E. Champarnaud, T.W. Knapman, A.E. Ashcroft, G. O'Connor, S.D.R. Chrisrtie, C.S. Creaser, Analyst 136 (2011) 3911.
[7] M. Cui, L. Ding, Z. Mester, Anal. Chem. 75 (2003) 5847.
[8] A.B. Kanu, P. Dwivedi, M. Tam, L. Matz, H.H. Hill Jr., J. Mass Spectrom. 43 (2008) 1.
[9] D.A. Barnett, B. Ells, R. Guevremont, J. Am. Soc. Mass Spectrom. 11 (2000) 563.
[10] R.W. Purves, R. Guevremont, S. Day, C.W. Pipich, M.S. Matyjaszczyk, Rev. Sci. Instrum. 69 (1998) 4094.
[11] I.A. Buryakov, E.V. Krylov, E.G. Nazarov, U.Kh. Rasulev, Int. J. Mass Spectrom. Ion Processes 128 (1993) 143.
[12] L.J. Brown, R.W. Smith, D.E. Toutoungi, J.C. Reynolds, A.W.T. Bristow, A. Ray, A. Sage, I.D. Wilson, D.J. Weston, B. Boyle, C.S. Creaser, Anal. Chem. 84 (2012) 4095.
[13] A.B. Hall, S.L. Coy, E. Nazarov, P. Vouros, Int. J. Ion Mobil. Spec. 15 (2012) 151.
[14] L.J. Brown, D.E. Toutoungi, N.A. Devenport, J.C. Reynolds, G. Kaur-Atwal, P. Boyle, C.S. Creaser, Anal. Chem. 82 (2010) 9827.
[15] S.A. McLuckey, J. Am. Soc. Mass Spectrom. 3 (1992) 599.
[16] Z. Yan, G.W. Caldwell, W.J. Jones, J.A. Masucci, Rapid Commun. Mass Spectrom. 17 (2003) 1433.
[17] C. Kubwabo, N. Vais, F.M. Benoit, Rapid Commun. Mass Spectrom. 19 (2005) 597.
[18] D.A. Barnett, B. Ells, R.W. Purves, R. Guevremont, J. Am. Soc. Mass Spectrom. 10 (1999) 1279.
[19] R.W. Purves, R. Guevremont, Anal.Chem. 71 (1999) 2346.
[20] C.H. Johnson, E. Karlsson, S. Sarda, L. Iddon, M. Iqbal, X. Meng, J.R. Harding, A.V. Stachulski, J.K. Nicholson, I.D. Wilson, J.C. Lindon, Xenobiotica 40 (2010) 9.

Analytical Methods

RSC Publishing

COMMUNICATION

View Article Online
View Journal | View Issue

Cite this: *Anal. Methods*, 2013, **5**, 3799

Received 23rd April 2013
Accepted 10th July 2013

DOI: 10.1039/c3ay40676h

www.rsc.org/methods

Direct analysis of potentially genotoxic impurities by thermal desorption-field asymmetric waveform ion mobility spectrometry-mass spectrometry

Robert W. Smith, James C. Reynolds, Sze-Ling Lee and Colin S. Creaser*

Thermal desorption has been combined with field asymmetric waveform ion mobility spectrometry and mass spectrometry for the rapid, direct analysis of isobaric potentially genotoxic impurities (PGIs) in a surrogate active pharmaceutical ingredient. FAIMS-selected PGIs were detected with limits of quantification <0.2 ppm, below the threshold of toxicological concern, with %RSD <8.4%, at the 1 ppm level.

1 Introduction

Potentially genotoxic impurities (PGIs) have characteristic structures that may exhibit carcinogenicity.[1,2] PGIs need to be monitored during the production of active pharmaceutical ingredients (APIs) to ensure that their concentrations remain below the threshold value of toxicological concern (TTC) required by the European Medicines Agency;[3,4] which is typically ~1.5 μg per day, equivalent to 1.5 ppm assuming a 1 g per day dose. Gas chromatography-mass spectrometry (GC-MS) and high performance liquid chromatography-mass spectrometry (LC-MS) are widely used techniques for monitoring the levels of PGI compounds in APIs. However, these conventional pharmaceutical analysis methods require lengthy sample preparation and chromatographic separation. Consequently, there is a need for new analytical strategies to meet the fast-paced pharmaceutical research and discovery environment.[5,6]

Thermal desorption is an extraction technique, where an analyte is transferred into the gas phase from a solid or liquid. The technique requires minimal sample preparation and is often interfaced with gas chromatography-mass spectrometry.[7] Desorbed PGIs have been ionised *via* extractive electrospray in an electrospray ionisation source (ESI) and detected by mass spectrometry.[8,9] Thermal desorption has also been interfaced with drift tube ion mobility-mass spectrometry (IM-MS) for the analysis of breath samples collected on solid adsorbents, with the ion mobility separation adding selectivity to the analyses.[10]

Field asymmetric waveform ion mobility spectrometry separates gas phase ions using a waveform with alternating low and high electric fields known as the dispersion field (DF). A compensation field (CF), is superimposed on the DF and may be scanned or fixed to transmit selected analytes based on their differential ion mobility under low and high electric fields conditions. FAIMS separation using a miniaturised, chip-based device is fast as a result of the short ion residence times (50–250 μs) and has been shown to enhance the selectivity of mass spectrometry analyses.[11,12] FAIMS separation is orthogonal to mass spectrometry and can distinguish between isobaric ions, making hyphenation of these techniques highly desirable.[11,13]

We report a rapid method for the determination of the isobaric PGIs, 2,4,6-trimethylaniline and *N*,*N*-dimethyl-*m*-toluidine (Fig. 1) by thermal desorption from a surrogate API with a FAIMS separation prior to detection using mass spectrometry. Good precision was observed at the 1 ppm level for the FAIMS pre-selected PGIs, with a limit of quantification established well below the required TTC.

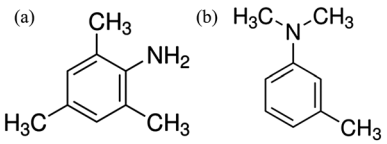

Fig. 1 The structures of (a) 2,4,6-trimethylaniline, and (b) *N*,*N*-dimethyl-*m*-toluidine.

2 Materials and methods

2.1 Chemicals

2,4,6-Trimethylaniline (2,4,6-TMA), *N*,*N*-dimethyl-*m*-toluidine (*N*,*N*-DMT), starch, and HPLC grade acetonitrile, methanol, water and formic acid were obtained from Sigma Aldrich (Gillingham, UK).

Centre for Analytical Science, Department of Chemistry, Loughborough University, Loughborough, LE11 3TU, UK. E-mail: C.S.Creaser@lboro.ac.uk; Fax: +44 (0)1509 223925; Tel: +44 (0)1509 222552

2.2 Sample preparation

Standard solutions of 2,4,6-TMA (50 ng mL^{-1}) and *N*,*N*-DMT (50 ng mL^{-1}) were prepared in methanol–water (50 : 50) with 0.1% formic acid for infusion studies and in acetonitrile for thermal desorption studies. The PGI mixture (4 μL, 2.5 μg mL^{-1}) was added to a surrogate API, starch (10 mg) which was immediately inserted into a thermal desorption tube between two pieces of Siltek Deactivated Wool (Borosilicate, Markes Int.), as shown in Fig. 2. The concentration of each of the PGIs in the starch was 1 ppm (w/w).

2.3 Instrumentation

TD-ESI-FAIMS-MS analyses were carried out using a Markes UNITY1 thermal desorption unit (Markes International, Swansea, UK) combined with an Agilent 6230 TOFMS (Agilent technologies, U.K.) fitted with a prototype chip-based FAIMS device (Fig. 2). 2,4,6-TMA and *N*,*N*-DMT were desorbed from the surrogate API (starch) at 230 °C for 2 min onto a cold trap (Tenax, −10 °C) and then rapidly desorbed from the trap (250 °C, >40 °C s^{-1}, 2 min). The thermal desorption cycle time was ~10 minutes. The heated transfer line from the thermal desorber, containing a fused silica capillary (0.25 mm i.d.) was maintained at 200 °C and introduced into the JetStream ESI of the TOFMS by removing the glass from a viewing window in the source housing. The tip of the fused silica capillary was positioned in the source at an angle of approximately 55° to the nebuliser, but set back ~10 mm to give the maximum response. Extractive electrospray and direct infusion electrospray were carried out in positive ion mode using a 10 μL min^{-1} infusion of methanol–water (50 : 50) with 0.1% formic acid. The ESI spray nebuliser pressure was set to 30 psig with an 8 L min^{-1} sheath gas flow at 250 °C. The nozzle voltage was set to 2000 V; the transfer capillary, spray shield and counter electrode were set to 3000 V and the drying gas flow to 6 L min^{-1} at 150 °C.

The miniaturised chip-based FAIMS (Owlstone Ltd., Cambridge), consisting of multiple parallel electrode gaps (100 μm) with a short path length (700 μm),[13–15] was located behind the spray shield of the TOFMS inlet. Scanning FAIMS-MS experiments were carried out by direct infusion of 2,4,6-TMA and *N*,*N*-DMT individually to evaluate the potential for separation of these isobaric compounds. The DF was stepped (10 Td) from 200 to 300 Td and the CF was scanned from −2 to +5 Td to determine optimum separation conditions. The mass spectrometer fragmentor voltage was set to 175 V for FAIMS-selected transmission experiments. The MS scan rates were 10 scans per s and 1 scan per s in the mass range *m*/z 70–1000 for direct infusion and thermal desorption experiments respectively.

3 Results and discussion

The thermal desorption of volatile compounds from a less volatile solid sample, such as an API, has the potential to speed

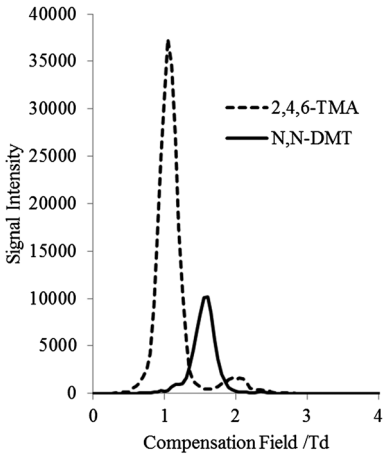

Fig. 3 FAIMS CF scan of 2,4,6-TMA (dashed) and *N*,*N*-DMT (solid) with DF set to 230 Td.

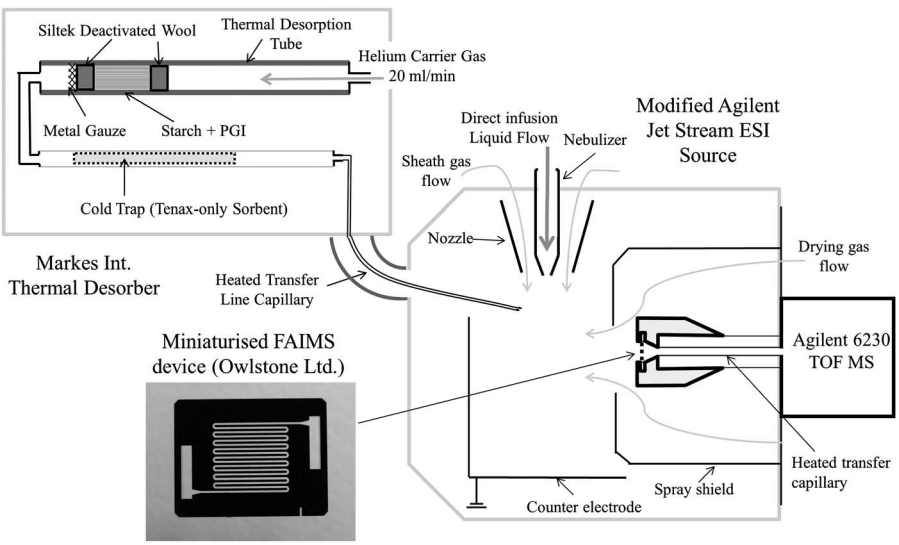

Fig. 2 A schematic diagram of the thermal desorber interfaced to the ESI-FAIMS-MS ion source.

up analysis by removing time consuming sample preparation and chromatographic separation steps. Furthermore, there is an even greater potential advantage in that such approaches are matrix independent and can be applied to the analysis of a wide range of APIs without the need to develop individual specific methods for each PGI/API combination. Increasing sample throughput is important for efficient quality control, but selectivity may be compromised to reduce analysis times, particularly for isobaric analytes that cannot be distinguished by mass spectrometry. Miniaturised, chip-based field asymmetric waveform ion mobility spectrometry incorporated into the ion source of a time-of-flight mass spectrometer (FAIMS-MS), was therefore investigated for the separation of the isobaric PGIs 2,4,6-trimethylaniline (2,4,6-TMA) and *N*,*N*-dimethyl-*m*-toluidine (*N*,*N*-DMT) (Fig. 1).[16,17]

3.1 Direct infusion FAIMS-MS studies

The two substituted anilines, 2,4,6-TMA and *N*,*N*-DMT, were introduced by direct infusion into the ESI-FAIMS-MS to explore the potential for a rapid separation step which would be compatible with the thermal desorption of these analytes. A DF stepping experiment, with the CF scanned at each DF, was used to determine the optimum DF for maximum separation without compromising sensitivity.[12] The CF spectrum obtained at the optimum DF, which was determined to be 230 Td, is shown in Fig. 3. The spectrum contains two peaks corresponding to 2,4,6-TMA and *N*,*N*-DMT centered at a CF at 1.0 and 1.5 Td respectively. There is also a small peak at CF 2 Td in Fig. 3, which is assigned to the protonated dimer of 2,4,6-TMA. The *N*,*N*-DMT peak lies between the 2,4,6-TMA monomer and dimer peaks where there is no significant interference from either. 2,4,6-TMA and *N*,*N*-DMT were sufficiently resolved at a DF of 230 Td to enable the selective transmission of each without significant interference from the other.

3.2 TD-FAIMS-MS analysis of 2,4,6-TMA and *N*,*N*-DMT

2,4,6-TMA and *N*,*N*-DMT are sufficiently volatile to be thermally desorbed from a surrogate API (starch) and transferred to the ESI source *via* a heated transfer line. The desorbed molecules were ionised using extractive electrospray (EESI) and detected using FAIMS-time-of-flight mass spectrometry (TOF MS). The FAIMS CF was set to transmit either 2,4,6-TMA (CF 1.0 Td) or *N*,*N*-DMT (CF 1.5 Td) selectively at a DF of 230 Td following ionization. Fig. 4 shows typical thermal desorption profiles (*m*/*z* 136) for the FAIMS pre-selected 2,4,6-TMA and *N*,*N*-DMT, spiked as a mixture into a surrogate API (starch) at 1 ppm (w/w). A good peak shape for the thermal desorption profile of each PGI was achieved by using a single sorbent (Tenax) in the desorber cold trap. The time axis corresponds to the mass spectrometry acquisition time, which was started 1 minute before the heating of the cold trap. Fig. 4a and b inserts show mass spectra corresponding to the maximum point of the thermal desorption profiles of FAIMS-selected 2,4,6-TMA and *N*,*N*-DMT respectively, showing the protonated ions at *m*/*z* 136. The use of a FAIMS

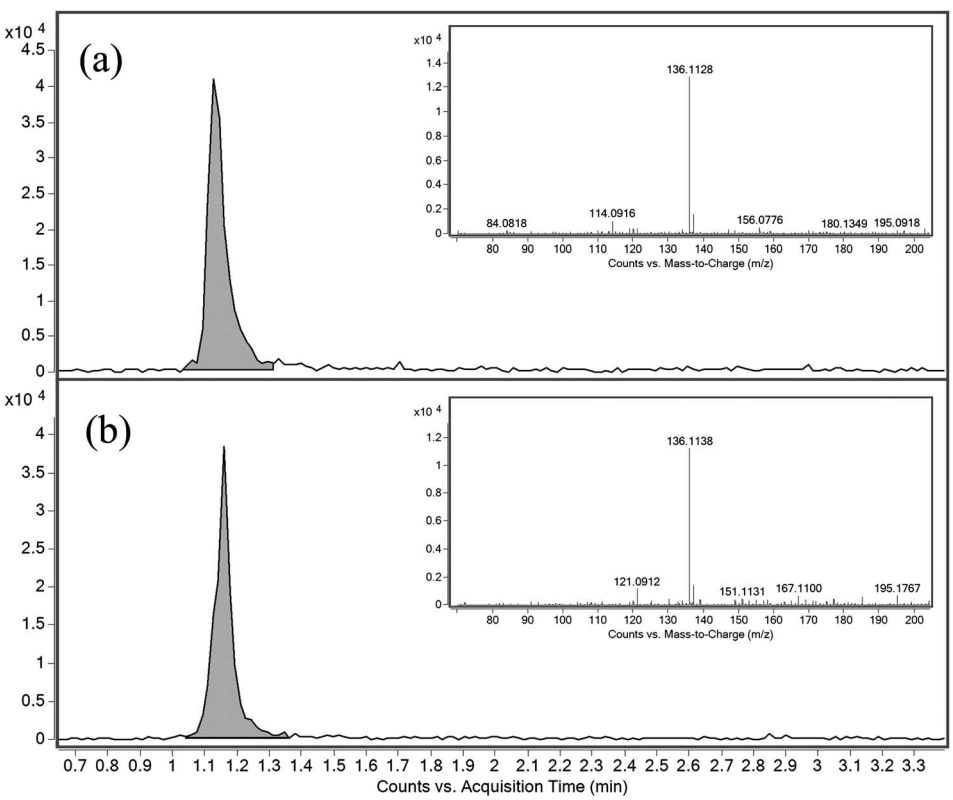

Fig. 4 TD-ESI-FAIMS-MS selected ion profiles (*m*/*z* 136.1) of (a) 2,4,6-trimethylaniline (CF = 1 Td, DF 230 Td); and (b) *N*,*N*-dimethyl-*m*-toluidine (CF = 1.5 Td, DF 230 Td), desorbed directly from starch at 1 ppm (w/w). Inset are the corresponding mass spectra at the desorption peak maxima.

Table 1 Quantitative determination of 2,4,6-TMA and *N*,*N*-DMT by TD-FAIMS-MS

Compound	LOQ/ppm	RSD/%
2,4,6-Trimethylaniline	0.19	8.4
N,*N*-Dimethyl-*m*-toluidine	0.13	7.5

separation at the appropriate DF and CF determined from the direct infusion studies, adds selectivity to the analysis by discriminating between *N*,*N*-DMT and 2,4,6-TMA.

The quantification limits and precision were evaluated to test performance of the prototype TD-FAIMS-MS analysis (Table 1). The limit of quantification (LOQ) was determined to be 0.19 ppm and 0.13 ppm for the FAIMS pre-selected 2,4,6-TMA and *N*,*N*-DMT respectively (10 : 1 signal : noise), spiked as a mixture into 10 mg of the surrogate API. These LOQs are approximately an order of magnitude below 1.5 ppm, the TTC limit assuming a 1 g per day dose (European Medicines Agency). However, detection of PGIs at 'as low as reasonably possible' (the so-called ALARP concept) levels[1,2] is encouraged, but not essential, for unusually toxic impurities where detection below the TTC may be required. This requirement is easily met using TD-FAIMS-MS, as well as reducing sample preparation and analysis times.

4 Conclusion

Chip-based FAIMS combined with TOF MS has been used for the rapid determination of the isobaric PGIs 2,4,6-TMA and *N*,*N*-DMT, without the need for a chromatographic separation. The ability to filter ions based on differential mobility, an orthogonal technique to mass spectrometry, provides an added dimension of separation to the TD-MS analysis. Direct thermal desorption of 2,4,6-TMA and *N*,*N*-DMT from a solid matrix was demonstrated at 1 ppm, below the TTC, with good precision (<8.4%). The combination of good reproducibility and limits of quantification almost an order of magnitude below the TTC, shows that TD-FAIMS-MS has the potential as a rapid, quantitative screening method for monitoring volatile PGIs in active pharmaceutical ingredients. Other API matrices would need to be investigated to demonstrate the ubiquity of this technique. The approach may also be used for the analysis of volatile organic compounds in other solid matrices.

Acknowledgements

The authors thank Owlstone Ltd. and Loughborough University for financial support. We thank Owlstone Ltd. and Agilent Technologies for the provision of instrumentation and technical support.

References

1 L. Muller, R. J. Mauthe, C. M. Riley, M. M. Andino, D. D. Antonis, C. Beels, J. DeGeorge, A. G. M. De Knaep, D. Ellison, J. A. Fagerland, R. Frank, B. Fritschel, S. Galloway, E. Harpur, C. D. N. Humfrey, A. S. Jacks, N. Jagota, J. Mackinnon, G. Mohan, D. K. Ness, M. R. O'Donovan, M. D. Smith, G. Vudathala and L. Yotti, *Regul. Toxicol. Pharmacol.*, 2006, **44**, 198–211.
2 *Genotoxic Impurities: Strategies for Identification and Control*, ed. A. Teasdale, John Wiley and Sons Inc., New Jersey, 2010.
3 http://www.ema.europa.eu/docs/en_GB/document_library/Scientific_guideline/2009/09/WC500002903.pdf, accessed 16 December 2012.
4 http://www.fda.gov/downloads/Drugs/…/Guidances/ucm079235.pdf, accessed 16 December 2012.
5 T. McGovern and D. Jacobson-Kram, *TrAC, Trends Anal. Chem.*, 2006, **25**, 790–795.
6 B. A. Olson, B. C. Castle and D. P. Myers, *TrAC, Trends Anal. Chem.*, 2006, **25**, 796–805.
7 J. F. Pankow, W. Luo, L. M. Isabelle, D. A. Bender and R. J. Baker, *Anal. Chem.*, 1998, **70**, 5213–5221.
8 J. Ding, S. Yang, D. Liang, H. Chen, Z. Wu, L. Zhang and Y. Ren, *Analyst*, 2009, **134**, 2040–2050.
9 J. C. Reynolds, G. J. Blackburn, C. Guallar-Hoyas, V. H. Moll, V. Bocos-Bintintan, G. Kaur-Atwal, M. D. Howdle, E. L. Harry, L. J. Brown, C. S. Creaser and C. L. P. Thomas, *Anal. Chem.*, 2010, **82**, 2139–2144.
10 N. A. Devenport, L. C. Sealey, F. H. Alruways, D. J. Weston, J. C. Reynolds and C. S. Creaser, *Anal. Chem.*, 2013, **85**, 6224–6227.
11 L. J. Brown, R. W. Smith, D. E. Toutoungi, J. C. Reynolds, A. W. T. Bristow, A. Ray, A. Sage, I. D. Wilson, D. J. Weston, B. Boyle and C. S. Creaser, *Anal. Chem.*, 2012, **84**, 4095–4103.
12 R. W. Smith, D. E. Toutoungi, J. C. Reynolds, A. W. T. Bristow, A. Ray, A. Sage, I. D. Wilson, D. J. Weston, B. Boyle and C. S. Creaser, *J. Chromatogr., A*, 2013, **1278**, 76–81.
13 L. J. Brown, D. E. Toutoungi, N. A. Devenport, J. C. Reynolds, G. Kaur-Atwal, B. Boyle and C. S. Creaser, *Anal. Chem.*, 2010, **82**, 9827–9834.
14 A. A. Shvartsburg, R. D. Smith, A. Wilks, A. Koehl, D. Ruiz-Alonso and P. Boyle, *Anal. Chem.*, 2009, **81**, 6489–6495.
15 A. A. Shvartsburg, K. Tang, R. D. Smith, M. Holden, M. Rush, A. Thompson and D. Toutoungi, *Anal. Chem.*, 2009, **81**, 8048–8053.
16 M. E. Kugler-Steigmeier, U. Friederich, U. Graf, P. Maier and C. Schlatter, *Arch. Toxicol., Suppl.*, 1998, **12**, 337–340.
17 G. Vanhoenacker, E. Dumont, F. David, A. Baker and P. Sandra, *J. Chromatogr., A*, 2009, **1216**, 3563–3570.

